Book of Invited Talks

DAE-BRNS TWO-DAY THEME MEETING ON Strategic Planning for Enhancing Research Reactor Utilization (RRU-2022)

Jointly Organized by
Reactor Group and Radiochemistry & Isotope Group
Bhabha Atomic Research Centre

May 6-7, 2022
DAE Convention Centre, Anushaktinagar, Mumbai-400094

Editors
Tej Singh, Kunal Chakraborty, C G Karhadkar, Reactor Group
and
Raghunath Acharya, P.K. Pujari, Radiochemistry & Isotope Group

Book of Invited Talks

DAE-BRNS TWO-DAY THEME MEETING ON Strategic Planning for Enhancing Research Reactor Utilization

(RRU-2022)

May 6-7, 2022

DAE Convention Centre

Anushaktinagar, Mumbai - 400094

Compiled by

Kamalakanta Singha
Avijit Das
Jainendra Kumar
Shantanab Banerjee
Tanay Mazumdar
Tej Singh
Abhishek Mishra
Paritosh Pandey
Y. S. Rana

Bhabha Atomic Research Centre

Board of Research in Nuclear Sciences

Jointly Organized by

Reactor Group and Radiochemistry & Isotope Group

Bhabha Atomic Research Centre

Sponsored by

Board of Research in Nuclear Sciences

आमंत्रित वार्ता पुस्तक

अनुसंधान रिएक्टरों के उपयोजन वृद्धि हेतु कार्यनीतिक आयोजना

पर दो दिवसीय पऊवि-बीआरएनएस थीम गोष्ठी

(आरआरयू-2022)

दिनांक 6-7 मई, 2022

पऊवि सम्मेलन केंद्र

अणुशक्तिनगर, मुंबई-400094

संकलन

कमलाकान्त सिंह *शान्तनब बनर्जी* *अभिषेक मिश्र*

अभिजीत दास *तनय मजुमदार* *परितोष पाण्डेय*

जैनेन्द्र कुमार *यशपाल सिंह राणा*

तेज़ सिंह

भाभा परमाणु अनुसंधान केंद्र **बोर्ड ऑफ़ रिसर्च इन न्युक्लियर साइंसेज**

रिएक्टर वर्ग तथा रेडियोरासायनिकी एवं आइसोटोप वर्ग
भाभा परमाणु अनुसंधान केंद्र
द्वारा संयुक्त रूप से आयोजित

प्रायोजक

नाभिकीय विज्ञान अनुसंधान बोर्ड

अस्वीकरण:

अंशदायी पत्रों की तकनीकी सामग्री तथा उनमें उद्धृत सन्दर्भों के लिए केवल उनके लेखक ही उत्तरदायी हैं।

DAE-BRNS TWO-DAY THEME MEETING ON

Strategic Planning for Enhancing Research Reactor Utilization

RRU-2022

May 6-7, 2022

National Advisory Committee

Shri K.N. Vyas	Chairman, AEC (Chair)
Dr. A. K. Mohanty	Director, BARC (Co-Chair)
Shri B. C. Pathak	CMD, NPCIL
Dr. B. Venkatraman	Director, IGCAR
Shri G. N. Rao	Chairman, AERB
Shri J. Srivastava	C & CE, HWB
Dr. Dinesh Srivastava	C & CE, NFC
Dr. R. A. Badwe	Director, TMC
Dr. D. K. Sinha	Director, AMD
Shri D. Singh	CMD, IREL
Dr. C. K. Asnani	CMD, UCIL
Dr. S. Bhattacharya	Director, RPG, BARC
Shri Vivek Bhasin	Director, NFG, BARC
Shri K. Jayarajan	Chairman, BSC, BARC
Dr. A. P. Tiwari	Director, KMG, BARC
Shri A. Sharma	Director, RDDG,BARC
Dr. Vivekanand Kain	Director, MG, BARC
Dr. D. K. Aswal	Director, HS&EG, BARC
Shri P. Mukherjee	CE, BRIT
Dr. (Smt.) A. Sharma	Director, BTDG, BARC
Shri K. T. Shenoy	Director, ChEG, BARC
Dr. T. K. Ghanty	Director, BSG, BARC
Dr. Amlan J. Pal	Director, UGC-DAE CSR

Organizing Committee

Dr. P. K. Pujari	**Director, RC&IG, BARC (Co-chair)**
Shri. C. G. Karhadkar	**Director, RG, BARC (Co-chair)**
Smt. Anita R. Behere	Director, E&IG, BARC
Dr. A. K. Tyagi	Director, CG, BARC
Dr. S. M. Yusuf	Director, PG, BARC
Dr. S. Kannan	AD, RC&IG, BARC
Shri R. N. Sen	AD, RPG, BARC
Dr. P. D. Babu	Director, UGC-DAE CSR (Mumbai)
Shri S. K. Jha	Head, AFD, BARC
Dr. (Smt.) Umasankari K.	Head, RPDD, BARC
Dr. R. Tewari	Head, MSD, BARC
Dr. P. K. Mohapatra	Head, RCD, BARC
Shri P. Sumanth	Head, RRMD, BARC
Shri Kunal Chakrabarty	Head, ROD, BARC
Shri Joe Mohan	Head, RPD, BARC
Dr. R. N. Singh	Head, MMD, BARC
Shri H. G. Gujar	Head, RRSD, BARC
Dr. M. S. Kulkarni	Head, HPD, BARC
Dr. (Smt.) B. K. Sapra	Head, RPAD, BARC
Dr. H. J. Pant	Head, IRAD, BARC
Dr. A. K. Gupta	Head, NPD, BARC
Dr. C. N. Patra	Head, ACD, BARC
Dr. A. Vinod Kumar	Head, EMAD, BARC
Dr. L. M. Pant	Head, TPD, BARC
Dr. S. Adhikari	Head, SIRD, BARC
Dr. A. K. Arya	Head, G&AMD, BARC
Dr. S. C. Parida	Head, PDD, BARC
Shri N. S. Joshi	Head, HRSS, RRSD
Dr. Tej Singh	**RRSD, RG, BARC (Convener)**
Dr. R. Acharya	**RCD, RC&IG, BARC (Co-convener)**

DAE Convention Centre

Anushaktinagar, Mumbai-400094

Bhabha Atomic Research Centre has state of art research reactor facilities at Dhruva and Apsara-U for radioisotope production as well as various R&D works. There is a need as well as scope to enhance the utilization of neutrons from research reactors by various R&D communities and users from various organizations for materials characterization, nuclear reaction & fission, health care and various societal applications. In this regard, a DAE-BRNS sponsored Two-Day Theme Meeting on "Strategic Planning for Enhancing Research Reactor Utilization (RRU-2022)" is being organized to commemorate Azadi Ka Amrit Mahotsav. The main objective of this Theme Meeting is aimed at interaction with the potential users of research reactors at BARC, other units of DAE as well as non-DAE government and private organizations including industries, research and academic institutes and Institutes/Universities that are pursuing projects under BRNS, UGC-DAE CSR , CSIR and other schemes.

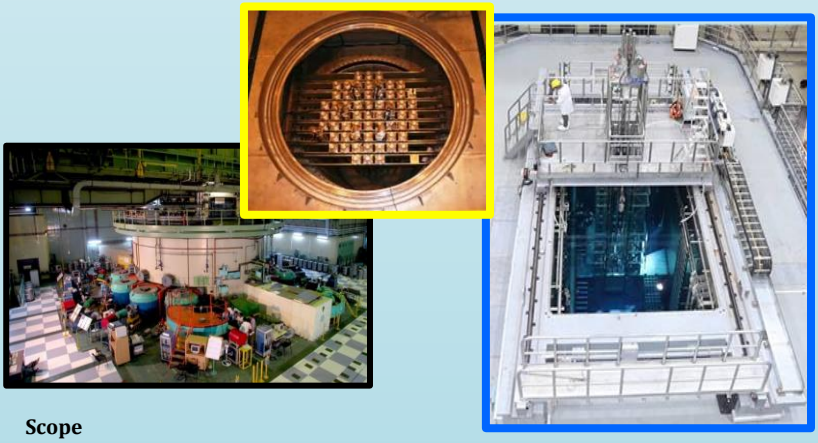

Scope

a) Research Reactor Facilities at BARC, Mumbai
b) Radioisotope Production & Various Societal Applications in Healthcare, Industry, Food & Agriculture
c) Neutron Scattering Studies utilizing Neutron Beams
d) Neutron Imaging (Radiography/Tomography) for Non-destructive Testing
e) Neutron Activation Analysis for Chemical Characterization of Materials
f) Nuclear Physics Studies (Neutron Capture Gamma-ray Spectroscopy, Fission Studies etc.)
g) Development and Testing of Radiation Detectors
h) Development and Testing of Shielding Materials for Neutron and Gamma-rays
i) Studies related to Materials Science, Reactor Materials, Ores, Minerals, Forensic Sciences, Industrial Applications, Geochronology
j) Reactor Physics Experiments
k) Neutron Transmutation doping studies for semiconductor devices
l) Education and Training for Human Resource Development

Jointly organised by

Reactor Group and Radiochemistry & Isotope Group, BARC

In association with

UGC-DAE CSR, Mumbai Centre and Society for Positron Annihilation and Nuclear Probes (SPAN) C/o. RCD, BARC

Website: http://www.barc.gov.in/symposia/RRU-2022

Correspondence E-mail: rru2020@barc.gov.in

National Advisory Committee

Shri K.N. Vyas	Chairman, AEC (Chair)	Mumbai
Dr. A. K. Mohanty	Director, BARC (Co-Chair)	Mumbai
Shri B. C. Pathak	CMD, NPCIL	Mumbai
Dr. B. Venkatraman	Director, IGCAR	Kalpakkam
Shri G. N. Rao	Chairman, AERB	Mumbai
Shri J. Srivastava	C & CE, HWB	Mumbai
Dr. Dinesh Srivastava	C & CE, NFC	Hyderabad
Dr. R. A. Badwe	Director, TMC	Mumbai
Dr. D. K. Sinha	Director, AMD	Mumbai
Shri D. Singh	CMD, IREL	Mumbai
Dr. C. K. Asnani	CMD, UCIL	Jaduguda
Dr. S. Bhattacharya	Director, RPG, BARC	Mumbai
Shri Vivek Bhasin	Director, NFG, BARC	Mumbai
Shri K. Jayarajan	Chairman, BSC, BARC	Mumbai
Dr. A. P. Tiwari	Director, KMG, BARC	Mumbai
Shri A. Sharma	Director, RDDG, BARC	Mumbai
Dr. Vivekanand Kain	Director, MG, BARC	Mumbai
Dr. D. K. Aswal	Director, HS&EG, BARC	Mumbai
Shri P. Mukherjee	CE, BRIT	Mumbai
Dr. (Smt.) A. Sharma	Director, BTDG, BARC	Mumbai
Shri K. T. Shenoy	Director, ChEG, BARC	Mumbai
Dr. T. K. Ghanty	Director, BSG, BARC	Mumbai
Dr. Amlan J. Pal	Director, UGC-DAE CSR	Indore

Organizing Committee

Dr. P. K. Pujari	Director, RC&IG, BARC (Co-chair)
Shri. C. G. Karhadkar	Director, RG, BARC (Co-chair)
Smt. Anita R. Behere	Director, E&IG, BARC
Dr. A. K. Tyagi	Director, CG, BARC
Dr. S. M. Yusuf	Director, PG, BARC
Dr. S. Kannan	AD, RC&IG, BARC
Shri R. N. Sen	AD, RPG, BARC
Dr. P. D. Babu	Director, UGC-DAE CSR (Mumbai)
Shri S. K. Jha	Head, AFD, BARC
Dr. (Smt.) Umasankari K.	Head, RPDD, BARC
Dr. R. Tewari	Head, MSD, BARC
Dr. P. K. Mohapatra	Head, RCD, BARC
Shri P. Sumanth	Head, RRMD, BARC
Shri Kunal Chakrabarty	Head, ROD, BARC
Shri Joe Mohan	Head, RPD, BARC
Dr. R. N. Singh	Head, MMD, BARC
Shri H. G. Gujar	Head, RRSD, BARC
Dr. M. S. Kulkarni	Head, HPD, BARC
Dr. (Smt.) B. K. Sapra	Head, RPAD, BARC
Dr. H. J. Pant	Head, IRAD, BARC
Dr. A. K. Gupta	Head, NPD, BARC
Dr. C. N. Patra	Head, ACD, BARC
Dr. A. Vinod Kumar	Head, EMAD, BARC
Dr. L. M. Pant	Head, TPD, BARC
Dr. S. Adhikari	Head, SIRD, BARC
Dr. A. K. Arya	Head, G&AMD, BARC
Dr. S. C. Parida	Head, PDD, BARC
Shri N. S. Joshi	Head, HRSS, RRSD
Dr. Tej Singh	RRSD, RG, BARC (Convener)
Dr. R. Acharya	RCD, RC&IG, BARC (Co-convener)

Technical Committee

Shri Kunal Chakrabarty	Head, ROD, BARC (Chairman)
Shri Pravin Kumar	DGM, BRIT
Shri Shibu Thomas	RS, Apsara-U
Dr. Mala N. Rao	Head, NIS, SSPD
Dr. Tej Singh	Head, RPNES, RRSD
Shri S. K. Mondal	Head, ISIS, RRSD
Shri N S Bhamra	RS, Dhruva
Shri V. Shivakumar	Head, FES, RED
Dr. B V John	Head, FPS, NPD
Dr. V. K. Aswal	Head, MSAS, SSPD
Dr. R. Acharya	Head, NA&ASS, RCD
Dr. K. K. Swain	Head, NAMS, ACD
Dr. S. Chakrabarty	Head, RChS, RPhD
Shri Abhishek Tripathi	SO/G, RPD
Dr. Mayank Shukla	SO/G, TPD
Dr. Suman Neogy	Head, RD&EMS, MSD
Dr. Tanay Mazumdar	SO/F, RRSD
Shri Abhishek Mishra	SO/E, RRSD

Local Organizing Committee (LOC)

Shri H. G. Gujar, Head, RRSD (Chairman)

LOC-1 Hospitality (Accommodation & Food) Committee

Shri Vikas Goel, RRSD
Dr. Rubel Chakravarty, RPhD
Dr. M. K. Tripathy, RRSD
Shri Sudeep Kumar Samanta, RCD
Shri Anil A. Naik, RRSD

LOC-2 Poster committee

Dr. Mala N Rao, SSPD
Shri Vikas Jain, ROD
Dr. Y.S. Rana, RRSD
Dr. Arijit Sengupta, RCD
Shri Jainendra Kumar, RRSD
Mr. Sk Wasim Raja, RCD
Dr. Somsundar Mukhopadhyay, NPD

LOC-3 Exhibition and Finance committee

Dr. R. Acharya, RCD
Dr. Kathi Sudarshan, RCD
Shri P.K. Dubey, RRMD
Dr. Manoj Mohapatra, RCD
Dr. Tushar Roy, TPD
Shri Avijit Das, RRSD
Dr. Ram Avtar Jat, PDD
Dr. K A Dubey, RTDD
Dr. Sudipta Chakraborty, RPhD
Dr. S.K. Sharma, RCD
Dr. D. Dutta, RCD

LOC-4 Transport Committee

N. K. Choudhary, ROD
Dr. K. V. V. Nair, RPhD
Dr. Saurabh Mukherjee, RCD
Dr. V. T. Aher, RRSD

LOC-5 Registration Committee

Dr. (Smt) Archana Mukherjee, RPhD
Kum. Nishtha Shreya, RRSD
Ms. Trupti Chavan, ACD
Ms. Mohini Guleria, RPhD
Ms. Kusum Vats, RPhD
Smt Nutan T. Tiwari, RRSD
Shri Kamalakanta Singha, RRSD

LOC-6 Hall management Committee

Shri Parag Punekar, RRMD
Dr. R. S. Sharma, RRSD
Shri Sachin Kumar, ROD
Shri Sparsh Sharma, RRMD
Shri Shantanab Banerjee, RRSD
Ms. Nicy Ajith, ACD
Smt. Archana Sharma, RRDPD
Ms. P. S. Remya Devi, ACD

LOC-7 Souvenir Committee

Dr. V. K. Aswal, SSPD
Dr. Y. S. Rana, RRSD
Shri Siddhartha Pramanick, ROD
Shri Sukumar Layek, ROD
Shri Paritosh Pandey, RRSD

के. एन. व्यास
K. N. Vyas

भारत सरकार
Government of India

अध्यक्ष, परमाणु ऊर्जा आयोग
व
सचिव, परमाणु ऊर्जा विभाग
Chairman, Atomic Energy Commission
&
Secretary, Department of Atomic Energy

MESSAGE

I am happy to know that the DAE-BRNS sponsored Two-Day Theme Meeting on "Strategic Planning for Enhancing Research Reactor Utilization (RRU-2022)" is going to be organized jointly by Reactor Group and Radiochemistry & Isotope Group during May 6-7, 2022 at DAE Convention Centre, Anushaktinagar, Mumbai.

Since commissioning of India's first nuclear reactor Apsara in 1956, DAE has been actively involved in utilization of research reactors for societal applications by producing medical radioisotopes as well as encouraging cutting-edge research with neutrons as probes in the field of condensed matter physics, nuclear physics, reactor materials, etc. Presently, research reactors at BARC – namely, Dhruva and Apsara-U are being extensively used by both DAE and non DAE users for a variety of applications in the field of reactor engineering, materials research, agriculture, material characterization, neutron imaging, etc.

I am delighted to know that about 200 delegates from DAE and Non-DAE institutes will be participating in this theme meeting. I am sure that the meeting will provide guidance and awareness among users for the effective utilization of these important research facilities. The two-day deliberations will inspire the researchers from academic institutes to take up new challenges by utilizing research reactors in India.

I wish the Theme meeting a grand success.

(K. N. Vyas)

राष्ट्र की सेवा में परमाणु
प ऊ वि
DAE
ATOMS IN THE SERVICE OF THE NATION

अणुशक्तिभवन, छत्रपति शिवाजी महाराज मार्ग, मुंबई - 400 001, भारत • Anushakti Bhavan, Chhatrapati Shivaji Maharaj Marg, Mumbai - 400 001, India
दूरभाष/Phone:+(91) (22) 2202 2543 • फैक्स/Fax: +(91) (22) 2204 8476 / 2284 3888
ई-मेल/E-mail: chairman@dae.gov.in

डॉ. अजित कुमार मोहान्ती
Dr. Ajit Kumar Mohanty

भारत सरकार
Government of India

निदेशक, भाभा परमाणु अनुसंधान केंद्र
Director, Bhabha Atomic Research Centre
सदस्य, परमाणु ऊर्जा आयोग
Member, Atomic Energy Commission

FOREWORD

On behalf of Bhabha Atomic Research Centre, I extend my gratitude to Reactor Group (RG) and Radiochemistry & Isotope Group (RC&IG) for organizing a DAE-BRNS sponsored Two-Day Theme Meeting on "Strategic Planning for Enhancing Research Reactor Utilization (RRU-2022)" to commemorate 75 years of Indian Independence - "Azadi Ka Amrit Mahotsav".

BARC is a premiere nuclear research centre under Department of Atomic Energy, which symbolizes an organization of multidisciplinary and broad-spectrum R&D excellence in the advanced domain of Nuclear Science, Engineering and Basic Sciences. It was none other than Dr. Homi Jehangir Bhabha, who conceptualized and laid the foundation of the research reactor programme in India by setting up Apsara in 1956 in order to commence beam tube research in nuclear physics, condensed matter physics and material science and production of radioisotopes for wide range of applications starting from medicine to industry to agriculture and research.

Presently, BARC has state-of-the-art research reactor facilities at Dhruva and Apsara-U for radioisotope production as well as various R&D activities. These Research Reactors are being well utilized by DAE and non-DAE organizations for Radioisotope production, Neutron Scattering and Spectroscopy experiments in beam tubes, Neutron Activation Analysis, Neutron imaging and its applications etc.

The main objective of the theme meeting is to enhance collaboration with potential users of research reactors at BARC including industries, research and academic institutes and thereby utilize the research reactors to their full potential.

I again wish to extend my heartfelt thanks to the organizers and the participants, who contributed to this programme and wish RRU-2022 a great success.

Ajit Kumar Mohanty

(Ajit Kumar Mohanty)

भाभा परमाणु अनुसंधान केंद्र, ट्रॉम्बे, मुंबई- 400 085, भारत • Bhabha Atomic Research Centre, Trombay, Mumbai 400 085, India
दूरभाष/Phone:+(91) (22) 2550 5300, 2551 1910 • फैक्स/Fax: +(91) (22) 2559 2107, 2550 5151
ई-मेल/E-mail: director@barc.gov.in

डॉ. आर. चिदंबरम

Dr. R. Chidambaram

सत्यमेव जयते

भारत सरकार
Government of India

पऊवि-होमी भाभा पीठाचार्य,
DAE - Homi Bhabha Chair Professor
भारत सरकार के पूर्व प्रधान वैज्ञानिक सलाहकार
पर्व अध्यक्ष, परमाणु ऊर्जा आयोग एवं
पर्व निदेशक, भाभा परमाणु अनुसंधान केंद्र
Former Principal Scientific Adviser to GOI,
Former Chairman, Atomic Energy Commission
Former Director, Bhabha Atomic Research Centre

The DAE BRNS Theme Meeting on Strategic Planning for Research Reactor Utilization (RRU-2022) is timely. The activities in BARC in neutron beam research for condensed matter physics and materials research, radio-isotope generation, etc. have been growing, and the experimental facilities have been made available to other units and universities in the country also.

The power reactor program in the country and that of the research reactors at BARC are closely intertwined. These research reactors have been providing our scientists and engineers much sought-after insights into the intricacies of design and construction of nuclear power reactors.

Since inception, our nuclear programme has been characterised by a holistic approach. Thus, while power generation is indeed a matter of priority, non-power applications of nuclear energy in areas such as medicine, agriculture and industry are given emphasis in our R&D programme. DAE has also extensively encouraged the university-BARC collaboration in the area of neutron beam research.

A new High-Flux Research Reactor is also coming up at the BARC campus at Vishakhapatnam, where our aim should be to build a robust R&D program, with the best-in-class neutron beam research instruments.

I believe the deliberations in the meeting would definitely lead to fruitful interactions amongst the participants and help in advancing research reactor utilisation in the country.

I extend warm wishes to all the participants and wish the conference all success.

R. Chidambaram
29.4.22

(R. Chidambaram)

राष्ट्र की सेवा में परमाणु
भा प अ कें
BARC
ATOMS IN THE SERVICE OF THE NATION

भाभा परमाणु अनुसंधान केंद्र, छठी मंजिल, सेंट्रल काम्प्लेक्स, ट्रॉम्बे, मुंबई - 400 085, भारत
Bhabha Atomic Research Centre, 6th Floor, Central Complex, Trombay, Mumbai 400 085, India
दूरभाष / Tel.: +91-22-2550 5305 • फैक्स / Fax : +91-22-2550 5132 • ई-मेल / E-mail : rc@barc.gov.in

सी. जी. कऱ्हाडकर

C. G. Karhadkar

सत्यमेव जयते
भारत सरकार
Government of India

उत्कृष्ट वैज्ञानिक एवं
निदेशक, रिएक्टर वर्ग
Outstanding Scientist &
Director, Reactor Group

MESSAGE

Research Reactors are an important platform for supporting research pertaining to material characterization using neutrons as probes, testing and qualification of reactor materials and related components under neutron flux environment and production of large variety of radioisotopes for health care, agriculture, industry and environmental related programme.

These reactors have provided a valuable support in development of the Indian Nuclear Power Program in many ways, viz. testing of materials, fuel, equipment, shielding experiments, validation of codes etc.

Presently BARC has state-of-the-art facilities, with neutron flux as low as 10^6 n/cm^2/sec to as high as 2.2 x 10^{14} n/cm^2/sec at Dhruva, Critical Facility and Apsara-U reactors. These Research Reactors are being utilized by DAE and some Non-DAE organizations for radioisotope production, Neutron Scattering experiments, Neutron Activation Analysis (NAA), Neutron Imaging, Material Research, Nuclear Reactions and Fission studies, Development and testing of detectors, Neutron Transmutation Doping (NTD)-Si, Reactor Physics experiments, Education and Training for Human Resources Development.

With a goal to enhance the collaboration with potential users of research reactors, Reactor Group (RG) and Radiochemistry & Isotope Group (RC&IG) are organizing a DAE-BRNS sponsored Two-Day Theme Meeting on ***"Strategic Planning for Enhancing Research Reactor Utilization (RRU-2022)"*** on May 6 & 7, 2022. I sincerely hope that this meeting will strengthen the bonds between the BARC-Reactor community, Non-DAE Government Industry, Private Industry & Academia and pave way for creation of a platform for regular interactions and enhancing research reactor utilization.

26.4.22

(C. G. Karhadkar)

भाभा परमाणु अनुसंधान केंद्र, ट्रॉम्बे, मुंबई - 400 085, भारत • Bhabha Atomic Research Centre, Trombay, Mumbai 400 085, India
दूरभाष / Tel.: +91-22-2559 4655 • आवास / Res.: +91-22-2085 4367 • फैक्स / Fax : +91-22-2550 5311
मोबाईल / Mobile: 098692 70145 • ई-मेल / E-mail : karhadka@.barc.gov.in

Dr. P.K. Pujari
Distinguished Scientist
Former Director, RC&IG, BARC
Co-Chair, Organizing Committee of RRU-2022
Email: pkpujari@yahoo.com

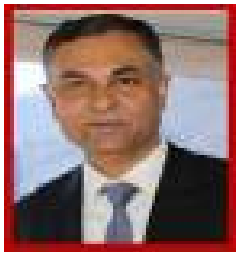

Message

I am glad that **DAE-BRNS sponsored Two-Day Theme Meeting on 'Strategic Planning for Enhancing Research Reactor Utilization (RRU-2022)**' is being jointly organized by Reactor Group and Radiochemistry & Isotope Group of BARC in association with UGC-DAE CSR Mumbai Centre and Society for Positron Annihilation and Nuclear Probes (SPAN) during May 6-7, 2022 at the DAE Convention Centre, Anushaktinagar, Mumbai to commemorate "**Azadi Ka Amrit Mahotsav**". The Theme Meeting will provide forum for interaction of Scientists and Engineers from BARC and researchers and potential users from non-DAE and private organizations including Industry. I am happy that 200 delegates will participate in this Meeting. The technical program of RRU-2022 consists of keynote and invited talks by experts as well as oral and poster presentations by more than 200 researchers from BARC, DAE, faculties from academic institutes, R&D personnel from Industry and research scholars.
Radiochemistry and Isotope Group of BARC is one of the beneficiaries of research reactors ever since the commissioning of Apsara reactor. In addition to various R&D works utilizing neutrons, RC&I group has very strong activities linked to societal applications in health care, industry as well as physical and chemical research. State of art facilities utilizing neutrons for studies in nuclear fission, neutron activation analysis, radiopharmaceuticals as well as isotope hydrology are in place at BARC. It is necessary to have enhanced utilization of neutrons from Dhruva and Apsara-U reactor facilities in key areas having societal importance and frontier areas of research like neutron radiography, imaging, non-destructive assay, PGNAA, neutrino research as well as intense positron facilities for materials characterization. BARC encourages users from Industry, academic institutes and government organizations for utilizing available research reactor facilities.

I am thankful to BRNS, DAE for the financial support and UGC-DAE-CSR and SPAN as organizing bodies. I wish the theme meeting RRU-2022 a grand success.

Date: 20th April 2022 (P.K. Pujari)

FAX : +91-22-2550 5151/2550 5345
Phone No.25593933, 25593604

Dr. S. Kannan

Director, RC&I Group,
BARC, Trombay, Mumbai 400085.
Email : skannan@barc.gov.in

सत्यमेव जयते

भारत सरकार
Government of India
BHABHA ATOMIC RESEARCH CENTRE
Radiochemistry & Isotope Group

April 21, 2022

Message

I am happy that the **DAE-BRNS sponsored Two-Day Theme Meeting on 'Strategic Planning for Enhancing Research Reactor Utilization (RRU-2022)'** is being jointly organized by Reactor Group and Radiochemistry & Isotope Group of BARC in association with UGC-DAE CSR, Mumbai Centre and Society for Positron Annihilation and Nuclear Probes (SPAN) during May 6-7, 2022 at the DAE Convention Centre, Anushaktinagar, Mumbai - 400094 to commemorate "**Azadi Ka Amrit Mahotsav**". The main objective of this Theme Meeting is aimed at interaction of experts from BARC, DAE with Potential Users of research reactors from non-DAE government and private organizations including academic and research institutes and Industries. It is heartening to note that more than 200 delegates will participate from various organizations having interest in utilizing research reactors and reactor produced radioisotopes and present their work plan. The technical program of RRU-2022 consists of keynote and invited talks by experts, Oral presentations by existing and prospective users and Poster presentation by researchers, faculties, R&D personnel and research scholars.

Radiochemistry and Isotope Group of BARC has been utilizing research reactors since 1956 for various R&D as well as applied works having applications in the area of health care, industry and research. R&D studies in the fields of Nuclear Fission, Neutron Activation Analysis and Radiopharmaceuticals are the key areas, where reactor neutrons have been extensively utilized by our group and also through collaboration with academic and research institutes under various schemes of BRNS and UGC DAE CSR. RC&I Group has a long-term R&D work plan aimed towards departmental as well as societal applications utilizing reactor neutrons and thermal neutron beam via Radioisotopes for health care and industry as well as Prompt Gamma-ray NAA and Positron Annihilation Spectroscopy for materials characterization utilizing Dhruva as well as Apsara-U reactor facilities.

I congratulate the organizers of RRU-2022 and wish the theme meeting a grand success via fruitful interaction among experts and users of research reactors.

(S . Kannan) 22/4/22

Dr. A. K. TYAGI
(FRSC, FNASc, FASc)
Director, Chemistry Group
Bhabha Atomic Research Centre
Mumbai-400 085

Email: aktyagi@barc.gov.in
Phone: 022-2559 5330

भाभा परमाणु अनुसंधान केंद्र
BHABHA ATOMIC RESEARCH CENTRE

MESSAGE

I am happy to know that the DAE-BRNS sponsored Two-Day Theme Meeting on "Strategic Planning for Enhancing Research Reactor Utilization (RRU-2022)" is being organized jointly by Reactor Group and Radiochemistry & Isotope Group during May 6-7, 2022.

The research reactors are important national facilities for supporting research and development in the areas of material characterization using neutrons as probes; testing of reactor materials, related components under neutron environment and production of a large variety of radioisotopes for societal applications including health care, agriculture, industry and environment. There are numerous industrial applications for research reactors. Another important application is in the area of neutron radiography/tomography of various objects utilizing neutron beam tubes of nuclear reactors.

Since late fifties, Chemistry Group, BARC has been utilizing reactor based neutron activation analysis (NAA) techniques for various applications including geological exploration, forensic investigations, archaeological studies and high purity material development program. Lunar samples made available to BARC were also analyzed by NAA. There was strong collaboration with Central Forensic Science Laboratory and Geological Survey of India for the specialized analyses for forensic exhibits and analysis of rock samples for precious metals respectively using NAA technique. With the availability of high flux research reactors the utilization of this technique will be extended to every branch of science and technology.

I am delighted to know that about 200 delegates including 80 participants from academic institutes will be attending this theme meeting. I am sure, RRU-2022 will provide an excellent platform for effective interaction among various users of research reactors and experts from DAE and Non-DAE. The two-day meeting will create awareness about the wide utility of existing facilities and inspire the young researchers to take up new challenges utilizing these research reactors.

I wish the Theme Meeting a grand success and fruitful time to all the delegates during RRU-2022.

Dated: 18-04-2022

(A. K. Tyagi)

डॉ. एस. एम. युसुफ
Dr. S.M. Yusuf, D.Sc (Hon.), FASc, FNASc
निदेशक, भौतिकी वर्ग
Director, Physics Group

सत्यमेव जयते
भारत सरकार
GOVERNMENT OF INDIA
भाभा परमाणु अनुसंधान केंद्र
BHABHA ATOMIC RESEARCH CENTRE
भौतिकी वर्ग
PHYSICS GROUP
Mumbai – 400085

भाभा परमाणु अनुसंधान केंद्र
BHABHA ATOMIC RESEARCH CENTRE

Message

It is my immense pleasure to be associated with the organization of “DAE-BRNS Theme Meeting on Strategic Planning for Enhancing Research Reactor Utilization (RRU-2022)”. The Theme meeting is being held during May 6-7 at Bhabha Atomic Research Centre, Mumbai, jointly organized by Reactor Group and Radiochemistry & Isotope Group, BARC.

Research reactor utilizations for neutron scattering, imaging and nuclear physics studies form a significant and unique implementation of radiation to probe and explore the properties of matter. Neutron scattering, in particular, has influenced many branches of science, ranging from fundamental physics to polymer science, nano-materials to soft matter, and biological systems to energy materials. The neutron scattering facilities, available at the National Facility for Neutron Beam Research at the Dhruva reactor, are enthusiastically used by faculty and students of many universities and other academic institutions in the country. These facilities are made available to users through research projects funded by various agencies.

The inter-disciplinary character of this Theme meeting would definitely lead to fruitful deliberations and birth of new ideas amongst the participating scientists and young researchers, not only in the field of basic research, but also in the application sector. Advancement of research reactor utilization is the need of the hour and in this respect, this Theme meeting is a step forward in this direction.

I extend my warm greetings to all the delegates and wish a grand success of this “DAE-BRNS Theme Meeting on Strategic Planning for Enhancing Research Reactor Utilization (RRU-2022)”.

Md. Yusuf

(S. M. Yusuf)

प्रो. अम्लान जे. पाल
निदेशक
Prof. Amlan J. Pal
Director

विश्वविद्यालय अनुदान आयोग–परमाणु ऊर्जा विभाग वैज्ञानिक अनुसंधान संकुल
UGC-DAE CONSORTIUM FOR SCIENTIFIC RESEARCH
[Centres: Kolkata, Mumbai, Indore; Node: Kalpakkam]
प्रधान कार्यालय: विश्वविद्यालय परिसर, खण्डवा रोड़, इन्दौर–452001, भारत
Head Office: University Campus, Khandwa Road, Indore- 452001, India
Phone: 0731-2463945, 2463914; EPBX: 2463913, 2472201, 2762267
email: director@csr.res.in

Message

I am happy to know that the **DAE-BRNS sponsored Two-Day Theme Meeting on 'Strategic Planning for Enhancing Research Reactor Utilization (RRU-2022)'** is being jointly organized by the Reactor Group and Radiochemistry & Isotope Group of BARC in association with UGC-DAE CSR, Mumbai Centre and Society for Positron Annihilation and Nuclear Probes (SPAN) during May 6-7, 2022 at the DAE Convention Centre, Anushaktinagar, Mumbai - 400094 to commemorate "**Azadi Ka Amrit Mahotsav**". The Theme Meeting will provide a forum for interaction of scientists and engineers from BARC and researchers and potential users from non-DAE and private organizations including universities and Indian industries. I am happy that about 200 delegates will participate in this meeting. I noted that the technical program of RRU-2022 consists of keynote and invited talks by experts as well as contributed abstracts for oral and poster presentations by younger researchers from BARC, DAE, and faculties from academic institutes and universities, R&D personnel from industries, and research scholars.

UGC-DAE CSR, Mumbai Centre is already coordinating the use of neutron scattering facilities by researchers from colleges, universities, and other research institutes for the last three decades. More than 300 collaborative research schemes have been completed. About 70 research scholars have obtained their Ph.D. degrees with their theses containing a significant amount of neutron data recorded from Dhruva and/or CIRUS reactors. In addition to CRS projects, many one-time users have also accessed these neutron facilities. Neutron diffraction of crystalline and amorphous systems and small-angle neutron scattering on soft matters remained the conventional techniques envisaged by the researchers. Users are gradually applying other neutron techniques as well.

A national facility for Research Reactor Utilization could be a useful idea for effective and enhanced utilization of research reactors for various R&D works and societal applications including human resource developments.

I wish the theme meeting a grand success.

Amlan J. Pal.

(Amlan J. Pal)

Director and JC Bose National Fellow
UGC-DAE Consortium for Scientific Research
University Campus, Khandwa Road, Indore 452001
E-mail: director@csr.res.in

On lien from:
School of Physical Sciences
Indian Association for the Cultivation of Science
Kolkata 700 032, India

DAE-BRNS TWO-DAY THEME MEETING ON
Strategic Planning for Enhancing Research Reactor Utilization

(RRU-2022)

May 6-7, 2022

Preface

Research Reactors are made for multifaceted application like radioisotopes production for medical, industrial and agricultural uses, neutron beam research, material characterization, imaging etc. In India, the journey of research reactors was started with the commissioning of Apsara in August, 1956. At present, Bhabha Atomic Research Centre (BARC) at Trombay has state of the art research reactor facilities like Dhruva and Apsara-U for radioisotope production, as well as various R&D works. Since 1985, Dhruva, which is a 100 MW_{th} reactor, remains one of the potential sources of radioisotope production and neutron beam research. 2 MW_{th} Apsara-U, which went critical in 2018, is the latest entry into the list of Indian research reactors. There is a need, as well as scope, to enhance the utilization of neutrons from research reactors by various R&D communities and users from various organizations for their intended applications. In order to do so in an organized manner, a DAE-BRNS sponsored Two-Day Theme Meeting on "Strategic Planning for Enhancing Research Reactor Utilization (RRU-2022)" is going to be organized jointly by Reactor Group and Radiochemistry & Isotope Group during May 6-7, 2022 at DAE Convention Centre, Anushaktinagar, Mumbai-400094. The main objective of this theme meeting is aimed at interaction with the potential users of research reactors at BARC, other units of DAE as well as non-DAE government and private organizations including industries, research and academic institutes and Institutes/Universities that are pursuing projects under BRNS, UGC-DAE CSR, CSIR and other schemes. In this meeting, a strategic plan will be developed for long-term sustainability in terms of 'marketing' the R&D facilities associated with the research reactors.

Over the years, research reactors are serving as precursor for wide variety of radioactive isotopes for use in many fields, including nuclear medicine, industry, agriculture and research. Globally, the use of radioisotopes for medical purposes is rapidly increasing. Every year, more than 30 million examinations and cancer treatments are being carried out worldwide. Radionuclides, which are produced at research reactors, are used in both diagnostic techniques and therapeutic treatments.

Sealed radioisotope sources such as ^{60}Co, ^{192}Ir, etc find also applications in level gauging, density monitoring, thickness gauging, radiometric scanning, gamma radiography, topography, blockage detection, etc. Some radioisotopes are also used as radiotracers for leak detection in pipelines and heat exchanger, residence time distribution, etc. Like ^{60}Co used for radiation processing in industry such as sterilization of medical appliances, hygienization of waste products and so on.

Through beam holes, neutron beam lines are utilized outside the reactor for research in nuclear physics, condensed matter physics and material science. Thermal neutrons have a typical wavelength ~ 0.1 nm (nanometres), which is perfect for studying crystalline structures through diffraction because of its similar order of magnitude as the interatomic spacing inside the crystals. Also, the order of energy of thermal neutrons allows to measure atomic/molecular dynamics in the system. The high penetrating power of neutrons, along with their magnetic moment and their unique sensing capabilities of light atoms, make them a unique probe. The nuclear structure studies employing prompt (n,γ) reactions using thermal neutrons and fission fragment spectroscopy are being carried out to investigate the properties (shape and structure) of the neutron-rich fragment nuclei. Dhruva reactor is best suited for such studies.

The research reactors are also serving as the facility for studying and qualifying nuclear fuels, structural materials and components used in power reactors (vessels, internal equipment, neutron absorbers, etc). Being a reliable source of high intensity fluxes of neutrons, gammas, neutrinos and other types of radiation, these reactors are used to determine the effect of radiation on materials, components and instruments in view of their performance in radiation environment.

Neutron activation analysis (NAA) is a qualitative and quantitative analytical technique for the determination of trace elements in a variety of complex sample matrices. It can be performed in a variety

of ways depending on the element and its levels to be measured, as well as on the nature and the extent of interference with other elements present in the sample. This is worthy to mention here that many of the trace element identification can be directly linked to potential economic benefits. Therefore, NAA should be considered as a key component in the strategic plans of Dhruva and Apsara-U research reactors. In one of the Apsara-U thermal neutron beam tubes, PGNAA facility is also going to be set up. Typical applications of PGNAA include analysis of samples in geological and atmospheric sciences. The technique is useful for analysing elements like H, B, C, N, P, S, Cd, Pb, Sm, and Gd.

There are numerous industrial applications for research reactors. Few of them, which are very common, are mentioned below. Firstly, neutron radiography/tomography of various objects is used for non-destructive testing in the aeronautical and space industries, nuclear sector, etc. Such facility has been commissioned in one of the Dhruva neutron beam tubes. Secondly, positrons are considered suitable probe to detect low concentrations of defects in materials. Thirdly, neutron transmutation doping of silicon (NTD-Si) through the formation of ^{31}P in silicon ingot upon its irradiation under thermal neutron flux is considered superior than the conventional doping technique. This method is used to achieve an excellent distribution of resistivity in silicon ingots, which is desirable in manufacturing components for the electronics industry, such as diodes, thyristors etc.

Research reactors have also established their legacy in education field in terms of manpower training in various branches of science and engineering, including the nuclear power plant staff. For safety and accessibility reasons, low power research reactors like Apsara-U are best suited for such training activities, which include neutron measurements and radiological protection measurements and characterization of reactor cores by establishing the neutron-absorbing rod worth curve and measuring the temperature coefficient etc. This type of reactor also enables trainees to acquire knowledge and practical experience of operating a nuclear reactor like approach to criticality, divergence etc.

This book is a compilation of about 200 abstracts, including 16 invited talks and 10 oral talks, contributed to the theme meeting and covers a whole gamut of the different aspects of utilization of research reactors.

It is quite evident that a theme meeting of this scale would not be possible without the support from many corners. On behalf of RRU-2022 Organizing Committee and Technical Programme Committee, we would like to thank the members of Trombay Council, BARC; Reactor Group and Radiochemistry & Isotope Group. We wish to express our sincere gratitude to Dr. K. N. Vyas, Chairman, AEC & Secretary, DAE; Dr. A. K. Mohanty, Director, BARC; Dr. R. B. Grover, Chairman, BRNS for their support and encouragement. We are indebted to all Unit Heads of DAE; Group Directors and Head of Divisions of BARC; Dr. S. Adhikari, Head, SIRD, BARC and his colleague Dr. M. Singh; all Advisory, Organizing, Technical and Local Organizing Committee members for their continuous and whole-hearted support. We thank Shri H. G. Gujar, Chairman, LOC for his untiring efforts for making RRU-2022 a grand success. Thanks are due to all Distinguished Guests, Session Chairs etc. We thank Director, DCSEM; Security Officers (DAE/BARC/DCSEM), Manager, DAE Convention Centre; AO (III), BARC Guest House for their cooperation. Thanks are also due to all Office and Technical Staff of Chairman, AEC; Director, BARC; BRNS Secretariat; Chairman, BRNS; Reactor Group; Radiochemistry & Isotope Group and concerned Divisions of BARC towards successful organization of RRU-2022.

Looking forward for fruitful scientific discussion in the RRU-2022 Theme Meeting.

Dr. Tej Singh
Convener, RRU-2022

Dr. Raghunath Acharya
Co-convener RRU-2022

Shri Kunal Chakraborty
Chairman, Technical Programme Committee, RRU-2022

DAE-BRNS TWO-DAY THEME MEETING ON
Strategic Planning for Enhancing Research Reactor Utilization
(RRU-2022)

DAY-1 Friday, May 06, 2022	
8:00-9:30	Registration of Participants
9:30-10:15	**Inaugural Function**
10:15-11:00	**Keynote Talk-1:** *Neutron Beam Research* **Dr. R. Chidambaram, Former Chairman, AEC, Former Secretary to the Govt. of India, DAE, Former Principal Scientific Adviser to the Govt. of India**
11:00-11:45	**High Tea**
11:45-13:00	**Technical Session I:**
11:45-12:10	**Invited Talk-1:** *Irradiation and experimental facilities at research reactors of BARC, Mumbai* **Shri Kunal Chakrabarty, BARC**
12:10-12:35	**Invited Talk-2:** *Reactor Physics Aspects of Research Reactor Irradiation Facilities at BARC* **Dr. Tej Singh, BARC**
12:35-13:00	**Invited Talk-3:** *Production and radiochemical processing of radioisotopes for use in healthcare utilizing research reactors at Trombay - Present scenario and future prospects* **Dr. S. Chakraborty, BARC**
13:00-13:45	**Lunch Break**
13:45-15:00	**Technical Session II:**
13:45-14:10	**Invited Talk-4:** *Clinical applications of indigenous ^{177}Lu: a decade of experience* **Dr. Sandip Basu, BARC**
14:10-14:35	**Invited Talk-5:** *Neutron Imaging for Aerospace Applications – past, present & future* **Dr. M. Nallaperumal, ISRO, Thiruvananthapuram**
14:35-15:00	**Invited Talk-6:** *Applications of Radioisotopes in Industry* **Dr. H. J. Pant, BARC**
15:00-16:30	**Poster Session-I** **Tea (Floating)**
16:30-18:30	**Technical Session III:**
16:30-16:55	**Invited Talk-7:** *Physics using Neutrons at Dhruva* **Dr. S. M. Yusuf, BARC**
16:55-17:20	**Invited Talk-8:** *Utilization of Neutron Scattering Facilities at BARC by Indian Universities and Institutes* **Dr. P. D. Babu, UGC-DAE CSR**
17:20-18:30	**Users' contributed presentation:**

DAE-BRNS TWO-DAY THEME MEETING ON
Strategic Planning for Enhancing Research Reactor Utilization
(RRU-2022)

DAY-2 Saturday, May 07, 2022	
9:15-11:15	**Technical Session IV:**
9:15-10:00	**Keynote Talk-2:** *Medical Applications of Radioisotopes* **Dr. Sudeep Gupta, ACTREC**
10:00-10:25	**Invited Talk-9:** *Basics of Neutron Imaging and its applications* **Dr. Y. S. Kashyap, BARC**
10:25-10:50	**Invited Talk-10:** *Functional Testing of Neutron detectors: Role of Research Reactors* **Dr. V. Balagi, BARC**
10:50-11:15	**Invited Talk-11:** *Chemical Characterization of Materials by NAA and PGNAA utilizing Research Reactors at BARC* **Dr. R. Acharya, BARC**
11:15-11:35	**Tea Break**
11:35-13:15	**Technical Session V:**
11:35-12:00	**Invited Talk-12:** *Utilization of Research Reactors for testing of Fusion Reactor Materials* **Dr. Shashank Chaturvedi, IPR**
12:00-12:25	**Invited Talk-13:** *Applications of Radioactive Particle Tracking Technique for Flow Visualization in Industrial Process System* **Dr. Rajesh Upadhyay, IIT (BHU)**
12:25-12:50	**Invited Talk-14:** *Enhancing the Efficiency of Chemical Processes: The Triad of Radiotracing, Radioactive Particle Tracking (RPT) And Computational Fluid Dynamics (CFD)* **Prof. Shantanu Roy, IIT Delhi**
12:50-13:15	**Invited Talk-15:** *Nuclear structure studies with thermal neutron induced reactions* **Dr. Bency John, BARC**
13:15-14:00	**Lunch Break**
14:00-16:00	**Technical Session VI:**
14:00-14:25	**Invited Talk-16:** *Ionizing Energy for Food Security, Safety and Promotion of International Trade of Agri-produce* **Dr. S Gautam, BARC**
14:25-15:50	**Users' contributed presentation:**
15:50-17:15	**Poster Session-II** **Tea (Floating)**
17:15-18:15	Panel Discussion
18:15-18:30	Valedictory session

KEYNOTE TALKS

Neutron Beam Research

Dr. R. Chidambaram

Former Director, Bhabha Atomic Research Centre, India
Former Chairman, AEC, Former Secretary to the Govt. of India, DAE,
Former Principal Scientific Adviser to the Govt. of India

Speaker Information

Dr. Rajagopala Chidambaram became the Director of the Bhabha Atomic Research Centre(BARC) in 1990. He was Chairman, Atomic Energy Commission from 1993 to 2000. He was the Principal Scientific Adviser to the Govt. of India and the Chairman of the Scientific Advisory Committee to the Cabinet from 2001 to 2018. He is presently the DAE-Homi Bhabha Professor in BARC.

Dr. Chidambaram has made important contributions to many aspects of our nuclear technology. He has D.Sc Degrees (h.c) from thirty Universities from India and abroad. He has more than 200 research publications in refereed journals and all his research work has been in India.

He was Chairman of the Board of Governors of the IAEA during 1994-95. During 1990-99, he was a member of the Executive Committee of the International Union of Crystallography, the last three years as its Vice-President. He has been Chairman, Board of Governors of IIT Bombay (1994-97) and of IIT Madras (2008-2011) and Member, Space Commission (2009-2014). Dr. Chidambaram is currently Chairman of the Board of Governors of IIT, Jodhpur and IIT, Delhi. He is also a Honorary Visiting Professor in the Department of Physics, Banaras Hindu University.

Dr. Chidambaram is a Fellow of all the major Science Academies in India and also of the National Academy of Engineering and the The World Academy of Sciences Trieste (Italy). He has received many awards and honours, notable among them are the C.V. Raman Birth Centenary Award of the Indian Science Congress Association in 1995, the Distinguished Materials Scientists of the Year Award of the Material Research Society of India (MRSI) in 1996, R.D. Birla Award of the Indian Physics Association in 1996, Homi Bhabha Lifetime Achievement Award of the Indian Nuclear Society(2006), The Lifetime Achievement Award of the Indian National Academy of Engineering (2009) and the C.V. Raman Medal of the Indian National Science Academy (2013). Lifetime Achievement Award of A.P. Akademi of Sciences (2014), Lifetime Achievement Award of the

Council of Power Utilites(2014). **Dr. Chidambaram was awarded the Padma Vibhushan, the second highest civilian award in India, in 1999.**

His initiatives as Principal Scientific Adviser to Government of India, include the setting up of the Core Advisory Groups for R&D in various technology sectors, the creation of RuTAG (Rural Technology Action Group) centered in 7 IITs, the establishment of SETS (Society for Electronic Transactions and Security), helping nucleate the Centres of Excellence in Nanoelectronics, the National Knowledge Network and initiating an R&D programme on the

design of the Advanced Ultra Supercritical Thermal Plant, through a consortium of IGCAR, BHEL and NTPC, which has now been completed.

Medical Applications of Radioisotopes

Dr. Sudeep Gupta, MD, DM

Professor of Medical Oncology, Director ACTREC (Advanced Centre for Treatment, Research and Education in Cancer), Tata Memorial Centre, Navi Mumbai-410210, India

Diagnostic and therapeutic radioisotope based techniques have gained increasing importance in cancer related healthcare in recent years. While radio-iodine scans and treatment of thyroid cancer is well known, many other applications of radioisotopes are now in routine clinical use. Increasing sophistication of techniques of conjugating radioisotopes to targeting molecules has enabled the new age radiopharmaceutical drugs to enter the molecular age of precision medicine for imaging, treatment and sometimes for both. An excellent example of such molecular targeted imaging is PSMA-PET for prostate cancer.

Radioimmunotherapy (RIT) is a technique wherein a radioisotope and a monoclonal antibody are administered as a conjugate with an intention to achieve synergy for tumor kill. This modality emerged about two decades ago, and at present there are two such radioimmunoconjugates (RIC) which are commercially available for human use – Bexxar and Zavelin for the treatment of Non Hodgkin's Lymphoma (NHL). Many investigators have now tried to develop RICs for other indications including breast cancer. While RICs offer several advantages, a single or limited dose administration being the most appealing, the complexities associated with formulating the conjugate as well as the cost had hitherto precluded widespread use of this modality in India. In India, Bhabha Atomic Research Centre (BARC) has the skill and expertise to make these conjugates. Coupled with the advent of biosimilars of important monoclonal antibodies such as rituximab and trastuzumab, the time is now most appropriate for the development of indigenous RICs. Tata Memorial Centre in collaboration with BARC has undertaken this project. Biodistribution studies in xenograft models of NHL and breast cancer has been completed. 131I-Rituximab and 131I-Transtuzumab RICs were evaluated in two separate studies using Raji cell xenograft (CD20+) bearing nude mice and MDA-MB-361 cell (Her2+) xenograft bearing NOD-SCID mice, respectively. More recently, human study of Lu-trastuzumab has been started in TMC.

Other radiopharmaceutical including alpha emitters will also be discussed during the presentation.

Speaker Information

Dr. Sudeep Gupta is the Professor of Medical Oncology, Director ACTREC (Advanced Centre for Treatment, Research and Education in Cancer), Tata Memorial Centre, Mumbai. He has done MBBS, MD and DM from All India Institute of Medical Sciences, New Delhi (completed 2000). He has been a faculty member in the Department of Medical Oncology at Tata Memorial Centre since June 2001. Dr. Gupta is an Internationally renowned breast and gynecological cancers oncologist.

He is a prolific clinical researcher who is actively involved in planning, organizing, conducting and analyzing Phase I, II and III clinical trials . He has been the Principal Investigator or Co-investigator in more than 120 trials. His special interest lies in breast and gynecological cancers and clinical genomics. His primary research themes include implementation science including access to medications, guideline development, testing concepts and technology in clinical trials, innovative therapeutic strategies, toxicity and quality-of-life studies, pharmacokinetics and translational studies involving next-generation sequencing technology. Dr. Gupta has published more than 250 papers in peer reviewed journals. He has been member of several national and international committees and taskforces of DBT, DST, DAE, ICMR, NITI, ESMO, and others.

INVITED TALKS

Irradiation and experimental facilities at research reactors of BARC, Mumbai

Vikas Jain*, Sanjit Pal, Prasit Mondal, Kunal Chakrabarty

Reactor Group, Bhabha Atomic Research Centre, Mumbai-400085, India
(**Corresponding author email:* vikasj@barc.gov.in)

1.0 Introduction

Research reactors have played a vital role in the development of nuclear technology in the country. The availability of high flux of neutrons in the research reactors facilitate basic and applied research in the field of chemistry, physics and biology, production of radioisotopes for application in the fields of medicine, agriculture and industry; irradiation and testing of reactor materials and nuclear fuels; neutron radiography and neutron activation analysis.

2.0 Inception and Developments in Research Reactor Program

The Indian nuclear program started with the building of a 1 MW_{th} pool type research reactor "Apsara' in the year 1956 at Bhabha Atomic Research Centre (BARC). A 40 MW_{th} reactor 'Cirus' and a low power test reactor 'Zerlina' for physics studies of future reactors were subsequently set-up during 1960 and 1961 respectively. Apsara & Cirus was utilized in a number of ways during its 50 years of safe operation and is presently under the process of decommissioning. Zerlina was decommissioned after carrying out required reactor physics studies.

As the experienced gained in design and operation of thermal research reactors was being fruitfully used to launch power program based on Pressurized Heavy Water Reactors (PHWRs), based on natural uranium-heavy water system, work was initiated to study the reactor systems based on Plutonium and Uranium-233 and various aspects of Thorium utilization. Towards this, construction and commissioning of Purnima series of reactors were undertaken during the period 1970-1992. Experiments were carried out to understand the physics of plutonium fuelled fast reactors as well as Uranium-233 fuelled thermal reactors. These experiments provided a thrust to the development of technology of Plutonium fuel fabrication, separation of Uranium-233 from irradiated Thorium, reactor control instrumentation etc. After required experimental studies these reactors were decommissioned.

Having gained expertise in diverse scientific and engineering discipline, decision to build 100 MW_{th} natural Uranium fuelled, heavy water cooled and heavy water moderated research reactor Dhruva was taken in early seventies and successfully commissioned in year 1985 through totally indigenous efforts. Dhruva is presently a workhorse for utilizing technologies related with high neutron flux.

India has abundant resources of Thorium as against limited resources of Uranium. Hence, in order to meet the energy needs of our country a new reactor concept with Thorium fuel cycle is being developed. This will provide long-term energy security by using available nuclear fuel resources in an optimal manner. To optimize and confirm the physics design parameters of such an Advanced Heavy Water Reactor (AHWR) a 'Critical Facility' for lattice investigations was commissioned in BARC in year 2007. The large Critical Facility is also ideally suited for Physics studies of loosely coupled cores, such as 700 MWe PHWR. The Critical Facility is a tank type, heavy water moderated reactor with natural uranium metal clusters. The reactor is designed for a nominal fission power of 100 Watt and an average flux of 10^8 $n/cm^2/sec$. For experiments the fuel clusters are suspended from lattice girder assemblies into the reactor vessel. The girder assemblies have the flexibility for configuring the reactor core at the designated pitch. With this feature, a core with precise geometry at the desire pitch can be achieved.

Unlike Dhruva reactor, Critical facility presently utilized for core physics studies with fuel assemblies warrantable in variable pitches.

Simple design of Apsara reactor, its vast utilization and its aging related issues called for construction of similar facility with some enhanced features as per operating experience with the old reactor. Accordingly, Apsara-U (U stands for upgraded) was designed and commissioned in the year 2018. The new reactor with increased flux is now ready for all challenges in terms of its utilization.

3.0 Operating Research Reactors at Trombay

Presently research reactor Dhruva, Apsara (U) and Critical Facility at Trombay complex are operational and meeting demands of a number of researchers in field of basic sciences & material testing. Apsara (U) and Dhruva have additional challenge to meet supply of radioisotopes for medical and industrial use. Important design aspects, facilities and utilization of these reactors have been explained below.

3.1 APSARA-U

Apsara-U is a 2 MW_{th} pool type research reactor, made critical on 10th September 2018. The reactor has a maximum thermal neutron flux of 6.1×10^{13} n/cm^2/sec and fast neutron flux of 1.4×10^{13} n/cm^2/sec. It uses indigenously developed low enriched uranium; plate type fuel made of Uranium Silicide dispersed in aluminum matrix. Light water is used as moderator and coolant and Beryllium Oxide as a reflector. The core is cooled by forced circulation of de-mineralized water while shutdown cooling is through natural circulation of coolant. A one meter thick thermally stratified layer of hot water at about 5°C temperature more than the bulk pool water temperature maintained at the top of bulk water which helps to keep the pool top radiation field practically negligible. This is first of a kind system for a reactor in India.

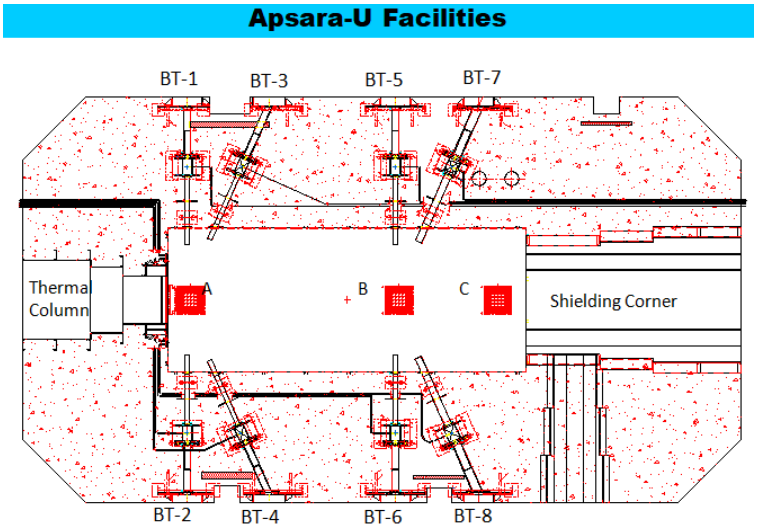

3.1.1 Facilities at Apsara-U

- Apsara-U is a versatile facility with flexibility of operating the reactor at three different positions A, B & C in the reactor pool, with easy access to the core; facilitating different experiments.
- There are eight beam tubes in position A and B of reactor core, where experimental facilities are being set up by researchers. These include facilities for neutron imaging and depth profile of different materials, prompt gamma neutron activation analysis, single-crystal alignment and neutron detector testing etc.
- Thermal column located at position A will be used for testing of various types of neutrons and gamma detectors as well as for neutron activation analysis. Graphite blocks are stacked in Thermal Column. It has 4 experimental holes, where maximum thermal neutron flux varies from 1.0×10^8 to 1.0×10^9 n/cm^2/sec (Cadmium ratio > 2000).

- Shielding experimental facility is located at position C with neutron flux ~10^{10} n/cm^2/sec, where shielding designs can be validated by carrying out experiments over wide energy ranges.
- There are 1 in-core and 7 out-of-core irradiation positions. Maximum 110 samples can be irradiated at a time in reactor core.
- Special tray Rod assemblies are provided in the reactor for production of radioisotopes. Each tray Rod can accommodate 15 capsules of target material.

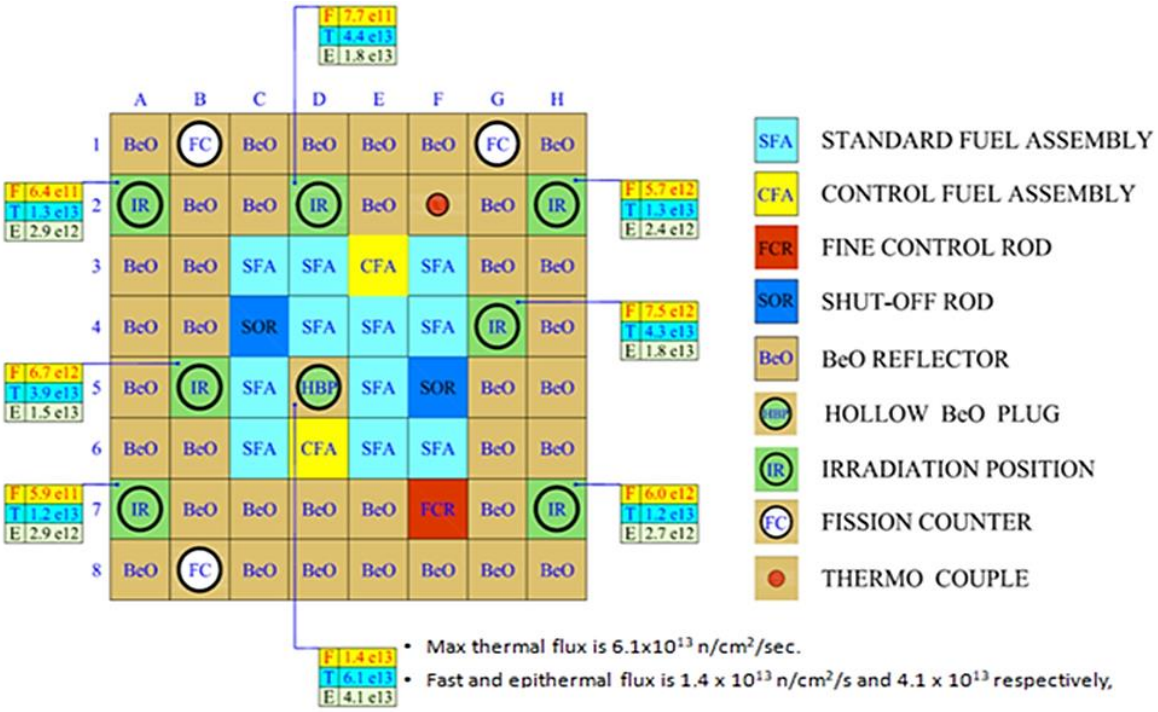

Core Configuration & Neutron Flux Distribution in Apsara-U

3.1.2 Utilization of Apsara-U

- The reactor is operated on a 24 x 7 basis and mainly utilized for production of radio isotopes. High specific activity Cu-64 in no-carrier added form was developed from Zn-64 by irradiation, which is a very promising isotope with its application in theranostics. After extensive trials, it has been approved for human use by regulator. Production Trials of Tc-99 through fission molly route is underway.
- It offers fast neutron flux (> 1 MeV) of about 1.4×10^{13} n/cm^2/sec, which can be utilized for material irradiation for nuclear technology.
- Feasibility of neutron transmutation doping of silicon (NTD-Si) is being explored in Apsara-U. A number of trial irradiations with small size silicon samples were successfully carried out to gather practical experience in various stages of the doping of silicon.
- Production of fission molly using fuel mini-plates and using fuel as the target is being planned.

3.2 CRITICAL FACILITY

Critical Facility (CF) is a low power reactor built as a part of the over-all technology development program to validate the physics design of the thorium based Advanced Heavy Water Reactor (AHWR). Salient design features of the reactor are:

- Nominal Power : 100 Watt.
- Thermal Neutron Flux : ~ 10^8 n/cm^2/sec.
- Reactor Tank : 330 cm Φ, 500 cm ht, vertical, cylindrical, made of Aluminum.
- Lattice pitch : Variable (minimum 215 mm)
- Moderator : Heavy water
- Shutdown system : 6 Cadmium shut-off rods & Moderator Dump

3.2.1 Facilities at CF:

Although the main objective of AHWR-CF is for conducting experiments and validating the physics design parameters of AHWR, the reactor has facilities in graphite reflector for sample irradiation, testing of neutron detectors etc.

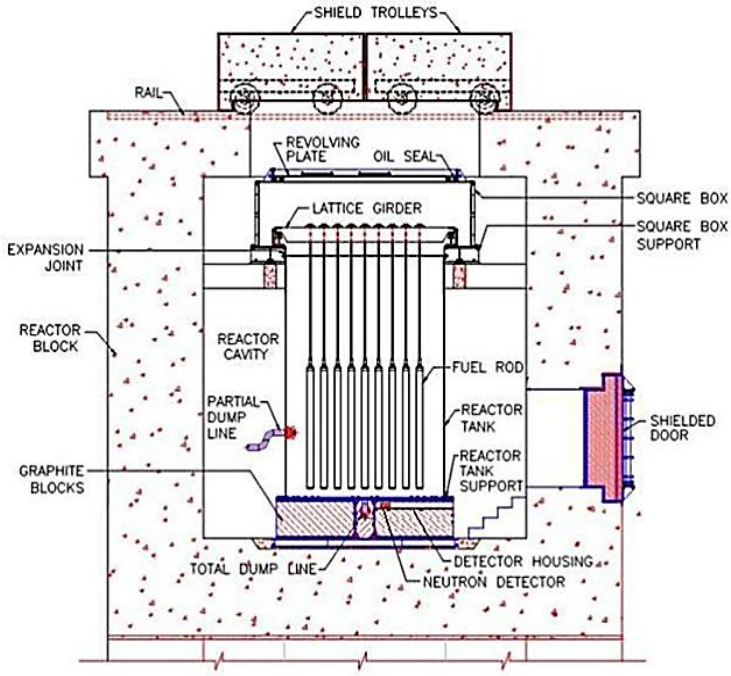

- The graphite reflectors at the bottom of the reactor houses two cuboidal shape positions for activation of various samples. The cuboidal positions have dimension of 150 cm × 10 cm × 10 cm. Thus, a large space is available for irradiation of irregular samples having bigger size. Maximum thermal neutron flux at irradiation position is 5 × 10^7 n/cm^2/sec. Installation and removal of the samples is manual and activated sample scan be availed within few minutes after activation for subsequent analysis.
- The graphite reflectors placed beneath the reactor tank has facilities for testing of neutron detectors and also to activate samples (Soil, geological rock, biological sample and metallic alloys) for neutron activation analysis (NAA). Both, the calibration of the neutron detectors and NAA are ongoing activities carried out almost on routine basis.
- Large size samples (up to 500 g) after packing in polythene can be activated in graphite reflector position. Higher masses of the samples (1 to 500 g) are used to obviate the error due to inhomogeneous distribution of analytes in small sub samples.

3.2.2 Utilization of CF:

The reactor is being utilized for validating the physics design parameters of AHWR Type Fuel. Reactor Physics Design Division (RPDD) in coordination with Reactor Engineering Division (RED) has carried out various experiments both in the standard reference core and extended core (by installation of six additional fuel cluster in standard core). Following is a list of important experiments carried out in the Critical Facility.

3.2.2.1 Reactor Physics Studies

- Reactor power calibration by absolute flux measurement by activation method.
- Axial flux distribution measurements on the central fuel cluster.
- Gold Cadmium-ratio measurement at infinite dilution.
- Measurement of level coefficient of reactivity of standard reference core by positive period method.
- Fine structure neutron flux measurement inside the central lattice cell of standard reference core.
- Gamma scanning of Natural. Uranium and thorium pin irradiated at central location of E5 cluster in reference core.
- Critical height measurement with various types of experimental clusters, [NU, ThO_2] Mixed Pin, Th-Pu (1%) Six Pin Cluster, Th-LEU Six Pin MOX Cluster.
- Measurement of the Moderator Temperature Coefficient of Reactivity (MTCR).
- Measurement of Westcott neutron spectrum parameters in reference core of AHWR-Critical Facility, using Lu and Cu foils.
- Axial, thermal and epithermal flux profile measurement inside (NU-ThO_2-NU) sandwich Cluster.
- Photo-neutron decay studies in standard reference core
- Commissioning of Online Flux Mapping System of AHWR-CF.
- Sub-criticality measurement using neutron noise method.
- Void coefficient with one (Th-1%Pu) MOX cluster in the extended reference core using water and HDPE as coolant simulating various voiding conditions.

3.2.2.2 Detector Testing:

- On an average nearly 30 neutron detectors were tested annually.
- Various types of neutron detectors like Fission chamber, Boron lined proportional counters, Helium-3 Detectors, Gamma compensated Ionization chamber, Micro fission Chamber, Transmission line fission chamber, Uncompensated Ionization chambers, Pre-start up equipment for Project-B with B-10 Proportional counters for different reactors were tested in CF. The testing of the detectors involves
    - Checking of the discriminator bias characteristics, HV characteristics, linearity of the flux measurement range, neutron sensitivity, gamma discrimination, long term count rate stability and response time etc.
    - Repeatability of detector response, measurement of count rate loss at high flux
    - Performance checking immediately after exposure to high fluence & at high flux etc.

CF is mainly used for characterizing the detector performances of pulse detectors as the maximum flux at the detector location is of the order of 2×10^7. For DC detectors, the full measurement range

may not be covered due to limited neutron flux at these locations. The DC detectors are checked for their response and initial signal calibration characterization.

3.2.2.3 Sample Irradiation for neutron activation analysis

Around 150 assorted samples were activated yearly in the graphite reflector. Large and irregular shape samples are being irradiated for neutron activation analysis in Graphite reflector region at bottom of the reactor.

3.2.3 Special Campaign at CF

Besides the above-mentioned experiments, following are a few important activities/experiments conducted in CF:

- Worth measurement of Hafnium absorber section of SOR and CSR for new Apsara-U reactor before installation in the Apsara-U reactor.
- Activation of DM water, dye and absorbent used in DP testing of welded joints for analysis of Chlorine and Br-82.
- Measurement of fission products of Uranium Silicide, type of fuel used in Apsara-U reactor.
- Sensitivity checking of modified critical accident dosimeter badge.
- Activation of medicine samples to see radiation damage on the medicine carried by astronauts during long term space missions.
- Activation of articles for special cores for testing and commissioning of the axial& integral gamma scanner and establish the procedural steps for bulk gamma scanning of the activated articles are such cores.

3.3 DHRUVA

Dhruva is a 100 MW_{th} research reactor using natural metallic Uranium fuel and heavy water as coolant, moderator and reflector. Maximum thermal neutron flux available at the rated power is 2.0 x 10^{14} n/cm^2/sec. The reactor core consists of a cylindrical stainless-steel vessel that is placed vertically in a light water filled Stainless Steel lined vault surrounded by 3 meter thick heavy concrete biological shield. There are a total of 146 lattice positions in the reactor vessel, out of which normally 128 positions are used for loading the fuel assemblies and 9 positions contain the cadmium shut-off rod. The remaining positions are used for isotope production and experimental facilities.

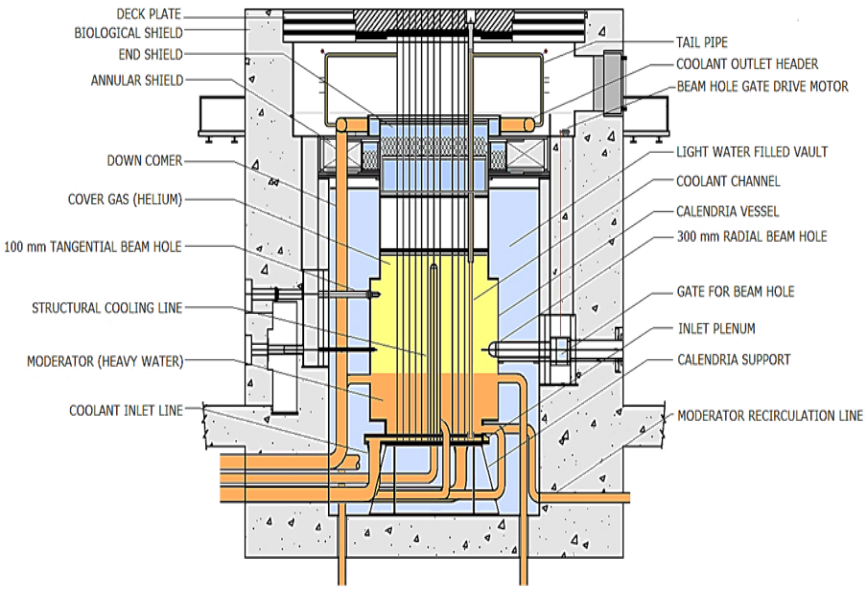

General arrangement of Dhruva Reactor

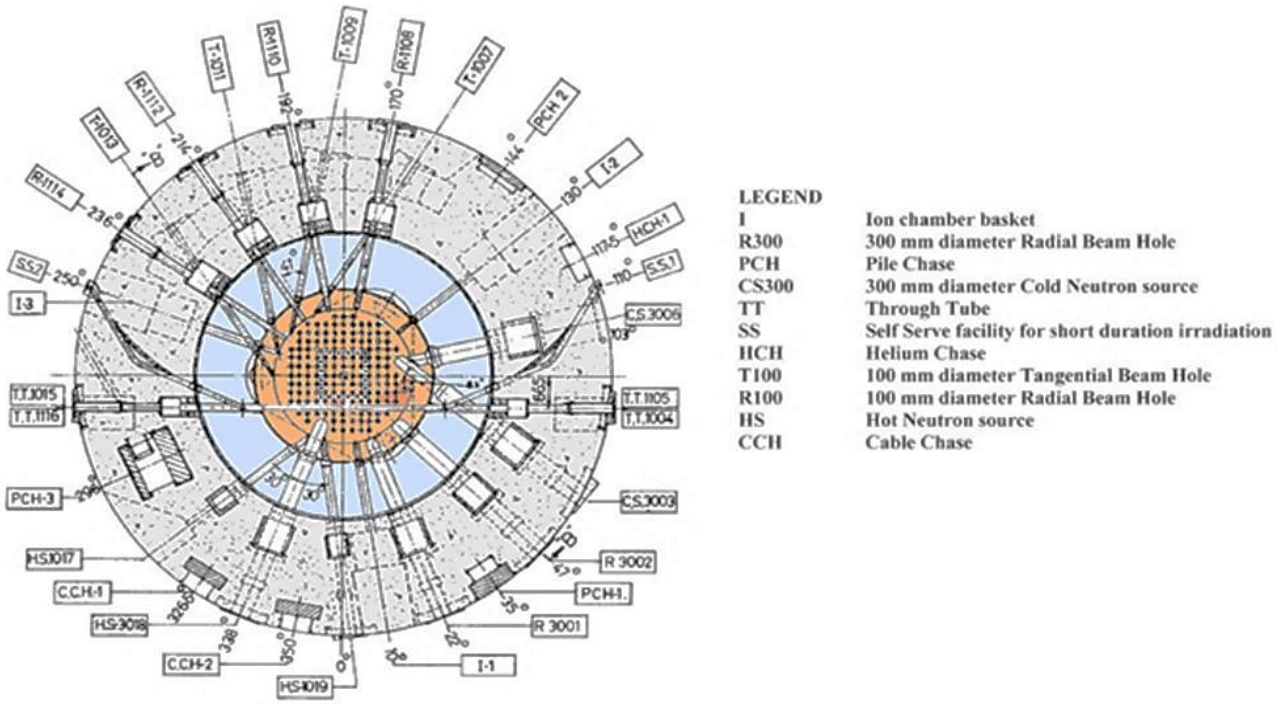

Cross-section of Dhruva Pile

In last 35 years of operation, Dhruva has been extensively used for basic research in neutron beam technology, radio -isotope production and neutron activation analysis. Besides such utilization, some of the fuel and other in-core positions have also been used for carrying out certain specific engineering experiments for material and special fuel testing. Reactor has been also been utilized for man power training in the field of nuclear technology.

3.3.1 Important features of Dhruva for its utilization*;*

For the prospective of Dhruva utilization, most important feature of the research reactor is its large core size, high thermal neutron flux (Max 2×10^{14} n/cm^2/sec), availability of excess reactivity in the core and feasibility of installation of experimental assemblies in any coolant channel. High neutron flux not only facilitates production of isotopes of higher specific activity in bulk, but also results in high neutron flux in beam tubes (~10^9 n/cm2/sec at pile face) for neutron beam utilization. Excess core reactivity permits a verity & bulk of material irradiation in the core. Each of the coolant channels in Dhruva is instrumented. Thus, any experimental assembly (with similar geometry of Dhruva fuel assembly and meeting specific safety requirement) can be installed in any fuel channel for material testing, special fuel irradiation or isotope production. Coolants flow though such experimental assemblies can be suitably controlled to meet thermal-hydraulics requirements and to limit vibration.

3.3.2 Irradiation facilities at Dhruva

3.3.2.1 Isotope Tray Rod

These provide facility for producing fairly large quantities of radioisotopes after appropriate period of irradiation at high flux levels. There are two tray rods for regular isotope production. Each tray rod can handle 90 capsules containing targets enclosed in cold weld standard aluminum Can (capsules of 22 mm diameter and 42 mm height). Three numbers of such aluminum containers are kept around the central rod to form a tier. Each tray rod assembly has 30 such tiers. The tube has a window in front of each tier. The central rod can be rotated to bring any of the three tiers for capsule removal and reloading fresh capsules in a shielded cell called tray rod Facility (TRF) with master slave manipulator. The tray rods are heavy water cooled.


Al Capsule for Isotope production

The demand for production of radio isotopes is to be met on a weekly basis. Earlier, for loading and unloading of samples to and from the tray rod, the reactor had to be shut down. To reduce the frequency of reactor shut downs on this account, further development work was carried out to enable the tray rod operations with reactor operating at high power. Regular irradiation in on-power tray rod was started at H-07 pile position since 1999. A second on-power tray rod was installed in K-09 pile position with provision for irradiation of Xenon gas in August 2008.

To meet the bulk demand of radioisotopes of higher half-life, additional isotope tray rods in fuel position (commonly called as off power tray rod) and Slug rods were also installed in to Dhruva core time to time. These tray rod /Slug rod are meant for long term (months to years) irradiation of target material and are handled during main coolant pumps in off condition only. The designs of such tray rods are similar to standard tray section to accommodate standard aluminum capsule for irradiation as in case of On-power tray rod. Slug rods can have specific design to accommodate slugs of target material (e.g. cobalt pencils) and coolant path. These assemblies can be installed in any coolant channel after certain modification in processing circuit of flow and temperature instrumentation as flow requirement for such assemblies are lesser as compare to channel containing standard fuel assemblies.

In past a number of tray rods in Fuel position and slug rods (such as Cobalt slug rods, antimony rods, Zircoally rods etc) were installed in pile on specific requirements.

A vast number of radioisotopes for application in healthcare, industries, agriculture and research are produced in Dhruva. Refer annexure-1 showing detail of important isotopes produced in Dhruva. For medical applications, presently, Dhruva is producing radioisotopes for meeting 40-50% demand of I-131 (annual production ~1200-1500 Ci), 10-15% demand of Mo-99 (annual production ~1000 Ci), 75-80% demand of Lu-177 (annual production ~500Ci) and 100% demand of Sm-153 (annual production~250-300 Ci) and I-125 (annual production 20-25 Ci) of our country.

3.3.2.2 Pneumatic Carrier Facility (PCF)

The facility is specially meant for the irradiation of short-lived samples which require minimum transit time between the completion of irradiation and counting. This facility has provision for shooting the sample into the core for irradiation and receiving back the same from a laboratory located outside reactor building. In this facility, the samples are encapsulated in 25 mm diameter and 38 mm long ethylene propylene capsules and are pneumatically transported to a carrier rod in the reactor from the fume hood located in attached laboratory. Samples are received back in the same fume hood after the required period of irradiation. Irradiation of samples is fully automated. The facility provides a neutron flux of the order of 5 x 10^{13} n/cm^2/sec at the irradiation location at a reactor power of 50 MW. The facility is mainly used for neutron activation analysis. This technique provides not only rapid quantitative simultaneous analysis down to ppb level or below but also provides critical validation support to other techniques. The growth and success have been mainly due to the availability of research reactors with high neutron flux and to the advances in high neutron spectrometry systems. A wide variety of samples were irradiated in PCF for application in material sciences, environmental and life sciences, forensic science and archaeology. PCF has also been used for determination of uranium by solid-state nuclear track detector (SSNTD) using fission track analysis (FTA).

View of PCF room and the control consol

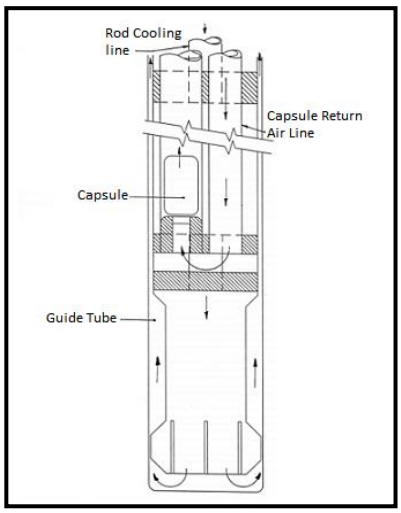

3.3.2.3 Self-Serve Facility

Self-serve facility is meant for producing smaller quantity of radioisotopes at relatively lower flux levels and for irradiation of samples with intermediate half-life for NAA. This irradiation can be carried out without affecting the reactor operation for a pre-determined time and is ideally suited for the production of short-lived radioisotopes. The irradiation period may be of few hours to couple of days as per users requirement. The Self-Serve unit is located at upper through tubes. At present one of Self-Serve unit is operational and being utilized for samples irradiation. The Self-Serve unit has five irradiation locations in reflector region of the Core. An Aluminum capsule containing target material is enclosed inside a spherical ball as shown in figure. The ball is rolled into the irradiation location under gravity and at the end of irradiation the ball is rolled out into a lead shielded flask. Refer diagram below showing setup of Self-Serve unit for sample movement. Further extraction and handling of sample is carried out in the tray rod facility hot cell.

SELF SERVE BALL WITH CAPSULE

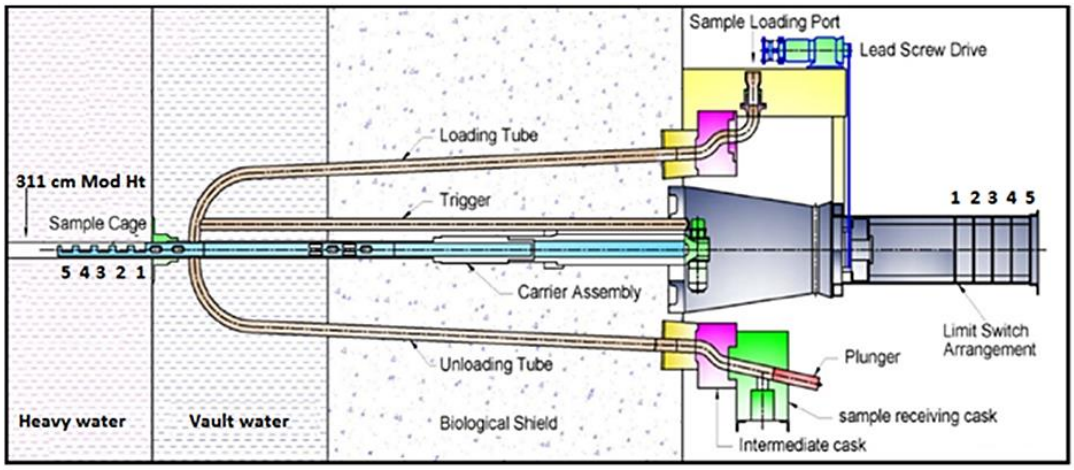

The facility provides a neutron flux of the order of 5 x 10^{12} n/cm^2.sec at the irradiation location. At three irradiated position the neutron flux was measured to be as follows at ~100 MW_{th} operation of reactor with moderator level of 327 cm

Position	Measured Thermal Flux
SS2-1	3.23 E +12
SS2-2	9.16 E +12
SS2-3	1.49 E +13

A number of rock and glass samples has been irradiated in Self-Serve for NAA.

3.3.2.4 Tray Rod facility (TRF)

For loading and unloading of isotope capsules from tray rod, a hot cell (commonly called tray rod facility) has been provided in Dhruva. The tray rod facility is a cubical cell of inner dimensions 2mx2mx3m. The hot cell is partly lined with 6mm SS sheet and can handle a maximum activity of 2x10^5 Ci of Cobalt-60. The ventilation provided in the cell ensures a negative pressure of 4m of WC. The cell is equipped with through-the-wall type master slave manipulator (MSM) having slave arm in hot cell and master arm in the control station. Radiation shielding window (RSW) has been provided in hot cell for handling various radio-isotopes with MSM. The construction of the window is such that it has one alpha protection glass and five shielding glasses of different thickness, size and density for protection from gamma.

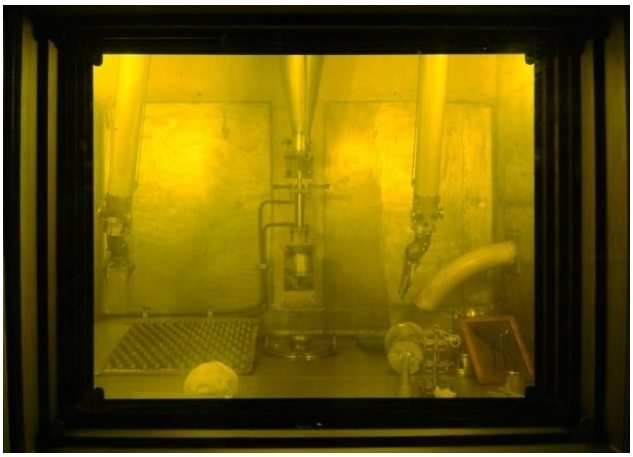

Radiation Shielding Window

3.3.2.5 Neutron Beam Holes in Dhruva

High intensity beams of continuous neutrons are produced by fission in the nuclear reactor Dhruva. Among the important uses of neutron beams from research reactors are their applications in basic research in the field of atomic physics & chemistry, material science research, nuclear fission investigations and neutron radiography. A large number of horizontal beam hole facilities have been provided in Dhruva reactor for neutron beam experiments as also for sample irradiations. Such beam neutrons are used in a variety of ways by means of sophisticated on-line computer-controlled instruments to investigate engineering, metallurgical, chemical, biological and other materials to determine characteristics pertaining to crystalline, magnetic structures, nature of atomic motions etc on which material properties crucially depend. In the figure various

beam tubes and their utilization by the researchers has been shown. In Dhruva, the following beam holes have been provided for experimenters:

- Four 100 mm diameter tangential beam holes
- Four 100 mm diameter radial beam holes
- Two 300 mm diameter radial beam holes
- Two through-tubes of 100 mm diameter providing four experimental ports.
- One 300 mm diameter beam hole, originally designed for installation of a cold neutron source, with a rectangular satellite port for installation of neutron guides.
- One 300 mm diameter beam hole originally designed for installation of a hot neutron source with a provision of two 100 mm diameter satellite ports for beam extraction.

The provision of tangential beam holes and through tubes for neutron beams are new features, built into the experimental facilities at Dhruva. Tangential beam holes provide better neutron to core gamma discrimination which is helpful to conduct experiments using neutron beam with reduced gamma flux from core. 100mm beam holes are used by for Solid state physics experiments related to neutron scattering using instrumented setup near pile face. The flux at pile face at $100MW_{th}$ operation is 10^9 n/cm^2/sec.

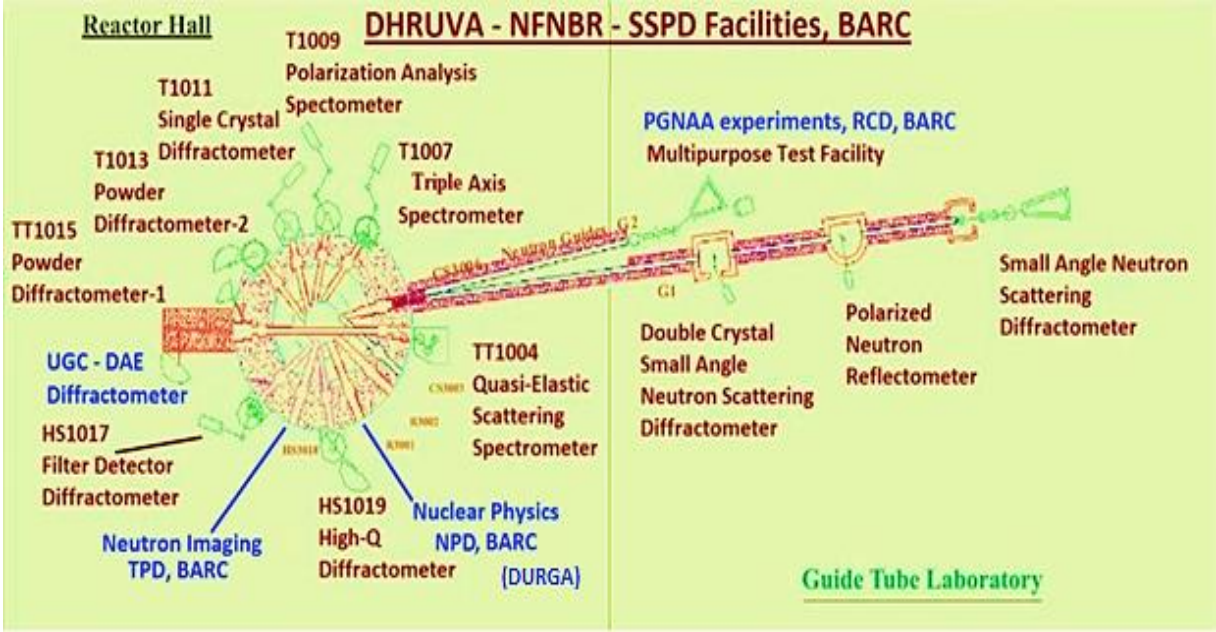

Special facilities have been setup at 300 mm diameter beam holes to utilize them for specific purpose. Presently facilities for neutron imaging and fission spectrum studies have been installed at 300 mm beam holes.

Each beam hole assembly is provided with two gates for shielding. The inner gate, located inside the biological shield and electrically operated, is used to open or close the neutron beam entering the experimental area. The outer gate is meant for shielding, whenever the beam hole is being utilized for irradiation of samples.

3.3.3 Neutron Beam research

3.3.3.1 Facilities available for utilizing 100 mm beam lines for basic research

There are four neutron scattering facilities at the tangential beam lines, three at the ends of the through tube, two at the radial beam lines and three instruments in the guide laboratory. Six diffractometers, (two small angle neutron scattering facilities, and one neutron reflectometer) help to study structures of magnetic materials, ferroelectrics, soft matter, nanomaterials, amorphous compounds, glasses, thin films, multilayer's, as a function of composition and/or temperature, pressure, and magnetic field.

Three neutron spectrometers facilitate the study of excitations (lattice vibrations, molecular/ magnetic/ diffusive) in materials (crystalline, soft matter, nanomaterials).

3.3.3.2 Guide tube Laboratory

Cold neutron beams can be transported using guides, to the laboratory located adjacent to the reactor building for conducting experiments in low gamma and neutron back ground condition. Two neutron guide tubes G1 and G2 (length: 21 m and 35 m, radius of curvature: 1916 m and 3452 m, characteristic wavelength: 3.0 Å and 2.2 Å respectively) transport neutron beams in to Guide-Tube Laboratory from the reactor hall. Average flux at the breaks, provided on the guides to accommodate various instruments, is ~ 10^7 n/cm2/sec.

3.3.3.3 UGC-DAE CSR facility

UGC-DAE consortium for Scientific research (CSR) facilitates utilization of the Nation facility for neutron beam research (NFNBR) at Dhruva reactor by scientists and students from Universities and various academic institutions across the country. CSR scientists have developed and installed neutron powder diffractometer along with a unique sample environment for carrying out neutron diffraction experiments at low temperatures and high magnetic field. The setup has been installed at beam hole of lower through tube the reactor. The diffractometer is mainly used for characterization of novel magnetic materials.

3.3.4 Utilization of 300 mm beam Holes

3.3.4.1 Thermal neutron imaging at beam hole HS-3018

Techniques such as radiography or tomography are very useful tools for various scientific investigations and industrial applications. Neutron radiography is complementary to X-ray radiography, as neutrons interact with nucleus as compared to X-ray interaction with orbital electrons. A neutron imaging beam-line has been designed and developed at 100 MW_{th} Dhruva research reactor for neutron imaging applications such as radiography, tomography and phase contrast imaging. Combinations of sapphire and bismuth single crystals have been used as thermal neutron filter/gamma absorber at the input of a specially designed collimator to maximize thermal neutron to gamma ratio. The maximum beam size of neutrons

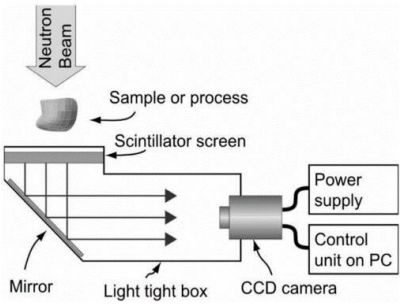

Experimental Hutch

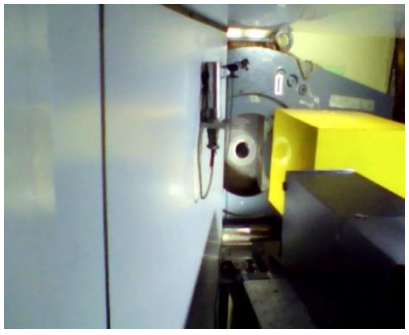

has been restricted to ~120 mm diameter at the sample position. A cadmium ratio of ~250 with *L/D* ratio of 160 and the thermal neutron flux is ~4×10^7 n/cm^2/sec at the sample position. Non-destructive radiography/tomography experiments on hydrogen concentration in Zr-alloy, aluminium foam; ceramic metal seals etc. have been carried out on this beam line.

3.3.4.2 DURGA for Fission spectrum studies at beam hole R-3001

Dhruva Utilization in Research using Gamma Array (DURGA) is a unique facility in the country to carry out prompt-gamma coincidence spectroscopy measurement using thermal neutron beam of Dhruva at beam hole R-3001. A unique facility in the country for nuclear structure studies of neutron-rich nuclei following thermal neutron induced fission reactions and Capture Gamma Spectroscopy (CGS). In the present configuration, the hybrid gamma detector array consists of six Compton-suppressed high-purity clover Ge detectors and an equal number of $LaBr_3$(Ce) fast Scintillators. The heart of the DURGA facility is a state-of-the-art, trigger less data acquisition system. Prompt and decay spectroscopy of neutron-rich fission fragment nuclei is one of the main research objectives of this facility. Apart from this, the facility is used heavily in studying Capture Gamma Spectroscopy (CGS). From application point of view, investigation of nuclear isomers and fuel cycles of actinides, relevant to reactor operation/designing, are planned to be carried out.

3.3.4.3 Testing of Neutron detectors

Neutron detectors of various types and sensitivities are developed by Electronics Division of BARC and ECIL Hyderabad. Before these detectors can be used for various reactor regulation or protection systems and they have to be tested for their performance under simulated conditions. One of the Dhruva beam holes has been utilized for accelerated life testing of newly developed ion chambers. 3 pitch Inconel SPNDs used in Indian PHWR were also tested in one of beam hole of Dhruva.

Spare positions of Ion chamber baskets of Dhruva are also being utilized for checking performance of detectors of new design.

3.3.5 Material and fuel testing

3.3.5.1 Irradiation of Zircaloy calandria tube samples

For Calandria tubes (CT) of Indian PHWR, to evaluate the relative irradiation performance of seamless Zircaloy calandria tubes vis-a-vis seam welded Zircaloy calandria tubes, a specially made assembly called Zicallory slug rod was irradiated in Fuel channel position in Dhruva. The assembly consists of various samples of Zicallory fabricated though different fabrication routes which were test irradiated in Dhruva reactor to study their comparative In-pile growth behavior. These studies along with subsequent studies done at FBTR for higher fluence, resulted in finalization of manufacturing route for the PHWR Calandria tubes.

3.3.5.2 Irradiation of Thoria assembly

A number of Thoria assemblies were irradiated in fuel positions of Dhruva. The irradiation program had helped in generating first-hand experience of Thorium-based fuel cycle, especially in U-233 production, and contamination level of U-232 in U-233.

3.3.5.3 Advanced Heavy Water Reactor (AHWR) fuel pin irradiation

2 clusters of AHWR fuel pins of different fuel compositions were irradiated in a regular fuel position of Dhruva. Such irradiation will be helpful in understanding irradiation behavior of Thoria based AHWR MOX fuel and for carrying out fuel cycle studies

3.4 Additional enhancements for meeting current demand of radioisotopes

3.4.1 Irradiation of Cobalt-60

In order to meet the increasing demand for low specific activity of Co-60, for supply of Gamma Chambers and Blood Irradiator to various users in countries and abroad, Nickel plated Cobalt-59 slugs of 36 gm each in standard Al-cans are being irradiated in off power tray rod in the reactor. For meeting requirement of Co-60 of very high specific activity (>200 Ci/gm), beads of Co are being irradiated in a specially made Zircoally capsule in new Adjuster rod of Dhruva. These capsules are designed to confine 10 gms of Cobalt pallets of 1 mm diameters and 1 mm height in its annuals space. The shape of capsule is such that it ready to use in Tele-therpy source and same need not to be cut to extract out pallets of cobalt. Capsules has been loaded in to a specially made tray section of the Adjuster rod of Dhruva shown in figure. 45 capsules can be loaded in to the tray section of the adjuster rod.

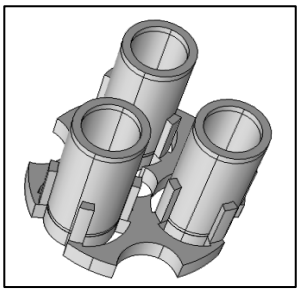

Zr capsules in Adjuster Rod Tray section

3.4.2 Proposal of Moly-99 Production by Fission Molly

Nuclear fission is the most widespread method to produce Mo-99 of very high specific activity. A preliminary analysis for production of fission moly in Dhruva reactor has been carried out with LEU-Al alloy (~20% U-235) as target material. The proposed Fission Moly target consists of a rectangular fuel meat plate of dimension 114 mm (Long) x 30 mm (Wide) x 0.8 mm (Thick) and clad of 0.3 mm thickness. The target fuel meat is UAl3 (where U is LEU of 19.75% enrichment) produced from dispersion of UAl2 in Aluminium-1S matrix. The cladding material of the fuel meat is Al.

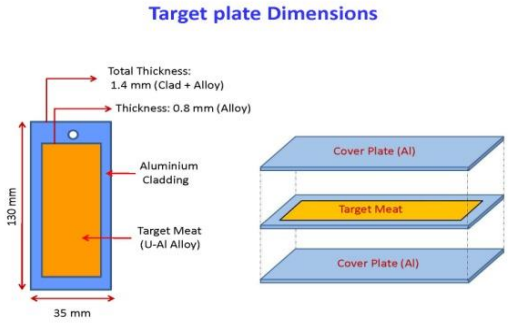

Target plate container

Target Container in Fission molly tray rod

The targets will be loaded in to containers and same will be further loaded and irradiated in a specially designed and fabricated tray rod assembly installed in a regular fuel Channel position. At rated operation of Dhruva Reactor, with 12 Target plates, Total activity of Mo-99 after pre calibration time (~8 days) can be 300Ci. The required setup for irradiation and handling has been designed and fabricated. Trails tests are in advance stage for all the processes involved in irradiation & handling of target material in Dhruva.

3.5 Special Experiments

3.5.1 Validation of Thermal Hydraulic codes with instrumented fuel rod.

The steady state and transient temperature of Dhruva fuel pin clad were evaluated theoretically using different thermal hydraulic models and codes. In order to validate the design, an instrumented fuel assembly was fabricated and irradiated at Dhruva to measure temperature of fuel pin clad during steady state and transients. Instrumented fuel assembly was similar to the regular fuel assembly of Dhruva. Five thermocouples were fixed at predicted hot spot elevations on four outer pins and one central fuel pin of the assembly. The steady state and rate of change of clad temperature of fuel pin clad were monitored during reactor operation and power changes. A flow coast down experiment was conducted at high reactor power by tripping all main coolant pumps simultaneously. The results matched reasonably well with the results obtained by COBRA-IV-I.

3.5.2 Neutron Noise Measurement

Establishing applicability of neutron noise measurement technique for diagnostics of in-core components for heavy water reactors a specially designed assembly consisting of five neutron sensors with integral cable assembly, mounted at different elevations was installed in one of the vertical experimental positions in reactor core. The AC component of the signal was electrically separated and recorded simultaneously with vibration signal tapped by accelerometers mounted on nearby core structure extensions. The recorded signal was analyzed by FFT analyzer. Prominent distinct frequency peaks could be identified both in the AC output of the neutron sensors of the special assembly and the mechanical vibration of in-core structures. This experiment indicated that neutron noise could be effectively utilized as an early diagnostic technique for in-core components in heavy water reactors.

3.6 Man Power Training

During the last 35 years a large number of Engineers, Scientists, operators and technicians have been trained at Dhruva reactor. This trained manpower is contributing to our nuclear programs in various capacities.

4.0 CONCLUSIONS:

The research reactors have provided valuable operating experiences of over 100 reactor-years. The insight gained in construction and operation of these reactors has played a significant role in developing India in all respects related to our nuclear program. The various irradiation and experimental facilities in these reactors are well utilized and helps in achieving new heights in production of radioisotopes and material testing.

Reference(s):

1. S.K. Agarwal et al., Dhruva: Main design features, operational experience and utilization, Nuclear Engineering and Design 236 (2006) 747
2. Kunal Chakrabarty & C.G. Karhadkar, "Research Reactors in BARC History, Development & Utilization" BARC Newsletter Jan-Feb 2021.
3. A K Tyagi & A K Mohanty, Non power applications of Nuclear Technologies, A BARC Publication (Oct 2021).

Annexure-1 : Radioisotopes produced in Dhruva

Sr. no.	Target Material	Isotope of Interest	Physical form of Target and normal weight	Reaction Natural Abundance of Target element (%) & Half Lifes	Uses of Isotope	Sp Activityat 100MW Delivery frequency, Irradiation Period
1	TeO2	I^{131} β= 0.6MeV γ=0.36MeV	Powder 28 gm/Cap	$Te^{130}(n,\gamma)Te^{131} \rightarrow I^{131} \rightarrow Xe^{131}$ N.A.(Te^{130}):34.49 %, $T_{1/2}Te^{131}$=25 min $T_{1/2}I^{131}$=8 days, $T_{1/2}Xe^{131}$=stable	Thyroid scanning & Therapy	125000 Ci/gm of I Weekly Delivery, 3-5 week irradiation
2	MoO_3	$[Tc^{99}]^*$ γ=0.14MeV	Powder 15 gm/Cap	$Mo^{98}(n,\gamma)Mo^{99} \rightarrow [Tc^{99}]^* \rightarrow Tc^{99}$ N.A. (Mo^{98})23.75 %, $T_{1/2}(Mo^{99})$=67 Hrs , $T_{1/2}[Tc^{99}]^*$ = 6 Hrs	Diagnosis & therapy	1 Ci/gm Weekly Delivery, 1-3 week irradiation
3	Ir	Ir^{192} γ=0.32MeV	Metal Pallets/seeds 3.4gm/Cap	$Ir^{191}(n,\gamma)Ir^{192} \rightarrow Pt^{192}$ N.A. (Ir^{191}) 38.5 % $T_{1/2}Ir^{192}$=74 days, $T_{1/2}Pt^{192}$=stable	Radiography source (γ)	300-400 Ci/gm Monthly Delivery, 5-6 mont irradiation
4	$LuCl_3$	Lu^{177} β=0.5, 0.4, 0.2 γ=0.208 &0.11	Enrich $LuCl_3$ 700mg Deposited on Quartz 1mg	$Lu^{176}(n,\gamma)Lu^{176} \rightarrow Hf^{177}$ N.A Lu-177.:2.6 % En.Lu176:>74% $T_{1/2}$ Lu177: 6.71Days	bone pain palliation Prostate Cancer Therapy	30000 Ci/gm Weekly Delivery, 2-3 Week irradiation
5	Sm_2O_3	Sm^{153} β=0.7, 0.8 γ=0.07, 0.1	Enrich Sm Powder 15 mg /Cap	$Sm^{152}(n,\gamma)Sm^{153} \rightarrow Eu^{153}$ N.A. Sm^{152}: 26.7% , En Sm^{152}: 98.4% $T_{1/2}$ (Sm^{153}):46.3 hr	Bone Pain Palliation	1350 Ci/gm, Weekly Delivery, 2-3 Week irradiation
6	S	P^{32} Pure β emitter β=1.71 MeV	Nat S Powder	$S^{32}(n,p)P^{32} \rightarrow S^{32}$ N.A. (S^{32}): 95.018 $T_{1/2}P^{32}$=14.3 days, $T_{1/2}S^{32}$=stable	Genetic studies & labeling, study of metabolism in plants	11.4 Ci/gm Delivery as required, 2-3 Mont irradiation
7	Red P		Red P Powder 100-400 mg	$P^{31}(n,\gamma)P^{32} \rightarrow S^{32}$ N.A. (P^{31}): 100% $T_{1/2}P^{32}$=14.3 days, $T_{1/2}S^{32}$=stable		11.4 Ci/gm, Delivery as required, 2-3 Mont irradiation
8	KCl	S^{35} Pure β Emitter β=0.167(max),	Nat. KCl powder	$Cl^{35}(n,p)\ S^{35} \rightarrow$Cl-35 N.A. Cl^{35}: 75.53 $T_{1/2}S^{35}$=87.4 Days	Study of Fungicides	4" special Flask Delivery as required
9	Co-59	Co^{60} γ=1.17 & 1.33 MeV	Pallets/Pins in Zr Capsules in AR	$Co^{59}(n,\gamma)Co^{60} \rightarrow Ni^{60}$ N.A. (Co^{59}):100% $T_{1/2}Co^{60}$=5.27 y, $T_{1/2}Ni^{60}$=stable	Tele-therapy (>200Ci/gm)	200-300 Ci/gm 2-3 Yr irradiation
10			Pencils in Special Slug rod		Irradiators (>40Ci/gm) GammaChamber (20-50Ci/gm)	40-200 Ci/gm 5-10Yr irradiation
11			Pins in Al or Zr Capsules in TR		GammaChamber (20-50Ci/gm) Blood Irradiator (2-3Ci/gm)	1-30Ci/gm 6-36 Mn irradiation
12	Xe Gas	I-125	Nat Xe Gas (4gm) in Special Container	$Xe^{124}(n,\gamma)\ Xe^{125}\text{-}^{(EC)} \rightarrow I^{125}\text{-}^{(EC)} \rightarrow Te^{125}$	Radio-Immunoassay Branchy therapy	4-8 Week irradiation Delivery Once in 2 months
In addition to above mentioned Radio isotopes, other isotopes that are also produced are given below. ^{166}Ho, ^{186}Re, ^{90}Y, ^{82}Br, ^{24}Na, ^{140}La, ^{45}Ca, ^{65}Zn, ^{32}P, ^{55}Fe, ^{59}Fe, Sc etc						

Annexure-2 Beam Hole Utilization for Neutron beam research

S. No	Beam Hole	Instruments	Research Area Covered by Instrument
1	**T-1007**	Triple Axis Spectrometer	Inelastic neutron scattering experiments from single crystals/ polycrystals/ glasses
2	**T-1009**	Polarized Neutron Spectrometer	Size/magnetization of magnetic domains or clusters at mesoscopic length scales
3	**T-1011**	Single Crystal Neutron Diffractometer	Used for study of high precision 3D structure of materials.
4	**T-1015**	Power Diffractometer- 1	Magnetic ordering/phases in technologically important polycrystals
5	**T-1013**	Power Diffractometer- 2	Chemical and magnetic structure phase diagrams of polycrystals
6	**HS-1017**	Time of Flight Spectrometer	Inelastic neutron scattering experiments from polycrystals
7	**HS-1019**	High –Q Diffractometer	Short and intermediate range order in glasses, liquids and disordered crystals
8	**TT-1004**	Quasi Elastic Spectrometer	Stochastic molecular motion in pico-second time scales. It provides both time scale and geometry
9	**Guide G1**	Double Crystal based SANS	Structural features in 20 nm to 1000 nm scale
10	**Guide G1**	Polarised Neutron Reflectometer	Depth dependent magnetic properties of thin films and multilayers
11	**Guide G1**	Small Angle Neutron Spectrometer	Structure and interactions at nanometre length scales
12	**Guide G2**	Multi Purpose Test Facility	A multipurpose neutron beam line for varied uses such as detector testing and also for

Author Information

Shri Kunal Chakraborty, Outstanding Scientist, is the Head, Reactor Operations Division, BARC. He is from 32nd batch of BARC Training School. His field of expertise is operations, utilization and safety Management of Research Reactors. He is responsible for effective utilization of the reactor like regular irradiation and supply of radioisotopes, irradiation of new fuels and other experimental assemblies, testing of detectors, utilization of beam tube by commissioning of neutron radiography facility etc. He is one of the key people for co-ordination with other services and sections as required for timely action to correct/rectify the deficiencies in the system and equipment.

Reactor Physics Aspects of Research Reactor (RR) Irradiation Facilities in BARC

Tej Singh[1*], Shantanab Banerjee[1]

[1]*Research Reactor Services Division, Bhabha Atomic Research Centre, Trombay, Mumbai-400085, India*
(* *Corresponding author email:* t_singh@barc.gov.in)

1.0 Introduction

Reactor physics has important role to play in the design as well as day to day operation of a nuclear reactor, be it power or research reactor. While power reactors are concerned with nuclear power generation, research reactors are mainly utilized for radioisotope generation, fundamental research, testing various nuclear & structural materials etc. Currently, in BARC, Trombay, there are three functional research reactors: 100 MW_{th} tank type reactor Dhruva [1], 100 W_{th} tank type reactor Critical Facility (CF) for Advanced Heavy Water Reactor [2] and 2 MW_{th} pool type reactor upgraded Apsara, i.e. Apsara-U [3]. Utilization of research reactors in a safe and efficient manner requires continuous technical support from reactor physics, which is a part of the responsibilities of operational reactor physicists. Operational Reactor Physics jobs can be broadly categorised into the following:

- Preparation of procedures for first approach to criticality with/without external neutron source & subsequent experiments for qualification of control rods from reactivity worth point of view, core excess reactivity, reactivity feedback coefficient, moderator level coefficient of reactivity etc.,
- Safety evaluation of proposals for various experimental irradiations, either in pile or neutron beam holes,
- Safety evaluation and approval of in-pile irradiation of samples in isotope tray rods (Pile Irradiation Requests),
- Estimation of core excess reactivity
- Calculation and measurement of core power/flux distribution,
- Reactor thermal power checks,
- Xenon transient estimation and preparation of start-up curves,
- Maintaining reactivity balance to plan & schedule irradiations in reactors,
- Working out different core configurations for various physics experiments,
- Thermal hydraulic analysis,
- Shielding calculations,
- Manpower training

Some of the instrumental role reactor physics plays in the utilization of RR, especially the irradiation facilities, is discussed below:

2.0 Irradiation of experimental samples

2.1 Different type of irradiation facilities in research reactors

Normally, various options are available for sample irradiation in research reactors (RR), namely the in-core irradiation facilities and beam-tubes. An in-core irradiation facility is a specialised position created within the core where potential samples can be inserted/removed while the reactor is operating (online) or in some cases while the reactor is shutdown (offline). These facilities can be designed to suit both short and long duration of irradiation. Long-term irradiation, such as for a few days to a few months, is useful for radioisotope production. These radioisotopes are important in various fields such as: nuclear medicine (diagnosis, therapy, palliation etc.), industries (radiography, process evaluation etc.), agriculture (genetic enhancements, preservation etc.) and other R & D activities. Short duration

irradiation (say, upto few minutes) is useful for Neutron Activation Analysis (NAA), which is a method for the qualitative and quantitative determination of elemental concentration and is used extensively in environmental studies, geological and geochemical sciences, forensic and medicinal studies, industrial material characterization, archaeology etc. Beam-tubes are specialised positions providing neutron source which are utilized for carrying out research work in the area of condensed matter physics, neutron radiography, fission fragment studies, neutron based scattering studies, neutron activation-based studies etc. Beam tubes can also be classified as hot neutron source and cold neutron source, depending upon the energy spectrum of the neutron beam available at the tube.

2.2 Description of irradiation facilities at research reactors situated in BARC

There are three research reactors currently operational in BARC, namely Dhruva, CF and Apsara-U. Currently, Dhruva core consists of two on-power rods and one off-power tray rod for radioisotope production, a pneumatic carrier facility (PCF) for very short time irradiation required in neutron activation analysis, a self-serve facility for short term irradiation and 15 experimental beam holes (including two through tubes) for neutron beam research. Standard Dhruva tray rod assembly houses 30 trays where each tray can hold a maximum of 3 sample-filled Al capsules, kept 120° apart. The maximum thermal neutron flux available in Dhruva tray rod position is about 2.0×10^{14} n/cm^2/s. The self-serve facility is designed for the irradiation of small quantity of sample in the region near of heavy water reflector for a short duration, with provision to load as well as remove the samples quickly. The PC facility has provision for shooting a sample into the core for a very short irradiation and then receiving back the same for rapid analysis using NAA technique. The experimental beam tubes are arranged radially, or tangentially, with respect to the core. These tubes are having either 300 mm dia. or 100 mm dia. Also, special provisions have been made in the calandria design to accommodate two engineering loop positions and three in pile creep and corrosion facilities.

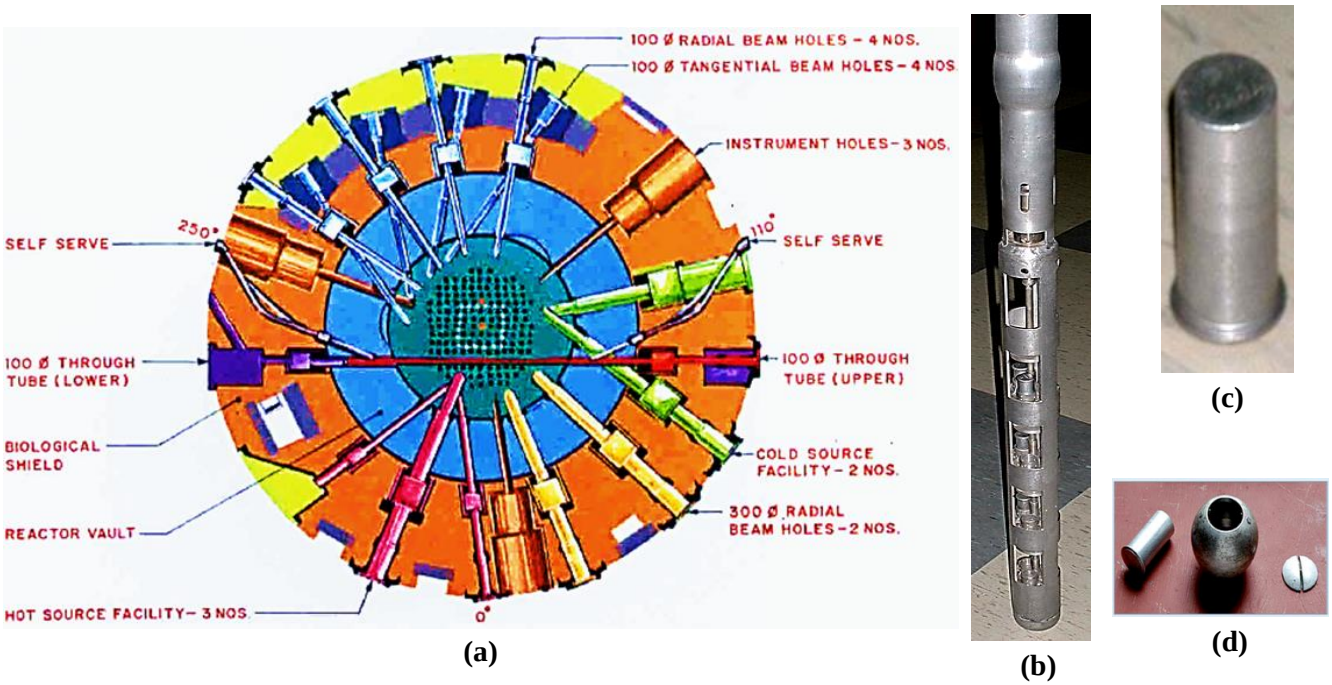

Figure-1: (a) Dhruva cross sectional view with beam tubes and other facilities, **(b)** Tray rod assembly, **(c)** Tray rod sample carrying capsule, **(d)** Self-serve sample carrying capsule

Apsara-U is a 2 MW swimming pool type research reactor cooled and moderated by light water and reflected by BeO. There is 1 in-core and 7 out-of-core irradiation positions (situated in the BeO reflector region) wherein tray rods can be loaded for radioisotope production (refer **Figure-2**). The maximum

thermal and fast neutron flux available at in-core irradiation position is 5.2×10^{13} and 2.1×10^{13} n/cm^2/s, respectively [4]. Apsara-U core is movable and can be operated at three different core positions inside the pool, viz. 'A', 'B' and 'C'. Core position 'A' contains graphite moderated thermal column in which provision for nuclear detector testing is provided. This position also contains four beam tubes. Core position C contains facility for carrying out shielding experiments. Reactor operation is mostly carried out at core position B which contains four beam tubes. Two beam tubes are of dia. 150 mm while the remaining two are of the dia. 100 mm. **Figure-3** shows the 3 core positions along with experimental facilities.

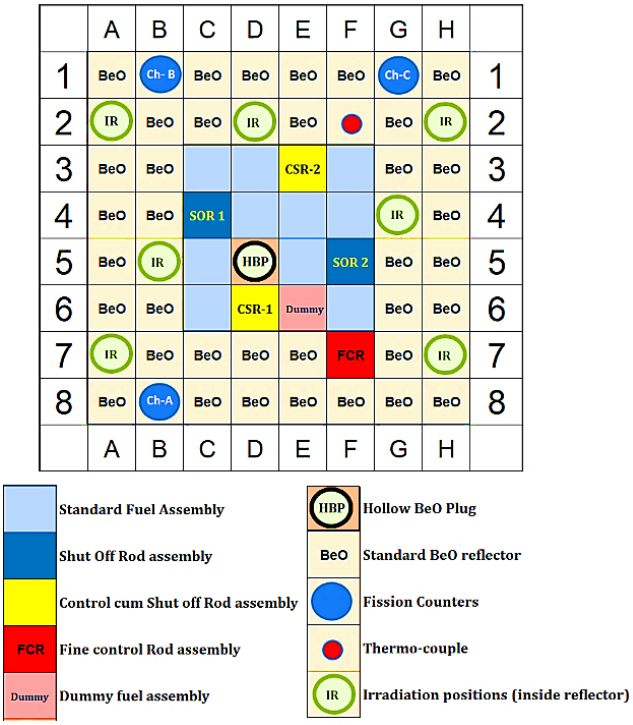

Figure-2: Irradiation positions of Apsara-U along with the core configuration

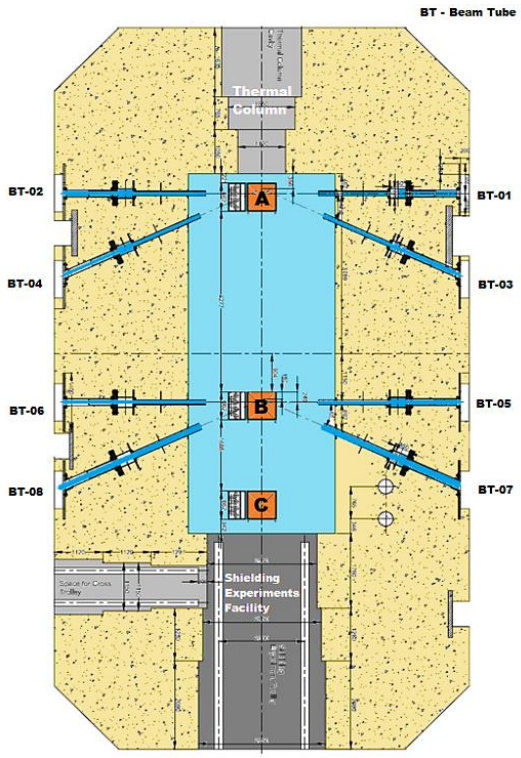

Figure-3: Beam tubes in Apsara-U along with different core positions

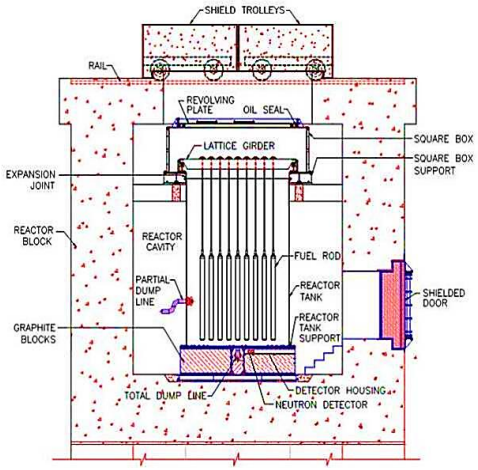

Figure-4: Reactor Block of Critical Facility [2]

CF is a low power research reactor with a nominal power of 100 W with an average thermal neutron flux of 10^8 n/cm^2/sec. Here fuels are suspended from movable support (which enable the reactor operate with a variable pitch, which is it's unique design feature) into an Al tank filled with heavy water moderator and bottom graphite reflector (refer **Figure-4**). The main objective of this reactor is conducting experiments and validating the physics design parameters of AHWR. Graphite reflector position of this reactor has facilities for testing neutron detectors and also to irradiate samples (Soil, Geological rock, Biological sample and Metallic alloys) for neutron activation analysis (NAA).

2.3 Characterisation of irradiation facilities

For utilization of RRs it is pertinent to characterize the irradiation positions. Reactor physics plays important role in this, by providing theoretically estimated and experimentally obtained values for (i) neutron and

gamma spectrum at irradiation locations, (ii) absolute value of the neutron flux and gamma flux (iii) epithermal shape factor (α) etc.

These fluxes and other parameters may be estimated theoretically using reactor physics codes, and may also be validated experimentally, if necessary. For theoretical estimation, Monte Carlo method-based stochastic code as well as deterministic method-based codes were employed [5], [6], [4], [7].

Maximum estimated neutron flux at the on-power tray rod locations in Dhruva (H-07 and K-09), PCF, self-serve facility and engineering loop are provided in **Table-1** [8]. Note that these values were estimated with typical core loading pattern along with a critical moderator height of 310 cm. Similarly, neutron and gamma flux are also estimated for all the beam holes. For example, for HS-3018 beam hole (hot neutron source tube), having 300 mm dia., the thermal, epithermal and fast neutron fluxes at the core facing incident face are about 8.6×10^{13}, 1.53×10^{13} and 1.06×10^{12} n/cm^2/s respectively. The corresponding values at the end of the beam hole in the biological shield are 4.4×10^{10}, 7.8×10^{9} and 5.6×10^{8} n/cm^2/s respectively. It may be noted that, among all the beam holes, the re-entrant can of HS-3018 penetrates maximum into the core and therefore the flux values for this beam hole are found to be highest among all beam holes [6]. Typical variation of estimated neutron flux (3 energy group) along with the estimated gamma flux (4 energy group) for HS-3018 beam tube in Dhruva, is given in **Figure-5** and **Figure-6**.

Table-1: Maximum neutron flux levels at tray rod locations in Dhruva at full power operation, with typical core loading and at critical moderator height 310 cm [8]

Type of facility	**Id. number**	**Maximum neutron flux at 100 MW (n/cm^2/sec)**		
		Fast (> 0.821 MeV)	**Epithermal (0.625 eV–0.821 MeV)**	**Thermal (<0.625 eV)**
Isotopic tray rods	H-07	1.8×10^{12}	2.7×10^{13}	2.0×10^{14}
	K-09	2.2×10^{12}	2.9×10^{13}	1.9×10^{14}
Pneumatic carrier	C-25	0.9×10^{12}	1.2×10^{13}	1.2×10^{14}
Engineering loop	G-13 (150 mm)	5.9×10^{12}	6.0×10^{13}	1.6×10^{14}
	G-19 (100 mm)	2.8×10^{12}	3.9×10^{13}	1.9×10^{14}
Self-Serve *	S-2-1	4.2×10^{10}	6.2×10^{11}	3.4×10^{12}
	S-2-2	8.5×10^{10}	1.3×10^{12}	6.9×10^{12}
	S-2-3	1.3×10^{11}	1.9×10^{12}	1.1×10^{13}

*** Reference** [5]

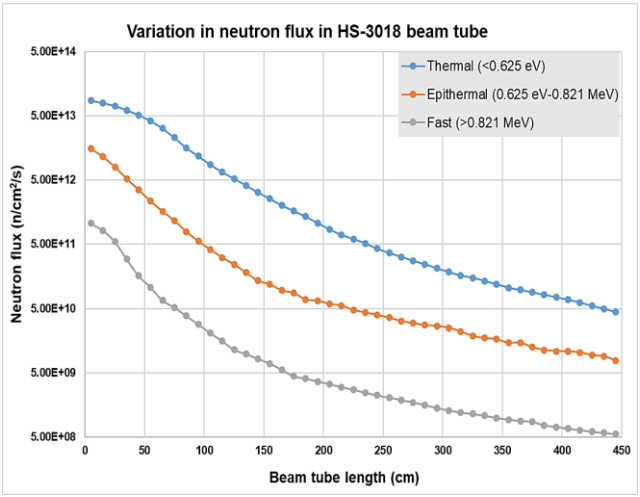

Figure-5: Typical variation in neutron flux in HS-3018 BT in Dhruva [6]

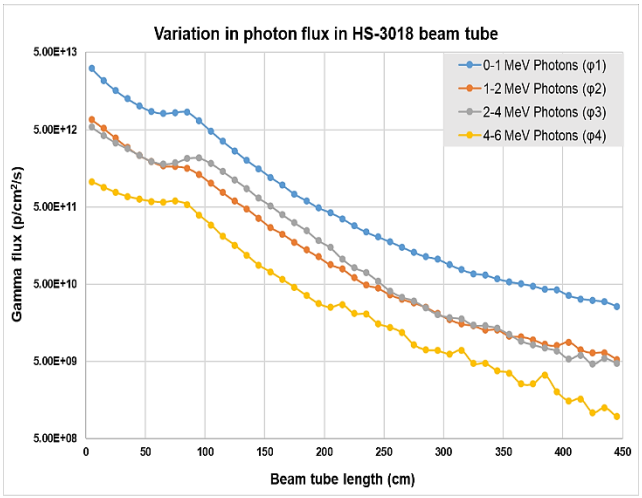

Figure-6: Typical variation in gamma flux at HS-3018 BT in Dhruva [6]

The maximum estimated neutron flux levels at tray rod locations in Apsara-U is provided in **Table-2**, while the typical variation of estimated neutron flux (3 energy group) along with the estimated gamma flux, for a 100 mm dia. beam tube in Apsara-U, is given in **Figure-7** and **Figure-8**.

Table-2: Maximum neutron flux levels at tray rod locations in Apsara-U (at BOC) at full power operation [4]

Tray rod position		**Maximum neutron flux at 2 MW (n/cm^2/sec)**		
		Fast (>0.821 MeV)	**Epithermal (0.625 eV–0.821 MeV)**	**Thermal (<0.625 eV)**
Out-of-core (in reflector region)	A-7	5.1×10^{11}	1.9×10^{12}	1.1×10^{13}
	A-2	5.4×10^{11}	2.0×10^{12}	1.1×10^{13}
	B-5	6.7×10^{12}	1.5×10^{13}	3.9×10^{13}
	D-2	7.1×10^{12}	1.6×10^{13}	4.1×10^{13}
	G-4	7.3×10^{12}	1.6×10^{13}	4.2×10^{13}
	H-7	5.8×10^{11}	2.2×10^{12}	1.2×10^{13}
	H-2	5.5×10^{11}	2.0×10^{12}	1.1×10^{13}
In-core	D-5	2.1×10^{13}	4.4×10^{13}	5.2×10^{13}

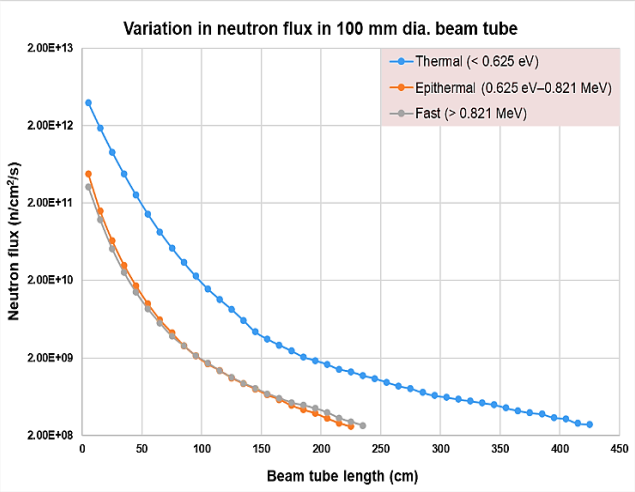

Figure-7: Typical variation in neutron flux in 100 mm dia. beam tube in Apsara-U [7]

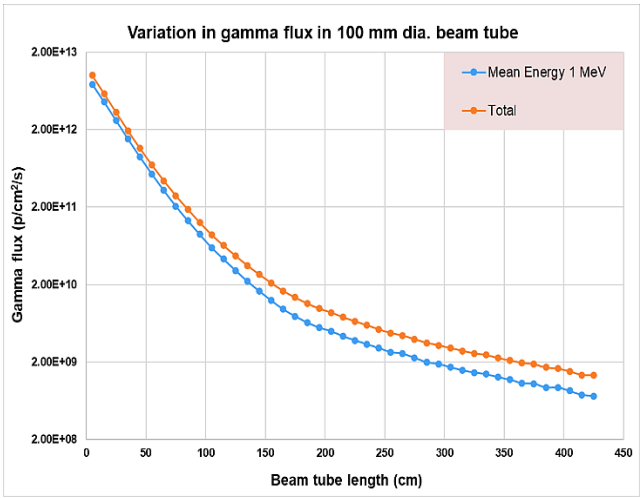

Figure-8: Typical variation in gamma flux in 100 mm dia. beam tube in Apsara-U [7]

Usually, the neutron spectrum in a thermal reactor can be described in parts by Maxwellian distribution (thermal energy region), slowing down spectrum (epithermal energy region), and fission spectrum (fast energy region). In an ideal thermalized reactor, the epithermal neutron flux distribution per unit energy interval is inversely proportional to $1/E_n$. However, this condition is rarely satisfied in a practical nuclear reactor. Therefore, deviations from the $1/E_n$ may occur, especially at irradiation position and the spectrum varies as $1/E_n^{1+\alpha}$ [9]. This α is called the epithermal neutron flux shape factor, the value of α is always positive for a well moderated reactor core, whereas it can take on negative values for the reactors with harder spectrum (e.g., LWR) as the population of neutrons in epithermal region will be significant. Thus, determination of α is essential to estimate proper interaction. If we assume, for capture type interaction, i.e. (n,γ) interaction, that contribution from fast neutron interaction is negligible, the reaction rate can be written as [10]:

$$R = \sigma_0\phi_0 + I_0\phi_e \qquad (1)$$

Where, ϕ_0 is the conventional thermal neutron flux, σ_0 is the microscopic neutron capture cross-section, I_0 is the resonance integral, defined in the epithermal range as $I_0 = \int_{E_{epithermal}} \frac{\sigma(E)dE}{E}$ and ϕ_e is the epithermal region flux. σ_0 and I_0 can be found in standard resources. Now, although for many nuclides, the reaction cross section varies as $1/v_n$ in the thermal energy region (v_n being the velocity of interacting neutron), some nuclides do not follow such rule (viz ^{176}Lu). For a non-$1/v_n$ target isotope, we need to account for the same using the temperature dependant Westcott g(T) factor.

Moreover, for a reactor where α is non-zero, I_0 becomes α-dependant. The relationship between I_0 and $I_0(\alpha)$ is also given by [11]:

$$I_0(\alpha) = \left(\frac{I_0 - 0.429\sigma_0}{(\bar{E}_r)^\alpha} + \frac{0.429\sigma_0}{(1+2\alpha)E_{Cd}^\alpha} \right) E_{arb}^\alpha = \int_{E_{Cd}}^{\infty} \alpha(E) \frac{E_{arb}^\alpha}{E^{1+\alpha}} dE \quad (2)$$

Where, E_r is the effective resonance energy and E_{Cd} = 0.55 eV is the cadmium cut off energy, E_{arb} =1 eV – arbitrary energy. Now, the epithermal neutron spectrum shape factor α at the sample irradiation position has been estimated using Monte Carlo based computer code. If we plot ϕ vs. E on log scale, which will be a straight line, the slope of the line is used to get the estimate of α [12]. For K-09 tray rod location in Dhruva, it was found to be ~ 0.1 [10].

2.3.1 Brief outline of flux measurement methods

One of the most well-known method to measure neutron flux is foil activation method. Multiple types of foil materials are chosen, such as gold, zirconium, sulphur, nickel etc. Sometimes, cadmium covers are used to cut off neutrons below the cadmium cut off energy (thermal neutrons).

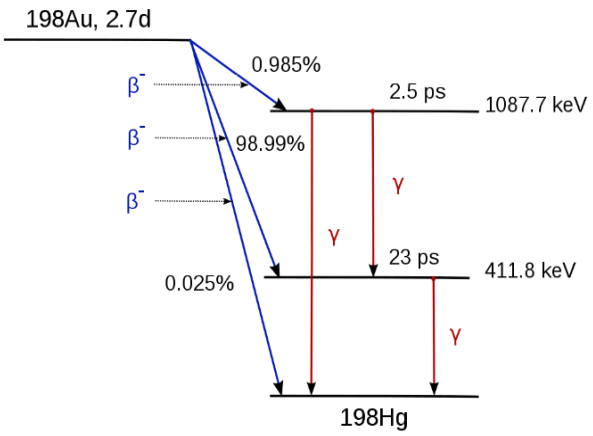

Figure-9: Decay scheme of ^{198}Au

For example, combination of bare gold foils and cadmium covered gold foils were used to measure thermal neutron flux in the Dhruva tray rods [5]. Natural gold (^{197}Au) captures neutron and forms ^{198}Au (half-life 2.7 days) which decays to ^{197}Hg in excited state via β-decay. ^{197}Hg comes to its ground state by emitting a number of gammas instantaneously. The decay scheme of ^{198}Au is shown in **Figure-9**.

After irradiation of the foils, sufficient cooling is provided to reduce radioactivity to a suitable level. HPGe detectors equipped with high resolution gamma-ray spectrometry system was used to count the signature emission (411 keV) of gamma rays from the active foils. Taking into account for the detector efficiency for the given energy, these counts can be used to estimate the residual radioactivity in the foil, which in turn can be used to find the reaction rate in each type of foil. The governing equation relating thermal flux with reaction rates are given as [13]:

$$\phi_{th} = \frac{R_S - F_{Cd} R_{S,Cd}}{g\sigma_0 G_{th}} \quad (3)$$

Where, g is the Westcott correction factor, G_{th} is the self-shielding factor for thermal neutrons, σ_0 is the thermal neutron cross section, and F_{Cd} is the cadmium correction factor. R_S and $R_{S,Cd}$ are the reaction rates per atom of bare and cadmium covered foil, both defined as follows:

$$R = \frac{A}{N_0 \varepsilon_1 \varepsilon_2 \varepsilon_3 G(\tau)\left(1-e^{-\lambda t}\right)e^{-\lambda T}} \tag{4}$$

Where A is photo-peak counting rate for the detector, N_0 is the number of atoms in the activation foils, ε_1 is isotopic abundance, ε_2 is yield of gamma ray, ε_3 is photo-peak counting efficiency, T is time elapsed between end of irradiation and start of counting, t is duration of irradiation, λ is decay constant for the gold isotope. This technique may also be used for other types of foils to deduce the neutron flux of different energies.

3.0 Safety evaluation of in-pile irradiation requests (PIR)

For in-pile irradiation of samples for radioisotope production, reactor physics analysis has to be performed before the target sample is cleared for irradiation. The main aims of the analysis are:

(i) For a typical sample, when put inside a reactor for irradiation, perturbs the steady operation of the reactor due to parasitic absorption of neutrons in the sample. As large perturbation has undesirable effects on smooth and safe operation of the reactor, it is very important to evaluate the reactivity effects due to loading of the target sample.

(ii) The target sample is heated due to absorption of various type of radiation. The rate of heat generation must be within the range allowed by the safety limit of the reactor.

(iii) For post irradiation handling of the samples, estimation of sufficient cooling period as well as necessary shielding required during transportation is very important. The activity produced during irradiation is calculated to find the residual activity with time, from which the safe cooling period and shield thickness are estimated.

In this regard, an interactive code system: Operational Reactor Physics Analysis Code, or ORPAC [14] had been developed to perform calculations related to operational reactor physics jobs of research reactors. The code is aimed at providing a handy tool for radioactivity estimation, safety analysis related with isotope irradiations and post irradiation handling etc through its SHARDA+ module. The code also has other modules which perform various other estimations related to regular operation such as estimation of xenon transient, start-up curve etc, Output power fraction (OPF).

Initially the code was developed to cater to the operational needs for Dhruva and hitherto operating CIRUS reactor. With the commissioning of new 2 MW_{th} Apsara-U reactor, and considering the differences in neutron spectra of heavy water moderated reactor Dhruva and light water reactor Apsara-U, it was imperative to use reactor specific spectrum-average cross-section library for extending its support for the newly commissioned reactor. The upgraded code, called "ORPAC-2" has user-friendly Graphical User Interface (GUI) written in Visual Basic platform, which offers the user a very handy tool for easy input and clearly interpreted output. User-selectable spectrum-averaged neutron cross-section libraries for Dhruva, Apsara-U as well as PWR and PHWR, along with photon data library as used in ORIGEN-2 code [15], have been successfully incorporated in ORPAC-2. For Apsara-U and Dhruva reactors, spectrum averaged cross section library has been generated using PREPRO-19 [16] and ENDF/B-VIII neutron data library. 69-group structure from WIMSD is used to estimate effective one-group cross section of isotopes using neutron spectrum of given irradiation position. A brief outline on how SHARDA+ module of ORPAC-2 operates is discussed in the following sub-sections

3.1 Estimation of flux depression factor

For estimation of accurate radioactivity and nuclear heating produced in a sample, the nature of depression in neutron flux profile inside the sample is important. Flux depression factor (f) depends upon the geometry of the sample.

$$f = \frac{\bar{\phi}}{\phi_0} \tag{5}$$

Where, $\bar{\phi}$ is the average neutron flux inside the sample and ϕ_0 in the flux at outer surface of the sample. It is approximately determined by solving the thermal neutron diffusion equation for a given geometry with appropriate boundary conditions, and can be written as:

For spherical geometry: $f = \frac{3}{k^2R^2}\left[kR\coth\left(kR\right)-1\right]$ (6)

For cylindrical geometry: $f = \frac{2I_1\left(kR\right)}{kRI_0\left(kR\right)}$ (7)

Where, $k = \sqrt{\frac{\Sigma_A}{D}}$ and Σ_A is the macroscopic absorption cross section and D is the diffusion coefficient, R is the sample radius, I_0 and I_1 are spherical Bessel functions. Although it may be noted that diffusion equation is only applicable where scattering cross section is larger than absorption cross section. Thus, for the grey and black absorbing material (viz Cd, B etc.), where this assumption is not true, accurate depression factor can only be calculated by using Mote Carlo method-based codes or neutron transport-based computer codes.

3.2 Estimation of reactivity load

The calculation of reactivity effect should account for neutron flux depression in the sample as explained in previous subsection. Special care has to be taken in the cases where the flux depression can be altered during irradiation itself, leading to change in reactivity. The relative neutron importance of the core location wherein the irradiation assembly is loaded is also to be properly considered.
Reactivity effect of the target isotope sample can be approximately estimated by

$$\Delta\rho = (N\sigma_a)fW \tag{8}$$

where N is the total number of target atoms, f is the flux depression factor, W is the so-called white absorption area (in mk/cm^2); For example, W = 0.0258 for H-07 & K-09 locations in Dhruva reactor. In tray rods, the typical flux variation along the length is approximately sinusoidal in nature $\phi = \phi_0 sin\left(\frac{\pi z}{H}\right)$. Reactivity load would normally be proportional to the square of the relative neutron flux in the core location. Thus, reactivity load (mk) due to a sample in any tray rod location in Dhruva may be given as follows

$$\Delta\rho = -0.0258\, f\, \delta\Sigma_A V_S \sin^2\left(\frac{\pi z}{H}\right) \tag{9}$$

Where f is flux depression factor in the sample, $\delta\Sigma_A V_S$ is referred to as white absorption area of sample (Σ_A is the effective macroscopic cross section of the sample and V_S is the surface area), ϕ_h is the flux at the sample location, ϕ_m is the maximum flux available (usually at the axial centre of moderator level), z is the axial location of a sample and H is the moderator level.

3.3 Estimation of radioactivity

Major fraction of the artificially produced radioisotopes come from nuclear reactors. The absorption of neutrons by target nuclides inside the reactor leads to a series of neutron induced nuclear reactions, generating many new radioisotopes in the process. In order to estimate the radioactivity of radioisotopes under consideration, the whole network of nuclear processes needs to be assessed by solving a large set of coupled differential equations governing temporal rate of change in the number of each nuclei. The equation governing decay and transmutation of an arbitrary mixture of N different nuclides in a homogenised material region can be written as:

$$\frac{dN_i}{dt} = -\lambda_i N_i - \sigma_i^a \phi N_i + \sum_{j\neq i}^{N} \gamma_{j\to i}\lambda_j N_j + \sum_{j\neq i}^{N} \sigma_{j\to i}\phi N_j + \sum_{j}^{N} \gamma_i \sigma_j^f \phi N_j; \qquad i = 1, 2, ..., N \tag{10}$$

Where, the first term = loss of nuclide i to decay, second term = loss of nuclide i to neutron absorption, third term = production of nuclide i from all possible parent isotope decays, fourth term = production of nuclide i from neutron induced reactions (e.g. (n,γ), (n,p) (n,α) etc.) in all possible parent isotopes and fifth term = production of nuclide i directly from fission reactions, if any. The above equations can be integrated to determine changes over the lifetime of the reactor if the time dependence of the flux is known. However, flux distribution depends on the compositions. In practice, a neutron flux distribution is calculated for the starting composition and this is used to integrate the composition equations over a depletion time step chosen suitably. Assuming that the flux is constant in the interval $t_i < t < t_{i+1}$, the production-destruction equations can be written in matrix notation as:

$$\frac{dN(t)}{dt} = A\{\phi(t_i)\}N(t) + F\{\phi(t_i)\}, \quad t_i < t < t_{i+1} \tag{11}$$

The general solution to these equations is of the form

$$N(t_{i+1}) = \exp[A(t_i)\Delta t]N(t_i) + A^{-1}(t_i)\{\exp[A(t_i)\Delta t]N(t_i) - 1\}F(t_i) \tag{12}$$

In general, it is economical to reformulate the physical production-destruction equations to eliminate short time scale phenomena that do not affect the overall result, so that $(\lambda_i + \sigma_i^a \phi)\Delta t << 1$. Eq. (9) can be written in terms of transition matrix **A** as

$$\frac{d\overline{N}}{dt} = \overline{\overline{A}} \cdot \overline{N}(t) \tag{13}$$

The transition matrix **A** describes the transition rate coefficients for each isotopic transition from neutron reactions and decay. Each individual element of **A** denoted as a_{ij} describes the relative transition rate from nuclide i to nuclide j

$$a_{ij} = \gamma_{i\to j}\lambda_i + \sigma_{i\to j}\phi \tag{14}$$

Where $\gamma_{i\to j}$ is decay yield from nuclide i to nuclide j and $\sigma_{i\to j}$ is spectrum averaged one group neutron cross section of the nuclide i resulting in nuclide j. The diagonal term of the transition matrix **A** is

$$a_{ii} = \lambda_i + \sigma_i^a \phi \tag{15}$$

Where λ_i is decay constant for nuclide i and σ_i^a is spectrum averaged one group total neutron absorption cross section of the nuclide i. Eq. (6) can be written in a compact form as

$$\frac{dN_i}{dt} = -\lambda_i^{eff} N_i + \sum_{j}^{N} b_{j,i}^{eff} \lambda_j^{eff} N_j; \qquad i = 1, 2, ..., N \tag{16}$$

Where N_i is the atomic density of nuclide i, λ_i^{eff} the effective decay constant of nuclide i, and $b_{j,i}^{eff}$ the effective branching ratio from nuclide i to j. These are defined as

$$b_{i,j}^{eff} = \frac{\gamma_{i\to j}\lambda_i + \sigma_{i,j}\phi}{\lambda_i^{eff}} \tag{17}$$

$$\lambda_i^{eff} = \lambda_i + \phi\sum_j \sigma_{i,j} \tag{18}$$

The set of first-order coupled linear differential equations written in the matrix form, involves a large number of isotopes. As the nuclear properties such as decay constants, cross-sections, etc. of isotopes appearing in the matrix equation vary widely, the eigenvalue of the coefficient matrix also has variation over several orders. This system of linear equations is solved using a semi-analytic model. The methodology adopted in this model involves discretization of total time duration into fine time steps. The analytic solution inside a time step is used along with proper initial conditions (at the start of time step) to get the solution at the end of this time step. The updated solution from this time step serves as initial conditions for the next time step. The process is continued to get the solution iteratively by updating solutions.

3.4 Preparation of data library

The new library of ORPAC consists of different sets of spectrum averaged cross sections for various type of reactions: (n,γ), (n,p), (n,2n), (n,3n), (n,α) and (n,f) corresponding to Dhruva, Apsara-U as well as LWR and PHWR type spectra. The unshielded group average cross section is defined as:

$$\sigma = \frac{\int \sigma(E)\Phi(E)dE}{\int \Phi(E)dE} \tag{19}$$

Using just thermal group average cross-section can give a fair estimate of activation for the cases where isotopes involved have relatively small cross-sections in epithermal and fast regions and the reactor is well thermalized. However, if the reactor spectrum is harder than thermal spectrum and/or the isotopes under irradiation have large resonance integrals, then accounting for the contribution of regions outside thermal also is necessary. As, the total activation (or reaction rate) depends also on the shape of the spectrum, cross-sections suitably averaged with the flux spectrum as indicated by Eq. (16) should be used for calculations.

Now, an evaluated nuclear data library such as ENDF/B format cannot be used directly in spectrum averaged cross section calculations. For this purpose, the ENDF/B pre-processing codes like PREPRO-19 [16], which is a collection of 18 computer codes designed to convert ENDF/B formatted neutron and/or photon data from the originally distributed form to a form in which the data can be used. For ORPAC-2, we obtain multigroup cross-sections using ENDF/B-VIII [17] library and PREPRO code. For example, the (n,γ) cross-sections for most frequent sample isotopes, as obtained from PREPRO-19 using ENDF/B-VIII library, are shown in **Figure-10** and **-11**. These multigroup cross-sections are then used along with reactor specific multigroup neutron spectra to obtain effective one-group spectrum dependent cross-sections. For calculation of effective one-group neutron cross section, over 69 neutron energy group flux values have been estimated using multigroup lattice code. The super cell calculation has been done to estimate real spectrum of a given irradiation position.

Also, complete neutron flux spectrum is needed for cross-section averaging. For this purpose, multigroup neutron flux has been obtained in fine group structure over the energy domain of reactor neutrons, using a Monte-Carlo based code and the lattice code DRAGON [18]. The spectrum at tray rod location of Dhruva reactor is shown in **Figure-12**. The Apsara-U core is under-moderated that means neutron spectrum in the core region will be harder. At the same time, the irradiation positions at the reflector region will have relatively softer spectrum. Neutron spectra at three different irradiation locations in Apsara-U are shown in **Figure-13.**

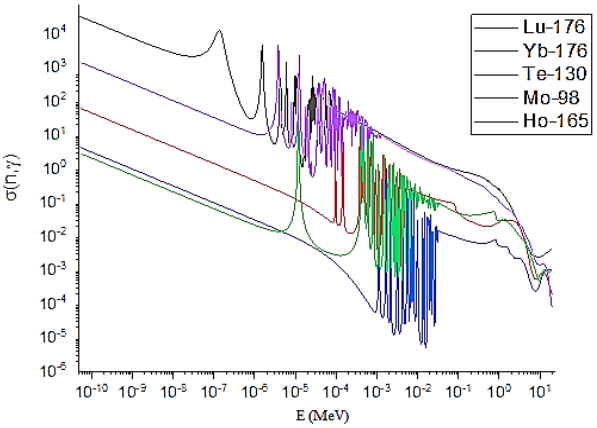

Figure-10: (n,γ) cross-section data generated using PREPRO-19 from ENDF/B-VIII library for Lu^{176}, Yb^{176}, Te^{130} , Mo^{98}, Ho^{165}

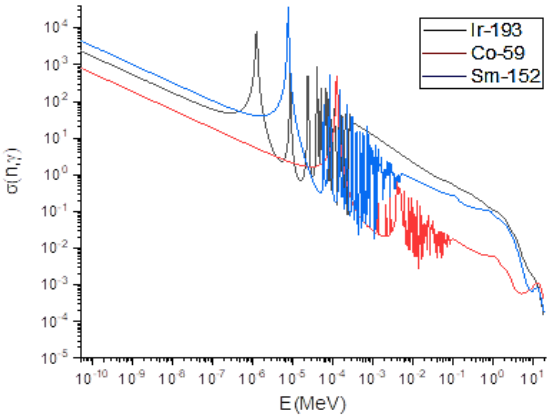

Figure-11: (n,γ) cross-section data generated using PREPRO-19 from ENDF/B-VIII library for Ir^{193}, Co^{59}, Sm^{152}

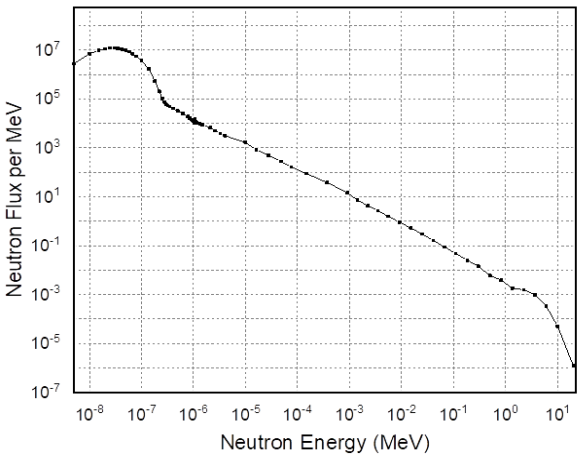

Figure-12: Neutron Spectrum at tray rod location in Dhruva

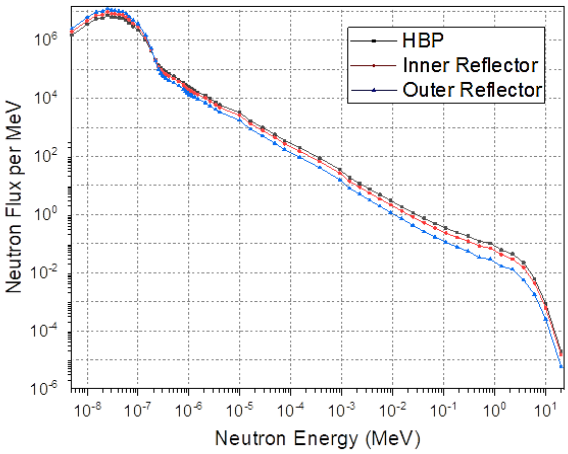

Figure-13: Neutron Spectrum at different irradiation locations in Apsara-U

Using these multigroup neutron spectra and cross-sections, estimated as shown above, one-group spectrum average cross-sections of various reactions are obtained.

Other than neutron, for dose rate and shielding analysis, estimation of photons emitted by each active nuclide produced in the irradiated sample is also required. In ORPAC-2, the photon library for each gamma emitting active nuclide is stored in 18 energy group structure as followed in ORIGEN-2. The calculation of gamma source strength, dose rate and gamma attenuation in shield medium are carried out in this 18-group structure. The final gamma source strength and dose rate is obtained by summing the respective quantity from all 18 groups. The shielding medium is fixed as the shielding casks used for transfer of active samples from our reactors are all made of lead with same material properties.

3.5 Estimation of dose rate

Bare dose rate (D_0) at a distance of 'r' cm from the irradiated sample is given as:

$$D_0 = \frac{5574C\sum_v E_v f_v}{r^2} \tag{20}$$

Where C = sample activity in Curie, E_V= photon energy of emergent gamma ray (MeV) and f_V = fractional yield of the gamma ray having photon energy E_V. Corresponding shielded dose rate (D):

$$D = D_0 \cdot e^{-\mu x} B(E_v, \mu x) \tag{21}$$

Where μx = attenuation coefficient for gamma radiation, x = shield thickness and B (E_v , μx) = Build-up factor for the specific shielding arrangement, look up tables for such factors are available.

2.6 Estimation of heating

Nuclear heating in a sample/capsule is on account of core radiations (neutrons and gammas), capture gammas/alpha/beta arising from thermal neutron absorption, radioactive decay (alpha, beta and gamma radiations) etc. For a sample with mass M and density ρ the total capture gamma heating rate is:

$$H = C_0 E_0 S_v (\psi_0 + a_1 \psi_1) \frac{\mu_A}{\mu} \frac{M}{\rho} \quad (22)$$

Where $C_0 = 1.6 \times 10^{-13}$ (Watt/MeV) is a conversion factor, $a_1 = 0.65$, E_0 = average energy of photons (MeV), S_V = no. of gamma photons/cc/sec. with energy E_0, μ_A = energy deposition coefficient for energy E_0 (cm^{-1}), μ = total linear attenuation coefficient (cm^{-1}), ψ_0 and ψ_1 are factors which depend upon sample geometry. Heating due to absorption of decay gamma is same as calculated in Eq. (22), only that S_V is replaced by specific activity C (Curie) of the sample.

$$H = C_0 \, E_0 C \, (\psi_0 + a_1 \psi_1) \times 3.7 \times 10^{10} \frac{\mu_A}{\mu} \frac{M}{\rho} \quad (23)$$

The energy deposition rate (H_{FN}) due to slowing down of fast neutrons is given by:

$$H_{FN} \propto N \bar{\sigma_s} \frac{A}{(A+1)^2} \quad (24)$$

Where A is the atomic number of the sample material and $\bar{\sigma_s}$ is the effective scattering cross section. Suppose value of H_{FN} is calculated for D_2O (say, H_{FN,D_2O}, then one may obtain, the nuclear heating $H_{FN,X}$, due to fast neutrons for any material 'X' can be scaled in terms of H_{FN,D_2O}

$$H_{FN,x} = H_{FN,D_2O} \times \frac{\left[N \bar{\sigma_s} \frac{A}{(A+1)^2}\right]_X}{\left[N \bar{\sigma_s} \frac{A}{(A+1)^2}\right]_{D_2O}} \quad (25)$$

The contribution to energy deposition from absorption of core gamma rays in the material is assumed to be approximately proportional to the electron population per gram of the material since the interaction between gamma and atom is essentially controlled by electrons. Provided N is the number of atoms per gram of sample material and Z is the atomic number of the nucleus, we can write:

$$H_\gamma \, \alpha \, NZ \quad (27)$$

Thus, similar to neutron heating, if the value of $H_{core\,\gamma}$ is calculated for D_2O then one may scale the power density $H_{core\,\gamma}$, due to interaction with core gamma radiation for any material X as

$$H_{core\,\gamma,x} = H_{core\,\gamma,D_2O} \times \frac{NZ_X}{NZ_{D_2O}} \quad (28)$$

Heat deposited due to charged particles like beta, alpha is due to deposition of all their kinetic energy in the sample can be written as

$$H = C \times 3.7 \times 10^{10} \times E \times 1.6 \times 10^{-13} \text{ watts} \quad (29)$$

Where C is the sample activity in Curies due to alpha and beta decay and E is the average energy of charged particles in MeV.

Finally, we need to account for post irradiation heating in the sample due to absorption of decay alpha, beta, and gamma in the sample itself. It can be calculated using Eq. (29) but here C is the residual sample activity in Curies; E is the average energy of charged particles in MeV.

4.0 Special irradiation being taken up recently in research reactors at Trombay

Other than the regular samples which are irradiated in designated positions, some of the new irradiation activities recently being taken up in Trombay research reactors are briefly discussed below

4.1 Doping of Silicon

Neutron transmutation doping (NTD) is the process of creating non-radioactive impurity isotopes from the host atoms of a material by thermal neutron irradiation & subsequent radioactive decay. In NTD of Si, specifically, phosphorus dopant atoms are produced by transmutation of ^{30}Si into ^{31}P by thermal neutron capture in nuclear research reactors. In conventional doping methods, the concentration of dopant atom is found to be inhomogeneous and so the resistivity, which leads to formation of hot spot and undesirable variation in the parameters like blocking voltage, turn-on characteristics, on-state voltage drop, reverse recovery, turn-off time etc. In NTD-Si technique, greater spatial uniformity of dopant concentration as well as precise control over the resistivity is achieved. Hence, NTD-Si has been used extensively in manufacturing of high-power semiconductor devices like thyristor (SCR), insulated-gate bipolar transistor (IGBT), integrated gate-commutated thyristor (IGCT), gate turn-off thyristor (GTO) etc.

The production process starts with ultra-pure polysilicon rod which is used to produce monocrystalline Si ingot, which is then taken up for initial characterization such as resistivity measurement and minority carrier life time (MCLT) measurement. The ingots are then irradiated according to irradiation plan. The length of irradiation is determined by the target resistivity. The design of Si-ingot irradiation assembly and the choice of irradiation site is such that a uniform neutron fluence profile is achieved. In parallel the actual neutron fluence can be measured either by activation detectors attached with the ingots or by online SPNDs. The irradiated ingot is then subjected to post-irradiation cooling and subsequent decontamination process. Now, the fast neutrons produce damage in the Si crystal during irradiation, resulting in increase in resistivity which must be repaired by an annealing process in a clean furnace so that predicted resistivity is reached. Finally wafer samples are taken from the ingot and various characteristics are re-measured such as resistivity variations, the carrier life time, impurities and the crystal deficiency. The stages of production are shown in **Figure-14**.

Figure-14: NTD-Si production stages

Several trial irradiations of small size silicon samples were carried out at Apsara-U to gather practical experience in various stages of NTD-Si, and a suitable position just outside reflector boundary has been found to be suitable (see **Figure-15**). As the concentration of dopant atoms will depend upon the thermal neutron fluence, the plot of thermal neutron fluence ($\phi \cdot t$) against inverse of resistivity ($1/\rho_{eff}$) will have a linear behaviour:

$$\phi \cdot t = \boldsymbol{K} \cdot \frac{1}{\rho_{eff}} \tag{30}$$

The slope of the line gives the value of doping factor, or resistivity-fluence correlation constant, called $\boldsymbol{K}$. From the trial irradiation data, if we plot thermal neutron fluence against inverse of resistivity of the silicon, as shown in **Figure-16**. We find for the designated irradiation position in Apsara-U, $\boldsymbol{K}$ = $2.75\pm0.05\times10^{19}$.

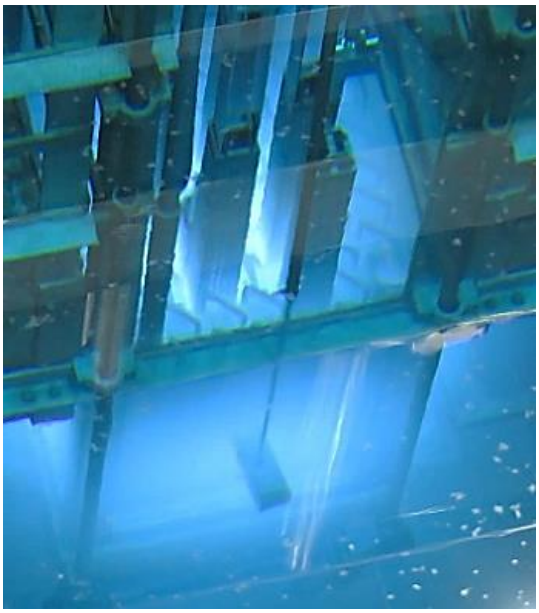

Figure-15: Trial irradiation of Si at outside reflector boundary position in Aspara-U

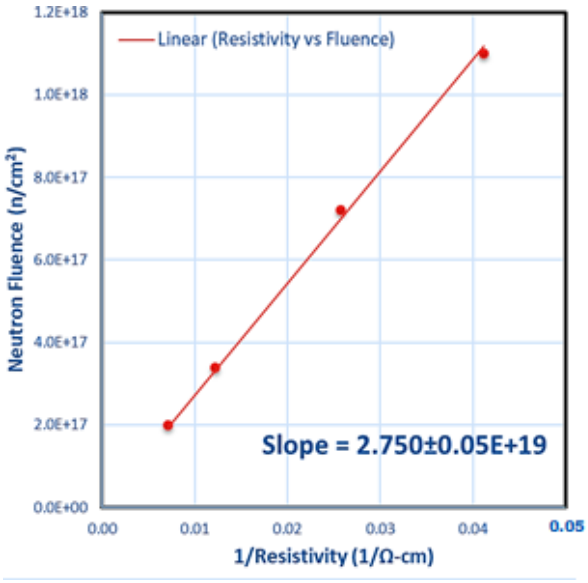

Figure-16: Resistivity-fluence correlation curve

For out of core irradiation under a fluence of 10^{17}-10^{18} n/cm^2, measured resistivity is found to be ~ 20 to 140 Ω-cm, which is adequate for power semiconductor device fabrication purpose. For commercial production of NTD-Si, it is possible to irradiate larger sized silicon (~ 4–8-inch diameter) ingot in Apsara-U.

4.2 Production of fission molly

Technetium-99m (^{99m}Tc) , the daughter product of ^{99}Mo, is one of the most commonly utilized radioisotope. It is very much suited for medical diagnostic applications because of the soft gamma (140 keV) produced by its radioactive decay. ^{99}Mo can be produced either by irradiating ^{98}Mo through (n,γ) reaction in the reactor (as currently being done in tray rods) or by fission route. However, the specific activity of ^{99}Mo is very low in case of direct irradiation route because of low neutron capture cross section of ^{98}Mo and due to the fact that only natural abundance of ^{98}Mo is only ~ 24%. On the other hand, fission yield of ^{99}Mo is around 6%. As a result, very high specific activity of ^{99}Mo can be produced via the fission route. To achieve this high specific ^{99}Mo activity, a special tray rod has been designed with two fission molly targets, each with 6 Lightly Enriched Uranium (LEU) fuel plates (^{235}U enrichment ~ 19.75±0.25 %) (see **Figure-17**).

Physics and safety analysis for the fission molly target has been carried out for Dhruva (F-11 core position) and Apsara-U reactor (in-core Hollow Beryllium Plug or HBP position at D-5). Estimations for heating in the two fission moly targets were carried using Monte Carlo code. In case of Dhruva, considering reactor operating at the nominal power of 100 MW, heating due to fission at in-core

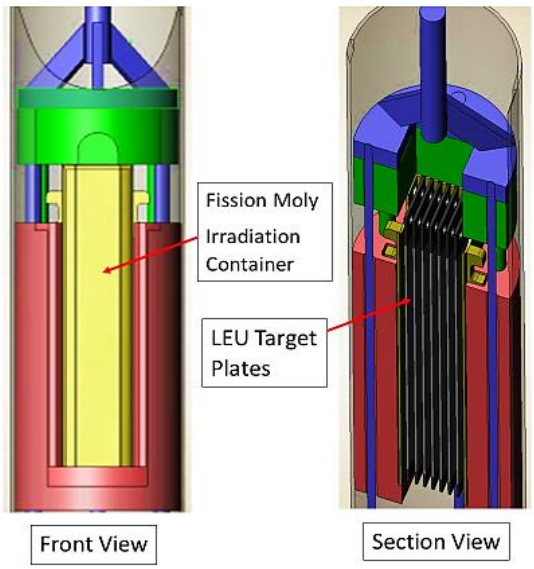

Figure-17: One of the two fission moly targets

irradiation position are estimated to be ~ 48 KW in upper target and ~ 39 KW in lower target at F-11 position. After 5 days' irradiation and 8 days of cooling, 99Mo activity is estimated to be ~ 360 Ci for reactor operation at 100 MW in two targets. The analysis was carried out using ORPAC-2.

Similarly, considering reactor operating at the nominal power of 2 MW, heating due to fission at in-core irradiation position are estimated to be ~ 13 KW in upper target and ~ 10 KW in lower target at D-5 position. After 5 days' irradiation and 5 days cooling ^{99}Mo activity is estimated to be ~ 77Ci. After 8 days of cooling, in case of both Apsara-U and Dhruva, the specific activity of ^{99}Mo remains about 10 KCi/g

5.0 Estimation and measurement of reactivity worth of shut off rods

Reactivity worth of shut off rods are one of the most critical physics parameters to ensure safe operation of the reactor. It may happen that loading of irradiation samples, change the reactivity worth of shut off rods. Thus, whenever a large disruption in core loading is anticipated, the reactivity worth of shut off rods are estimated by theoretical means and also measured via experimental methods.

5.1 Theoretical estimation

The reactivity worth can be estimated theoretically either via stochastic codes or deterministic codes. Monte Carlo method-based codes are able to simulate the reactor components and materials in quite exact manner, but generally need higher computation time to simulate enough particle history to provide results with good accuracy. Deterministic codes, on the other hand, solve neutron transport equation to generate the results quickly, but may not be able to handle intricate and non-standard geometries. Usually, deterministic calculation is done by first dividing the core into individual two-dimensional lattices. Neutron transport method-based codes, such as WIMSD [19], DRAGON5 [18] etc. are used to generate few group homogenized macroscopic neutron cross sections for each lattice type. Then, all lattices are represented in a neutron diffusion method-based three-dimensional core level code such as NEMSQR [20]. The core level code is able to compute important physics parameters such as core neutron multiplication factor (k). The measure of k is representative of the excess (or lack thereof) reactivity of the core, for example k=1 means core is just critical and has no excess reactivity, k>1 means the core is "super-critical" and k<1 means the core is "subcritical". The difference between the neutron multiplication factors, with and without the presence of shut off rods, is indicative of the reactivity worth of the said rods.

$$\rho = \frac{1}{k_{with}} - \frac{1}{k_{without}} \tag{31}$$

Usually, both of these methods are employed to verify the results.

5.2 Experimental methods

Due to high absorbing nature of shut off rods and uncertainty related to input parameters used in theoretical estimation, reactivity worth measurements are also performed to verify the estimated worth. Few of the most popular methods are:

5.2.1 Asymptotic period measurement

When a critical reactor is perturbed by a step change in properties, the asymptotic period may be determined from the response R(t) of neutron detectors by $\frac{1}{T} = \frac{d\left(\ln R(t)\right)}{dt}$; then the period reactivity relation $\rho = \frac{\Lambda}{T} + \sum_{i=1}^{6} \frac{\beta_i}{1+\lambda_i T}$ can be used to infer the reactivity ρ. Here Λ is mean neutron generation time. This method is limited to super critical reactor (ρ>0) measurements, for which above equation can be written as $\rho \approx \sum_{i=1}^{6} \frac{\beta_i}{1+\lambda_i T}$

5.2.2 Rod drop method

In this method, the control rod, whose worth is to be measured, is raised to the top limit and the reactor power is stabilized at low power (P_0) with the help of other control rods. Then, that particular rod, which is at top limit, is dropped. The response of the neutron detector immediately before ($R_0 \sim n_0$) and after ($R_1 \sim n_1$) a shut off rods is dropped into a critical reactor are related by $n_1 / n_0 = \beta / \left(\beta - \rho_1\right)$, which allows determination of reactivity worth of the rod.

5.2.3 Source jerk method

For a sub critical system that is maintained at equilibrium with neutron concentration as $n_{0,}$ and neutron precursor (fission products which emit delayed neutrons during decay) concentration as $c_{i0,}$ only by the presence of an extraneous neutron source rate (S), the neutron balance equation is:

$$\left(\frac{\rho-\beta}{\Lambda}\right) n_0 + \sum_{i=1}^{6} \lambda_i c_{i0} + S = 0 \tag{32}$$

If the source is then jerked, the prompt jump approximation for the neutron density immediately after the source jerk is $\left(\frac{\rho-\beta}{\Lambda}\right) n_1 + \sum_{i=1}^{6} \lambda_i c_{i0} = 0$ because the delayed neutron precursor population will not change immediately. These equations and the equilibrium precursor concentrations $c_{i0} = \frac{\beta_i n_0}{\lambda_i \Lambda}$ may be used to relate the response of the neutron detector immediately before ($R_0 \sim n_0$) and after ($R_1 \sim n_1$) the source jerk to the reactivity of the system.

5.2.4 Sub-critical method

In this method, stabilized detector (usually fission counters in pulse mode) readings are noted for three sub-critical states of the reactor-first for a given reference core configuration, second for the same core with a known load ρ_1 installed (say, fine control rod) and the third with the shut off rods inside the reference core. From the observed readings, reactivity worth of the rods (ρ_2) can be calculated. If C_0, C_1, C_2 are the response of fission counter, then the reactivity worth of the control rod is given by:

$$\rho_2 = \rho_1 \times \frac{C_1}{C_2} \times \frac{C_0 - C_2}{C_0 - C_1} \tag{33}$$

5.2.5 Inverse kinetics method

After reactor shut down, power profile as a function of time is stored in a fast recorder and the data is then used to estimate reactivity worth of shut off rods by inverse point kinetics method-based computer codes, such as POINTK [21]. The code solves the following set of equations:

$$\rho(t+\Delta t)=\beta+\frac{\Lambda}{n(t)}\left(\frac{n(t+\Delta t)-n(t)}{\Delta t}-\sum_i \lambda_i c_i(t+\Delta t)-s(t+\Delta)\right) \tag{34}$$

$$c_i(t+\Delta)=e^{-\lambda_i \Delta t}\left[c_i(t)+\frac{\beta_i}{\Lambda}\int_0^{\Delta t} n(t+\Delta t')e^{-\lambda_i(\Delta t-\Delta t')}d(\Delta t')\right] \tag{35}$$

6. Conclusion

Reactor physics is essential in safe and smooth operation of the reactors in Trombay. Reactor physicists undertake various analyses of core physics (core loading, reactivity worth of shut down devices etc.), thermal hydraulic analysis for fuel thermal safety, safety evaluation of experimental and irradiation assemblies etc. Reactor physics calculations are required for activities related to not only reactor operation but also for in-pile irradiations of the samples. The frequency and complexities of these calculations make it necessary to use computer codes. The computer "Operational Reactor Physics Analysis Code-2" (ORPAC-2) has been upgraded with these issues in mind. It is designed with user-friendly GUI to streamline the input process of required information from user side and offers clearly interpreted output, including reactivity load penalty, irradiation heating, required shielding and cooling time for handling of irradiated samples etc. Moreover, knowledge of the reactivity worth of all safety devices is very important for safe reactor operation. The values of reactivity worth of shut off rods are thus estimated theoretically, as well as assessed experimentally, whenever a significant change in core loading is postulated.

Acknowledgement

The authors are thankful to all the officers working in the Reactor Physics & Nuclear Engineering Section for providing technical support. The authors are also thankful to ROD for providing necessary help in carrying out irradiation of Silicon samples. Thanks are due to Shri H. G. Gujar, Head, Research Reactor Services Division for continuous support to sectional activities. Finally, the authors are grateful to Shri C. G. Karhadkar, Director, Reactor Group, for his continuous motivation and encouragement.

References

[1] S. Agarwal, C. Karhadkar, A. Zope and K. Singh, "Dhruva: Main design features, operational experience and utilization," *Nuclear Engineering and Design*, vol. 236, no. 7-8, pp. 747-757, 2006.

[2] S. Sengupta, S. Chafle, S. Mammen, K. Sasidharan and V. Raina, "Critical facility for AHWR and PHWRs," in *Proceedings of International Conference on Peaceful Uses of Atomic Energy* , New Delhi, 2009.

[3] T. Singh, P. Pandey, T. Mazumdar, K. Singh and V. K. Raina, "Physics design of 2 MW Upgraded Apsara Research Reactor," *Annals of Nuclear Energy*, vol. 60, pp. 141-156, 2013.

[4] J. Kumar, P. Pandey and S. Banerjee, "Final Safety Analysis Report (rev. 0) for Reactor Core Physics (Apsara-U)," BARC, 2021.

[5] Y. S. Rana, A. Mishra, T. Singh, P. V. Varde, S. Bhattacharya, S. Samanta, R. Kumar, A. Mallick, K. Deo, U. Kannan, S. Prasad and R. Sharma, "Life Cycle Reliability and Safety Engineering," *Thermal neutron flux measurements in self-serve and tray rod facilities of Dhruva reactor,* vol. 6, p. 149–166, 2017.

[6] J. Kumar, Y. S. Rana, T. Singh and P. V. Varde, "Monte Carlo modelling of Dhruva Reactor and characterization of experimental beam holes," BARC, 2018.

[7] A. Das, P. Pandey and T. Singh, "Neutron-gamma flux distributions in cylindrical beam tubes," *Life Cycle Reliability and Safety Engineering,* p. 161–169, 2020.

[8] Y. S. Rana and T. Singh, "Design & Operating Manual (Rev. 2)," BARC, 2020.

[9] T. Ryves, "A New Thermal Neutron Flux Convention," *Metrologia,* vol. 5, no. 4, pp. 119-124, 1969.

[10] T. Singh, P. Pandey, Y. Rana, P. Varde and S. Bhattacharya, "Estimation and measurement of Mo99 activity in natural molybdenum metal and oxide samples irradiated in Dhruva," BARC, 2017.

[11] Y. Rana, A. Mishra, T. Singh, P. Varde, S. Samnta, R. Kumar, A. K. Mallick, K. Deo, U. Kannan, S. Prasad and R. Sharma, "Experimental measurement and theoretical simulations for neutron flux in self-serve facility of Dhruva reactor," BARC, 2016.

[12] K. Inour and K. Katori, "Measurements of deviation from 1/E distribution in," *Journal of Nuclear Science and Technology,* vol. 1, no. 1, pp. 1-6, 1964.

[13] R. Sogbadji, B. Nyarko, E. Akaho and R. Abrefah, "Determination of Neutron Fluxes and Spectrum Shaping Factors in Irradiation Sites of Ghana'S Miniature Neutron Source Reactor (mnsr) by Activation Method After Compensation of Loss of Excess Reactivty," *World Journal of Nuclear Science and Technology,* vol. 1, no. 2, pp. 50-56, 2011.

[14] J. Kumar, K. Singh and K. Singh, "Operational Reactor Physics Analysis Code (ORPAC)," BARC, 2007.

[15] A. Croff, "ORIGEN2: a revised and updated version of the Oak Ridge isotope generation and depletion code," Oak Ridge National Lab, 1980.

[16] D. Cullen, "PREPRO 2019: 2019 ENDF/B Pre-processing Code," 2019.

[17] D. A. Brown, M. B. Chadwick, R. Capote, A. C. Kahler, A. Trkov, M. Herman, A. A. Sonzogni, Y. Danon, A. D. Carlson, M. Dunn, D. L. Smith, G. Hale, G. Arbanas, R. Arcilla, C. Bates, B. Beck, B. Becker, F. Brown, R. Y. Casperson and Y. Zhu, "ENDF/B-VIII.0: The 8th Major Release of the Nuclear Reaction Data Library with CIELO-project Cross Sections, New Standards and Thermal Scattering Data," *Nuclear Data Sheets,* vol. 148, pp. 1-142, 2018.

[18] A. Hébert, "DRAGON5 and DONJON5, the contribution of École Polytechnique de Montréal to the SALOME platform," *Annals of Nuclear Energy,* vol. 87, no. 1, pp. 12-20, 2015.

[19] J. Askew, F. Fayer and P. Kemshell, "A General Description of Lattice Code WIMSD," *Journal of the British Nuclear Scociety,* p. 564, 1966.

[20] T. Singh, T. Mazumdar and P. Pandey, "NEMSQR: A 3-D multi group diffusion theory code based on nodal expansion method for square geometry," *Annals of Nuclear Energy,* vol. 64, pp. 230-243, 2014.

[21] P. Pandey, T. Mazumdar, T. Singh and P. Varde, "Worth measurement of reactiviry devices using Inverse Kinetics method," BARC, 2015.

[22] H. Yücel H and M. Karadag, " Experimental determination of the α-shape factor in the 1/E(1+α) epithermal-isotopic neutron source-spectrum by dual monitor method.," *Annals of Nuclear Energy,* vol. 31, p. 681–695, 2004.

Author Information

Dr. Tej Singh, is a postgraduate in Physics from Agra University, Uttar Pradesh, joined Research Reactor Services Division in the year 1990 after completion of one year orientation course in Nuclear Engineering from 33rd batch (Physics Discipline), BARC training school. He did his PhD in physics from Mumbai University. His areas of expertise are reactor physics, safety & shielding design optimization, core management studies & operational reactor physics of present and upcoming research reactors. At present, he is heading the reactor physics and nuclear engineering section of Research Reactor Services Division. He is responsible for providing reactor physics support for safe and smooth operation of the research reactors at BARC. He has developed computer codes NEMSQR and HEXNEM, based on nodal expansion method, for reactor core design calculations & core management studies, respectively. He also developed safety analysis codes IQSHEX & DINHEX Space time kinetics based on nodal expansion methods and RITAC & SACRIT based on point kinetics model coupled with thermal hydraulics for research & power reactors for analysis of reactivity-initiated accidents.

Production and radiochemical processing of radioisotopes for use in healthcare utilizing research reactors at Trombay – Present scenario and future prospects

Sudipta Chakraborty

Radiopharmaceuticals Division, Bhabha Atomic Research Centre, Trombay, Mumbai-400085, India
(*Author email:* sudipta@barc.gov.in)

1.0 Introduction

Production, radiochemical processing and deployment of radioisotopes for their use in human healthcare has come a long way since its inception in India after the commissioning of Apsara reactor in 1956. Commissioning of Radiological Laboratories at Trombay in 1969 and availability of CIRUS reactor marked the modest beginning of radioisotope production at a routine commercial scale in India. Availability of 100 MW Dhruva research reactor in 1985 was an important milestone in the development and implementation of indigenous nuclear technology in the field of radioisotope production, which resulted in augmentation of production capacity. Radioisotopes produced in research reactors find extensive applications in several fields that include human healthcare, industry, agriculture and research. Production of radioisotopes in research reactors to service different sectors of economic significance constitutes an important ongoing activity at Bhabha Atomic Research Centre (BARC). Radiochemicals Section of Radiopharmaceuticals Division, BARC shoulders the responsibility to ensure the steady availability of reactor produced radioisotopes in suitable radiochemical formulation as per their requirement in India.

The technique of radioisotope production and radiochemical separation are being continually improved. Radioisotopes have become an indispensable tool in most area of human endeavour. Radioisotope production and their applications are among the most prominent peaceful uses of atomic energy. One of the most important contributions of nuclear science has been the vital application of radioisotopes in medicine, for both diagnosis and therapy.
Last couple of decades have witnessed momentous development in the use of radioisotopes in human healthcare, both diagnostic and therapeutic radiopharmaceuticals using a variety of radionuclides have contributed to this. Currently, a large number of radiopharmaceuticals are produced and supplied by commercial manufacturers for patient application in the hospitals. Availability of radioisotopes with attractive decay characteristics in suitable radiochemical form have contributed to the accelerated growth of nuclear medicine. In recent times, the therapeutic products have come into greater prominence. With the revival of interest in therapeutic applications, identification of promising radioisotopes having attractive features suitable for radiotherapy, their production and radiochemical preparation has assumed importance.

In this article, aspects of production, radiochemical processing and deployment medically useful radioisotopes namely, ^{99}Mo, ^{131}I, ^{153}Sm and ^{177}Lu, routinely produced in Dhruva research reactor at BARC, are discussed. Apart from these, various aspects of large-scale production of relatively unexplored reactor-produced radioisotopes and new routes of production of radioisotopes established for medical use are also discussed. Introduction of 2 MW Apsara-U research reactor is another major milestone in production of new radioisotopes for nuclear medicine. Fast neutron flux available in Apsara-U have been successfully utilized in the production of NCA ^{64}Cu by ^{64}Zn(n,p)^{64}Cu route.

2.0 Radioisotope production utilizing Dhruva reactor for nuclear medicine

Radioisotopes are produced mainly by thermal neutron activation of suitable target chemical in Dhruva research reactor, Trombay. Target chemicals are neutron irradiated from few days to several weeks at neutron flux in the range of 1.8×10^{13} n.cm^{-2}.s^{-1} to 1.8×10^{14} n.cm^{-2}.s^{-1}. Measured amounts of respective target to be irradiated in the reactor for production of radioisotopes are weighed and sealed in standard aluminum capsules by cold welding (**Fig. 1**). Certain precious target materials, particularly isotopically enriched targets are first encapsulated in quartz ampoules which are placed inside the irradiation containers. The amount of target is calculated and optimized for obtaining the desired radioactivity content on irradiation at a known neutron flux for adequate length of time duration.

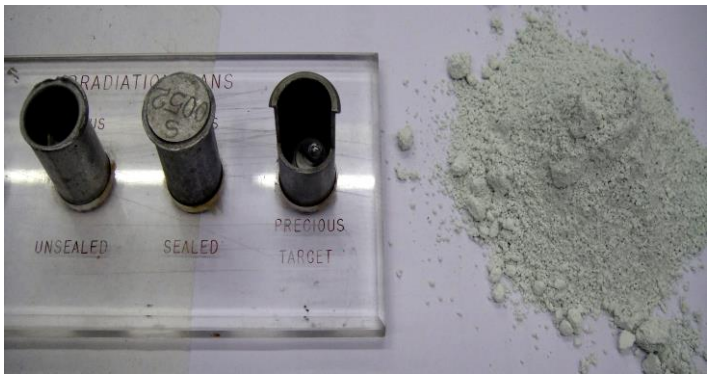

Fig. 1. Target encapsulation for irradiation

Presently, two tray rods are dedicated for irradiation of targets for regular production radioisotopes. **Table 1** lists medically useful radioisotopes routinely produced in Dhruva research reactor along with target chemicals, nuclear reactions involved in their production.

Table 1. List of medically useful radionuclides regularly produced in Dhruva reactor

Radio-isotope	Target used	Activation cross section (b)	Natural abundance (%)	Nuclear reaction	Frequency of production
^{99}Mo	MoO_3 (natural)	0.13	^{98}Mo-24.4%	$^{98}Mo(n,\gamma)^{99}Mo \xrightarrow{\beta^-} {}^{99m}Tc$	Weekly
^{131}I	TeO_2 (natural)	0.18	^{130}Te-34.5%	$^{130}Te(n,\gamma)^{131}Te \xrightarrow{\beta^-} {}^{131}I$	Weekly
^{153}Sm	Sm_2O_3 (enriched: 98.6% ^{152}Sm)	206	^{152}Sm-26.7%	$^{152}Sm(n,\gamma)^{153}Sm$	Weekly
^{177}Lu	Lu_2O_3 (enriched: 74.5% ^{176}Lu)	2065	^{176}Lu-2.59%	$^{176}Lu(n,\gamma)^{177}Lu$	Weekly
^{125}I	Xe gas (natural)	111	^{124}Xe-0.1%	$^{124}Xe(n,\gamma)^{135}Xe \xrightarrow{Ec} {}^{125}I$	Quarterly
^{90}Y	Y_2O_3 (natural)	1.28	^{89}Y-100%	$^{89}Y(n,\gamma)\,^{90}Y$	Monthly
^{166}Ho	Ho_2O_3 (natural)	61.2	^{165}Ho-100%	$^{165}Ho(n,\gamma)\,^{166}Ho$	Monthly

Detailed protocols for production and radiochemical processing of four major radioisotopes routinely produced for medical use are as follows:

(i) ^{99}Mo

Molybdenum-99 is the parent radionuclide for ^{99m}Tc [$T_{1/2}$ = 6.02 h and E_γ = 140 keV], which is estimated to be used in about 30 million medical diagnoses annually throughout the world and is considered as the workhorse of nuclear medicine procedures. Availability of ^{99m}Tc for preparation of diagnostic agents is ensured in the form of ^{99}Mo/^{99m}Tc generator system from which ^{99m}Tc is separated at regular intervals. ^{99}Mo for this purpose is produced by thermal neutron activation of natural MoO_3 target and 10-50 Ci of ^{99}Mo is processed and supplied weekly from BARC for nuclear medicine applications. The specific activity of ^{99}Mo varies between 600-1000 mCi/g of Mo depending on power at which Dhruva is operated. Irradiated natural MoO_3 target is dissolved in 4 M NaOH solution with addition of H_2O_2 as oxidizing agent to obtain [^{99}Mo]MoO_4 solution as the radiochemical precursor to obtain ^{99m}Tc from ^{99}Mo/^{99m}Tc gel generators.

(ii) ^{131}I

Iodine-131 in the form of [^{131}I]NaI radiochemical is extensively used in the diagnosis and treatment of thyroid disorders including differentiated thyroid cancer. Iodine-131 decays by emission of both β^--particles with a maximum energy of 0.61 MeV and γ photons [principal γ photon energy 364 keV (81%)]. The 8.04 d half-life is logistically favorable for shipment of ^{131}I radiopharmaceuticals to places far away from the reactors. With expanding areas of applications and growing interest in the use of ^{131}I labeled radiopharmaceuticals, the domestic demand of ^{131}I has increased several folds over the last decade. In the quest for an effective method for large-scale routine production of ^{131}I to cater the increasing domestic requirements, dry distillation technology for radiochemical separation of ^{131}I from neutron irradiated natural TeO_2 target was developed [1]. Briefly, the procedure involves heating of neutron irradiated high purity TeO_2 target at 740° C inside a furnace with simultaneous purging the ^{131}I released using an inactive carrier gas and trapping it in NaOH solution containing Na_2SO_3 to obtain ^{131}I as radiochemically pure [^{131}I]NaI solution [1]. The set-up for radiochemical separation of ^{131}I by dry distillation method inside the shielded glove box is shown if **Fig. 2**. The reported method has been successfully used for the routine production of 30-60 Ci of ^{131}I every week. Iodine-131 produced is utilized for the preparation of [^{131}I]MIBG, [^{131}I]NaI therapeutic capsules, ^{131}I-lipiodol and other ^{131}I labeled biomolecules apart from its regular use as orally administered doses of [^{131}I]NaI solution.

Fig. 2. Set-up for radiochemical separation of ^{131}I by dry distillation method inside the shielded glove box

(iii) ^{153}Sm

Samarium-153 [$T_{1/2}$ = 46.3 h] decays by emission of both β^--particles with a maximum energy of 0.81 MeV and γ photons [principal γ photon energy 103 keV (28%)]. Favorable nuclear characteristics coupled with feasibility of its large-scale production made this radioisotope a good choice for palliative care of painful skeletal metastases. From a modest beginning of 1 batch per month in year 1998, around 5 Ci of ^{153}Sm is produced every week for formulation of [^{153}Sm]Sm-EDTMP (EDTMP = Ethylenediaminetetramethylene phosphonic acid) radiopharmaceutical. Samarium oxide enriched in ^{152}Sm (98.6%) is used for production of ^{153}Sm. About 5 mg of target is encapsulated by cold-press welding in an aluminum container is irradiated in Dhruva reactor at a thermal neutron flux of ~1.2×10^{14} n.cm^{-2}.s^{-1} for 3-7 days. Under the stated optimized conditions of irradiation, the specific activity ^{153}Sm is found to be ~ 1.2 Ci/mg at EOI, which is sufficient for preration of [^{153}Sm]Sm-EDTMP for its end use palliative care painful skeletal metastases in cancer patients.

(iv) ^{177}Lu

Lutetium-177 decays to stable ^{177}Hf with a half-life of 6.65 d by emission of β^- particles having E_{max} of 497 keV (78.6%), 384 keV (9.1%) and 176 keV (12.2%). The emission of low-energy gamma photons [E_γ=113 keV (6.6%), 208 keV (11%)] enable imaging and therapy with the same radiolabeled preparation and allow dosimetry to be performed before and during treatment as well. Direct thermal neutron activation of enriched (in ^{176}Lu) lutetium target in Dhruva could be utilized to produce ^{177}Lu having specific activity more than 20 mCi/mg, which can be used for targeted cancer therapy applications.

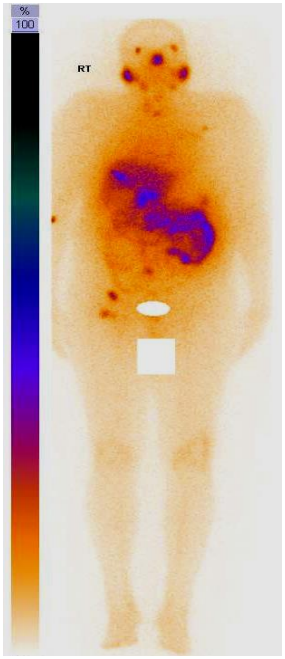

Fig 3. A typical post-therapy scan of a patent suffering from prostate cancer with liver metastases 24 hrs after administration of therapeutic dose of [^{177}Lu]Lu-PSMA-617 indicating site specific localization of the formulation

Our pursuit of (n,γ)^{177}Lu method of production of ^{177}Lu for targeted tumor therapy in India was driven mainly by the need to provide the required activity of ^{177}Lu for its use in the treatment of patients suffering from neuroendocrine tumor (NET) at an affordable cost. Evolution and continued success of [^{177}Lu]Lu-DOTA-TATE and [^{177}Lu]Lu-PSMA-617 therapy in our country, has been, in large part, due to the cost-effective availability of ^{177}Lu of required quality. The specific activity of indigenously produced ^{177}Lu available every week at nuclear medicine clinics in India is around 18-20 mCi/mg, considering the decay loss of 48 h during transit. This is adequate to formulate ^{177}Lu-labeled target specific biomolecules with specific activity of >1 mCi/μg of biomolecule with high radiochemical purity, which is the benchmark requirement for target cancer therapy [2].

Radiopharmaceuticals Division is currently supplying 25-30 Ci of radiopharmaceutical grade [^{177}Lu]$LuCl_3$ radiochemical every week to the leading nuclear medicine centres across India. More than 100 cancer patients receive ^{177}Lu-therapy every week from this. A typical post-therapy scan of a patient suffering from neuroendocrine originated cancer with liver metastases recorded 24 h after administration of therapeutic dose of [^{177}Lu]Lu-PSMA-617 is given in **Fig. 3** emphasizing the clinical utility of BARC [^{177}Lu]$LuCl_3$.

3.0 Future prospective -emerging radioisotopes and their newer applications

With the successful utilization of radioisotopes in various nuclear medicine procedures, both diagnostic and therapeutic, efforts are on to identify and establish newer radioisotopes with attractive radionuclide features and production feasibility using Dhruva and Apsara-U. In this regards, reactor production and radiochemical processing of radioisotopes such as ^{64}Cu, ^{90}Y, ^{47}Sc, no-carrier added ^{177}Lu and ^{161}Tb are our focus of attention.

Copper-64 [$T_{½}$ = 12.7 h., EC 45%, β^- 37.1%, β^+ 17.9%) is a promising radionuclide for positron emission tomography (PET) imaging, which is generally produced by ^{64}Ni(p,n)^{64}Cu reaction in a cyclotron. Despite excellent attributes of ^{64}Cu for PET imaging, utility of this radioisotope is still limited to countries having good cyclotron facilities and excellent production logistics. We have explored the feasibility of using ^{64}Cu produced in a research reactor by (n,p) route using fast neutron flux of Apsara-U reactor. A robust radiochemical separation technique based on 2-step solvent extraction using dithizone as extractant was developed to obtain [^{64}Cu]$CuCl_2$ in no carrier form from irradiated ZnO target [3]. [^{64}Cu]$CuCl_2$ solution thus obtained was successfully used as a probe for tumor imaging by PET. **Fig. 4** shows PET image of brain of a suspected glioblastoma patient after administration of [^{64}Cu]$CuCl_2$ showing stite-specific localization of Cu^{2+} at tumor lesion.

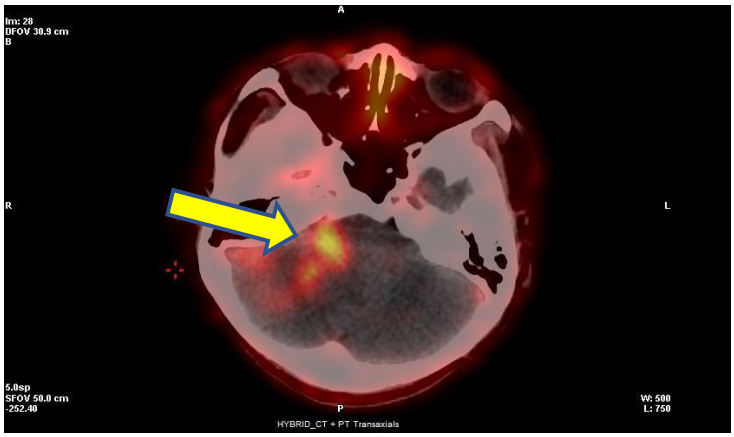

Fig. 4. PET image of brain of a suspected glioblastoma patient after administration of [^{64}Cu]$CuCl_2$ showing stite-specific localization of Cu^{2+} at tumor lesion

In another significant development, we have, for the first time, successfully demonstrated the suitability of ^{90}Y [$T_{1/2}$ = 64.1 h, $E_{\beta(max)}$ = 2.28 MeV] produced by neutron activation route in Dhruva reactor in the treatment of arthritis of knee joints in the form of ^{90}Y-labeled hydroxyapatite (HA) microparticles [4]. The treatment efficacy of this product is clearly demonstrated in **Fig. 5,** which shows the bone scans of the arthritic knee joints of a patient at different time post administration of 185 MBq of ^{90}Y-HA preparation.

Holmium-166 [$T_{1/2}$ = 26.9 h, $E_{\beta(max)}$ = 1.85 MeV, E_γ = 81 keV (6.4%)] also holds good promise as a therapeutic radioisotope in India, thanks to the feasibility of its large-scale production in adequate specific activity. We have demonstrated its potential in treatment of arthritis [5], which could be extended to the treatment of liver cancer and multiple myeloma. Scandium-47 [$T_{½}$ = 3.35 d, $E_{\beta(max)}$ = 600 keV, Eγ = 159.4 keV (68.3%)] has excellent attributes for use in nuclear medicine as an intrinsically theranostic radioisotopes. Feasibility of production of ^{47}Sc have already been investigated following ^{46}Ca(n,γ)^{47}Ca$\xrightarrow{\beta^-}$ ^{47}Sc route using thermal neutron flux of Dhruva as well as following ^{47}Ti(n,p)^{47}Ca route using fast neutron flux in Apsara-U.

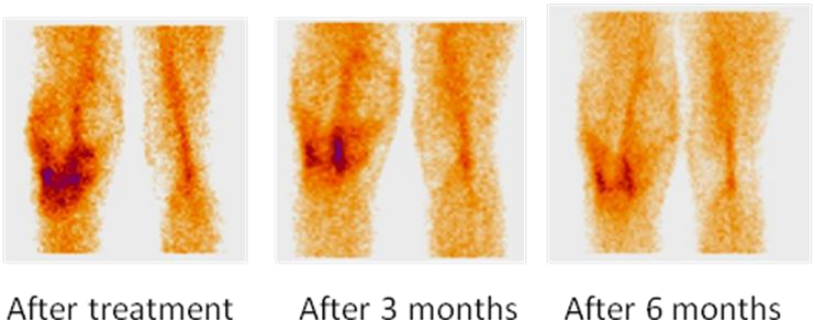

Fig 5. Bone scans of the arthritic knee joints of a patient at different time post administration of 185 MBq of ^{90}Y-hydroxyapatite showing the therapeutic efficacy of the preparation

Acknowledgements

Time bound production, radiochemical processing and supply of radioisotopes for clinical use requires excellent team work. This is an on-going program and several people have contributed significantly to the success of the programme over many years. The authors gratefully acknowledge their contributions and specially thank the staff members of Radiochemicals Section, and Irradiation Co-ordination Group of Radiopharmaceuticals Division, BARC.

References

[1] R.N. Ambade, S.N. Shinde, M.S.A. Khan, S.P. Lohar, K.V. Vimalnath, P.V. Joshi, S. Chakraborty, M.R. A. Pillai and A. Dash. J Radioanal Nucl Chem 303 (2015) 451.

[2] S. Chakraborty, K. V. Vimalnath, S.P. Lohar, P. Shetty and A. Dash. J Radioanal Nucl Chem 302 (2014) 233.

[3] R. Chakravarty, A. Rajeswari, P. Shetty, K. C. Jagadeesan, Ramuram, S. Jadhav, H.D. Sarma, A. Dash, S. Chakraborty. Appl Radiat Isot (2020) 109341.

[4] K.V. Vimalnath, S. Chakraborty, A. Rajeswari, H.D. Sarma, J. Nuwad, U. Pandey, K. Kamaleshwaran, A. Shinto and A. Dash. Nucl Med Biol 42 (2015) 455.

[5] S. Chakraborty, K. S. Sharma, A. Rajeswari, K. V. Vimalnath, H. D. Sarma, U. Pandey, Jagannath, R. S. Ningthoujam, R. K. Vatsa and A. Dash. J Mater Chem B 3 (2015) 5455.

Author Information

Dr. S. Chakraborty is presently heading Radiochemicals Section of Radiopharmaceuticals Division and also serving as an Associate Professor of Homi Bhabha National Institute. He is looking after the production, radiochemical processing and deployment of radioisotopes for use in human healthcare and leading a team carrying out frontline research on radiolabeled probes for molecular imaging and targeted cancer therapy. He did his M.Sc. in Chemistry from Jadvapur University, Kolkata and subsequently joined Bhabha Atomic Research Centre (BARC) in 1999 graduating from 42nd Batch of Training School (Chemistry Discipline). He did his Ph.D. from University of Mumbai in 2005. He has worked as a visiting research scientist at the School of Health Sciences, Purdue University, USA, during 2008-2009. He has also worked as visiting scientist in Institute of Nuclear Chemistry, Johannes-Gutenberg University, Germany, as a part of Indo-German Bilateral Research Project. He is has served as Principal Scientific Investigator/Consultant for a number of research projects of International Atomic Energy Commission (IAEA). He has co-authored 128 papers in peer-reviewed international journals.

Clinical Applications of indigenous ^{177}Lutetium: a decade of experience

Sandip Basu[1,2]

[1]Radiation Medicine Centre, Bhabha Atomic Research Centre, Tata Memorial Centre Annexe, Jerbai Wadia Road, Parel, Mumbai - 400012, India, [2]Homi Bhabha National Institute, Mumbai, India
(*Author email:* drsandipb@gmail.com)

1.0 Introduction

Targeted radionuclide therapy and Nuclear Theranostics in India have been greatly boosted by the production of ^{177}Lu from enriched ^{176}Lu targets via the direct (n,γ) route in the medium-flux Dhruva reactor and its successful radiolabelling with various ligands, either directly or through bifunctional chelating agents, in the Radiopharmacy units of the country (*1-2*). Based upon this, 3 radionuclide therapies have been developed over the last decade that has been widely employed clinically for treatment of cancer patients:

(a) ^{177}Lu-DOTA-TATE Peptide Receptor Radionuclide Therapy (PRRT) in metastatic/advanced neuroendocrine neoplasms (NENs)

(b) ^{177}Lu-PSMA-617 peptide receptor radioligand therapy (PRLT) in metastatic castration resistant prostate cancer (mCRPC) and

(c) ^{177}Lu-EDTMP for painful skeletal metastasis from different cancers.

The physical characteristics of ^{177}Lutetium (Max β=497 keV, t1/2=6.7 days, γ=208 keV and half-life of 6.7 days) and relatively easy radiolabeling (related to the chemistry of the radiolanthanide Lu^{3+}) makes this a preferred and popular therapeutic radionuclide in the field of Nuclear Medicine. The two major success stories in targeted radionuclide therapy in cancer over the past decade have been development of a variety of cell-surface receptor targeted peptide-based radiopharmaceuticals, ^{177}Lu-DOTA-TATE and ^{177}Lu-PSMA-617. Both these receptor-based therapies are also *proof-of-concept* of the 'Theranostics' approach (popularly described as "*Treat what you see & See what you treat*"), which employs the combination of one radiotracer to identify/diagnose the disease (the diagnostic radiopharmaceutical, usually a PET based radiotracer) and the second radioactive molecule towards the same target to deliver treatment (the therapeutic radiopharmaceutical) (*1-7*).

With years of successful use & promising results, both these treatments have made in-roads into the main clinical treatment algorithms of metastatic neuroendocrine tumors and metastatic prostate cancer respectively and frequently being considered in the oncological parlance. We need to state here that India had been one of the frontrunners in these treatments, and the clinical PRRT & PRLT services in this country was a result of joint combined effort by the Radiation Medicine Centre (RMC), Bhabha Atomic Research Centre (BARC), and Gastrointestinal services of Tata Memorial Hospital (TMH) at the TMH-RMC premises, with strong support from the Reactor Group and Radiopharmaceutical division, Bhabha Atomic Research Centre and BRIT (*1, 5, 6, 7*). The indigenous production and availability have enabled these very specialized therapies to be delivered at a very affordable cost at RMC (BARC) which could be viewed as a major societal contribution of the Department of Atomic Energy (DAE) to this country (*1, 5, 6, 7*).

Two alternative routes are available for production of ^{177}Lu with adequate specific activity required for its utility in PRRT: (a) the first is the "direct" route which involves the thermal neutron activation of highly enriched (in ^{176}Lu) lutetium target [^{176}Lu (n, γ) ^{177}Lu] in research reactors with medium to high

thermal neutron flux. (b) The second route or the "indirect" route is based on neutron irradiation of highly enriched (in ^{176}Yb) ytterbium targets leading to the formation of no-carrier-added (NCA) ^{177}Lu from the β- decay of the short-lived activation product ^{177}Yb ($T_{1/2}$ =1.9h). The post-irradiation radiochemical processing in the former case involves simple dissolution of the irradiated target, whereas the latter route involves elaborate procedure to separate ^{177}Lu from ytterbium targets as well as its radionuclides. In India, more than 90% of the PRRT procedures (nearly all government centres and majority of the private centres) are undertaken using ^{177}Lu obtained via the first pathway indigenously in the research reactor.

A. [^{177}Lu]Lu-DOTATATE in Metastatic/Advanced Neuroendocrine Neoplasms

Somatostatin receptors (SSTRs), comprises of five somatostatin receptor family gene product proteins (*SSTR1* to *SSTR5*), of which high expression of SSTR2 are commonly observed in the Neuroendocrine tumors (NETs). Octreotide and lanreotide, two synthetic somatostatin analogs (SSAs) bind primarily to SSTR2 and SSTR5 and are used as therapeutic agents in patients with advanced NETs. Octreotate, the radioligand employed in peptide receptor radionuclide therapy (PRRT), differs from octreotide in that the C-terminal threoninol (corresponding amino alcohol) is replaced with threonine. The resultant effect is nine-fold increase in affinity for the SSTR-2 for [DOTA-0, Tyr 3]octreotate when compared with [DOTA-0,Tyr-3]octreotide. Thus, in summary, [^{177}Lu]Lu-DOTATATE (DOTATATE = DOTA^{0}-(Tyr^{3})-octreotate) used for treatment of metastatic or advanced Neuroendocrine tumors, primarily targets SSTR2 receptors with high affinity. The pre-treatment work-up entails PET/CT imaging of the NETs by the radiopharmaceuticals like ^{68}Ga-DOTA-TATE/^{68}Ga-DOTA-NOC, with semiquantitative Krenning's grading for decision making for the therapy (*1, 5, 6*). Several innovative clinical algorithms have been evolved over the last decade in the PRRT approach, which involves:

(A) expanding PRRT therapy in a wide spectrum of tumors with SSTR overexpression as their characteristics. We have, in our practice have employed PRRT in (i) Gastroenteropancreatic NENs (GEP-NENs), (ii) Metastatic NEN with unknown primary (CUP-NEN) (iii) Bronchopulmonary, Mediastinal and Thymic NENs, (iv) Medullary thyroid carcinoma (MTC), (v) non-[^{131}I]I-MIBG concentrating metastatic Paraganglioma & Pheochromocytomas, and (vi) other miscellaneous tumors (non-iodine concentrating metastasis of differentiated thyroid carcinoma or TENIS, metastatic Merkel Cell carcinoma, Meningioma, recurrent/inoperable Phosphaturic Mesenchymal Tumor and sinonasal neuroendocrine carcinoma). (*1*)

(B) Secondly, 'Sandwich Chemo-PRRT' in patients with avid [^{68}Ga]Ga-DOTATATE and [^{18}F]F-FDG uptake on dual tracer PET-CT, indicating a relatively aggressive tumor biology. (*1, 3*)

(C) Thirdly, employing PRRT in neoadjuvant setting (*1, 4*)

(D) Using PRRT in carcinoid heart disease that could be potentially helpful in enhancing the chances of corrective vulvular surgery. (*1*)

(E) Duo-PRRT regimen: Combining ^{90}Y-DOTATATE with ^{177}Lu-DOTATATE PRRT as sequential duo-PRRT to treat non-responding large-sized tumors. (*1*)

An illustrative example of *post-PRRT complete response* in a known patient of grade I pancreatic NET with multiple hepatic metastases is depicted below (*Fig 1*, reproduced with permission):

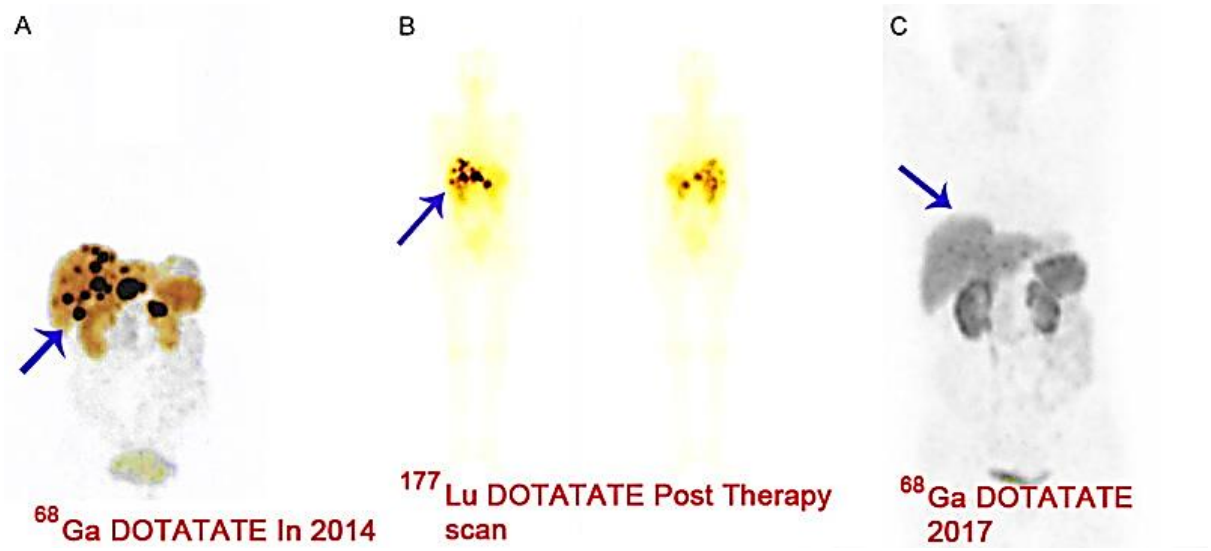

Fig 1. An illustrative example of *post-PRRT complete response* in a known patient of grade I pancreatic NET with multiple hepatic metastases

B. [^{177}Lu]Lu-PSMA-617 PRLT in Metastatic Castration Resistant Prostate Cancer (mCRPC)

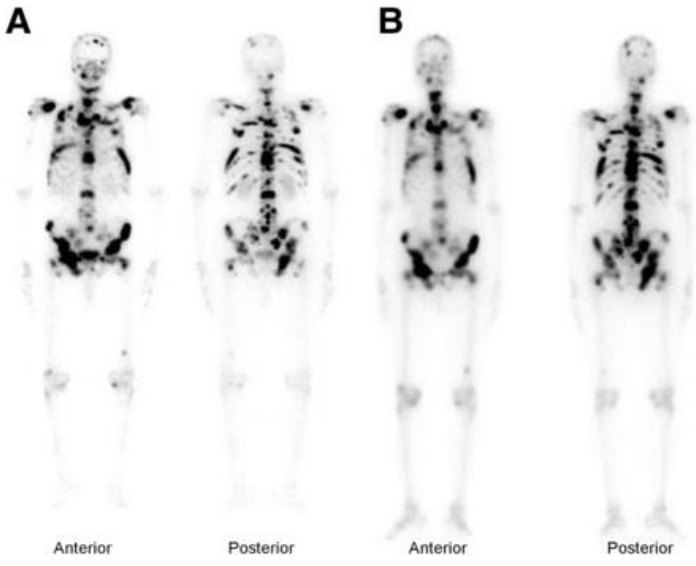

Fig 2. ^{99m}Tc-MDP bone scan **(A)** and post-therapy ^{177}Lu-EDTMP planar scan **(B)** of 69-y-old man with known case of prostate adenocarcinoma (Gleason score, 9; operated primary tumor) who presented with multiple painful skeletal metastases. Patient was on oral nonsteroidal antiinflammatory drugs 3 times per day (analgesic score, 3) and had received pelvic radiotherapy 6 mo previously. Parameters before 177Lu-EDTMP therapy: Visual Analogue scale (VAS), 9; Serum Bone-Alkaline Phosphatase (BAP), 109.6; EORTC Quality of life scale score, 68; Karnofsky Score, 80; ECOG score, 2. Post-therapy parameters: VAS, 4; BAP, 87; EORTC, 40; Karnofsky, 80; ECOG, 1. Post-therapy analgesic score was zero. (Reproduced with Permission).

Prostate-specific membrane antigen (PSMA) is a type II membrane glycoprotein, that is overexpressed in prostate cancer cells. PSMA protein comprises of a unique 3-part structure: a 19-amino-acid internal portion, a 24-amino-acid transmembrane portion, and a 707-amino-acid external portion. The PSMA gene is located on the short arm of chromosome 11 in a region that continues to be expressed in prostate cancer. Multiple small-molecule and low-molecular-weight peptidomimetic Glu-ureido–based PSMA inhibitor radioligands (PSMA-617, PSMA-11, PSMA-1007) have been clinically introduced for the diagnosis and radioligand therapy (RLT) of prostate cancer esp. in metastatic settings (mCRPC).

^{177}Lu-EDTMP has been developed as an attractive alternative to ^{153}Sm-EDTMP for systemic radionuclide therapy of bone pain palliation (*Fig 2*), in view of the logistical advantage of relatively longer half-life of ^{177}Lu and possibility of rationing it for other radiopharmaceuticals prepared with other ligands such as DOTATATE and PSMA-617 (*8*).

2.0 Foreseeing future developments with ^{177}Lu-based therapeutic radiopharamceuticals

Basic dosimetry work is currently in progress in the area of radioimmunotherapy (RIT) after tagging monoclonal antibodies with ^{177}Lu. The two such successful examples include, (I) radiolabelled anti-CD20 antibodies against lymphoma cells, where ^{177}Lu/^{131}I-Rituximab has been used for therapy of relapsed refractory lymphoma and (II) HER2/NEU receptor targeting on breast cancer cells by ^{177}Lu-trastuzumab for metastatic, advanced breast carcinoma. (III) The CXCR-4 receptor based Pentixafor/Pentixather ligands (for Multiple myeloma and Lymphoma) and (IV) αvβ-3 integrin targeting RGD peptides and (V) Tumour associated fibroblasts targeting FAPI (both of these being investigated in a wide range of cancers e.g. breast, lung, brain, TENIS), are other interesting developments in the field of Nuclear Theranostics, where ^{177}Lutetium is likely to find potential application as therapeutic radionuclide.

References:

1. Basu S, Chakraborty S, Parghane RV, Kamaldeep, Ranade R, Thapa P, Asopa RV, Sonawane G, Nabar S, Shimpi H, Chandak A, Vimalnath KV, Ostwal V, Ramaswamy A, Bhandare M, Chaudhari V, Shrikhande SV, Sirohi B, Dash A, Banerjee S. One decade of 'Bench-to-Bedside' peptide receptor radionuclide therapy with indigenous [^{177}Lu]Lu-DOTATATE obtained through 'Direct' neutron activation route: lessons learnt including practice evolution in an Indian setting. Am J Nucl Med Mol Imaging. 2020 Aug 25;10(4):178-211.
2. Sitani K, Parghane RV, Talole S, Basu S. Long-term outcome of indigenous ^{177}Lu-DOTATATE PRRT in patients with Metastatic Advanced Neuroendocrine Tumours: a single institutional observation in a large tertiary care setting. Br J Radiol. 2021 Jan 1;94(1117):20201041.
3. Parghane RV, Ostwal V, Ramaswamy A, Bhandare M, Chaudhari V, Talole S, Shrikhande SV, Basu S. Long-term outcome of "Sandwich" chemo-PRRT: a novel treatment strategy for metastatic neuroendocrine tumors with both FDG- and SSTR-avid aggressive disease. Eur J Nucl Med Mol Imaging. 2021 Mar;48(3):913-923.
4. Parghane RV, Bhandare M, Chaudhari V, Ostwal V, Ramaswamy A, Talole S, Shrikhande SV, Basu S. Surgical Feasibility, Determinants, and Overall Efficacy of Neoadjuvant ^{177}Lu-DOTATATE PRRT for Locally Advanced Unresectable Gastroenteropancreatic Neuroendocrine Tumors. J Nucl Med. 2021 Nov;62(11):1558-1563.
5. Basu S, Parghane R, Ranade R, Thapa P, Ramaswamy A, Ostwal V, et al. Peptide receptor radionuclide therapy in the management of neuroendocrine tumors (Neoplasms)*: Fundamentals and salient clinical practice points for medical oncologists. Indian J Med Paediatr Oncol 2019;40:165-71.
6. Basu S, Parghane RV, Kamaldeep, Chakrabarty S. Peptide Receptor Radionuclide Therapy of Neuroendocrine Tumors. Semin Nucl Med. 2020 Sep;50(5):447-464.
7. Loharkar S, Basu S. The evolving concept of Theranostics in Nuclear Medicine: Potential for Targeted Radionuclide Therapy of Cancer patients in the next decade. INS Newsletter 2022. Vol 22, Issue 1. Pg 9-11.
8. Thapa P, Nikam D, Das T, Sonawane G, Agarwal JP, Basu S. Clinical Efficacy and Safety Comparison of 177Lu-EDTMP with 153Sm-EDTMP on an Equidose Basis in Patients with Painful Skeletal Metastases. J Nucl Med. 2015 Oct;56(10):1513-9.

Dr. Sandip Basu is Consultant Physician and the Head, Nuclear Medicine Academic Programme of the Radiation Medicine Centre (BARC), Tata Memorial Centre Annexe, Parel, Mumbai. He is Dean-Academic (Medical & Health-Sciences), BARC at Homi Bhabha National Institute and is actively involved in Clinical patient services, research and post-graduate teaching and training activities of the Centre. Authored over 440 publications in peer-reviewed journals, and 30 text-book chapters, he serves as the Editorial Board member of multiple national & international journals. The CSIR, the apex agency of the Government of India for scientific research, awarded him the Shanti Swarup Bhatnagar Prize in Medical Sciences in 2012. He is also the recipient of DAE Homi Bhabha Science and Technology Prize in 2017, Alavi-Mandell Award from the Society of Nuclear Medicine, USA in 2010, and the DAE Scientific and Technical Excellence Prize in 2007. Dr. Basu delivered the Homi Bhabha Memorial Oration 2019 of the Society of Nuclear Medicine India and Dr. Gour Gopal Das Memorial Oration 2014 by the Indian Physical Society.

Neutron Imaging for Aerospace Applications – past, present & future

M. Nallaperumal*, Girish N. Namboodiri, Moideenkutty K K

Rocket Propellant Plant, Vikram Sarabhai Space Centre, Thiruvananthapuram-695022, India
(**Corresponding author email:* m_nallaperumal@vssc.gov.in)

Neutron imaging has been extensively used by Indian Space Research Organization (ISRO) for imaging and quality assurance of explosive laden pyrotechnic devices used in Indian space programme. NR of pyro components for launch vehicles application started during the initial days at APSARA reactor at BARC. The first NR facility in Indian Space Research Organization (ISRO) was developed at Satish Dhawan Space Centre, SHAR, Sriharikota using 15 MeV LINAC. Subsequently, neutron imaging activity was shifted to reactor-based neutron imaging at KAMINI reactor facility of IGCAR Kalpakkam, India. In recent years, due to increased production of pyros to meet the tight launch schedules of various types of launch vehicles / satellites as well as difficulty in transportation of explosive loaded pyro devices to IGCAR each time, there was a strong requirement to have an in-house neutron radiography facility. This led to setting up a neutron radiography facility using a Deuterium–Tritium-based neutron generator with the technical support of BARC, Mumbai.

The Neutron Radiography facility established at VSSC with the expertise of BARC Team has been used for clearance of pyro components for all important missions of ISRO since 2016. But the system uses D-T based Neutron generator bought from M/s. Sodern, France. As a part of "Make in India" policy, it is essential to have an indigeneous Neutron Generator of similar size and easiness of operation like the present Neutron Generator. In future, it will be difficult to depend upon a single source for meeting ISRO's NR requirements. It is essential to consider the above requirements and develop neutron generators which are very compact and of sufficient flux close to nuclear reactor source. D-D or D-T based compact Neutron Generators with flux as high as 10^{12} to 10^{14} n/cm^{2}s will be the need of the hour considering the increased number of launches in the coming years as ISRO is under a trasnformation stage with increased participation of private players in the Space sector. The neutron generator shall be user friendly and simple to operate without the support of a nuclear expert. Since the flux levels in such systems will always be less than nuclear reactor based NR facilities, suitable provisions of carry out NR of pyro components containing explosives also shall be planned in the future. Above mentioned facilities do not have sufficient penetartion to detect explosives in Pyro components in its assembled stage. In such typical scenarios, NR facilities at BARC/IGCAR only could offer support. IGCAR, Kalpakkam permits entry of ISRO flight components in KAMINI reactor for NR but do not have digital NR systems. BARC, Mumbai has expertise in digital NR which needs to be made available for pyro devices from ISRO that can support radiography as well as studies related to failure analysis during new development of pyros etc in future.

Acknowledgements:
AGM & GM, RPP Deputy Directors ASOE & SPRE, VSSC,
Dr. Tushar Roy. BARC

Author Information

Dr. M. Nallaperumal has an M.Sc degree in chemistry and PhD in the topic of Composite Explosives . He is a first rank holder and gold medallist in the High energy materials course conducted by Defence Institute of Armament Technology, Pune.

He has joined VSSC, ISRO in 1986 and served in the area of high explosives-based space ordnance systems for 30 years. Currently he is Deputy General Manager of Non-Destructive Testing Facility of Rocket Propellant Plant, Vikram Sarabhai Space Centre, Trivandrum.

This is the centralised NDT facility for all rocket motors, composite nozzles, ignition systems and the host of pyro devices used in ISRO's launch vehicles and satellites. The major techniques used are X-ray, Neutron Radiography and Ultrasonic testing equipment.

He has 45 technical papers, two publications and three patents to his credit.

He has been awarded the HEMCE rolling trophy instituted by HEMRL, Pune in 1997 and the first HEMSI-M R KURUP gold medal for young scientist by HEMSI, Trivandrum-Sriharikotta chapters in 2008.

In addition to his scientific activities, he is a national athlete and ISRO overall champion for two terms.

Applications of Radioisotopes in Industry

H.J. Pant

Isotope and Radiation Application Division, Bhabha Atomic Research Centre, Mumbai- 400085, India
(Author email: hjpant@barc.gov.in*)*

1.0 Introduction

Applications of radioisotopes and radiation technology in industry, medicine and agriculture form an important part of India's programme of using nuclear technology for societal benefits. Radioisotope production in India started on a modest scale soon after 1 MW APSARA reactor at Trombay, Mumbai became critical in 1956. The scope of activities expanded thereafter. With the commissioning of 40 MW CIRUS reactor in 1960, the setting up of modern radioisotope processing laboratories in late sixties and the production of cobalt-60 in power reactors in megacurie quantities in late seventies made India self-sufficient in radioisotope production. The radioisotope production received a major boost in 1985 with the commissioning of high flux 100 MW DHRUVA reactor, which provided opportunity to extend the range of radioisotopes available in the country both in quantity as well in specific activity. The CIRUS reactor has been shutdown in year 2010 and 1 MW APSARA reactor has been upgraded to 2 MW, and renamed as APSARA-U. Today, The DHRUVA and APSARA-U reactors are operating at their optimum capacity for production of 100 different radioisotopes for use in industry, agriculture and medicine.

As a consequence of an early realization of importance of radioisotopes and radiation technology, India today has a fairly advanced base for applications of radioisotopes and radiation technology in medicine, industry and agriculture. The infrastructure has been further strengthened over last two decades by modernizing the existing radiological laboratories for radioisotope processing and hot-cell facilities for fabrication of high intensity gamma sources; and finally establishing R & D groups for each area of application.

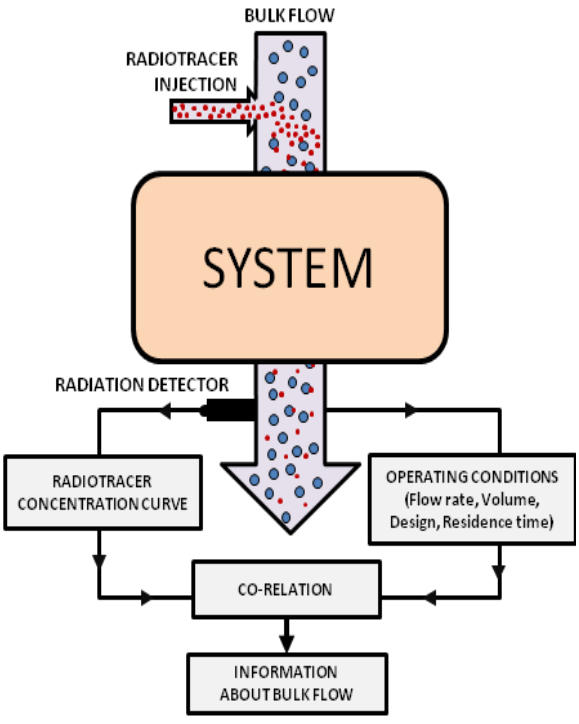

Fig.1: General principle of tracer technique [1]

Board of Radiation and Isotope Technology (BRIT), Department of Atomic Energy (DAE) supplies radioisotopes and radiation equipment to the various users in the country and abroad and along with the Bhabha Atomic Research Centre (BARC), Mumbai offers professional services to meet the country's demand in various fields of applications. The R&D programmes for advanced applications of radioisotopes are pursued at BARC, Mumbai.

2.0 Radioisotope applications in industry

Radioisotope techniques have been widely used in industry for troubleshooting, measurement of hydrodynamic parameters, process visualization and optimization of designs of process equipment. The applications are broadly classified into two categories i.e., radiotracer and sealed source applications. The two categories of applications are briefly discussed below.

2.1 Radiotracer applications

Radiotracers have been widely used in industry for troubleshooting and process optimization in industry, and in research applications all over the world because of their specific advantages over conventional tracers. The main advantages of radiotracers are physico-chemical compatibility, high detection sensitivity, in-situ detection, availability of a number of radiotracers for different phases; stability in harsh industrial environment and limited memory effects [1,2,3]. Some of the commonly used radiotracers in industry are listed in Table 1 [1].

The principle of radiotracer technique is shown in Fig.1. The technique involves instantaneous injection of a suitable radiotracer into the system at the inlet and monitoring its passage at the outlet or at strategically selected locations along the system using collimated radiation detectors. The monitored tracer concentration data is plotted as a function of time and interpreted to obtain information about process parameters, hydrodynamic behavior of the system and occurrence of malfunctions, if any. The commonly carried out applications of radiotracers in industry in India include [1,2,3].

- Leak detection in buried pipeline and industrial systems
- Flow rate measurements
- Mixing/blending time measurements
- Residence time distribution in process vessels
- Sediment transport investigations in ports
- Effluent dispersion studies in water bodies
- Radioactive particle tracking technique for flow visualization and design optimization
- Radiotracer applications in oil field investigations

Table 1: Commonly used radiotracers in industry [1]

Isotope	Half-life	Radiation and Energy (MeV)	Chemical Form	Tracing of Phase
^{3}H	12.6 y	β: 0.018 (100%)	Tritiated Water	Aqueous
^{24}Na	15 h	γ : 1.37 (100%), 2.75 (100%)	Sodium carbonate	Aqueous
^{82}Br	36 h	γ : 0.55 (70%), 1.32 (27%)	Ammonium bromide Paradibromo-benzene and dibrobiphenyl Methyl bromide	Aqueous Organic Organic Gas
^{131}I	8.04 d	γ : 0.36 (80%), 0.64 (9%)	Potassium or Sodium iodide, Iodobenzene	Aqueous Organic
^{99m}Tc	6 h	γ : 0.14 (90%)	Sodium technetate	Aqueous
^{140}La	40 h	γ : 1.16 (95%), 0.92 (10%) 0.82 (27%), 2.54 (4%)	Lanthanum chloride	Solid (Adsorbed)
^{46}Sc	84 d	γ : 0.89 (100%), 1.84 (100%)	Scandium oxide	Solid (Particle)
^{198}Au	2.7 d	γ : 0.41 (99%)	Chloroauric acid	Solid (Adsorbed)
^{197}Hg	2.7 d	γ: 0.077 (19%)	Mercury metal	Mercury
^{79}Kr	35 h	γ : 1.37 (%)	Krypton	Gas
^{41}Ar	110 min	γ : 1.29 (99 %)	Argon	Gas

Since early sixties, Bhabha Atomic Research Centre (BARC), Mumbai has made pioneering contribution to the development and promotion of radiotracer technology in India and Asia Pacific region for troubleshooting and process optimization in industry. Isotope and Radiation Application

Division (IRAD), BARC alone has carried out over 350 field-scale radiotracer investigations to benefit the Indian industry during last five decades.

2.1.1 Leak detection in heat exchangers

Occurrence of leakage in heat exchangers and underground pipelines is one of the commonly encountered problems in process industry leading to contamination of the product or loss of process efficacy. There are no conventional techniques available for online detection of leak(s) in heat exchangers as they operate at high temperature and pressures. Various radiotracer techniques have been developed and used for online leak detection in industrial systems [4]. An illustrative example of leak detection in a heat exchanger system carried out in a petroleum refinery in India is briefly discussed.

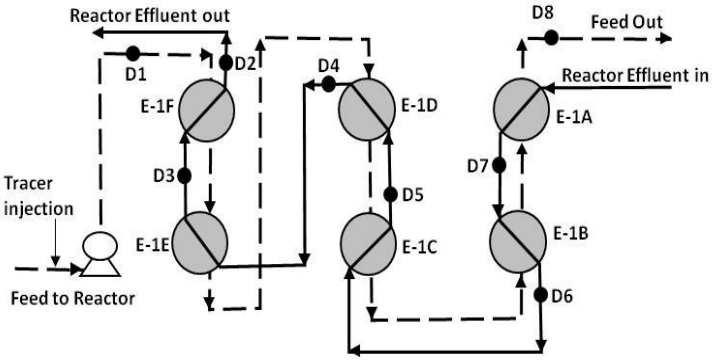

Fig.2: Schematic diagram of heat exchanger system and tracer monitoring locations (D1-D8: Radiation detectors)

A high-pressure heat exchanger system had been in operation in a hydro-processing plant in a refinery. The schematic diagram of the heat exchanger system is shown in Fig. 2. The heat exchanger system consisted of a series of six shell-tube type heat exchanger connected in series. The heated desulphurised effluent from a process reactor flows through the tube side of the heat exchangers, thus transferring the heat to the incoming feed flowing counter-currently through the shell side of the heat exchangers. The pressure in the shell side of the exchangers ranges from 125-130 kg/cm^{2}g, whereas the pressure in the tube side of the exchangers ranges from 107-110 kg/cm^{2}g. Since the shell side of each heat exchanger is at higher pressure, therefore any leakage in the heat exchanger will result in flow of untreated feed into the tube side of the exchanger and contaminate the product i.e., high speed diesel (HSD). During routine laboratory analysis, the sulfur content in the product was found to be higher (>100 ppm) than the specified value i.e. <30 ppm) indicating leakage of untreated feed from shell-side to the tube side of the exchanger system. The maintenance and servicing of the shell-tube type of heat exchanger is a difficult and expensive task and thus requires hiring of a specialized agency before the shutdown is planned. Therefore, a radiotracer investigation was carried out to identify the leaking heat exchanger(s). A suitable radiotracer (Bromine-82 as dibromobiphenyl)

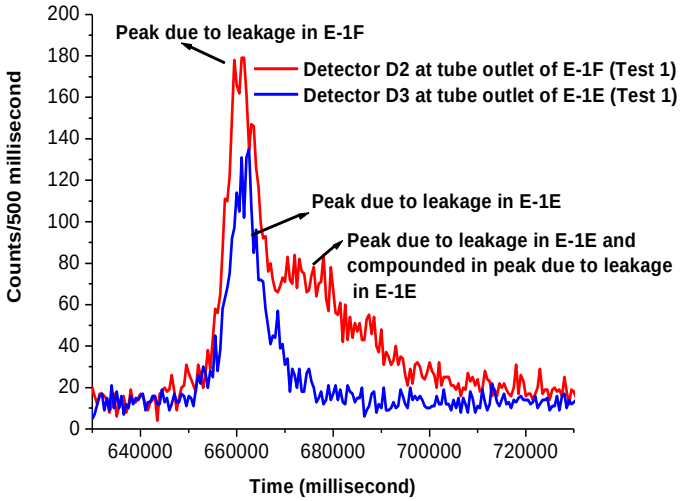

Fig.3: Tracer concentration curves monitored at tube outlets of heat exchanger E-1E and E-1F

was instantaneously injected at the inlet of the shell-side (feed) and monitored at the strategically selected locations in the counter-currently flow stream through the tube-side (Fig.2). Figure 3 shows the radiotracer concentration curves monitored at the tube-outlets of the exchanger E-1E and E-1F indicating occurrence of leakages in them. Based on the results of the radiotracer investigation, the leaking exchangers were identified and accordingly the shutdown was planned for remedial measures. The timely identification of leaking heat exchangers reduced the shutdown time of the plant leading to significant revenue saving to the industry.

2.1.2 Flow rate measurements in a canal

Measurement of flow rates of process fluids is an essential requirement in industry. Usually, suitable flow meters are used for measurement of flow rates in industrial plants. However, there are certain situations where neither flow meters nor any conventional techniques can be used. Radiotracer techniques are routinely used for flow rate measurements in industrial systems, particularly in situations where there is need to calibrate the installed flow meters, highly accurate measurements are needed and conventional techniques cannot be applied [1,2,3]. Radiotracer dilution method was used for measurement of water flow rates in four different pumping stations (PS2, PS3, PS4 and PS5) constructed for pumping water along a 104 km long section of a canal [5]. Each pumping station comprised of 5-6 identical Concrete Volute (CV) pumps. The objective of the measurements was to validate the efficacy of the CV pumps used. Flow rate measurements were carried out with a single pump operating at each pumping station. Radiotracer solution of Idone-131 (gamma energies: 0.36 MeV (80 %); half-life: 8 days) of concentration C_1 was injected into the suction end of the pump at a flow rate of Q_1 and its concentration C_2 was measured in water samples collected at a downstream location. The samples are collected from a location at which the radiotracer is uniformly mixed across the entire cross-section of the canal. The flow rate of the canal Q_2 is measured using the following relation [2,3,5]:

$$Q_2 = Q_1 \times [C_1/ C_2] \quad (1)$$

The values of flow rate measured at four different pumping stations are given in Table 2. The flow rates generated and measured were found to be in good agreement with the theoretically estimated efficacy (20 m^3/s) of the pump.

Table 2: Results of flow rate measurements in the canal [5]

Q_1 (ml/min)	C_1 (Counts/ 2 min)	C_2 (Counts/ 2 min)	Q_2 (m^3/s)
Pumping station, PS2			
135	5.662×10^{10}	6275	20.30±0.29
Pumping station, PS3			
156	9.304×10^{10}	11760	20.62±0.26
Pumping station, PS4			
143.81	2.197×10^{11}	25811	20.47±0.22
Pumping station, PS5			
144.07	1.0426×10^{11}	12179	20.60±0.37

2.1.3 Residence time distribution measurements in a soaker

A soaker operating in a refinery for production of heavier hydrocarbon products was producing gaseous hydrocarbons than the expected amount. The process engineers suspected inappropriate flow patterns within the soaker leading to over-production of gaseous hydrocarbons. Residence time distribution (RTD) approach was used in investigate the cause of over-production of lighter hydrocarbons. Figure 4 shows the schematic diagram of the soaker and the experimental setup for RTD measurements. Bromine-82 as dibromobiphenyl was used as radiotracer for tracing the petroleum residue. About 370 MBq (10 mCi) activity was used in each run. The radiotracer was instantaneously injected at the inlet of the soaker at the bottom and monitored at the inlet and outlet using collimated NaI(Tl) scintillation detectors (D1, D2) connected to a multi-input data acquisition system (MIDAS) as shown in Fig. 4. The MIDAS was connected to a laptop that was programmed to record radiotracer concentration at an interval of 1 minute. The measured RTDs were treated and mean residence times (MRTs) were determined. The measured RTD data was simulated using a combined model i.e., axial dispersion model in parallel with tanks-in-series with stagnant volume and exchange [6]. The results of the model simulation fitted very well to the experimentally measured data and identified bypassing or existence two parallel flow paths within the soaker. A representative plot showing the comparison of experimental and model simulated curve is shown in Fig. 5. The results of model simulation showed that there exist two parallel flow paths inside the soaker. One of the paths having lesser mean residence time (MRT) represents the bypassing of the fluid while the other path having the larger MRT represents the back-mixed flow. Based on the results of the RTD study, the design of the soaker was modified (sectionalizing) by inserting the baffles at various axial locations to minimize the bypassing and backmixing.

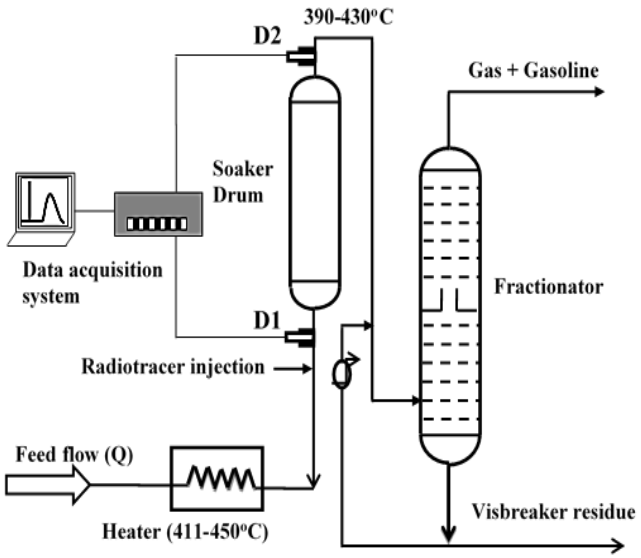

Fig. 4: Schematic diagram of the soaker plant and experimental setup [6]

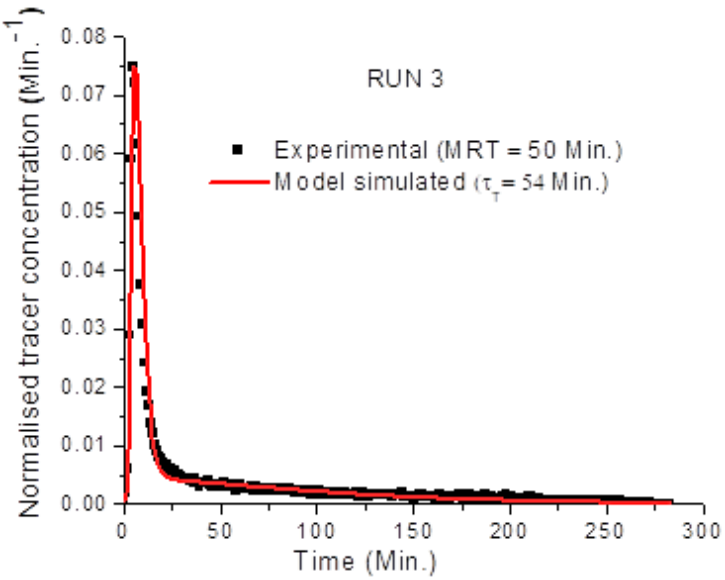

Fig. 5: Comparison of experimental and model simulated curves [6]

2.1.4 Sediment transport investigations in ports

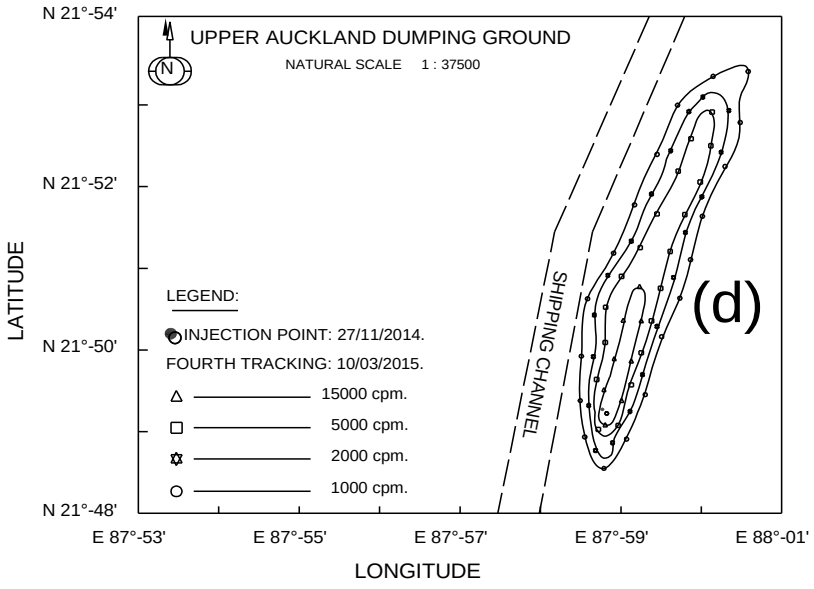

Fig.6: Iso-activity contours monitored at Upper Auckland Dumping Ground at Kolkata Port [7]

The knowledge of movement of sediment either on sea-bed or in suspension is required for maintenance of depth of existing shipping channels or development of new harbor projects. Radiotracer techniques are well-established tool to investigate the dispersion of sediments on sea-bed or suspended sediments in ports or coastal areas and estimate parameters such as direction of movement, velocity and quantity of bed load transport [7]. The procedure involves preparation of a radioactive particulate tracer having similar physicochemical properties as the bed material, injection of the tracer at the desired point, tracking of the tracer on sea-bed or in suspension using waterproof scintillation detectors and finally interpretation of iso-activity contours to evaluate the above-mentioned parameters. The radiotracer used for sediment transport investigation on sea-bed is scandium-46 as glass powder having the same density and grain size distribution as that of the bed material being traced. Most of the radiotracer investigations are aimed at:

- Examining the suitability of the existing dumping ground for dredged silt.
- Selection of a suitable dumping ground for new projects
- Examining the suitability of alignments of proposed navigation channels
- Pollution studies in coastal areas

More than 80 large-scale radiotracer studies have been conducted for studying sediment dispersion on sea-bed in all the major ports in India [7]. In Kolkata Port, Kolkata alone, more than 20 large-scale sediment transport investigation have been carried out since 1967. Recently a series of three radiotracer investigations have been conducted at three different locations along the shipping channel in Haldia estuary, West Bengal, India [8]. The main objective of these investigations was to investigate the sediment movement and examine the suitability of the dumping sites for the dredged material during the maintenance dredging of the shipping channel. A typical plot of iso-activity contours plotted after monitoring the injected radiotracer at a particular site (Upper Auckland Dumping Ground) after a period of 115 days is shown in Fig.6. The contours indicate that the movement of the sediments is parallel to the shipping channel and do not find its way into the channel. This showed that the selected site is suitable for dumping the dredged sediments.

2.2 Sealed source applications

In second category of applications, a radiation source is encapsulated in a metal capsule and never directly comes in contact with either process material or equipment. The penetrating radiation from the radiation source capsule is directed at the desired location in the equipment under investigation or material of interest and the intensity of transmitted or scattered radiation intensity is measured and

analysed to obtain information about content of the system or physical properties of the material. The commonly carried out applications of sealed sources include:

- Radiography
- Radiometry or gamma scanning
- Computed tomography
- Nucleonic gauges
- Radiation processing applications

2.2.1 Radiography

Radiography testing (RT) is a non-destructive technique (NDT) used to examine the integrity and internal structures of materials and assemblies without destroying them and altering their size, shape, physical or chemical properties [8]. It is employed in quality control monitoring in various industries including nuclear, aerospace and automobile. The technique involves exposing the object with energetic electromagnetic radiations emitted either from a sealed radioisotope source or X-ray machine and recording the intensity of the transmitted radiations on a recording medium like chemical-based film, phosphor imaging plate or a flat panel detector [8]. Distribution of optical density on the recording medium provides information about defects, flaws, voids and internal structure of the object.

The gamma emitting sealed radioisotope sources used in RT are listed in Table 3. BARC has played a pivotal role during the last five decades in developing radiography equipment, production of radioisotope sources for RT and promoting the technique in India. BRIT, DAE supplies radiography equipment and sources to the Indian industry on regular basis. As on June 2021, there are 3176 RT equipment registered with Atomic Energy Regulatory Board (AERB), 647 actual number of licensees for radiography cameras, 740 industrial X-ray devices and similar equipment, 676 entities carrying out commercial activities in the countries and 1454 total number of RSOs registered with the AERB. Training courses are regularly carried out by BARC for various levels of radiography personnel such as operators (RT-1), supervisors (RT-2) and managers (RT-3). More than 10,000 personnel have been trained at different levels to carry out radiography testing for quality control of industrial products.

Table 3: Commonly used radioisotopes sources for radiography testing

Radioisotope	**Half-life**	**Gamma ray energy (MeV)**	**Activation cross-section (Barn)**	**Radiation output R/hr/Ci @ 1 m**	**Optimum working thickness**
Co-60	5.27 years	1.17-1.33	37	1.37	50-200 mm equivalent of steel
Cs-137	30.1 years	0.66	---	0.382	50-125 mm equivalent of steel
Ir-192	74.4 days	0.296-0.613	370	0.592	10-60 mm equivalent of steel
Tm-170	129 days	0.052-0.084	130	0.0062	2-10 mm equivalent of steel
Yb-169	32 days	0.063-0.308	11000	0.327	2-12 mm equivalent of steel
Se-75	120 days	0.009-0.400	26	0.859	5-40 mm equivalent of steel
Am-241	432.2 years	0.0595	750	0.314	2-18 mm equivalent of aluminium

2.2.2 Radiometry

Gamma radiometry technique, also known as gamma scanning technique, is used to determine the density of the intervening material between the source and the detector, holdup or voidage in multiphase flow systems, testing of shielding integrity of transportation casks/lead blocks/civil structures, scanning of industrial process columns and blockage detection in pipelines in industry [1,2]. The gamma radiometry technique involves mounting of a collimated-sealed radiation source and a detector on the diametrically opposite sides of an object under investigation and recording the intensity of the transmitted radiations in terms of counts per unit time (Fig. 7). An example of radiometry is discussed below.

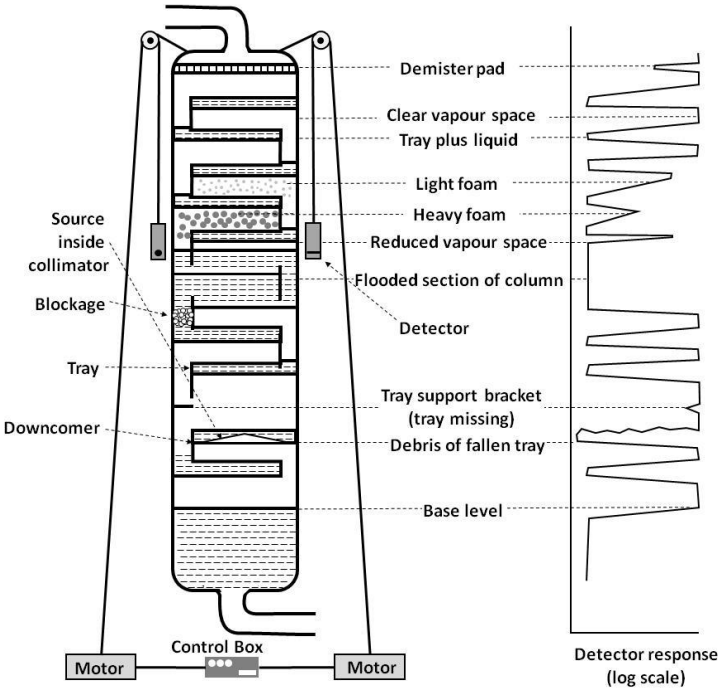

Fig. 7 : Radiometry (Gamma scanning) of industrial process columns

During the operation of the industrial process columns, a number of malfunctions are developed hampering the normal operation leading to deterioration in product quality and reducing the process efficacy. Radiometric measurements or gamma scanning technique is the only tool to identify the location of the problem within the column without shutting down the operation [1,2]. Fig. 7 shows a schematic diagram of a typical column with scanning arrangement and a typical scan (density profile) of the column. The scan is interpreted to identify the malfunctions and their locations within the column. It is always desirable to scan the column during its normal operation and keep it for future reference. The comparison of the normal scan with the scan obtained during abnormal operations helps to identify and confirm the malfunctions. The gamma scanning services are regularly offered by BRIT, DAE to the Indian industry. In addition to this, there are a few private companies which are also offering the gamma scanning services to the Indian industry.

2.2.3 Computed tomography for NDT and process applications

Computed tomography (CT) is and advanced imaging technique based on attenuation of X-ray or gamma-ray across a plane of an object. The technique involves obtaining large number of attenuation data obtained at different angular positions in a plane and creating an image of density distribution across the plane. The cross-sectional images are obtained through a mathematical process called image reconstruction. The images generated across multiple planes are used to even generate three-dimensional images which can be viewed on a computer monitor, printed on film or transferred to electronic media [9]. The obtained cross-sectional images are used for flaw detection, internal details, failure analysis, metrology, assembly analysis, reverse engineering, conservation of museum artifacts and many others [10]. In recent times, the technique has been applied for flow visualization in industrial process systems with different modalities.

Bhabha Atomic Research Centre (BARC), Mumbai has been actively involved in research and development (R&D) activities pertaining to advanced industrial applications of X-ray and gamma-based industrial imaging for more than two decades. Development programmes undertaken earlier resulted the setting up of an experimental facility for X-ray radiographic imaging and cone-beam computed tomography (DR&CT). The system consists of a 40-450 kV (variable anode voltage) constant potential X-ray generator having focal spot sizes of 0.4 mm and 1.0 mm, a flat panel detector and a multi-axis precision manipulator for positioning source, detector and specimen. It is capable of scanning specimen having maximum dimension up to 400 mm in any orientation. Components and assemblies for scanning are selected based on their radiation attenuating capacities and physical shape and size.

2.2.4 Nucleonic Gauges

Nucleonic gauges (NG) are the devices based on the ionizing radiations emitted from sealed radiation sources that are used for online monitoring of the various physical parameters and quality control during the production processes in industry [11, 12]. A NG consists of one or more than one radiation sources and a detector system integrated with a data acquisition system. They are arranged in a fixed geometrical configuration depending upon the type of application. The types of radiation sources used in NGs include alpha, beta, gamma, neutron and X-rays. The activity of the sources varies from several kBq to few GBq and X-ray operating in the energy range of 30-160 keV. The various applications of nucleonic gauges and typical sources in use are as given in Table 4 [12]. Some of the NGs used in industry are also based on the measurement of the natural radiation emitted from the material under study. The applications of nucleonic gauges are well-established and their socio-economic benefits have been amply demonstrated and recognized. The commonly used applications of NGs include measurement of density, thickness and level of process material in industrial systems, analysis of ores and minerals and measurement of moisture content in various systems.

One of the most important advantages of NGs is the online measurement without direct contact between the radiation source and the material being examined. As a consequence of this, NGs are preferred in high-speed production lines and harsh process conditions such as high temperature, pressure and corrosive medium. The measurements are accomplished non-destructively and without disturbing and changing properties of the examined material. The penetrating nature of high energy gamma radiation enables measurements to be made through the walls of sealed containers. The sampling volume of most of the NGs is usually larger than that sampled by conventional methods for laboratory analysis.

Indian Industry has made extensive use of nucleonic gauges such as level, density, thickness, moisture and well logging gauges. The gauges have been manufactured, marketed, supplied and installed by many national and international commercial companies. Electronic Corporation of India Limited (ECIL), a public sector company of Department of Atomic Energy (DAE) also manufactures a range of nucleonic gauges and supplies to the industry

Table 4. Radiation sources, technique and applications of nucleonic gauges in industry [12]

Type of gauge	**Technique**	**Radiation sources used**	**Typical applications**
Level and interface	Transmission	Cesium-137 (Gamma) Cobalt-60 (Gamma)	Level and interface measurements in process vessels in industry
	Backscattering	^{241}Americium-Beryllium (Neutron)	Level measurements of hydrogenous materials
Thickness or mass per unit area	Transmission, Backscattering	Krypton-85 (Beta) Strontium-90 (Beta) Promethium-147 (Beta) Thulium-170(Beta)	Thickness measurement of paper and plastic sheets
	Transmission, Backscattering	Cesium-137 (Gamma) Cobalt-60 (Gamma) Americium-241(Gamma)	Aluminum and metal sheets in industry, mass of materials on conveyor belts
Coating thickness	Differential transmission method	Krypton-85 (Beta) Strontium-90 (Beta)	Coatings on textiles papers and leather clothes
	Backscattering	Promethium-147 (Beta) Thulium-170 (Beta)	Metal coatings on metal sheets and coatings on photographic paper
	X-ray fluorescence	Iron-55, Cadmium-109, Americium-241 (Gamma) etc.	Measurements of thickness coating on metal sheets
Density	Transmission	Krypton-85 (Beta) Strontium-90 (Beta) Promethium-147 (Beta) Thulium-170 (Beta)	Cigarettes, fluids and slurries in pipes and tanks, gas and gas-fluidized solids, gas-liquid emulsions, steam-water ratios etc.
	Transmission	Americium-241 (Gamma) Cesium-137 (Gamma) Cobalt-60 (Gamma)	Fluids and slurries in pipes and process vessels in industry
Bulk density	Transmission, Backscattering	Americium-241 (Gamma) Cesium-137 (Gamma) Cobalt-60 (Gamma)	Soil, borehole cores, rocks and ore measurements in boreholes
Moisture	Slowing down of neutron and backscattering	Americium-241/Beryllium (Neutron)	Soil, rocks and ores, agricultural products.
Elemental analyzer	Emission of characteristic X-rays and their backscattering	Iron-55 (Gamma) Cadmium-109 (Gamma) Americium-241 (Gamma) Characteristic X-rays	Elemental analysis in metals, minerals, petroleum product etc.
Air quality/Dust monitor	Absorption of low energy beta radiations	Carbon-14 (Beta) Promethium-147 (Beta) Krypton-85 (Beta)	Environmental control

2.2.5 Radiation processing applications

Radiation processing or irradiation is an intentional exposure of products and materials to high-energy ionizing radiations for beneficial purposes. The irradiation generates highly reactive free radicals, ionic species and defects at any temperature and in any phase (solid, liquid and gas). The high energy radiations mainly interact with orbital electrons and excite the absorbing molecules to higher excited states that results in the formation of highly reactive ions or radicals. Subsequent reactions of these reactive species lead to biological, chemical and physical effects in the irradiated material and form the basis of industrial radiation processing. Gamma radiation from cobalt-60 and cesium-137 as well as electron beam (EB) radiations are two main sources used for industrial radiation processing applications. Some of the common applications of radiation processing are mentioned below:

- Sterilization of medical products
- Sterilization of packaging material
- Improvement in polymeric materials
- Processing of hydrogels
- Preparation of polymer blends and composites
- Preparation of polymeric matrices for separation purposes
- Preparation of heat shrinkable polymeric matrices
- Food irradiation
- Hygienisation of dry sewage sludge
- Coloration of diamonds and precious stones

The above applications are discussed elsewhere in details [13,14,15].

3.0 Conclusions

Radioisotope techniques are well-established and widely used for troubleshooting and process monitoring in Indian industry leading to significant economic benefits. The applications will continue to expand following substantial developments in supporting technologies and meet the growing needs of the Indian industry. It is generally realized that the level of application of the radioisotope techniques in industry is presently confined to only a few well-informed industries. It is thus essential to explore and plan for a much wider application of these unique techniques to help the Indian industry.

Radiation processing is clean, reliable, reproducible and easy to upscale technology which enriches the quality of our life in many ways. It finds applications for spectrum of industrial applications. It is expected the unique characteristic of high energy radiation to deposit energy to initiate chemical reactions in the any matrix without any significant rise in temperature would be exploited for many more industrial applications in near future. Presently there are 24 gamma irradiator plants and 18 electron beam machines operating in India for various radiation processing applications on commercially basis. These numbers are expected to increase significantly in near future.

References

1. Charlton, J. S., 1986. Radioisotope Tracer Techniques for Problem Solving in Industrial Plants. Leonard Hill, Glasgow and London.
2. International Atomic Energy Agency, 1990. Guide book on Radioisotope Tracers in Industry. Technical Report Series, No. 316, Vienna, Austria. 374p.
3. Pant, H.J., Applications of the radiotracers in the industry: A review, 2021.Appl. Radiat. Isot.,https://doi.org/10.1016/j.apradiso.2021.110076.

4. Pant, H.J., Sharma, V.K., Goswami, S., Samantray, J.S. and Singh, G., 2013. Development and application of radiotracer technique for online leak detection in high-pressure heat exchangers. BARC Newsletter, Issue No. 330, pp.8-15.
5. Pant, H.J., Goswami, S., Biswal, J., Samantray, J.S., Sharma, V.K., 2016. Discharge rate measurements in a canal using radiotracer methods. Appl. Radiat. Isot. 112, 89-97.
6. Pant, H.J., Sharma, V.K., 2015. Radiotracer investigation in an industrial-scale oxidizer. Appl. Radiat. Isot. 99, 146–149.
7. Sharma, V.K., Pant, H.J., Goswami, S. and Bhar, K.K., 2020. Radiotracer investigations in Kolkata Port Trust, India for evaluation of dumping sites for dredged sediments. Appl. Radiat. Isot, 2021, 168, 109524.
8. Baldev Raj and Venkataraman, B., Practical radiography, Alpha Science Int'l Ltd., Narosa Publishing House, 2004.
9. Kak, Avinash C., Malcolm Slaney, and Ge Wang. Principles of computerized tomographic imaging, 2002, 107-107.
10. International Atomic Energy Agency TECHDOC Series-1931, 2020. An Introduction to Practical Industrial Tomography Techniques for Non-destructive Testing (NDT), IAEA, Vienna, Austria.
11. Johansen, G.A., Jackson, P. (Eds.), 2004. Radioisotope Gauges for industrial process measurements, John Wiley &Sons, Ltd., pp.331.
12. Pant, H.J., Sen, A., Application of nucleonic gauges in industry, In Non-power applications of nuclear technologies. A. K. Tyagi and A. K. Mohanty (Eds.) (ISBN: 978-81-954733-2-8) published by SIRD, BARC pp. 153-164.
13. K. Makuuchi, S. Cheng; In Radiation Processing of Polymer Materials and its Industrial Applications. (2012) John Wiley & Sons, Inc., Hoboken, New Jersey.
14. Sarma, K.S.S., Rawat, K.P., Benny, P.G., Khader, S.A. 2011. Developments in electron beam processing technology. BARC Newsletter, 323 Nov.-Dec. 38-41.
15. Sarma, K.S.S., 2015, A report on the industrial applications carried out since 2001 using ILU-type electron beam accelerator at BRIT-BARC Vashi complex, Navi Mumbai. BRIT Bulletin, pp. 45-52.

Author Information

Dr. H.J.Pant obtained his M.Sc Degree in Physics from H. N. Bahuguna Garhwal University, Srinagar Garhwal, Uttarakhand in 1985 and joined erstwhile Isotope Division, Bhabha Atomic Research Centre, Mumbai in 1988 after graduating from the 31st Batch of BARC training school. He obtained his Ph.D degree in Physics from Mumbai University in 2000. He is currently serving as the Head, Isotope and Radiation Application Division of BARC.

He is a specialist in Industrial Applications of Radioisotope Techniques and has developed a number of radiotracer techniques and applied them in various industries in India for troubleshooting, measurement of hydrodynamic parameters, process visualization and evaluation of design of chemical process systems.

He was awarded "DAE Scientific and Technical Excellence Award-2010" for his outstanding contribution in the field of "Radiotracer Applications in Industry". He has more than 100 publications in international journals and about 150 publications in international/national conferences/symposiums.

He is a member of International Atomic Energy Agency's expert panel on Industrial Applications of Radioisotopes and was deputed to Thailand, Algeria, Indonesia, Egypt, Republic of Korea, Czech Republic, Philippines, Austria, Malaysia and Kenya as a Technical Cooperation Expert. He was National Project Coordinator of various IAEA/RCA Projects on "Industrial Applications of Radioisotopes" during 2008-2016. He was also Chief Scientific Investigator for various IAEA-Coordinated Research Programmes during last two decades.

He is a life member of many professional bodies such as, Indian Nuclear Society (INS), National Association of Applications of Radioisotope and Radiation Technology in Industry (NAARRI), Indian Society of Radiation Physics (ISRP), Indian Association of Nuclear Chemists and Allied Scientists (IANCAS).

Physics using neutrons at Dhruva reactor

S M Yusuf

Physics Group, Bhabha Atomic Research Centre, Mumbai 400085
(Author email: smyusuf@barc.gov.in

Abstract

Neutron was discovered by Chadwick in 1932. It is a charge less particle with magnetic moment. Neutrons are useful for technological developments as well as fundamental science. In this regard, the National Facility for Neutron Beam Research (NFNBR) at Dhruva reactor has contributed immensely in condensed matter physics research in the subject domain of advanced magnetic materials, structure and dynamics of functional materials, soft matters, quantum materials, thin films and multilayers, and nano structures. Neutron beams have also been used in the area of nuclear physics and imaging technology.

A brief overview of current neutron beam research program at Trombay using the thermal research reactor Dhruva is presented. A few specific examples of recent studies are also elaborated with emphasis on collaborative research with national users.

1.0 Introduction

Neutrons have several interesting properties that make them an indispensable tool in a variety of investigations in Condensed Matter Physics, Chemistry, Biology and Materials Science. The high penetrating power, sensing capabilities of both light as well as heavy atoms simultaneously, isotope sensitivity, comparable wavelength/energy to the atomic length scale/basic excitations in materials, capability of measuring atomic magnetic moment, *etc*. have made thermal neutron a unique probe for materials' characterization and in-depth investigations. Unlike x-ray photons with a similar wavelength, that interact with the electron-cloud surrounding the nucleus, neutrons interact primarily with the nucleus [1, 2]. This makes neutron very sensitive to light atoms like hydrogen, which are difficult to detect using x-rays. Neutrons can also distinguish between the neighbouring atoms of the periodic table like iron, cobalt, and nickel due to their large varying scattering lengths. Scattering and absorption cross sections of neutron vary widely among the isotopes of an element and thus neutron can distinguish between the isotopes. Another important property of neutron is its magnetic moment, which allows it to interact with the atomic magnetic moments of a sample through dipole–dipole electromagnetic interaction. Therefore, neutrons can be used to investigate microscopic magnetic structures in the atomic length scale.

It is nearly 65 years since study of materials began in India with facilities at the then Atomic Energy Establishment Trombay (later renamed as Bhabha Atomic Research Centre or BARC), using India's first nuclear research reactor, Apsara. Over the following decades, CIRUS and Dhruva research reactors became operational in BARC. Further, after decommissioning of Apsara reactor in 2009, its upgraded version Apsara-U reactor became operational in 2018. Today, the neutron scattering activity in India [3] is mainly centered around the indigenously built Dhruva reactor and it serves as the National Facility for Neutron Beam Research (NFNBR). Neutron beams have also been used in the area of nuclear physics and imaging technology. A brief overview of the applications of these facilities is depicted along with some recent results on structure and dynamics in various condensed matter systems obtained through neutron scattering based research at Dhruva reactor.

2.0 Neutron beam facilities at Dhruva

All the instruments have been fabricated in the in-house workshops, and have automated means of data acquisition. Short description of various neutron scattering facilities at Dhruva reactor is mentioned below.

Description of property determined	Facility	Application
Structure	Powder Diffractometer I (PD-I)	This diffractometer is employed in the study of magnetic ordering/phases in technologically important polycrystalline magnetic materials.
Structure	Powder Diffractometer II (PD-II)	Delineation of chemical and magnetic structures, phase diagrams of poly-crystalline materials with respect to temperature and composition
Structure	Single Crystal Diffractometer (SCD)	Based on four circle Eulerian geometry. Used for study of high precision 3D structure of materials.
Structure	Powder Diffractometer III (PD-III)	Study of chemical and magnetic structures of materials using the low temperature-high magnetic field sample environment
Structure	High Q Diffractometer (Hi-Q)	Study of short and intermediate range order in glasses, liquids and disordered crystals, and High-pressure structural phase transitions
Structure	Polarized Neutron Spectrometer (PNS)	Enables the study of size/magnetization of magnetic domains or clusters at mesoscopic length scales and study of magnetic correlations
Structure	Double Crystal Based Medium - resolution Small- Angle Neutron Scattering (MSANS)	The medium resolution Small Angle Neutron Scattering (SANS) instrument is used to study structural features in materials in the range of 40 nm to 1000 nm.
Structure	Small Angle Neutron Scattering (SANS) Instrument	SANS instrument is used to determine the structure and interactions at nanometre length scales
Structure	Polarised Neutron Reflectometer (PNS)	This facility enables the study of depth dependent magnetic properties of thin films and multilayers
Dynamics	Triple Axis Spectrometer (TAS), Time of flight spectrometer (TOF)	For inelastic neutron scattering experiments from single crystals/ polycrystalline samples. For measurements of phonon dispersion curves, phonon density of states, crystal field excitations, and quasielastic scattering at any point in (Q, E) space
Dynamics	Quasi Elastic Neutron Spectrometer (QENS)	Study of stochastic molecular motion in pico second time scales. It provides both time scale and geometry of motion
Non-destructive characterization	Advanced Neutron Imaging Beamline	Capable of acquiring data in radiography, tomography and real - time imaging mode. It can detect the presence of hydrogen down to ppm level and also conforms to ASTM class-I standard for industrial users.
Coincidence gamma-ray spectroscopic investigation	Dhruva Utilization in Research using Gamma Array (DURGA)	1) Fission Fragment Spectroscopy using fissile targets/samples; 2) Capture Gamma Spectroscopy; and 3) Decay spectroscopy

3.0 Some recent results:

3.1 Structure in Advanced Functional Materials

Advances in technologies are heavily reliant on functionalities of materials. The functionalities of material are intrinsically dependent on the internal arrangement of atoms, collective excitations, and electron and defect distributions in matter. Neutron scattering is an invaluable tool to provide information about the atomic-scale structure of materials [1-4]. Neutron diffraction can be used for the investigation of crystalline, hybrid nanostructured materials, and to determine the static structure factor of glasses, liquids or amorphous materials. Some selected examples based on neutron diffraction are outlined here.

3.1.1 Quantification of Phase Fraction in Nuclear Materials

Uranium –Thorium (U-Th) alloys are considered to be potential nuclear fuel materials. With the incorporation of Mo in the U-Th alloy, the alpha phase of Uranium (α-U) changes to gamma phase of Uranium (γ-U) crystalline phase. γ-U exists in bcc crystal structure. This gamma phase of Uranium is desired in fuel materials due to its isotropic thermal expansion character. To optimize the amount of Mo in the alloy, it is essential to determine the correct phase fraction of Uranium as a function of Mo concentration. In addition to this, the Thorium metal also gets oxidized and forms ThO_2 layer on the surface of materials along with being present in bulk. Thus, to obtain higher quality of nuclear fuel, it is essential to quantify phase fraction of each identities present in materials [5, 6].

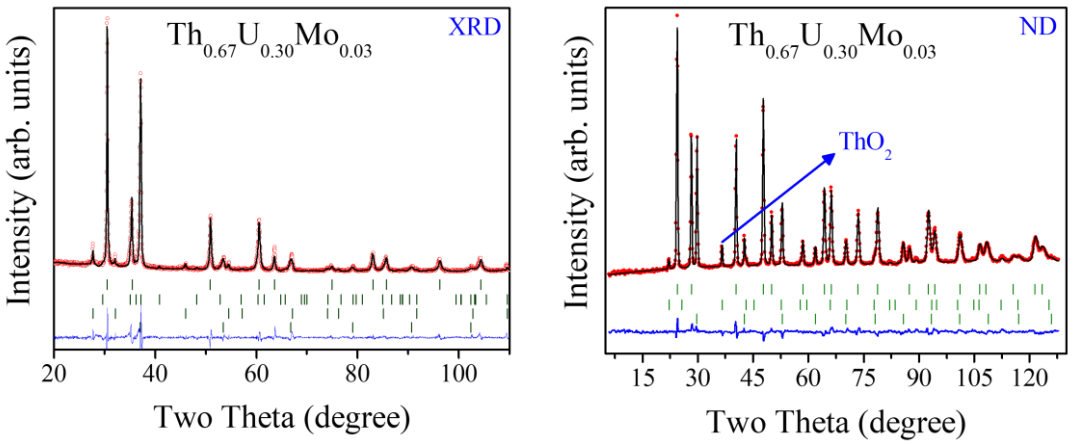

Fig. 1: Rietveld refinement fit of Th-U-Mo alloy using X-ray and neutron diffraction technique (Ref: AIP Conference Proceedings 1832, 060012 (2017); Nuclear Engineering and Technology, 2021)

The $Th_{0.67}U_{0.30}Mo_{0.03}$ alloy was investigated using both X-ray and neutron diffraction (Fig. 1). Different values of weight fraction of ThO_2 phase was found; in X-ray study is ~15% and in neutron study it is 3%. As the oxidation of Th is more prominent on surface and X-rays are scattered from surface predominantly, a larger weight fraction (15%) of ThO_2 phase was observed in x-ray diffraction study. On the contrary, neutron diffraction can penetrate inside these materials and gives us the more accurate information of the weight fraction of the different phases in the bulk samples. From neutron diffraction, the phase fraction of ThO_2 was found to be around 3% and is in agreement with chemical analytical techniques. In summary, neutron diffraction can be utilized for an accurate determination of phase fraction for nuclear materials, and is non-destructive in nature [7].

3.1.2 Investigation of microstructure and network connectivity in Functional Glasses

Tellurite glasses are being continuously explored and studied to develop novel properties and produce functional materials. These network glasses are covalently bonded like oxides but can also form homo polar bonds making a richer combination of structural motifs. Incorporation of ferroelectric material like $LiNbO_3$ into TeO_2 glass matrix opens wide range of applications in mouldable intra-red optics and fibers, lenses, memory devices, dielectric super capacitors, and phase change materials.

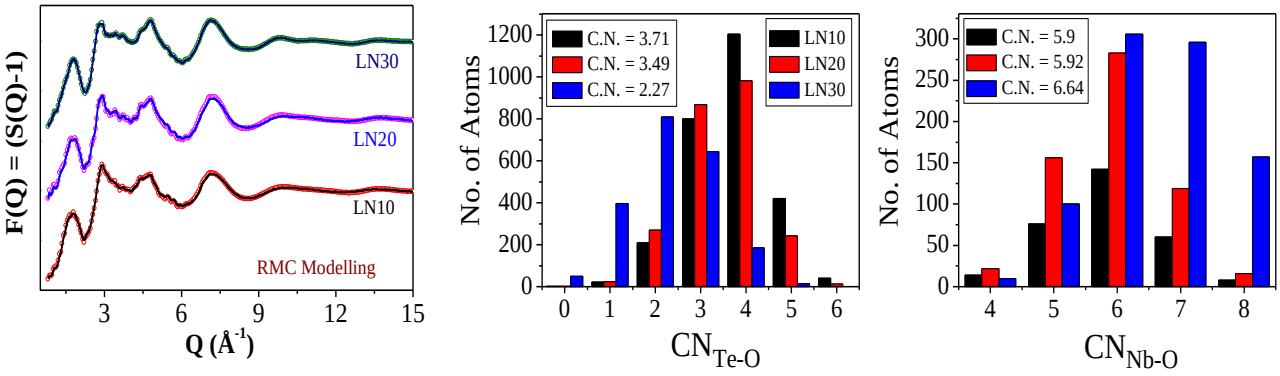

Fig. 2. Total neutron diffraction data of experimental structure factor F(Q) (empty circles) and RMC simulated F(Q) (solid line) for all compositions of lithium niobium tellurite glasses. Each S(Q) is shifted upward by 0.4 units for each composition for clarity. Histogram comparison of distribution of coordination numbers for Te-O atom pairs in the r range of 1.68 Å to 2.36 Å and Nb-O atom pairs in 1.8 Å – 3.12 Å interval (Ref: AIP Conference Proceedings. 2020).

The microstructure and network connectivity in lithium niobium tellurite glasses of the compositional formula (1-x) (TeO_2)-x $(LiNbO_3)$ for composition x = 0.10, 0.20 and 0.30 were investigated using neutron diffraction and reverse Monte Carlo modelling [8]. Detailed analysis of structural data using Reverse Monte Carlo modelling suggests that on increasing concentration of $LiNbO_3$ in TeO_2 matrix, more and more TeO_4 units get converted to TeO_3 units via an intermediate TeO_{3+1} structural unit. The average value of Nb-O coordination number is around 6 and it does not change much with $LiNbO_3$ concentration even though deformed polyhedra too are present in the glass matrix. This is clearly evident from the co-ordination number distributions shown in Fig. 2. On increasing $LiNbO_3$ concentration, strength of glass network and its thermal stability are increased.

3.1.3 Structural investigation of microscopic defects in irradiated graphite

Graphite has been used in high radiation environment, as neutron moderator or reflector, in many nuclear reactors. The irradiation of graphite in a nuclear reactor results in the knocking out of carbon atoms from their equilibrium sites. Defects in graphite are unusual since they involve very large potential energy and are prevented from annealing at ambient or moderately high temperatures due to a large energy barrier. Consequently, on heating of the irradiated graphite at high temperatures of around 200^o C, the annealing of the defects is spontaneous with release of an unusually large energy, called the Wigner energy.

Several graphite samples [9] irradiated with neutrons at various levels of fluence were taken out from a block of irradiated nuclear-grade graphite originally used in the reflector section of the CIRUS research reactor at Trombay. The highest fluence of the neutrons encountered by the samples is 2.6×10^{21} neutrons/cm^2 over a period of several decades. The neutron fluence seen by various samples is depicted in Fig. 3. Further, an un-irradiated sample was used for reference. While irradiation results in defects at various length scales, our studies have focussed on atomic level defects that are most relevant to the large Wigner energy release.

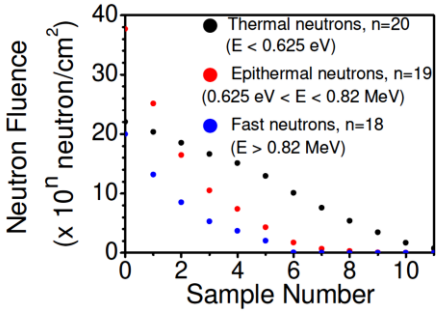

Fig. 3 Neutron fluence as seen by various graphite samples. The irradiated samples are numbered as S0 to S11 in the order of decreasing neutron fluence seen by them; i.e., S0 and S11 have seen the maximum and minimum neutron fluence, respectively. Another unirradiated sample for reference is assigned as sample number S12. The unit (10n neutrons/cm2) of the vertical axis is different for thermal (n=20), epithermal (n=19) and fast neutrons (n=18) (Ref: Physical Review B, 2020. 102(6): p. 064103.).

The experimental neutron diffraction data were obtained using the High-Q powder diffractometer at the Dhruva reactor, and are shown in Fig. 4a. It can be seen that peaks in the diffraction patterns of the highly irradiated graphite are broader in comparison to that in the fresh sample. Fig. 9b shows the pair distribution function for the unirradiated and several irradiated samples. It is evident from this figure that an additional peak in the real-space pair-distribution function g(r) plot of the irradiated samples appears at r=2.17 Å with a redistribution of intensity in the g(r) function. As discussed below it was found that this peak arises when an atom in the hexagonal layer is knocked-out resulting in a deformed pentagon. The peak at 2.17 Å results from one of the C-C distances in the deformed pentagon from where a vacancy has been created (Fig. 4c). The intensity of the peak at 2.17 Å gradually decreases with decrease of neutron fluence. This provides the experimental evidence for the defect and deformation in the hexagonal structure.

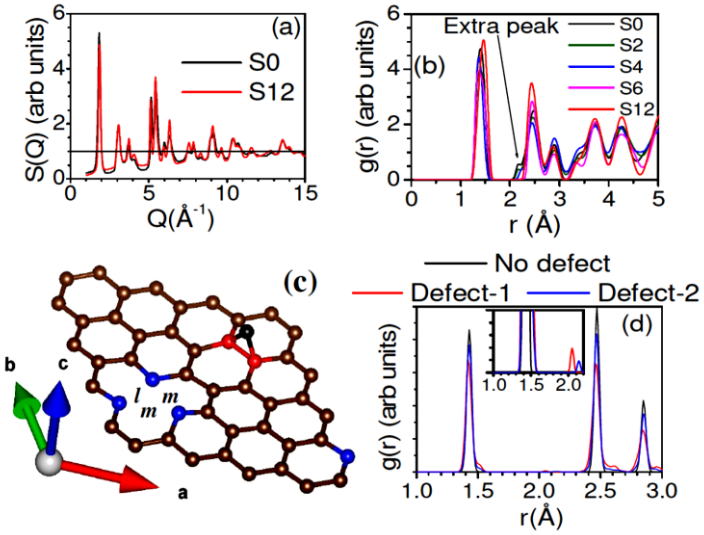

Fig. 4 Topological structures in defected graphite. **(a)** The neutron diffraction data (S(Q) vs the neutron wave-vector transfer Q) for the un-irradiated (S12) and maximum irradiated (S0) samples. **(b)** The Pair distribution function of irradiated (S0, S2, S4, S6) and un-irradiated (S12) graphite as obtained from powder neutron diffraction data. **(c)** A graphite layer with a single Frankel defect in a 4×4×1 supercell. "l" and "m" correspond to the interatomic distance of 2.06 Å to 2.66 Å respectively. The interstitial atom, and the 2-, 3- and 4-coordinated carbon atoms are shown by black, blue, brown and red colors, respectively. (d) The calculated pair correlation functions in the perfect and defected graphite structures. The labels Defect-1 and Defect-2 indicate the defect structures containing a single Frankel defect in 4×4×1 and 4×4×2 supercells, respectively. In the inset, a part of the figure is zoomed (Physical Review B, 2020. 102(6): p. 064103).

3.1.4 Unravelling the enigma of hydrogen bond interactions in crystalline solids with the help of single crystal neutron diffraction

Almost all the materials around us are made up of molecules that are made up of different atoms linked together by chemical bonds. When the various processes and functions performed by these materials are investigated it is observed that these do not usually involve making or breaking of chemical bonds but instead it is the manipulations of much weaker and more flexible "intermolecular interactions" that play a primary role in making these materials workable. In a hydrogen bond interaction D-H---A, a hydrogen atom H acts like a bridge between two other atoms called the donor (D) and acceptor A atoms, which are usually more electronegative than the H atom. Single crystal neutron diffraction is the only experimental technique which can give accurate atomic positions particularly that of H atom in a crystalline solid hence it can reveal details of hydrogen bond interactions better than any other technique. Following is a recent example of studies conducted at the instrument demonstrating the power of the instrument to unravel the minute details of hydrogen bonding in crystals.

Deterioration of hydrogen bonded superprotonic conductors belonging to $CsHSO_4$–CsH_2PO_4–H_2O solid solution system: Single crystal neutron diffraction investigation on $Cs_4(HSO_4)_3(H_2PO_4)$ and $Cs_6H(HSO_4)_3(H_2PO_4)_4$ superprotonic crystals belonging to $CsHSO_4$–CsH_2PO_4–H_2O solid solution system was under taken to elucidate the precise hydrogen atom positions in these crystals [10]. The investigation revealed that these crystals are very sensitive to the ambient conditions and can undergo deterioration due to fluctuation in air moisture content. Crystal structure of $Cs_6H(HSO_4)_3(H_2PO_4)_4$ was obtained both before and after deterioration, it was found that the asymmetric O-H···O hydrogen bond between the PO_4 and SO_4 ions (Figure-10) of this crystal becomes stronger after deterioration, this led to the shrinkage of the unit cell, and most likely prevented further deterioration. The change in the hydrogen bonding is expected to affect the overall proton conductivity of the crystal.

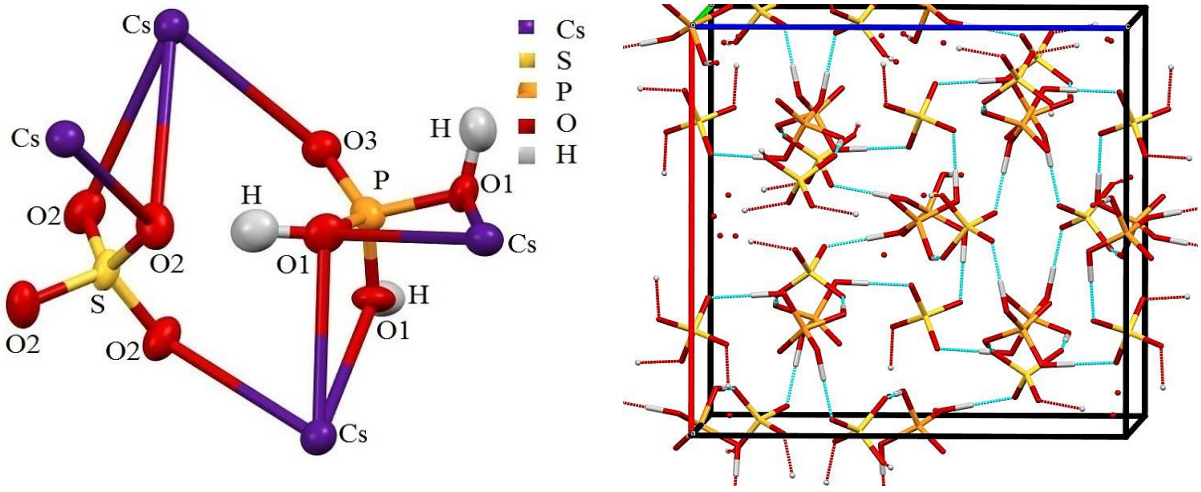

Fig. 5. Asymetric unit of $Cs_6H(HSO_4)_3(H_2PO_4)_4$. Hydrogen bonding network in $Cs_6H(HSO_4)_3(H_2PO_4)_4$ (Ref: Bulletin of Materials Science, 2021. 44(2): p. 1-8)

3.2 Microscopic spin-spin correlations in advanced magnetic materials

Knowledge of the microscopic spin-spin correlations is a key factor not only for the fundamental understanding but also to design new magnetic materials for practical applications from Spintronics to quantum devices. Neutron scattering being a novel direct probe for the microscopic spin-spin correlation in the atomic scale, it plays an indispensable tool for research in magnetism. Some selected examples based on magnetic neutron diffraction studies are outlined here.

3.2.1 Search for Quantum Magnetic States: An Insight from Neutron Diffraction

Competing magnetic interactions in low-dimensional quantum magnets can lead to the exotic ground state with fractionalized excitations. The low-dimensional magnetic systems with large spin have not been studied extensively as the quantum effects are not prominent in these materials. Herein, the results of neutron diffraction studies on several novel spin systems are presented that illustrate the microscopic spin-spin correlations.

Fig. 6 shows the neutron diffraction patterns of $Bi_3FeMo_2O_{12}$ at different temperatures over 6-50 K. Neither additional magnetic Bragg peaks nor an enhancement in the intensity of the fundamental nuclear Bragg peaks has been observed down to 6 K, indicating the absence of magnetic long-range order [11].

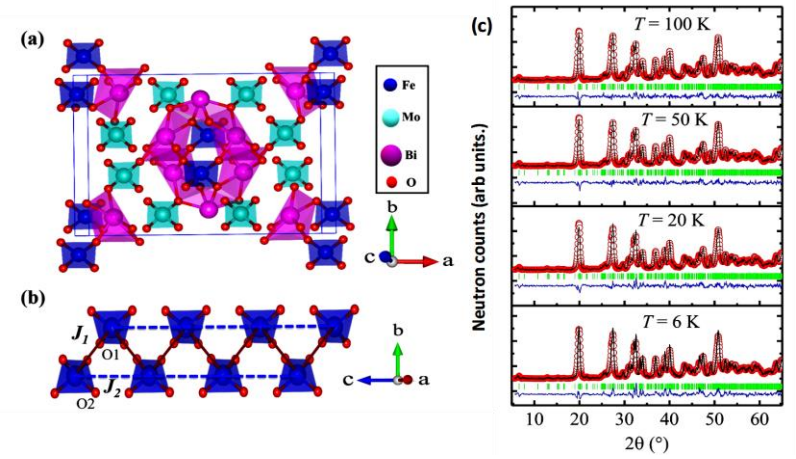

Fig. 6. (left) Schematic crystal structure of $Bi_3FeMo_2O_{12}$ having very well separated, infinite zigzag S =5/2 spin chains. (Right) Rietveld refined neutron powder diffraction patterns at 50, 20, and 6 K. [Ref: Phys. Rev B 104, 1844402 (2021)].

3.2.2 Investigations of magnetization compensation and its correlations with other physical properties

Technologically important phenomenon of magnetization compensation leading to magnetization reversal has been recently studied in several magnetic oxide systems [12-19]. In these systems, study of ordering of the involved magnetic sublattices including their temperature dependence, by employing neutron diffraction, is crucial to understand their magnetization reversal behavior. Some of our recent results on the magnetization compensation system, $YbCrO_3$ [23] are presented here.

DC magnetization and neutron diffraction studies have revealed reversals of magnetization and exchange bias (EB) across the compensation temperature (T_{COMP}) ~ 16.5 K) in $YbCrO_3$ compound [Figs. 7 (a), (b)]. Our neutron diffraction study has revealed a G_z-type canted antiferromagnetic ordering of Cr^{3+} moments below T_N (~120 K) involving a weak ferromagnetic component of magnetization (M_{Cr}) and a finite ordered moment (M_{Yb}) for Yb^{3+} sublattice [Figs. 7 (c), (d)]. The novel phenomenon of magnetization reversal, observed in the dc magnetization study, has been explained in terms of the competition between the antiparallelly coupled M_{Yb} and M_{Cr} moments. Similarly, EB, arising due to the atomistic antiferromagnetic coupling between M_{Yb} and M_{Cr} moments, also changes sign at the T_{COMP}. This sign reversal of EB is attributed to the change of dominance of competing M_{Cr} and M_{Yb} moments across the T_{COMP} [23].

The present understanding of magnetization compensation in this and similar materials, and their correlations with other physical properties may open up the possibility for making thermomagnetic switches, spin-valve, and other spintronic devices.

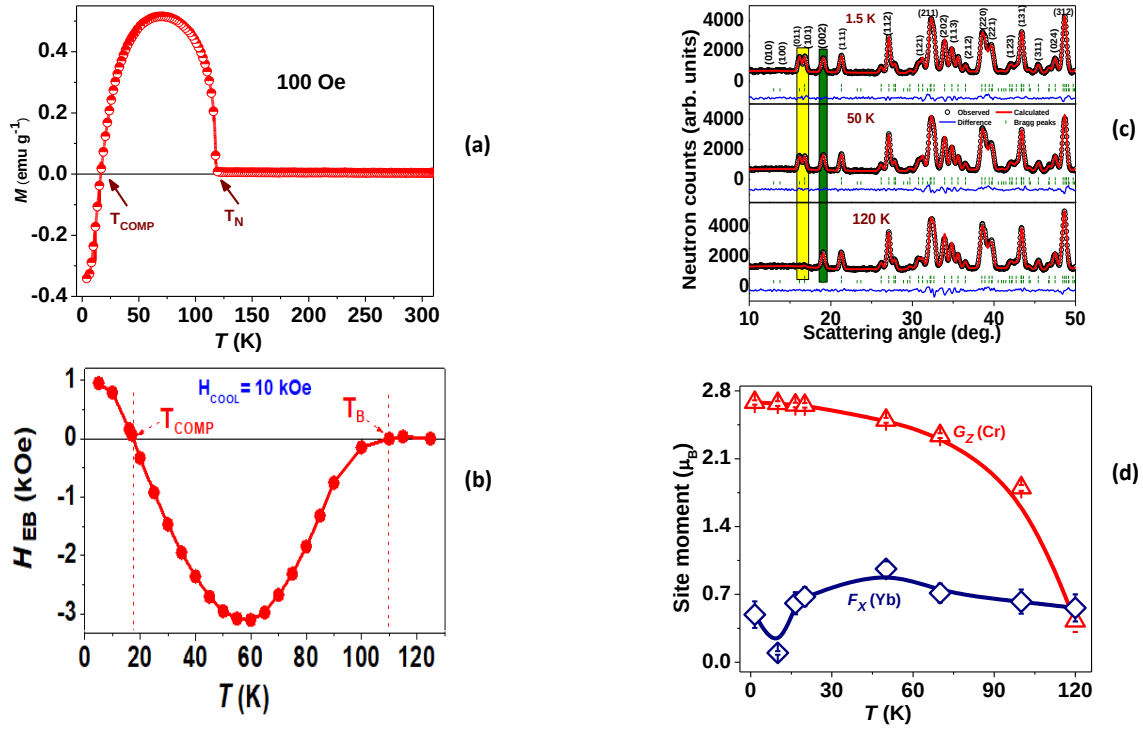

Fig. 7. Temperature dependence of (a) dc magnetization and (b) exchange-bias in $YbCrO_3$. (c) neutron diffraction patterns showing temperature evolution of magnetic Bragg peaks. (d) Temperature dependence of ordered antiferromagnetic (G_z) Cr^{3+} and ferromagnetic (F_x) Yb^{3+} moments. [Ref: Phys. Rev. Matter. 5, 124402 (2021)].

3.2.3 Na-Ion Conduction in the 2D Layered Magnetic Materials and their Battery Applications: An insight from neutron diffraction

The search for efficient ionic conductors for high-energy density battery applications under renewable energy technology (to replace conventional fossil fuels) is one of the most active fields in materials research. The cost-effective sodium conducting materials, an alternative to Li-ion batteries, are promising for medium- and large-scale energy storage applications. The Na-ion conduction materials based on the 2D layered magnetic materials are of special interest. Understanding ion-conduction pathways inside crystal structure and the role of underlying crystal structure on ion-conduction are the main decisive parameters for the Na-ion conductivity, and hence to design new high efficient materials.

The visualization of the sodium-ion conduction pathways in the 2D layered magnetic material $Na_2Ni_2TeO_6$ was reported where a coexisting commensurate and incommensurate magnetic ordering was found [20] through high-temperature neutron powder diffraction experiments and sophisticated analysis using soft bond valence sum method. Our results reveal a 2D Na ionic conduction within the Na-ion layers and provide site-specific contribution of Na-ion conduction [21]. At room temperature, only the Na ions located at the Na1 and Na2 sites, among the three Na crystallographic sites [Fig. 8(a)], are involved in the ionic conduction process. However, with increasing temperatures above ~500 K, continuous ionic conduction pathways occur involving the Na3 site as well.

Another important parameter is the crystal structural stacking faults that can affect the battery performance significantly. Comprehensive neutron diffraction results are reported to determine the role of stacking faults on the ionic conduction and magnetic properties of $Na_2Mn_3O_7$ [Fig. 8(b) and (c)]. Neutron diffraction pattern yields asymmetric broadening of selective nuclear Bragg peaks [Fig. 8(b)] suggesting the presence of stacking faults. Detailed analysis of the neutron diffraction pattern yields

that the stacking faults are due to the in-plane sliding of the manganese-oxygen $Mn_3O_7^{2-}$ layers. A substantial narrowing of the (012), (102), and (-203) Bragg peaks

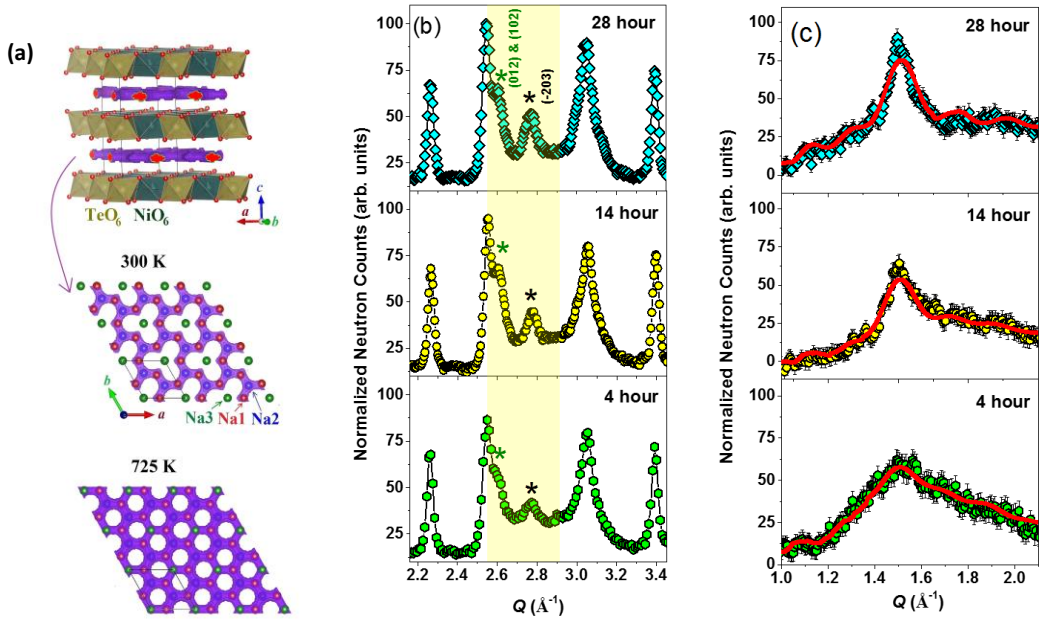

Fig 8. (a) The layered crystal structure of $Na_2Ni_2TeO_6$ and the Na-ion conduction pathways at 300 and 725 K, respectively. **(b)** and **(c)** Neutron diffraction patterns) of $Na_2Mn_3O_7$ samples synthesized with annealing times of 4, 14, and 28 hours, respectively, revealing the evolution of nuclear and magnetic peaks with the annealing time. The red curves in (c) are the RMC fitted curves of magnetic diffuse scatterings. [Ref: J. Phys. Chem. C 124, 4421 (2020) and ACS-Applied Energy Materials 4, 6040 (2021)].

[Fig. 8(b)] has been found with the increasing of annealed time (4, 14, and 28 h) during the sample synthesis, and confirms a reduction of the stacking faults with the increasing annealing time of the samples [22].

The present study provides an experimental realization of Na-ion conductions in the promising battery material based on 2D magnetic system $Na_2Ni_2TeO_6$ and facilitates the understanding of the microscopic mechanism for Na+-conductions. Further it is shown that the ionic conductivity can be enhanced by reduction of the stacking faults in the crystal structure.

3.2.4 Investigation of intermetallic alloying at the interfaces of heterostructures using polarized neutron reflectivity.

Intermetallic alloys with specific stoichiometry are known to exhibit enhanced mechanical, thermal, transport, magnetic and corrosion resistance properties. One of the prospective routes of formation of intermetallic composites is considered to be via annealing of multi-layered thin films [23]. Temperature involved in this process is usually much lower than the melting temperature of individual elements of the constituent layers, allowing controlled growth at the interfaces [24, 25]. Annealing-induced exchange bias in and emergent crystalline alloy phase (Fe_3Ge) at the interfaces of ultrathin Fe/Ge multilayers [26] has been investigated using Polarized neutron reflectivity (PNR) as a primary technique.

Interfacial ferromagnetic alloy phase in Fe/Ge multilayers

Ferromagnetic (FM) alloy phase at the interfaces of the FM/semiconductor (SC) heterostructure is essential for possible application of FM/SC system for spintronics [26]. The formation of a crystalline alloy phase (Fe_3Ge) at the interfaces on growing ultrathin Fe/Ge multilayers at an elevated substrate temperature of ~ 523 K as well as on annealing the multilayer at a temperature > 523K is investigated. The alloy phase formation at interfaces is achieved at a much lower temperature than the Fe_3Ge phase formation in bulk material (~973 K), mainly due to rapid inter-diffusion of Fe and Ge at the interfaces which is about 4 (~2) order higher in magnitude than the diffusion of Ge (Fe) in the bulk crystalline phase. Ultrathin Fe/Ge multilayers were characterized using PNR (Fig. 9) provided a detailed depth profile of the nuclear and magnetization in the system and suggested formation of alloy phase, which is FM at room temperature.

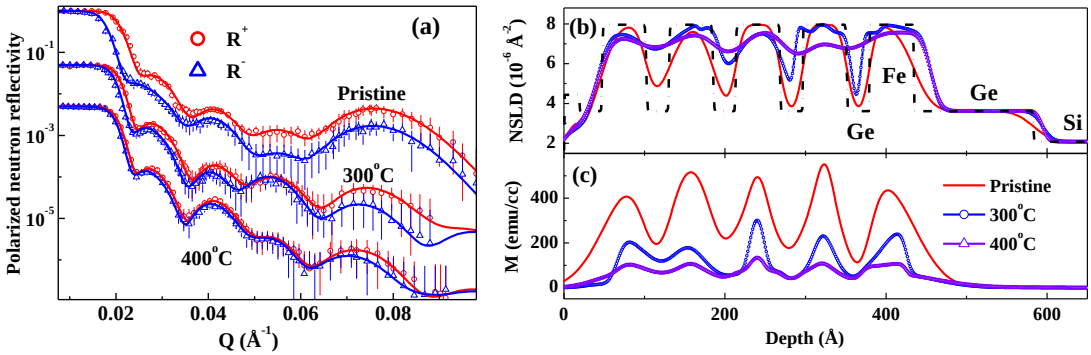

Fig. 9. a) *PNR data with best fits,* ***b)*** *Nuclear Scattering length density (NSLD) and d) magnetization (M) depth profiles for Fe/Ge multilayer grown on Si substrate at different annealing temperatures (Ref:* Applied Surface Science, 2021. **570**: p. 151193*).*

In short, using polarized neutron reflectometer, the interface magnetism of technologically important heterostructures was successfully studied.

3.3 Mesoscopic Structure and interaction in Soft Matter and Nanostructured Materials

3.3.1 Tuning of micelle adsorption on nanoparticles by combination of surfactants

The complexes of nanoparticles with surfactant (surface active agents) have myriad of applications such as enhanced oil recovery, foam stability, detergency, synthesis of photonic nanomaterials, ultra-filtration of nanoparticles etc. [27]. Most of these applications require an understanding of surfactant adsorption on nanoparticle surface. In this work, the adsorption behaviour of surfactant micelles on nanoparticles has been tuned by using a combination of surfactants. The systems have been probed by employing the unique advantage of contrast variation in SANS [28-31].

Figure 10 shows SANS data of the 1 wt% anionic silica nanoparticles (HS40) with (a) non-ionic (C12E10) surfactant and (b) non-ionic (C12E10) and anionic (SDS) mixed surfactant, in the nanoparticles contrast-matched condition. Total concentration of the surfactants is fixed to 0.5 wt%. The scattering build-up at the low Q range (Fig. 10a) suggests the formation of large structure, due to the redistribution of surfactant. The non-ionic surfactant C12E10 is known to interact with silica nanoparticles through hydrogen bonding, resulting into direct adsorption of the micelles (micelle decoration model) [29]. In this case, scattering comprises four terms self-correlation of nanoparticles, self-correlation of micelles, cross-correlation between adsorbed micelle and nanoparticle, and cross-correlation in micelle-micelle, respectively. This complicated scattering can be simplified by contrast-matching the nanoparticles with the solvent, vanishing contributions from self-term of nanoparticles

and cross term of nanoparticle-micelle interaction. Data analysis shows that around 15 micelles adsorb on each nanoparticle, whereas nanoparticles do not undergo any changes (Fig. 10b). When the nanoparticle interaction with the non-ionic (C12E10) /anionic (SDS) mixed surfactant is examined (Fig. 10b), it is found that the ionic character of the surfactant dominates and strong electrostatic repulsion between the mixed micelles and nanoparticles does not allow any direct adsorption [31]. As can be seen in Fig. 10b, the data of 1 wt% nanoparticles + 0.5 wt% C12E10-SDS system resembles with that of 1 wt% nanoparticles + 0.5 wt% SDS system.

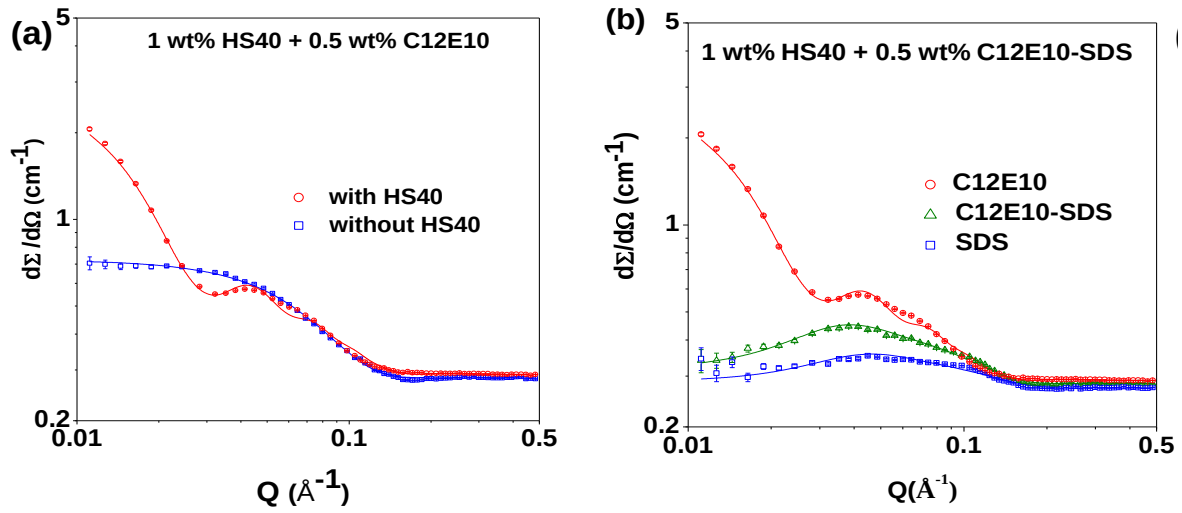

Fig. 10. SANS data of the 1 wt% nanoparticles with (a) non-ionic C12E10 surfactant (0.5 wt%) and (b) 0.5 wt% C12E10-SDS (0.25 wt % C12E10 + 0.25 wt% SDS), in the nanoparticles contrast-matched condition. The SANS data of the 0.5 wt% C12E10 is shown in (a). SANS data of 1 wt % HS40+0.5 wt% SDS under same contrast-matched condition are shown (b). (Ref: Physical Review E, 2020. 102(6): p. 062601, Langmuir, 2012. 28(25): p. 9288-9297, Journal of Physics: Condensed Matter, 2010. 23(3): p. 035101)

In short, SANS measurements under nanoparticles contrast-matched reveal that nonionic C12E10 micelles adsorb to nanoparticles. Mixed micelles of nonionic and anionic surfactants provide a very effective way to control the charge of the micellar system, and hence their interactions with nanoparticles. The systematic transition from adsorption to non-adsorption has been found in the mixed micellar system of C12E10-SDS. Overall, the study provides pathways to tune the surfactant adsorption on nanoparticles by using a combination of the surfactant.

3.3.2 Unravelling Structural Hierarchy in Self-assembled Nano-Structured Spheres

Micro-emulsion templated dendritic fibrous nanospheres (DFNS) have attracted considerable attention owing to their unique accessible pore structure coupled with high-surface area [32, 33]. However, their complex structural hierarchy is still intriguing. To establish a structure-function correlation of the DFNS, it is necessary to understand the internal morphology of the fibrous network. In this regard, small-angle scattering investigation (SAS) has been carried out over a wide Q-range of 0.003 to 2.5 nm^{-1} to unravel the structural hierarchy of DFNS [33, 34].

Fig. 11(a) shows the scanning electron micrograph of a DFNS sphere revealing multi-level structure. The hierarchical nature of the internal structure of the DFNS is reflected in the combined (both SAXS and SANS) scattering data (Fig. 11(b)). There exists a hump like feature around 1 nm^{-1} (zone B-I; Q ~0.5 to 2.5 nm^{-1}) in the scattering profile. Then, in the intermediate Q region (zone B-II; Q ~0.15 to 0.5 nm^{-1}) the intensity increases towards low Q. Next comes in the zone B-III (Q ~0.015 to 0.15 nm^{-1}) which

also shows an increasing trend but with slightly modified functionality, and ultimately the rate of increase in the intensity gets significantly reduced below Q ~0.01 nm^{-1} (overall nanosphere).

Fig. 11(b) shows a typical fitting of a suitable model with a two-level bicontinuous structure to the scattering profile. It is evident that the consideration of just two levels of bicontinuous micro-emulsion cannot represent the experimental profile over the entire Q-range, particularly in the intermediate Q-regime (~0.3 to 0.5 nm^{-1}). Thus, it was necessary to consider three levels of bicontinuous contributions (*k*=3) to fit the scattering data. In fact, this emphasizes the need of scattering experiments accessing a wide Q-range for such hierarchically structured materials [34].

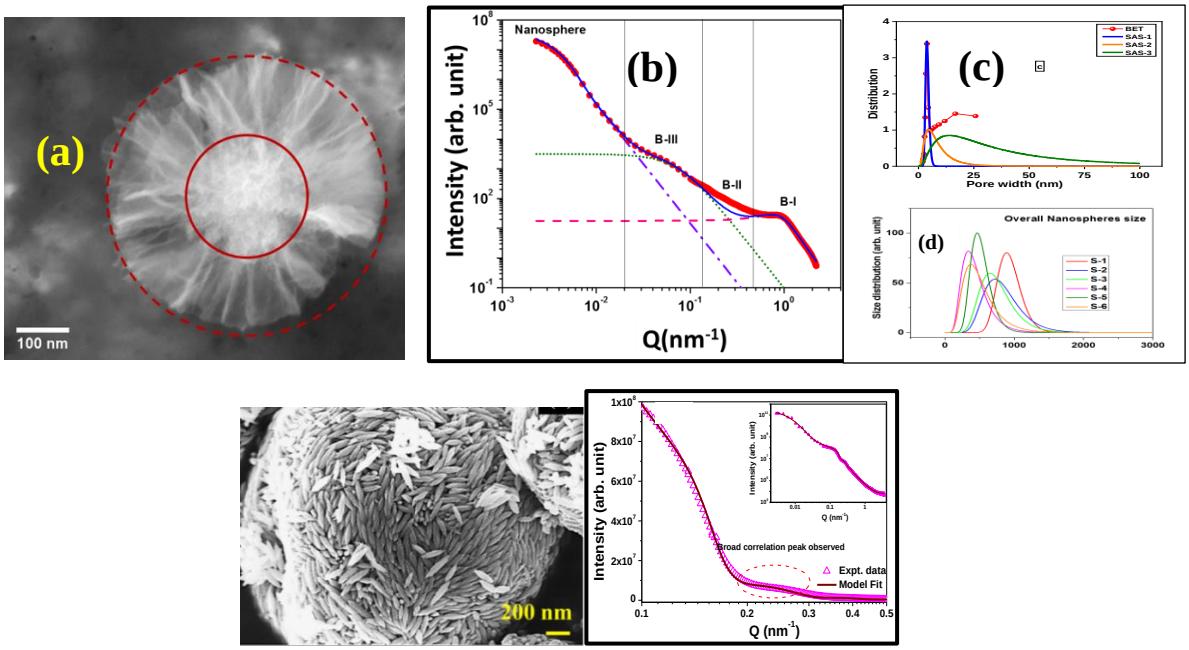

Fig. 11: **Top Panel: (a)** SEM micrograph of the DFNS sphere revealing multi-level structure. **(b)** Combined SAS intensity profile over a wide Q range. The continuous blue curve with two-levels (k=2) of bicontinuous structure is compared with the experimental data. It is evident that the model deviates at around q~0.4 nm^{-1} and consideration of three levels (k=3) of bicontinuous contributions is found indispensable to explain the SAS data over the entire accessed Q range. **(c)** Comparison of Pore size distribution from BET and small-angle scattering **(d)** Estimated Size distribution of nanospheres synthesized with different processing parameters. **Bottom panel:** SEM and scattering profile from microgranules with ellipsoidal NP (Ref: Langmuir, 2021. **37**(21): p. 6423-6434, Microporous and Mesoporous Materials, 2021. **323**: p. 111234., Langmuir 2022, 38, 12, 3832–3843).

The close packing of anisotropic particles is of fundamental importance. A novel approach has been elucidated for determination of the packing fraction of strongly correlated nano-ellipsoids in a microsphere using small-angle scattering (SAS).

SAS profile [Fig. 11 bottom panel] does not show any prominent correlation peak, even though the packed ellipsoids possess strong positional correlation. Owing to the shape anisotropy, the relative orientation of the packed ellipsoids plays a deceiving role by smearing out the structural correlation peak resulting in the underestimation of the packing fraction through conventional analysis. A new approach, by introducing an inter-particle distance distribution function in the structure factor involving the effective correlation among the correlated ellipsoidal particles, faithfully extracts the realistic positional correlation vis-à-vis the packing fraction of the jammed ellipsoidal particles from the scattering data[35].

In summary, an in-depth insight into the complex hierarchical structure of the high surface-area dendritic fibrous nanospheres and nanostructured microgranules has been obtained [32-34] by small-angle scattering techniques.

3.4. Periodic and Stochastic dynamics in Materials

3.4.1 Lattice Dynamics of Cu_2ZnSnS_4: Inelastic Neutron Scattering studies

Copper zinc tin sulphide (Cu_2ZnSnS_4, CZTS) is a semiconductor compound suitable for applications in photovoltaics. While the solar cells based on III-V semiconductors exhibit high efficiency, cheaper solar cells are required for wide spread applications. In recent years, kesterite-type Cu_2ZnSnS_4 (belonging to I_2-II-IV-VI_4 chalcogenide quaternary group) has become promising alternative in thin film solar cell applications. CZTS usually crystallizes in the body centred tetragonal kesterite-type structure with space group I4 and has two formula units per unit cell.

The lattice dynamics of CZTS was investigated using inelastic neutron scattering measurements. The computation of the lattice dynamics helps to understand the low thermal conductivity of this material in terms of the dispersion and life-times of phonons. Employing the phonon frequencies and thermal conductivity, the thermoelectric figure of merit was computed.

The phonon spectrum extends to 55 meV in this compound. Fig. 12a [36] shows the results of inelastic neutron scattering measurements on Cu_2ZnSnS_4. The experimental data compare well with the computed spectrum of the neutron-weighted phonon density of states. The low energy part of the spectrum has intense peaks that are well reproduced by the calculations, which is most important for the thermal properties of the material.

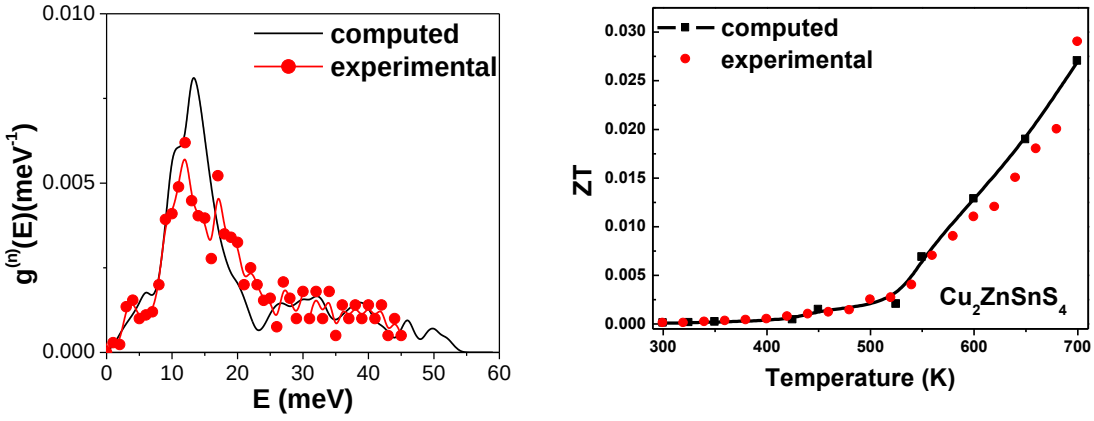

Fig. 12. (a) Experimental (from Dhruva) and computed neutron-weighted phonon density of states of Cu_2ZnSnS_4. (b) Temperature dependence of the figure of merit of Cu_2ZnSnS_4. Experimental data is from Ref [Yang et al., Nano Letters 12 (2012) 540.] (Ref: Journal of Physics and Chemistry of Solids, 2021. 150: p. 109819.

The effectiveness of a thermoelectric material is represented by the dimensionless figure of merit $ZT = S^2 T\rho^{-1} \kappa^{-1}$, where S is the Seebeck coefficient, T is the absolute temperature, ρ is the electrical resistivity and κ is the thermal conductivity. The computed temperature dependence of the ZT is shown in Fig. 12b, after normalization at 300 K. The calculated ZT increases with increasing temperature, and the rise becomes rapid beyond about 525 K, which is in excellent agreement with the experiments [37]. Overall, the agreement with experimental data [37] is reasonable, with a discrepancy of around 16% at 680 K.

3.4.2. Investigating Effects of Cholesterol on the Microscopic Dynamics of Metallosomes

Metallosurfactants (MT) are a new class of material in which the polar headgroup of the surfactant molecule contains a metal centre as an integral structural component [38]. In aqueous solution, under suitable conditions, MTs self-assemble and form metallosomes which are the closed bilayer structures encompassing an aqueous core and are surrounded by water. Owing to the various functions derived from the metal centres together with their surface activity, MT can be potentially used in various applications as drug delivery vehicles, catalysts, medicines, and precursors for nanoparticles.

Bishexadecylpyridiniumcopper tetrachloride (Cu:CPC) , an archetypal MT, has a single polar head group and two alkyl tails. Cu:CPC forms metallosomes, a model biomembrane system, when dispersed in aqueous media. Cholesterol is a vital component of eukaryotic membranes that plays a critical role in the membrane organization, dynamics, function, and sorting.

The microscopic dynamics of Cu:CPC based metallosomes are investigated using QENS technique [39]. QENS experiments indicate presence of localized motion which is described using localized translational diffusion within a sphere. Effect of cholesterol on the microscopic dynamics of metallosomal membrane is also studied and indicates that cholesterol hinders the dynamics of membrane[39]. D_2O Subtracted QENS spectra for Cu:CPC metallosome (Fig. 13a) showed significantly quasielastic broadening over the instrument resolution indicating presence of stochastic molecular motion of metallosurfctant.

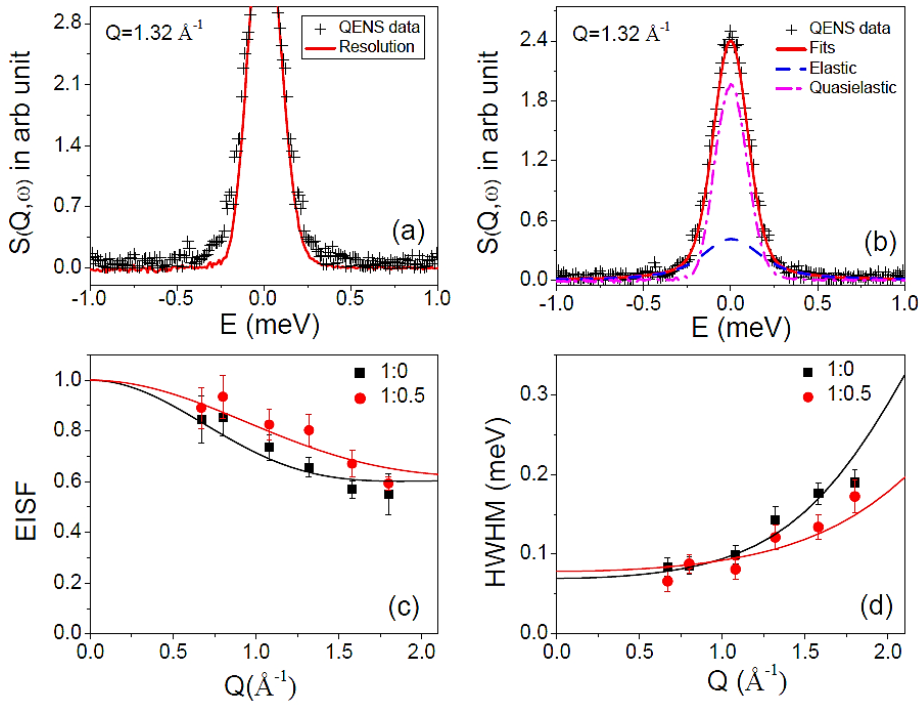

Fig. 13. (a) Typical observed quasielastic broadening after D2O subtraction for pure metallosomes over the instrument resolution as shown by the solid line. **(b)** Fitting of the QENS spectra based on eq. (1) for pure metallosomes. The elastic and quasielastic components are also explicitly shown **(c)** The variation of EISF with respect to Q for metallosomes with and without cholesterol. The solid lines are fits based on fractional localised translational diffusion model. (d) The variation of HWHM of the Lorentzian associated to the localised diffusion with respect to Q. The solid lines indicate theoretical modelling based on fractional localised translational diffusion model described in the text. (Ref: Journal of Molecular Liquids, 2020. 318: p. 114034**.**

Typically, a fitted QENS spectrum is shown in the Fig. 13 b. A non-zero Q-dependent value of EISF is obtained, which indicates the presence of localized motion. The variation of the EISF and HWHM of Lorentzian for Cu:CPC membrane in absence and presence of cholesterol are shown in Figs. 13c and 13d. It is evident that EISF for Cu:CPC membrane with cholesterol is always higher compared than pure Cu:CPC membrane, indicating that incorporation of cholesterol reduces flexibility of the Cu:CPC in metallosome and makes membrane more order. This is found to be consistent with the obtained HWHM values (Fig. 13d) which showed that for pure Cu:CPC metallosome, large quasielastic broadening is observed compared to Cu:CPC with cholesterol which indicates that dynamics of MT in Cu:CPC metallosome with cholesterol is restricted with respect in pure Cu:CPC metallosome.

Observed dynamic is explained based on the fractional localized diffusion model, in which a fraction of hydrogen atoms of Cu:CPC undergo localized translation diffusion which a spherical volume.

The observed EISF for Cu:CPC metallosomes with and without cholesterol is described very well by the solid lines in Fig. 13c and the fitting parameters, fraction of immobile hydrogen (p_x) and radius of confining sphere (a) are obtained. It is found that for pure Cu:CPC metallosomes, about 39 % fraction of hydrogen are mobile in a sphere of radius of 2.4 Å. It is found that incorporation of cholesterol, leads to decrease in radius of confining sphere from 2.4 Å to 1.8 Å. This indicates that addition of cholesterol reduces flexibility of metallosurfctant and makes membrane more ordered.

Fig. 13d show the fits of the QE widths as obtained assuming the localised translational diffusion model to describe the dynamics of metallosurfctant in metallosomes with and without cholesterol. For pure Cu:CPC metallosomes, diffusion coefficient for metallosurfctant is found to be 1.4×10^{-5} cm^2/s. Incorporation of cholesterol restricted dynamics of metallosurfctant and diffusion coefficient is found to be 1.1×10^{-5} cm^2/s.

In short, the dynamics of bishexadecylpyridiniumcopper tetrachloride (Cu:CPC) metallosurfctant in metallosomes was studied using Quasielastic neutron scattering (QENS) [40] technique. Significant quasielastic broadening is observed for Cu:CPC metallosomal membrane and observed QENS data could be described by a scattering law consisting an elastic and a quasielastic component, suggesting presence of the localized motion of the metallosurfctant. The observed dynamics of metallosurfctant using fractional localised translational diffusion model was successfully described in which a fraction of hydrogen atoms undergo localised translational diffusion within a sphere. It is found that incorporation of cholesterol reduces flexibility of the metallosurfactant in metallosomes and makes membranes more ordered. Dynamics of metallosurfactant is found to be restricted due to incorporation of cholesterol.

3.5. Investigation of hydrogen dynamics employing Neutron Imaging

Understanding the hydrogen diffusion kinetics in the materials used in the reactor materials is an important scientific problem. Zirconium alloys are used as core structural materials for reactors due to their low neutron absorption cross-section, irradiation stability and excellent corrosion resistance. Though the initial hydrogen content in core components is kept as low as possible, it can pick up hydrogen during reactor operation resulting in a steady increase of hydrogen during service. This hydrogen has a deleterious influence on the integrity of the core components, which is manifested as gross or bulk and local embrittlement. Neutron imaging provides an important probe for studying and estimating variation parameters for hydrogen diffusion kinematics that can be validated with theoretical models and hence can contribute in mitigation of structural failures or tailoring/characterization of new alloys. Systematic studies on hydrogen diffusion in Zr-2.5%Nb alloy pressure tube samples were carried out [41] at different temperatures and the possibility of quantifying hydrogen content using neutron

radiography was explored. The transmission values of neutron radiographs were used to determine the diffusion coefficients.

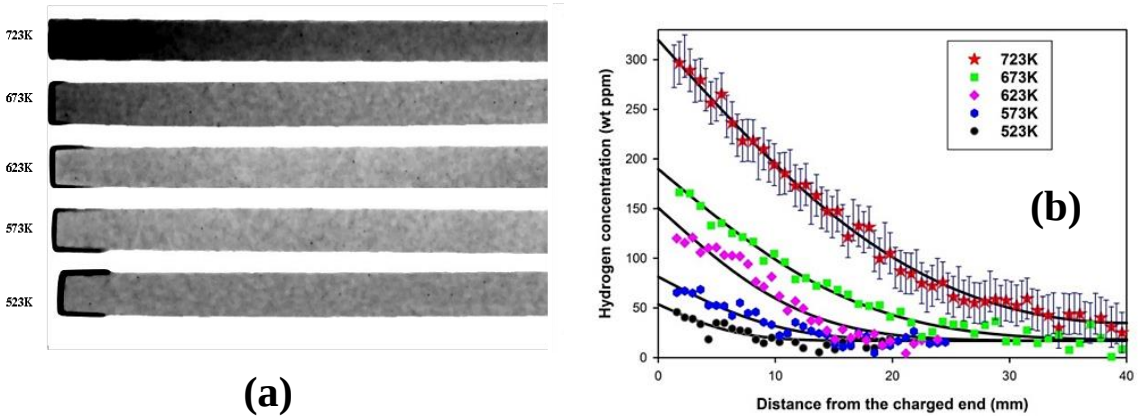

Fig. 14. (a) Radiograph for samples annealed at different temperatures. **(b)** Depth profile of hydrogen in Zr-2.5%Nb annealed at various temperatures obtained using radiography (Ref: Journal of Nuclear Materials, 2020. 544: p. 152879.

3.6. Capture Gamma Spectroscopy measurements to determine the vibrational structure of a deformed nucleus

Recently, a Capture Gamma Spectroscopy measurement has been carried out which has yielded interesting insights into the vibrational structure of a deformed nucleus (^{164}Dy). It is noteworthy that this is the first such nuclear structure investigation in India using thermal-neutron beam, and the results are encouraging to carry out further measurements in this direction.

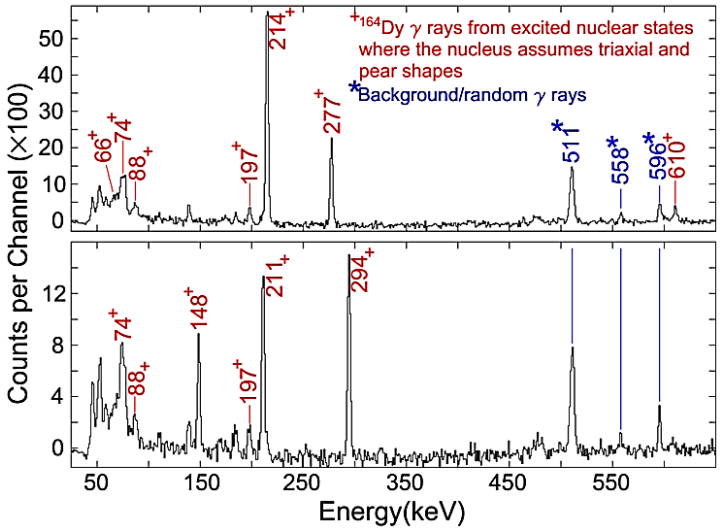

Fig. 15. Data from Capture Gamma Spectroscopy measurements on ^{164}Dy at DURGA (S. Mukhopadhyay et al., unpublished).

A certain rare type of nuclear excitation which deals with the geometrical interpretation of vibration of a nucleus with triaxial shape (*i.e.,* with three unequal axes, such as, a potato shape) has been observed. The relevant excited states and gamma rays, as a consequence of such nuclear excitations, have been identified [42].

4.0 Neutron Detectors for NFNBR: an in-house development

All the instruments at Dhruva reactor under NFNBR are supported with indigenously developed durable neutron detectors, such as neutron beam monitor, proportional counters and one-dimensional and two-dimensional position sensitive detectors (PSD), which are tailor-made for the beam size and intensity.

^{3}He remains as a basic detection medium for most of the neutron scattering instruments. Other alternative such as BF_3 gas is conveniently used for arrays as well as for other area monitoring applications. Imaging monitor is useful to evaluate the intensity profile and mount neutron optics in high intensity region.

Facilities supporting detector development

In-house facility consists of hardware design and fabrication, fine wire handling, gas filling and characterization of these detectors at the multipurpose test beam facility. BF_3 gas is generated from the $CaF_2(BF_3)$ complex with ^{10}B enrichment >90%. Generation of the BF_3 gas involves various steps, Purity of gas is further improved by repeated distillations carried out at triple point temperature of -127° C with the fine flow rate.

Fig. 16. (a) BF_3 gas generation and distillation facility

Fig. 16. (b) Various detectors developed in-house

5.0 Neutron Instrumentation for the Upcoming facilities at HFRR (Vizag) and Apsara U (Mumbai) Research Reactors

Neutron scattering is an important and indispensable technique providing unique information about bulk condensed matter spanning 10 orders of magnitude in length scales and 7 orders of magnitude in time scales. National facility for neutron beam research (NFNBR) at the Dhruva research reactor, BARC, Mumbai is conceived and operated by Solid State Physics Division (SSPD). In addition to the in-house experimental neutron beam research program, SSPD caters to (i) users from other divisions from BARC, (ii) UGC-DAE Collaborative research schemes from Indian universities and other academic institutions like IITs, National Labs etc., and (iii) Direct collaboration experiments from University and National lab users. NFNBR, Dhruva contains 12 beamlines developed by SSPD along with 1 beamline each developed by Nuclear Physics Division, Technical Physics Division and UGC-DAE CSR, Mumbai respectively. These facilities attract a strong national user base of over 200 groups from Universities and other academic institutions. At present, this is one of a kind of facility in the entire country. We also need to mention here that the neutron beam instrumentation at NFNBR benefited greatly from in-house development of all the neutron diffractometers/spectrometers with (i) self-reliance in design optimization, (ii) indigenous fabrication of shields and mechanical parts of spectrometers, (iii) design and fabrication of control and data acquisition systems, (iv) design and development of various kinds of neutron detectors required for each instrument. SSPD scientists have also exported neutron spectrometers to other countries like South Korea, Philippines, Bangladesh etc.

5.1 High Flux Research Reactor, Vizag:

HFRR is a 30 MW swimming pool type research reactor with 2.5 times neutron flux availability compared to the 100 MW Dhruva research reactor. SSPD is involved in making a liquid hydrogen (20K) based cold neutron source for HFRR with a possibility of high gains (~20) of cold neutron flux over the thermal source. With these parameters in place this reactor will be a world class research reactor for neutron beam research. Increased thermal flux at HFRR compared to Dhruva will help in improving resolutions in general for all types of neutron beam instruments and also helps to do experiments with smaller samples, both desirable characteristics. The total number of neutron beam instruments that can be accommodated at HFRR is about 25 instruments if we use the end of all the guides too.

5.2 Apsara-U reactor, BARC, Mumbai:

Apsara-U reactor is operating at BARC, Mumbai. Apsara-U is also envisaged for neutron scattering experiments.

New instrumentation at Apsara-U:

1. **Neutron Detector Test facility:** Design and development of gas proportional detectors for neutrons is a unique strength of SSPD, and for the testing of these custom-made detectors and Position Sensitive Detectors (PSDs), a permanent neutron beam line is a pre-requisite. The new neutron detectors that are being developed will be tested at the APSARA-U facility. This facility will be installed at beam tube # 8, APSARA-U.
2. **Single-crystal Alignment Facility:** This facility will be used to check the quality of single crystals, grown by the optical floating technique and to align single crystals or multi-crystal arrays in preparation for other neutron scattering experiments. This facility will be installed at beam tube # 6, APSARA-U.
3. Neutron Imaging beam line: A neutron imaging beamline has been proposed to be set-up at BT-7 beamport of Apsara-U for implementing conventional Neutron Tomography advanced neutron imaging techniques. The beam-line consists of an advanced neutron collimator,

shielded experimental hutch, enclosed within shielded walls, roof and a movable shielded door. This facility will be used for both Neutron Radiography and Neutron depth Profile applications.

4. CEvNS beam line: For the exploration of highly interesting physics, beyond the standard model, which is a very challenging and frontier field in experimental physics, it is proposed to carry out Coherent elastic neutrino nucleus scattering (CEvNS) measurements using the neutrinos produced from Apsara-U reactor at BARC. Due to the low power of the reactor (LEU fuelled low power ~ 2 MW), the facility would be as close as possible to the biological shielding, inside the Apsara-U reactor hall.

Thus, new research reactors offer new opportunities and possibilities for extending existing capabilities of the facilities operating at the Dhruva Reactor, BARC, Mumbai. Physics Group, BARC is equipped to utilize these new research reactors to advance fundamental and applied science with the help of optimized neutron instrumentation.

6.0 International Collaboration on Neutron Scattering Activities

BARC's international collaboration on neutron scattering activities began in the early Sixties under the regional collaboration agreement (RCA) in South East Asia. Under the aegis of the International Atomic Energy Agency, Vienna, neutron researchers from BARC trained scientists from other countries like the Philippines, Korea, Indonesia, Thailand, Taiwan, Bangladesh, etc., in methods of neutron scattering. BARC also donated home-built diffractometers and spectrometers to the Philippines, South Korea and Bangladesh. BARC has been collaborating with the ISIS facility, Rutherford Appleton Laboratory, UK since the early eighties. India was the first non-European country to join the international neutron research facility at the Institut Laue-Langevin (ILL) in Grenoble, France, one of the most intense neutron sources in the world in 2012. India was an ILL member country for 4 years. The ILL and India have cooperated on technology transfer in various fields including the development of supermirror-based polarizers. BARC also had an active collaboration with, 1) Paul Scherrer Institute, Switzerland, 2) HMI, Berlin, 3) Argonne National Laboratory, USA, 4) KEK, Japan towards various scientific problems including, diffraction, interferometry, small angle neutron scattering (SANS), inelastic neutron scattering (INS), quasielastic neutron scattering (QENS) etc.

At present, scientists from BARC carry out neutron experiments first with their own facility at the DHRUVA reactor and then follow up with international facilities when essential, for getting neutron data with energy high resolution over a wide dynamic wave vector transfer range for their research problem, by submitting a proposal through peer review.

7.0 Neutron Scattering Society of India (NSSI):

Neutron Scattering Society of India (NSSI), originally named as Indian Neutron Scattering Society (INSS), was formed on 11 June 2008 during a meeting of neutron users at Mumbai with an objective to promote the research and development activities of neutron-scattering science and applications. Another aim to form NSSI was to represent the neutron users in the Asia-Oceania Neutron Scattering Association (AONSA), which is an affiliation of neutron scattering societies, which directly represent users in the Asia-Oceania Region. By this, NSSI could become one of the founder members of the AONSA along with, Japan, South Korea, Australia and Taiwan.

7.1 Symposium and conferences

To promote neutron-based research in the country and to enhance the collaboration among the researchers, SSPD, BARC has been organizing several conferences in association with Neutron

Scattering Society of India (NSSI), and UGC- DAE Consortium for Scientific Research in a regular interval. Aim of these events is both showcasing of research in the area of condensed matter at neutron facilities and meeting of an active scientific user community.

Important events organized in last few years are **(i) the 7th Conference on Neutron Scattering 2021 (Hybrid), Mumbai, India** (25-27 November 2021) **(ii) 47th National Seminar on Crystallography (NSC47)** (June 19-22, 2019), (iii) **Theme meeting on Neutron scattering (**August 19, 2017) **(iv) 6th Conference on Neutron Scattering (CNS 2016) (**November 21-23, 2016) **(v) The 5th Conference on Neutron Scattering (CNS2015)** (February 2 - 4, 2015). Particular emphasis was given on the application of neutron scattering in the topics of strongly correlated electron systems, critical phenomena and phase transitions, functional materials, nanomaterials, soft matter and biological systems, energy and green materials, thin films and multilayers, and neutron instruments. The conference provided very useful scientific discussions and platform for collaborations among the national and international neutron scattering researchers.

8.0 Conclusions:

In brief, owing to the special attributes of neutrons, neutron scattering technique is unique and it provides the crucial information on structure, dynamics, imaging in materials. A strong and focused neutron-based research, encompassing interdisciplinary fields, is being carried out at Dhruva reactor, Bhabha Atomic Research Centre, under NFNBR, based on the indigenously developed facilities at the Dhruva reactor involving single crystal diffraction, powder diffraction, small-angle scattering, high Q diffraction, reflectivity, in-elastic and quasi-elastic scattering, and imaging beam line. A wide variety of technologically relevant materials, including magnetic, ceramics, alloys, glass, biological, granular materials, nano-structured materials, and industrial materials are investigated using these facilities. Very recently nuclear structure study has also been initiated using a Gamma Spectroscopy beam line. Under the NFNBR, a large number of user communities from Universities and institutes, all over the country, use these facilities apart from the dedicated in-house research. Neutron Scattering Society of India (NSSI) promotes the research and development activities of neutron-scattering science and applications. In addition to the existing Dhruva based neutron scattering facility, a newly proposed high flux reactor (HFRR) at BARC, Vizag will be a new horizon for neutron scattering activity in the country. The upcoming high-flux reactor will open up possibilities for more sophisticated neutron scattering experiments enabling scientific breakthroughs related to novel materials, energy & its storage, and health addressing some of the most important scientific challenges.

Acknowledgements: The author acknowledges contributions from all colleagues whose work has been cited in this manuscript. The author sincerely thanks all colleagues from Physics Group, BARC, whose valuable inputs helped to prepare this manuscript.

References:

[1] G. L. Squires, *Introduction to the theory of thermal neutron scattering* (Courier Corporation, 1996).
[2] S. W. Lovesey, Theory of neutron scattering from condensed matter, (1984).
[3] A. K. Bera, J. Bahadur, A. Kumar, D. Sen, and S. M. Yusuf, *Neutron Scattering Program at Dhruva Reactor: Applications to Advanced Materials Research*, 2022).
[4] S. K. Mishra, P. S. R. Krishna, and A. B. Shinde, in *Fundamentals and Properties of Multifunctional Nanomaterials* (Elsevier, 2021), p. 1.
[5] S. Thakur, P. S. R. Krishna, A. B. Shinde, R. Kumar, and S. B. Roy, (AIP Publishing LLC, 2017), Vol. 1832, p. 060012.

[6] R. Kumar, S. Gupta, S. Wajhal, S. K. Satpati, and M. L. Sahu, Effect of process parameters on the recovery of thorium tetrafluoride prepared by hydrofluorination of thorium oxide, and their optimization, Nuclear Engineering and Technology (2021).

[7] P. S. R. Krishna, S. Wajhal, A. B. Shinde, R. Kumar, and S. B. Roy, (Manuscript under preparation).

[8] S. Wajhal, A. B. Shinde, and P. S. R. Krishna, in *AIP Conference Proceedings* (AIP Publishing LLC, 2020), Vol. 2265, p. 030240.

[9] R. Mittal, M. K. Gupta, S. K. Mishra, S. Wajhal, H. K. Poswal, B. Singh, A. B. Shinde, P. S. R. Krishna, P. D. Babu, and R. Mishra, Defect topology and annihilation by cooperative movement of atoms in neutron-irradiated graphite, Physical Review B **102**, 064103 (2020).

[10] R. R. Choudhury, R. Chitra, I. P. Makarova, E. V. Selezneva, and V. A. Komornikov, Deterioration of hydrogen-bonded superprotonic conductors belonging to $CsHSO_4$–CsH_2PO_4–H_2O salt system: a single-crystal neutron diffraction investigation, Bulletin of Materials Science **44**, 1 (2021).

[11] K. Boya, K. Nam, A. K. Manna, J. Kang, C. Lyi, A. Jain, S. M. Yusuf, P. Khuntia, B. Sana, and V. Kumar, Magnetic properties of the S= 5 2 anisotropic triangular chain compound Bi 3 FeMo 2 O 12, Physical Review B **104**, 184402 (2021).

[12] A. Kumar and S. M. Yusuf, The phenomenon of negative magnetization and its implications, Physics Reports **556**, 1 (2015).

[13] A. Kumar, S. M. Yusuf, and C. Ritter, Nd-ordering-driven Mn spin reorientation and magnetization reversal in the magnetostructurally coupled compound NdMn O 3, Physical Review B **96**, 014427 (2017).

[14] A. Kumar and S. M. Yusuf, Microscopic experimental evidence of sublattice decoupling and negative magnetization in a spinel ferrite, Journal of Applied Physics **121**, 223903 (2017).

[15] M. Ghanathe, A. Kumar, I. d. Silva, and S. M. Yusuf, J. Magn. Magn. Mater. **523**, 167632 (2021).

[16] Deepak, A. Kumar, and S. M. Yusuf, Intertwined magnetization and exchange bias reversals across compensation temperature in YbCr O 3 compound, Physical Review Materials **5**, 124402 (2021).

[17] M. Ghanathe, A. K. Bera, A. Kumar, and S. M. Yusuf, Mixed Ionic–Electronic Conduction and Magnetoelectric Coupling in Li0. 5Fe2. 5–x Cr x O4 (x= 1.0, 1.1, 1.3, 1.5, and 1.6) Involving Magnetization Compensation Phenomenon, ACS Applied Electronic Materials (2022).

[18] M. Ghanathe, A. Kumar, and S. M. Yusuf, J. Appl. Phys. **125**, 093903 (2019).

[19] Deepak, A. Kumar, and S. M. Yusuf, J. Appl. Phys. . **127**, 213903 (2020).

[20] A. K. Bera, S. M. Yusuf, L. Keller, F. Yokaichiya, and J. R. Stewart, Phys. Rev B **105**, 014410 . (2022).

[21] A. K. Bera and S. M. Yusuf, Temperature-Dependent Na-Ion Conduction and Its Pathways in the Crystal Structure of the Layered Battery Material Na2Ni2TeO6, The Journal of Physical Chemistry C **124**, 4421 (2020).

[22] B. C. Saha, A. K. Bera, and S. M. Yusuf, Mechanism of Na-Ion Conduction in the Highly Efficient Layered Battery Material Na2Mn3O7, ACS Applied Energy Materials **4**, 6040 (2021).

[23] S. Singh, M. Swain, and S. Basu, Kinetics of interface alloy phase formation at nanometer length scale in ultra-thin films: X-ray and polarized neutron reflectometry, Progress in Materials Science **96**, 1 (2018).

[24] M. A. Basha, H. Bhatt, Y. Kumar, C. L. Prajapat, M. Gupta, S. Basu, and S. Singh, Formation of an intermetallic GdCo2 alloy on controlled annealing of a Gd/Co multilayer, Materials Letters **283**, 128879 (2021).

[25] S. Singh, M. Basha, H. Bhatt, Y. Kumar, and M. Gupta, Interface morphology driven exchange interaction and magnetization reversal in the Gd/Co multilayer, Physical Chemistry Chemical Physics (2022).

[26] S. Singh, H. Bhatt, Y. Kumar, C. L. Prajapat, A. Mishra, S. Bedanta, and S. Basu, Interface-driven static and dynamic magnetic properties of ultrathin Fe/Ge multilayers, Applied Surface Science **570**, 151193 (2021).

[27] H. Heinz, C. Pramanik, O. Heinz, Y. Ding, R. K. Mishra, D. Marchon, R. J. Flatt, I. Estrela-Lopis, J. Llop, and S. Moya, Nanoparticle decoration with surfactants: molecular interactions, assembly, and applications, Surface Science Reports **72**, 1 (2017).

[28] H. Singh, D. Ray, S. Kumar, S.-i. Takata, V. K. Aswal, and H. Seto, Probing the adsorption of nonionic micelles on different-sized nanoparticles by scattering techniques, Physical Review E **102**, 062601 (2020).

[29] S. Kumar, V. K. Aswal, and J. Kohlbrecher, Size-dependent interaction of silica nanoparticles with different surfactants in aqueous solution, Langmuir **28**, 9288 (2012).

[30] S. Kumar and V. K. Aswal, Tuning of nanoparticle–surfactant interactions in aqueous system, Journal of Physics: Condensed Matter **23**, 035101 (2010).

[31] H. Singh and V. K. Aswal, Tuning of micelle adsorption on nanoparticles by combination of surfactants, Journal of Applied Physics **129**, 234703 (2021).

[32] J. Bahadur, A. Maity, D. Sen, A. Das, and V. Polshettiwar, Origin of the Hierarchical Structure of Dendritic Fibrous Nanosilica: A Small-Angle X-ray Scattering Perspective, Langmuir **37**, 6423 (2021).

[33] A. Maity, A. Das, D. Sen, S. Mazumder, and V. Polshettiwar, Unraveling the formation mechanism of dendritic fibrous nanosilica, Langmuir **33**, 13774 (2017).

[34] D. Sen, A. Maity, J. Bahadur, A. Das, and V. Polshettiwar, Unravelling the structural hierarchy in microemulsion droplet templated dendritic fibrous nano silica, Microporous and Mesoporous Materials **323**, 111234 (2021).

[36] S. P. Kandare, M. N. Rao, S. S. Dahiwale, R. Rao, S. D. Dhole, and S. L. Chaplot, Lattice dynamics in kesterite-type Cu2ZnSnS4: Inelastic neutron scattering studies and thermoelectric properties, Journal of Physics and Chemistry of Solids **150**, 109819 (2021).

[37] H. Yang, L. A. Jauregui, G. Zhang, Y. P. Chen, and Y. Wu, Nontoxic and Abundant Copper Zinc Tin Sulfide Nanocrystals for Potential High-Temperature Thermoelectric Energy Harvesting, Nano Letters **12**, 540−545 (2012).

[38] F. Gu, M. Hashizume, S. Okada, Y. Sasaki, J.-i. Kikuchi, and T. Imori, Metallosomes: artificial cell membranes with ultrathin metallic surfaces derived from cationic cerasomes through electroless plating, Journal of the Ceramic Society of Japan **116**, 400 (2008).

[39] B. Kaur, G. Kaur, G. R. Chaudhary, V. K. Sharma, H. Srinivasan, S. Mitra, A. Sharma, S. L. Gawali, and P. A. Hassan, An investigation of morphological, microscopic dynamics, fluidity, and physicochemical variations in Cu-decorated metallosomes with cholesterol, Journal of Molecular Liquids **318**, 114034 (2020).

[40] R. Mukhopadhyay, S. Mitra, S. K. Paranjpe, and B. A. Dasannacharya, Quasielastic neutron scattering facility at Dhruva reactor, Nuclear Instruments and Methods in Physics Research Section A: Accelerators, Spectrometers, Detectors and Associated Equipment **474**, 55 (2001).

[41] Shefali Shukla, Prashant Singh, Tushar Roy, Y S Kashyap, Mayank Shukla, and R N Singh, J Nucl Materials 544 (2020) 152679

[42] S Mukhopadhyay, unpublished

Author Information

Dr. S M Yusuf currently serves as Director, Physics Group of BARC, Mumbai. He is a fellow of the Indian Academy of Sciences, and National Academy of Sciences, India. He also served as Director, Institute of Physics, Bhubaneswar. He was a post-doctoral fellow at Argonne National Laboratory, USA, and a visiting scientist at the Institute of Materials Science, Spain. He has made noteworthy contributions in the area of 1-D and 2-D magnetism driven by quantum fluctuations, phenomenon of magnetization reversal, magnetic proximity effect, high magnetocaloric effect, collosal magnetoresistance effect, coexistance of magnetic phases, etc. His H-index is 48.

Presently, he serves as (i) Vice Chair, Division of Condensed Matter Physics, Association of Asia Pacific Physical Society, (ii) Vice-President and Board member of Asia-Oceania Neutron Scattering Association, (iii) Vice-President, Materials Research Society of India, (iv) INSA nominated member of the National Committee for IUCr, and (v) also serves in various committees of DST, CSIR, UGC, and DAE.

He also served as (i) President, Neutron Scattering Society of India, (ii) Vice-President of Indian Physics Association, (iii) Vice President, Indian Crystallographic Association, (iv) Member of Neutron Science Review Committee, Oak Ridge National Laboratory, USA for eight years during 2013 – 2021.

Dr. Yusuf is the recipient of (i) D. Sc(Hon.), (ii) MRSI Distinguished LecturerShip Award (iii) PK Iyenger memorial award, Indian Phys. Association, (iv) Raja Ramanna Prize Lecture in Physics, JNCASR, (v) DAE Homi Bhabha Science & Technology Award, (vi) DAE SRC outstanding research investigator award, (vii) DAE Group Achievement Awards (viii) MRSI Materials Science Annual Prize, (ix)MRSI Medal, (x) NS Sathya Murthy Memorial Award of IPA, (xi) 1st prize in Young Physicist Colloquium from Indian Physical Society. Recipient of U.S. Depart. of Energy Fellowship, & Spanish Ministry of Science && Education Fellowship.

Utilization of Neutron Scattering Facilities at BARC by Indian Universities and Institutes

P. D. Babu

UGC-DAE Consortium for Scientific Research, Mumbai Centre, 246-C CFB BARC Campus, Mumbai – 400085, India
(*Author email:* pdbabu@csr.res.in)

1.0 Introduction

UGC-DAE Consortium for Scientific Research (UGC-DAE CSR), formerly known as Inter University Consortium for DAE Facilities came into existence following an MOU (and MOA) between University Grants Commission (UGC) of MHRD, GOI and Dept. of Atomic Energy (DAE) with a mandate to promote and coordinate the use of major DAE facilities by university research community. Mumbai centre (CSR) has been instrumental in facilitating the use of neutron scattering facilities at the "National Facility for Neutron Beam Research" (NFNBR), by the university scientists. The NFNBR, which includes a wide variety of neutron spectrometers, is being increasingly utilized by a number of university groups for research problems in front-line areas of science and technology.

Mumbai Centre of UGC-DAE CSR has been coordinating and promoting the use of neutron scattering facilities by the university research community for last three decades. For this purpose, neutron schools/workshops are organized every year in different parts of the country, including remote areas from far east (Nagaland) to Jammu. During these workshops, few days dedicated to hands on training with neutron scattering instruments at Dhruva. Over the period of time, more than 500 university users from all over country have been trained in the use of neutron scattering as well as with neutron data analysis.

2.0 Collaborative Research Schemes

The collaborative research scheme (CRS), initiated by the consortium, is a peer-reviewed, long-term collaborative program wherein a university researcher, in collaboration with BARC/CSR scientists, could carry out neutron scattering experiments at the Dhruva reactor, BARC or utilize the state-of-art in-house facilities of the CSR. Once a research proposal is accepted under the CRS program, CSR provides grants for travel to BARC, contingency and, in deserving cases, fellowship for a student. A large number of scientists of various disciplines like physics, chemistry, materials science, chemical engineering, etc, from many universities and research institutions of the country benefited from the use of neutron facilities at Dhruva reactor using this program.

Neutron diffraction (normal, small angle and hi-q), quasielastic scattering, inelastic scattering techniques and activation analysis are the most popular techniques among university groups in India. Till date more than 300 collaborative research projects have been completed. Every year there is a steady increase of CRS projects as can be seen from Fig.1(a). The CRS project users are distributed throughout the length and breadth of the country, even remote corners as can be seen from Fig.1(b). At any point of time, there 30 to 40 ongoing CRS projects by university groups per year who are utilizing the neutron scattering facilities. In addition to long term CRS projects, UGC-DAE CSR has been supporting one-shot experiments (duration ranging from one to two weeks) where a single or series of samples are studied using neutrons by a university group. On the average, about 30 to 40 publications arise out of these university collaborations per year and had led to large number Ph.D.'s being awarded using the data take at Neutron Facilities.

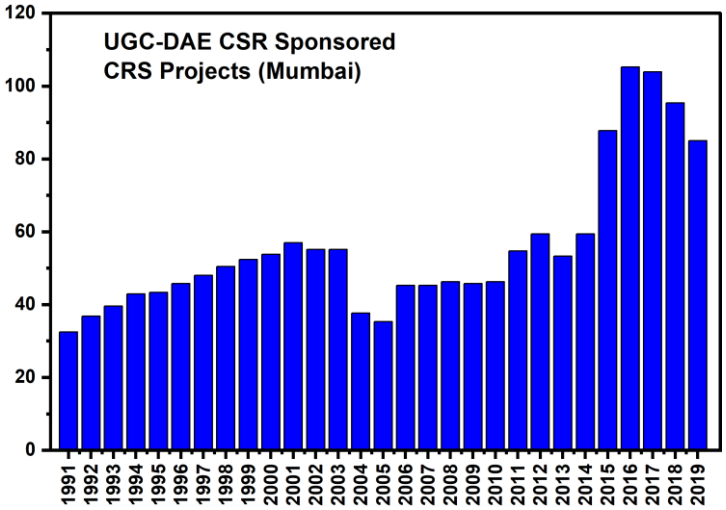

Fig. 1(a) Growth of CRS projects of Mumbai Centre in Blue over the years

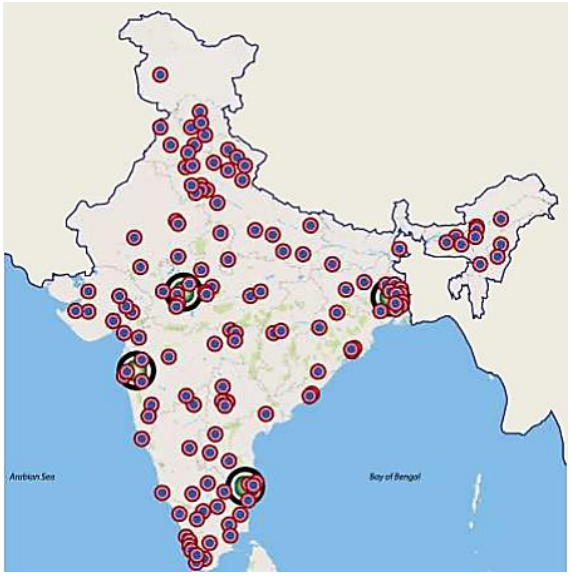

Fig. 1(b) Distribution of university/college/ Institute users of Mumbai Centre (neutron

The neutron scattering users come not only from the colleges and smaller universities, a significant numbers users are also from the premier institutions such as central universities, I.I.T.s, I.I.Sc. TIFR, CSIR labs, etc. With the help of neutrons, some of these grops have obtained very significant results leading top quality publications. Relaxaor ferroelectric behaviour, complex magnetic structures, study and development ferrofluids suitable for applications, study multi head surfacnts and other micellar systems, variety of polymers based systems, dynamics in porous zeolites, probing acheoligically important potter samples, stydying toxicity in crop patterns of certain regions, etc. are some of the exotic phenomena that were studied using neutrons by university groups.

These programs resulted in large number publications from university users in internationally refereed journals. Neutrons not only helped in increase in publications, but also let to significant raise in the quality publications which appeared in top journals. This raised the qualify of research in many universities.

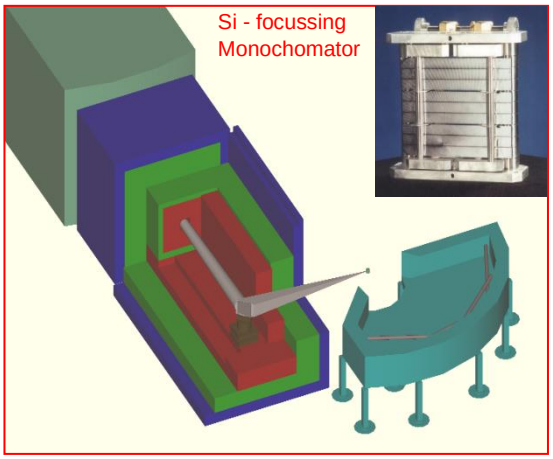

Fig. 2(a). Schematic cross-sectional view of Neutron beamline and powder diffractometer designed, developed and commissioned by UGC-DAE CSR on TT1015 beam port. Inset show double bent perfect Silicon Single crystal Monochromator

Fig. 2(b). Actual photograph of Neutron beamline and powder diffractometer. Monochromator is capable of providing different wavelengths by computer controlled goniometer.

CCR with integrated VTI

Fig. 3(a). Closed Cycle Refrigerator for temeraature variation of sample (3K to 300K)

7 Tesla Cryogen-Free Magnet with 1.5 K VTI

Fig. 3(b). Cryogen Free magnet with split pair coils capable of proving 7Tesla at any temperature inrange of 1.6K to 300K.

It would not be an exageration to say that these programs resulted in research being under taken in many colleges where none existed previously.

With large demand for powder diffraction from university community, UGC-DAE CSR Mumbai Centre has designed, development and commission a tandem neutron beamline (Fig.2(a)) with focusing crystal based high resolution and high intensity neutron powder diffractometer as shown in Fig.2(b). This diffractometer employs doubly bent asymmetrically cut Silicon single crystal-based monochromator that is mounted on a computer-controlled goniometer. Different wavelengths can be accessed with a simple rotation and tilt adjustment of the monochromator, which gives enormous flexibility to run instrument optimally for different situations. This diffractometer, generally referred to as "Focusing Crystal Diffractometer (FCD) or PD-III, is equipped with unique sample environment facilities like low temperature down to 1.6 K and high magnetic fields up to ±7 Tesla. These sample environmental facilities help in study samples as function of temperature as well as under the influence of magnetic

Fig. 4(a). Boron Rubber developed by R Prof. R.V. Upadhyay of Bhavnagar Univ. under CRS Project

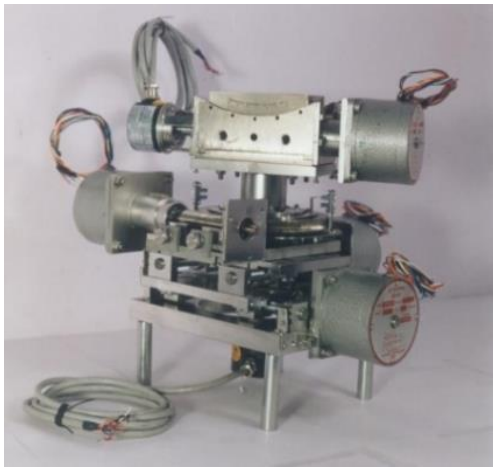

Fig. 4(b). Computer controlled goniometer consisting of x-y stage, 360º rotation table and ±15º tilt stage by Prof.V. N. Bhoraskar under CRS Project

field. There are about 15 CRS projects and 25 one-shot university users per year on an average on this diffractometer and is heavily utilized by university community.

3.0 University Participation in Beamline Development:

In the development of this tandem neutron beamline, five university groups were involved in the development of different aspects of instrumentation. (a) One Pune university group was involved in the development of monochromator bending devices while (b) another Pune university group was involved in the development of computer-controlled goniometer. (c) The Goa university group was involved in the shielding calculations whereas (d) the group from Rajasthan university was involved with the development of low temperature cryostat for neutron scattering experiments. And (e) the group from Bhavnagar University was involved with the development of Boron Rubber – a neutron shielding material. These projects were successful to various extents. The Boron rubber project was the most successful one, it not only led to the development of flexible Boron Rubber (content of B from 5 to 52% available) as shown in Fig. 4(a) and Boron impregnated Polyethylene (hard plastic) with 1% to 30% B loading. This product was developed with a tie-up from a small-scale industry from Bhavnagar. This company not only made Boron Rubber and Plastics with required B content it has successfully marketed the same withing the country and abroad. It has now Christened as "Boron Rubbers India" and has now grown in much larger company. It is supplying Boron based products to various DAE and defense organizations as well as exporting to USA and Europe. Figure 4(b) shows the computer-controlled goniometer developed by Prof. V. N Bhoraskar of Pune University, which was another completely successful project.

On the whole, UGC-DAE CSR is instrumental in spreading the neutron scattering activities around the country and played a significant role in raising quantity and quality of research output from universities.

Reference: The material present in this report is taken from various internal reports of UGC-DAE CSR and its annual reports.

Author Information

Dr. P. D. Babu, is the Centre Director, UGC-DAE Consortium for Scientific Research, Mumbai Centre. His areas of research are Experimental Condensed Matter, Magneto Structural Properties, neutron diffraction and other physical properties of Novel magnetic materials. He completed his PhD from University of Hyderabad. He won best thesis award at DAE Solid State Physics Symposium -1996. He was a UGC- CSIR NET Fellow (1988-1993). He was a visiting Scientist in Tamkang University, Taipei, Taiwan (April 2004 – Dec 2005). He has performed experiments at several International Neutron Scattering Centres, such as ILL, Grenoble, France; Paul Scherrer Institute (PSI), Switzerland; Synchrotron Facility, Taiwan.

His research experience includes design, development and installation of Tandem Neutron Beam line, High Resolution Neutron Powder Diffractometer (with unique sample environment of low temperatures and high magnetic fields) and development of triple axis spectrometer. He was one of the key people involved in development of Material preparation Laboratory at CSR, Mumbai Centre and also in the development of low temperature and high magnetic field laboratory.

He has worked on Synchrotron Techniques - (Thin Films, nanomaterials & bulk samples) such as X-ray absorption/EXAFS/XANES; Photoelectron spectroscopy (PES); Scanning Photoelectron Microscopy (SPEM); X-ray Magnetic Circular Dichroism (XMCD). He has, till date, published 210 articles in referred journals.

Basics of Neutron Imaging and its Applications

Yogesh Kashyap*, Tushar Roy, Shefali Shukla and Mayank Shukla

Technical Physics Division, Bhabha Atomic research Centre, Mumbai-400085, India
*(*Corresponding author email:* yskashyap@barc.gov.in)*

1.0 Introduction:

It has been dream of scientist to look inside the materials and see the unseen. A good understanding of microscopic and submicroscopic properties or atomic decorations is not only a scientific fancy, but it has revolutionized the field of science and engineering. Understanding attributes at this scale is crucial not only for characterization of materials, but also for discovering new materials and developing revolutionary material development procedures. There are a variety of destructive and non-destructive approaches available today to achieve this objective. A vast variety of these approaches rely on visible light, electrons, microwaves, X-rays, and neutrons, among other things. These methods rely on the interactions of radiations with matter to extract the relevant parameters. Because each of these radiations has a distinct characteristic, each of these methods is best suited to a certain application or the extraction of a tiny portion of relevant data. Light microscopy, for instance, is a great tool for optically transparent materials. Similarly, when it comes to obtaining information about a material's surface, electron microscopy-based techniques provide extremely accurate and thorough results.

Neutrons, unlike all other types of radiation, have the ability to penetrate the bulk of the material. Neutrons penetrate comparably thick samples and thus allow a deep look inside a sample rather than only at its surface. Moreover, neutron-based imaging techniques are inherently non-destructive in nature and no detailed sample preparation is necessary. For example, unlike electron microscopy, the sample does not need to be placed in a vacuum chamber or needs to be conducting in nature. We will briefly discuss some of the key factors that distinguish neutron as a unique probe in the non-destructive examination of matter:

a) Neutrons are useful for investigating biological materials and samples under in-situ condition of pressure, temperature, within chemical reactors because of large penetration depth into most materials.
b) Neutrons have a magnetic dipole moment; they are affected by magnetic fields produced by unpaired electrons in materials. As a result, they are used as a probe to examine nuclear spin, and analyse magnetic properties of materials.
c) The interplanar distance in polycrystalline materials is comparable to the wavelength of neutrons (1A to 10A). As a result, they're suitable for determining microstrains in large structures through use of neutron diffraction.
d) Because neutrons interact with nuclei in a quasi-random way, lighter atoms may be detected even in the presence of heavier atoms, and neighbouring atoms can be discriminated from one another. Furthermore, contrast may be changed by isotopic substitution (for example, D for H or one nickel isotope for another); specific structural characteristics can thus be emphasised. As neutrons are highly sensitive to hydrogen, they are an effective probe for hydrogen storage materials, organic molecular materials, and biomolecular samples or polymers.

In following section, we describe the basic concepts of attenuation-based neutron imaging and show its potential through its application various scientific and engineering fields.

2.0 Basics of Neutron imaging:

A plethora of imaging technologies are used in almost every branch of research at some point. In this regard neutron imaging plays the complimentary role as compared to X-ray imaging due to their interaction mechanism. Neutrons are strongly attenuated by low Z materials and, with the exception of a few, and transparent to most high Z materials. The first radiography experiments by H. Kallman in 1935 [1] were also carried out soon after the discovery of neutron radiation by J. Chadwick in 1932 [2]. Unlike X-rays, which interact mainly with the electrons in the atomic shell, the neutron attenuation coefficient of a material is determined by the neutron-nucleus interactions. Figure 1 shows a typical comparison of neutron mass attenuation coefficient and that of thermal neutrons [3]. As can be seen from this plot, its quite clear that, for thermal neutrons, the attenuation coefficients show no simple dependence on the atomic number and can vary significantly also between neighboring elements or even between the isotopes of the same element.

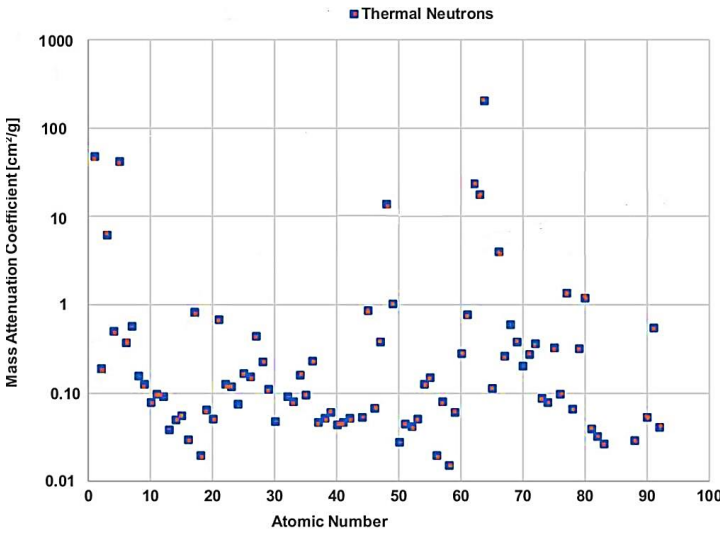

Figure 1 Plot of neutron mass attenuation coefficient as a function of atomic number.

The neutron matter interaction can be simply modeled through the complex refractive index for neutrons with a wavelength λ propagating through a medium can also be described as (as shown in Figure 2):

$$n(\mathbf{r},\lambda) = 1 - \delta(\mathbf{r},\lambda) - i\beta(\mathbf{r},\lambda). \tag{1.1}$$

Where the real part δ corresponds to the phase of the propagating neutron wave and β represents the absorption of the neutron in the medium. Consider a plane wave with amplitude A_0, and initial wave-vector k, incident on a material with thickness *d* and refractive index *n*. The amplitude of the unperturbed wave after the material is $A = A_0 e^{i(kd-\omega t)}$ where $k = \omega/c$ and amplitude of the perturbed wave after the object is given by:

$$A = A_0 e^{i(k'd-\omega t)} = A_0 e^{-i\frac{\omega}{c}\delta d} e^{-\frac{\omega}{c}\beta d} e^{i(kd-\omega t)} \tag{1.2}$$

where $k' = n\omega/c$. Eq. (1.2) contains a phase factor $\exp(-i\phi(d))$ with $\phi(z) = \omega\delta d/c$ which represents the phase difference between matter and vacuum. Similarly, the amplitude attenuation of the wave is given by $\exp(-\omega\beta d/c)$. Hence the intensity in the exit plane of the object is $I = |A|^2 = I_0 e^{-2k\beta d} = I_0 e^{-\mu d}$, which is

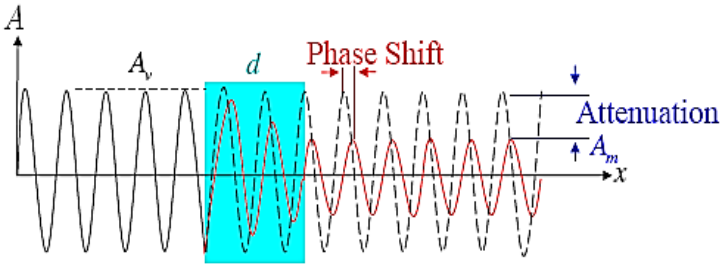

Figure 2 The effect of transmission of a wave through matter with complex refractive index.

nothing but Lambert-Beer's law where $I_0 = |A_0|^2$ and attenuation coefficient μ is defined as $\mu = 2k\beta = 4\pi\beta/\lambda$. This is the basic principle of radiography where the information based on differential attenuation or absorption is recorded.

More precisely, the Beer-Lambert law, can be expressed as follows:

$$I = I_0 e^{-\int \mu dl} \tag{1.3}$$

where I_0 and I are the incident and attenuated neutron beam intensities respectively, μ is the attenuation coefficient of the material (combining the interaction cross-section and nuclear density) and *dl* is the path length through the sample. Radiography, as shown in Eq. (1.3), gives integrated information on the amount of attenuation along the ray path, and the contributions arising from distinct elements ore quantity of material corresponding to the path length cannot be separated. Although ill-posed, this common "inverse problem" may be solved using the radon transform [4] and Fourier back-projection techniques, as well as iterative reconstruction methods [5], and is referred to as Computer Tomography (CT). The tomographic scan generates three-dimensional spatially resolved images (volumetric data) that depict the distribution of attenuation coefficients in the sample volume [6].

3.0 Neutron Imaging Facility at Dhruva Research Reactor:

In 2016, a new Neutron Radiography and Tomography Facility, as shown in Figure 3, was commissioned at Dhruva. Dhruva is also India's main neutron beam research centre, with digital neutron radiography and tomography capabilities. At the Beam-hole HS-3018, a dedicated neutron imaging beam line has been built up for real-time neutron imaging and neutron tomography. Hydrogen ingress in zircaloy, study of pressurised heavy water reactor (PHWR) fuel pins, fractures in failed turbine blades, real-time inquiry, and other research are all possible using this neutron imaging Facility.

Figure 3 Photograph of Advanced neutron imaging beamline at Dhruva Research Reactor

The neutron collimator is an important ingredient for neutron imaging and has been constructed in such a manner that it may be used for both neutron radiography and tomography as well as phase contrast imaging investigations on the same setup. A customized conical collimator with a 1mm pinhole is installed in the main collimator for phase contrast imaging applications. As a neutron shielding material for the experimental hutch, borated polythene (1% Boron content) was employed. This experimental hutch was built with modular and simple-to-assemble blocks of borated polythene (400mm thick for the walls and 600mm thick for the door) and lead (200mm thick). In the path of the beam, an extra shutter composed of 250mm thick borated polythene (20% boron concentration) and 200mm thick lead was employed to allow easy change the samples during experiments.

The digital imaging detector system used for experiments consists of a scintillator (LiF/ZnS(Ag)), a front coated mirror and a high resolution CCD camera kept inside a light tight box. The L/D ratio and the beam size at the sample position (at 1100mm from the collimator output) was found to be ~ 160 and ~140mm respectively. The cadmium ratio was determined to be 250. A high cadmium ratio suggests a thermal beam with a minimal contribution of higher energy neutrons.The thermal neutron flux at the collimator

output was measured to be $4x10^7 n/cm^2/s$. A 170µm spatial resolution has been achieved with the 100µm scintillator and the optics used in the camera. The sample manipulator is kept in front of the imaging system for mounting the samples. The material is directly imaged for Neutron radiography using CCD based digital detector or off-line neutron sensitive Films. Tomography involves rotating samples in stages of 180/360° and recording the radiography projection image data to rebuild the distribution of components in the sample. Figure 4 shows some applications of Neutron imaging chosen from variety of disciplines to illustrate the potentials of this technique. In the following sections we discuss, some applications of neutron imaging.

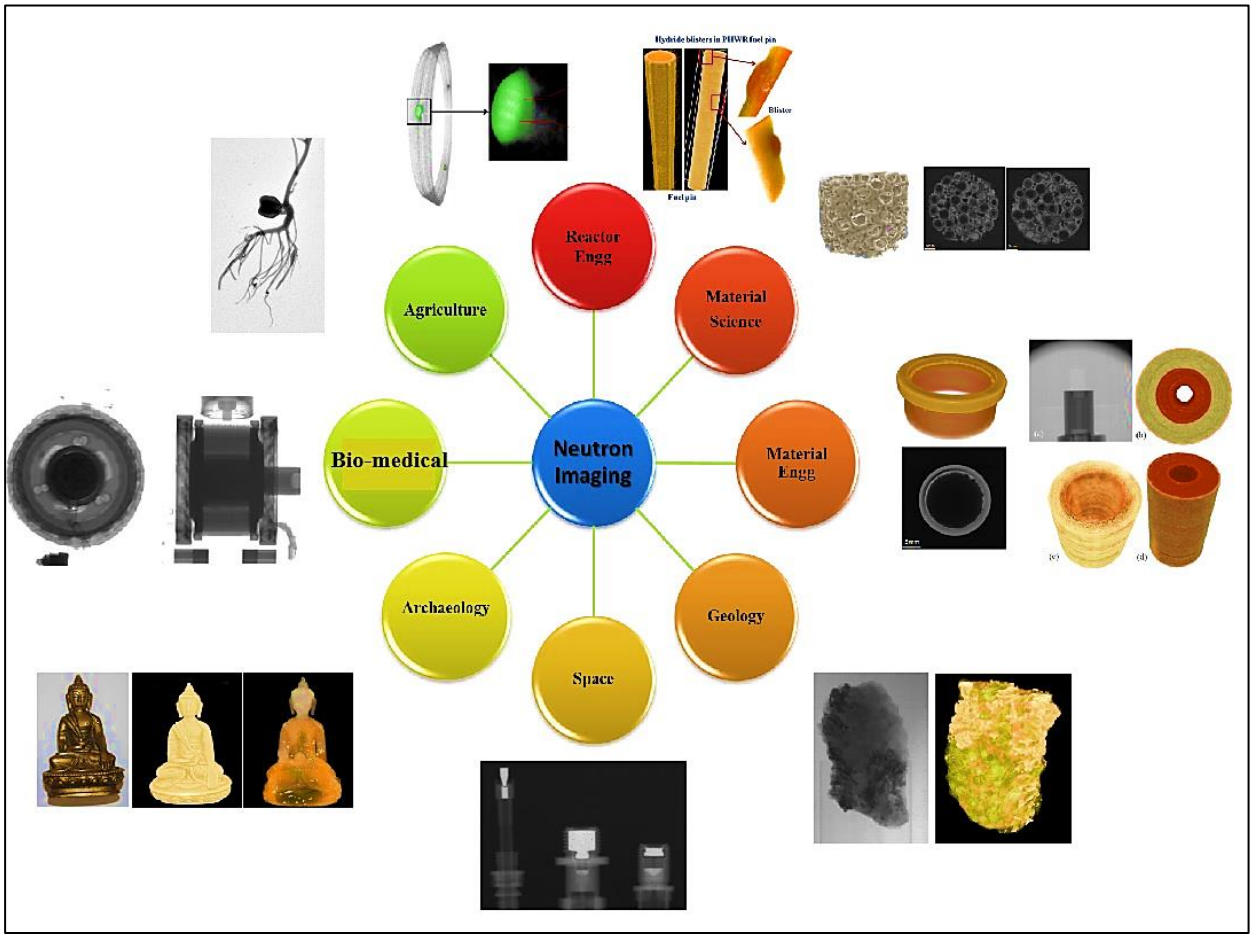

Figure 4 Applications of neutron imaging as shown through some representative examples

4.0 Neutron imaging for Engineering Applications:

Because of neutrons' unique interaction capabilities, they are widely utilised as probes for characterising materials for the improvement of process parameters, novel material development, and a different variety of engineering science disciplines.

In many applications where new materials are developed to meet safety requirements, the health of the materials is critical since the application's success is dependent on the material's fitness.

For example, when metals are welded, local deformation due to heat stress may be created, and therefore and an in-depth investigation of the fusion site is critical. Figure 5 and Figure 6 show use of neutron imaging in non-destructive evaluation of different kinds of engineered samples.

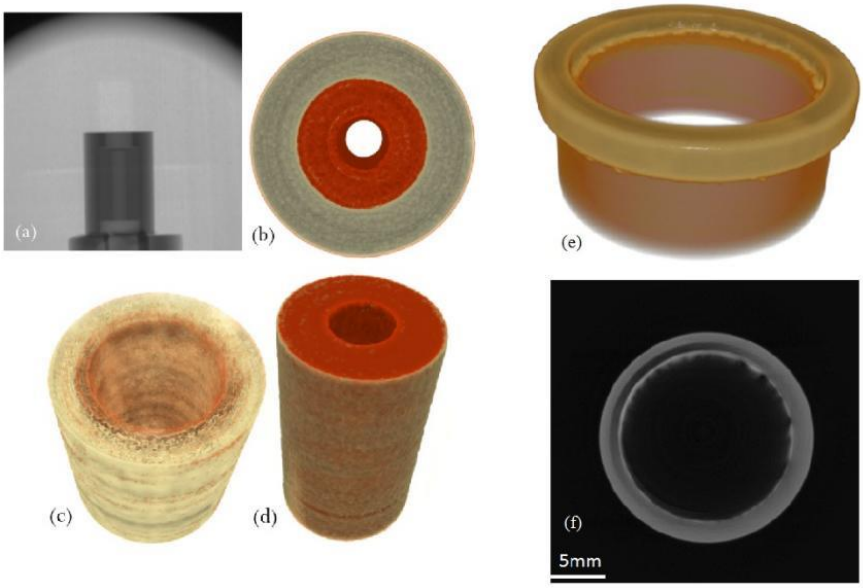

Figure 5 (a) Neutron radiograph of Ti-SS bonded material (b-d) Neutron tomography of the same showing the internal and surface details (e-f) Neutron tomography of SS-Ceramic joints showing the deformation at the welding part [7]

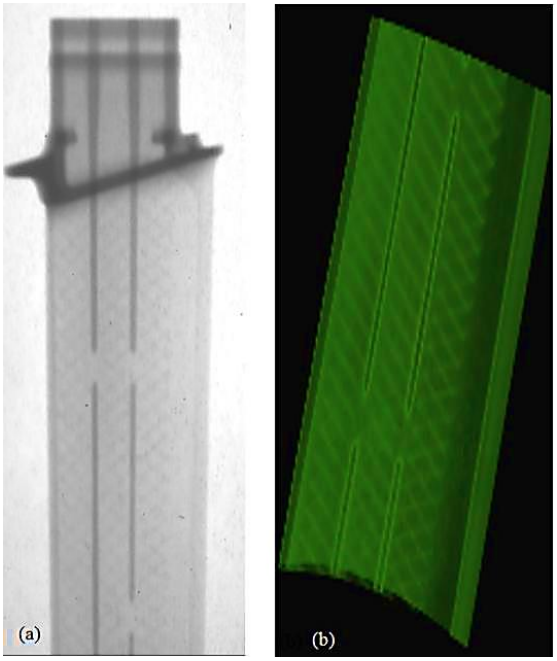

Figure 6 (a) Neutron radiograph of a gas turbine blade (b) Neutron tomography of the same showing the details of internal part

5.0 Neutron imaging for Agricultural applications:

Land degradation is affecting around 38% of the world's agriculture owing to decreasing water and fertiliser availability, as well as lower rainfalls. Over the last 40 years, over one-third of the world's agricultural (1.5 billion hectares) has been abandoned due to soil erosion, excessive fertiliser usage, ground water depletion, and other factors. For example, The United States is losing soil at a rate that is ten times faster than natural replenishment. Therefore, Its important to carry out scientific investigation in exploring and modifying root development, as well as managing the rhizosphere, to boost water and nutrient absorption and minimise root dysfunction caused by infection and disease, as well as drought,

resulting in increased crop yield. Figure 7 show some examples of applications of neutron imaging in agriculture sciences.

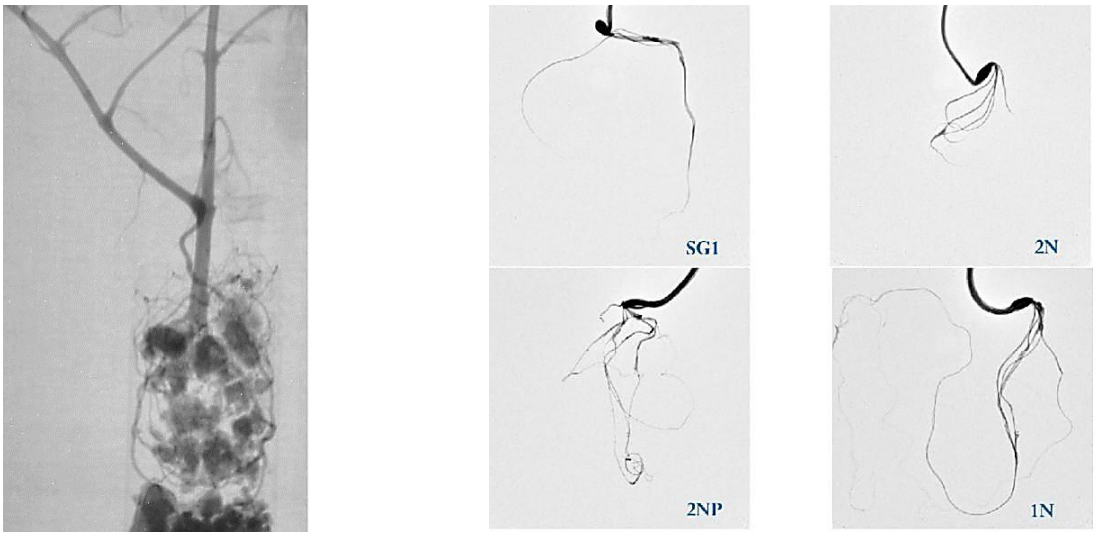

Figure 7 (Left) Neutron radiograph of the plant with rizhosphere, (Right) Neutron radiograph of seeding grown with varieties of nutrients

6.0 Neutron imaging for cultural heritage and archaeological applications:

Archeology is the study of the ancient and modern past of human civilization via tangible remnants, and it is one of the interesting sciences that has drew scientist's attention to its past over the millennia. A systematic study of archeological materials gives us the tools and procedures to investigate our past and developmental over the course of history.

Neutron imaging is a nondestructive technology which has advantage over destructive techniques that have restricted applications, as the preservation of archeological artifacts is one of main concerns. Neutron imaging has the unique ability to characterise the composition and mechanical properties of ancient materials, allowing it to answer questions about the production process and the degree of deterioration etc. Neutron based techniques are increasingly being employed for quantitative, non-invasive study of various areas of cultural heritage preservation in general: museum collections, artefacts, books, manuscripts, musical instruments, archaeological finds Geomaterials, and so on [8-11]. Figure 8 shows an example of neutron tomography that reveals internal decorations of a metallic Buddha statute.

Figure 8 (a) Photograph (b) Neutron radiograph (c-d) neutron tomography of a Budhha statue

7.0 Neutron imaging for Nuclear Industry:

The increasing demand for electric energy necessitates an increase in global nuclear power generation. Nuclear power generation is becoming safer and more efficient as a result of ongoing research and development in this industry. Neutron imaging has a wide range of uses in the nuclear sector, from evaluating new fuels and reactor materials to investigating irradiated failure components to determine the underlying cause of damage. For example, presence of hydrogen in both pressure tubes and fuel cladding is detrimental to long and continuous reactor operations, and neutron imaging techniques can be used to detect the presence of hydrides in these components, as shown in the Figure 9 and Figure 10 respectively.

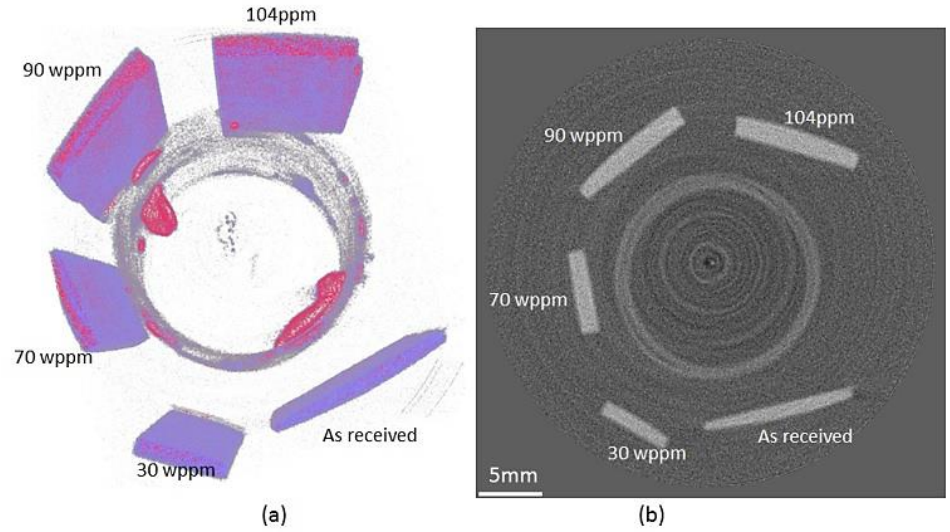

Figure 9 (a-b) Neutron tomography of Zr-alloy with varying amount of Hydrogen content [5]

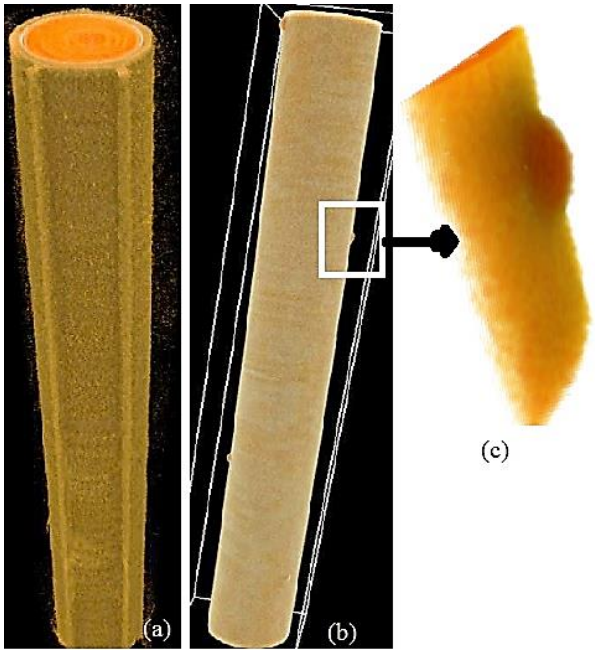

Figure 10 (a-b) Neutron tomography of Fuel Pin (c) showing presence of hydride blisters

8.0 Neutron imaging for Space industry:

Neutron imaging has become critical in the aerospace industry. Many aircraft and spacecraft components, such as turbine blades, ejection mechanisms, explosive signal transfer systems, and payload separation mechanisms, must be carefully tested to verify that they perform as intended, since any flaw or defect in the samples might result in mission failure. In recent years, neutron radiography (NR) has become a required inspection technology for aircraft applications. It has become an essential approach in the quality control and inspection of explosive-based mechanical devices used in the aerospace sector, as illustrated through a simulated devise in Figure 11.

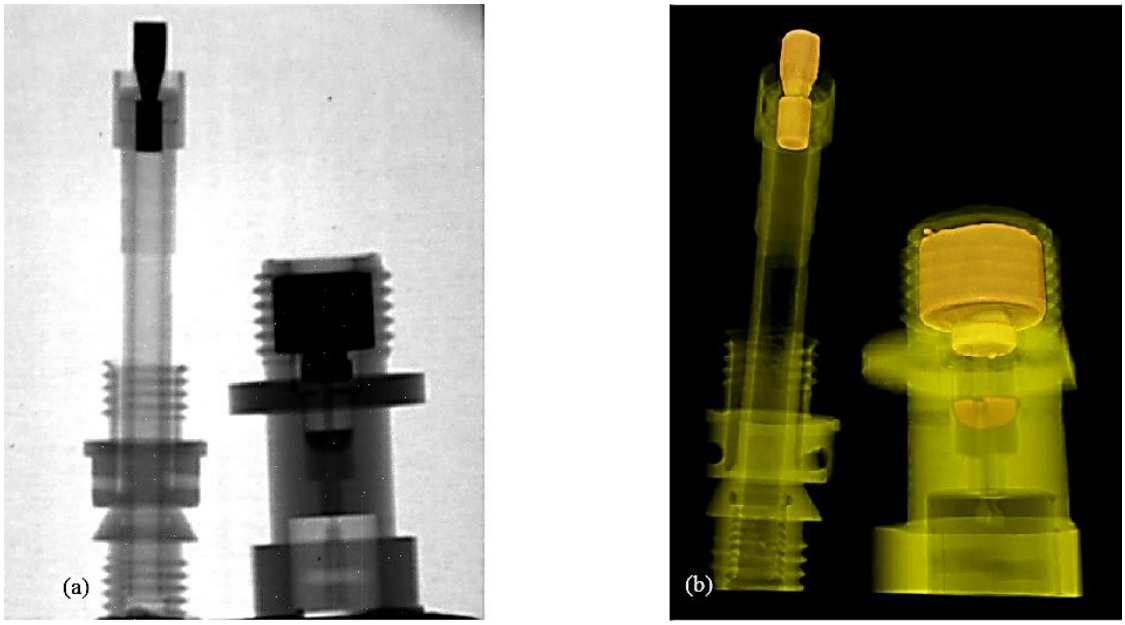

Figure 11 (a) Neutron radiography (b) Neutron tomography of a simulated pyrodevice used in space applications

9.0 Conclusion:

We have illustrated the potentials of neutron imaging in various diverse fields of science and engineering through some representative examples. This shows that advancement in the detector technology and availability of high flux research reactors have contributed significantly to the successful widespread application of neutron imaging techniques.

10.0 Acknowledgments:

We are grateful to Dr. L. M. Pant, Head TPD and Dr. S. M. Yusuf, Director Physics Group for providing necessary support for carrying out neutron beam research activities. We are also grateful to Head ROD, and Director, Reactors Group for encouragements towards developing various the engineering application of the neutron imaging beamline.

References:

1. Kallmann, H., "Neutron Radiography," Research, Vol. 1, No. 6, pp. 254-260 (1948).
2. Chadwick, J. Possible Existence of a Neutron. Nature 129, 312 (1932).
3. Podurets, K.M., Kichanov, S.E., Glazkov, V.P. et al. Modern Methods of Neutron Radiography and Tomography in Studies of the Internal Structure of Objects. Crystallogr. Rep. 66, 254–266 (2021).

4. J. Radon, "On the determination of functions from their integrals along certain manifolds" [in German], *Math Phys Klass*, **69**: 262–277, (1917)
5. G. T. Herman: Image reconstruction from projections: The fundamentals of computerized tomography, Academic Press (1980)
6. A. C. Kak and M. Slaney, Principles of Computerized Tomographic Imaging (Society for Industrial and Applied Mathematics, 1987).
7. Mayank Shukla, Tushar Roy, Yogesh Kashyap et. Al. , Development of neutron imaging beamline for NDT applications at Dhruva reactor, India, Nuclear Instruments and Methods in Physics Research Section A 889 (2018) 63-68.
8. Neutron Imaging and Applications: A Reference for the Imaging Community, Ed. by I. S. Anderson (Springer, US, 2009).
9. H. Berger, Neutron Radiography: Methods, Capabilities, and Applications (Elsevier, Amsterdam, 1965).
10. Neutron Methods for Archaeology and Cultural Heritage, Ed. by N. Kardjilov and G. Festa (Springer, 2017).
11. A. Kaestner, P. Vontobel, and E. Lehman, Neutron Imaging Methods in Geoscience. Advances in Computed Tomography for Geomaterials (Wiley, USA, 2013).

Author Information

Dr. Yogesh Kashyap has been working in the field of X-ray and neutron-based imaging techniques. He was involved in installation & commissioning of Neutron imaging beamlines at CIRUS and Dhruva research reactor, Trombay. He has also made significant contribution in the development of X-ray imaging beamline at Indus-2, synchrotron source, India. He is a faculty member of Homi Bhabha National Institute (HBNI), Mumbai, as Associate professor in the discipline of Physical sciences. He has contributed two book chapters, edited a book on "Neutron imaging: Basics, Techniques and Applications" and published around 90 papers in journal/conference.

Functional Testing of Neutron detectors: Role of Research Reactors

V. Balagi

Electronics Division, Bhabha Atomic Research Centre, Trombay, Mumbai—400085, India
(*Author email:* balagiv@barc.gov.in)

1.0 Intorduction

Nuclear Power provides a viable and cleaner alternative to fossil-fuel based power plants by harnessing clean energy generated through nuclear fission and helping in decarbonisation of the environment. A nuclear reactor is at the heart of a Nuclear Power Plant, which is engineered to carry out a controlled nuclear chain reaction for generating heat to be converted to electrical power. Nuclear reactor instrumentation (NIS) is a sine qua non for any nuclear reactor and its importance cannot be overemphasised. By reactor instrumentation is chiefly meant the systems deployed in any nuclear reactor for the control and safety of the core during all the stages of operation and otherwise. Apart from the electronics, the neutron detector, which detects the neutrons is an integral part of any NIS.

It must be emphasised that reactor instrumentation is different from conventional instrumentation [1]. The reason for this is fairly simple, though not obvious. Conventional power plants have continuous fuel feed while Nuclear power plants have stored fuel for several years of operation, and hence, increasing nuclear reaction rate due to equipment failure or malfunction will not be stopped by exhaustion of fuel. In other words, the system is not self-limiting. While, concentration of heat energy in the fuel is 40 x 109 BTU / lb of pure nuclear fuel, the value is 14 x 103 BTU / lb of coal, a factor of ~ 3 million. This means, that nuclear fuels can generate intense heat, exceeding the capabilities of the coolant to remove heat. Further, the presence of high nuclear radiation fields and high temperature in core regions of a nuclear reactor causes deterioration in signal and system performance.

The heat generated by the fission of nuclei like U-235 is utilized in these reactors. Since, the fission is caused and controlled by neutrons, the neutron flux is proportional to the instantaneous reactor power and is a true indicator of the operating status of the reactor. The control system of a reactor maintains / regulates the neutron flux and it's rate of change within the permissible limits, as demanded by the power requirements, while the safety system generates ALARM and TRIP signals to restore the neutron flux and it's rate of change to safe values whenever the regulation deviates beyond permissible limits or whenever there is a breach of integrity in some part of reactor system and the required response time is beyond the capabilities of the regulating system

2.0 Neutron Detectors:

The majority of neutron sensors for reactor applications are of the gas-filled type. Their advantages for this application include: Wide dynamic range, long term stability, tolerance to radiation damage and Inherent gamma-ray discrimination [2], [3]. Since neutrons are uncharged particles and so do not ionize the medium through which they pass, they are detected by causing them to interact with some target material and measuring the ionization caused by the resultant charged particle. The most common reactions used in gas-filled detectors for reactor instrumentation are $^{10}B(n, \alpha)^{7}Li$ and the fission reaction in ^{235}U. The energetic charged particles produced by the reaction ionise the gas inside the detector and the movement of these charges under the influence of an electrical field constitutes the signal. In some cases, especially in detectors using the 10B reaction, gas multiplication is used to increase the number of ions from each event.

The reactions of neutrons with various isotopes are given below:

$$^{10}_{5}B + ^{1}_{0}n \rightarrow \begin{cases} ^{7}_{3}Li + ^{4}_{2}\alpha + 2.792MeV \text{ (ground state)} \\ ^{7}_{3}Li^{*} + ^{4}_{2}\alpha + 2.310MeV \text{ (excited state)} \end{cases} \quad (1)$$

$$^{6}_{3}Li + ^{1}_{0}n \rightarrow ^{3}_{1}H + ^{4}_{2}\alpha + 4.78MeV \quad (2)$$

$$^{3}_{2}He + ^{1}_{0}n \rightarrow ^{3}_{1}H + ^{1}_{1}p + 0.764MeV \quad (3)$$

3.0 Range of Neutron Flux:

Typically, a single set of detectors can be used to measure only a limited part of the range and is complimented by additional sets of detectors. Safety and reliability considerations dictate sacrificing a part of the range of the detectors by having them duplicate the range of other detectors. This duplication or overlapping (typically 2 decades) is necessary for the smooth transfer of control and safety from one set of detectors to the next. It must be mentioned that with fission detectors it is possible to use one detector to cover the entire range of reactor neutron flux by operating the device in three modes of operation viz., pulse counting, Mean Square Voltage (MSV) or Campbell and DC mode. The great range in reactor power (from watts to hundreds of megawatts) makes it impossible to use one set of detectors with one circuitry. For convenience the reactor power is divided into three ranges: source, intermediate and power ranges (Fig 1).

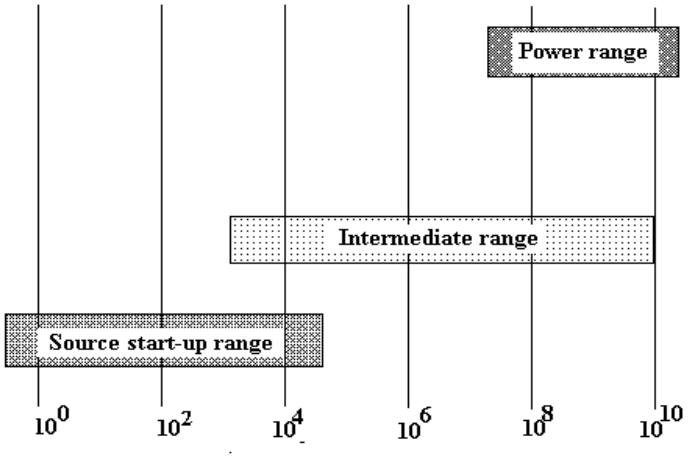

Fig.1 The typical neutron flux at ex-core detector locations

The limits of the source range (counting range) are determined by the permissible counting rates, expressed in counts per second. The low end of this range is dictated by the minimum counting rate for safe condition as specified by reactor safety norms (1-10cps). The upper limit of neutron flux that can be measured with good accuracy depends on the maximum counting rate. This latter depends on the pulse width (or the system resolving time, whichever is longer) and the maximum resolution loss that is acceptable. As a rough rule of thumb, for a counting loss of less than 10%, the maximum counting rate would be $1/10\tau$, where τ is resolving time. Thus, a system with 200ns resolving time would have maximum counting rate of $5x10^5$cps.

Since gamma background is almost always present at the detector location, the selection of detectors for source range monitoring is dictated by the ability of the device to measure 'few' neutrons in the presence of 'many' gammas. Counting individual pulses helps eliminate the unwanted short gamma induced pulses by pulse height discrimination. Here fission detectors are ideal candidates because of their superior gamma tolerance capability. ^{10}B lined proportional counters are also used in this range.

The intermediate range overlaps the source range and here the gamma background is less severe. However, the higher neutron flux makes it impossible to resolve individual pulses and the signal takes on the garb of

DC current and becomes indistinguishable from the gamma background. ^{10B}-lined gamma compensated ion chambers are the most commonly used detectors in this range.

Another means of measuring the neutron flux is the so called Mean Square Voltage or Campbell mode.

In the DC mode operation only the mean value of the generated current is considered. However, the standard deviation σ of the fluctuating component of this mean current is proportional to the square root of the neutron flux. This is called the Campbell's method or Mean Square Voltage (MSV) method employed in the intermediate range with fissions detectors [4] [5].

In the power range, the neutron detectors are operated in DC mode where-in the mean value of the generated current is considered. The intermediate range usually extends into and completely overlaps the power range. The power range covers from 1 to 150% of full power to provide some allowance for small power excursions. ^{10}B-lined ion-chambers with or without gamma compensation or fission chambers are employed in this range.

The detector-electronics system need to be tested to establish it suitability to provide the necessary safety and control functions in the environment of the facility for which they are designed. However, it is not possible to test the system in the actual facility as is obvious. This is where the research reactors play an important role. The present article gives details of the various detectors that have been tested in different research reactors in DAE.

4.0 Parameters to be measured

Among the parameters that are relevant for establishing the performance of a neutron detector are: capacitance and insulation resistance, charge collection time, sensitivity, operating voltage, linearity of response, maximum operating temperature and gamma tolerance. Of these, sensitivity, operating voltage, and linearity of response over 5-6 decades of neutron flux are difficult, nay, even impossible, to establish in laboratory testing.

Establishing the sensitivity of a detector necessitates the irradiation of the detector sensitive volume with neutrons in near 4π geometry. While facilities such as the neutron STAG at RSSD, BARC provide such a possibility, for detectors with long sensitive length the variation of the neutron flux along the length could pose problems is assessing the sensitivity. Research reactors, on the other hand, have irradiation locations, like the Thermal Column in Apsara or D9, D10 locations in CF, where the detectors can be extensively tested for sensitivity and linearity over the intended dynamic range of operation.

Further, it is possible to introduce systems into the research reactors for either modifying the flux profile and/or changing the environmental conditions. It goes without saying that such introductions are subject to through safety review.

5.0 Utilization of APSARA Reactor

Apsara was a swimming pool type thermal Reactor operational since August 4,1956 with 1 MW thermal power. It had Enriched uranium -aluminium alloy in the form of plates as fuel. From the very inception, thermal column and the core dry tubes of Apsara Reactor were extensively used for testing various types of neutron and gamma detectors as a part of research and development programme in that area. The type of control instrumentation tested in Apsara includes radiation monitors, intermediate range monitors, self-powered neutron detectors, ion chambers and reactor regulation instrumentation for our research and power reactors.

Detector Type	Sensitivity
High sensitivity B-10 lined proportional counters	17 cps/nv
In-core Boron lined proportional counters	0.15 cps/nv & 1 cps/nv
B-10 lined proportional counters - Seven cathode assembly	5.5 cps/nv
B-10 lined proportional counters – Three cathode assembly	10 cps/nv
B-10 lined proportional counters – Baffle structure	0.8 cps/nv

Detector Type	Meant for	Use	Testing Location
Un-compensated Neutron Ion Chambers	235 MWe & 540 MWe reactors	For reactor control and safety in the range of $10^4$to 10^{10}nv	Thermal column hole No. 5
Compensated Neutron Ion Chambers	TAPS #1 & #2 (PRM)	For reactor control and safety in the range of $10^4$to 10^{10}nv	Thermal column hole No. 5
Source Range Monitors	TAPS 1 & 2	For the measurement of in – core n neutron flux in the range of 10^3 to 10^8nv	Thermal column hole No. 5
Intermediate Range Monitors	TAPS 1 & 2	For the measurement of in-core neutron flux in range of 10^6nv to 10^{10}nv by using Campbell technique	Thermal column hole No. 5
Miniature Fission Chamber	TAPS 1,2 & TAPP-4	For the measurement of in-core neutron flux	Thermal column hole No. 5 & Dry tube
Travelling In-core probe – Miniature Fission Chambers	TAPS 1,2 & TAPP-4	Measurement of in-core neutron flux for calibration of LIQHs and SPNDS, etc.	Thermal column hole No. 5 & Dry tube
Self-Powered Neutron Detectors (SPNDs)	500 MWe PHWR	In-core neutron flux mapping	Dry tube
Source Range Monitors – Miniature Fission Detectors	AHWR critical facility	Reduced neutron sensitivities (10^{-4}cps)	Thermal column hole No. 5

a. Uncompensated ion chambers
Used in ex-core locations in the intermediate and power ranges of the reactor, with typical neutron sensitivity of 10fA/nv and gamma sensitivity of 1pA/nv. The dimensions are typically 85 mm OD X 400mm length

b. Compensated ion chambers
Used in ex-core locations in the intermediate and power ranges of the reactor, with typical neutron sensitivity of 10fA/nv and gamma sensitivity of 0.1pA/nv. The dimensions are typically 85 mm OD X 400mm length

c. Source range monitors
Used in the in-core location of BWRs like, TAPS 1 and 2, in the source range with typical sensitivity of 10^{-3}cps/nv and dimensions of 6mm OD with 25mm overall length

d. Intermediate range monitors
Used in the in-core location of BWRs like, TAPS 1 and 2, with typical sensitivity of 10^{-3}cps/nv and dimensions of 6mm OD with 25mm overall length

e. SPNDS
Used in in-core locations, with typical sensitivity of 10^{-21} to 10^{-20} A/nv and dimensions of 6mm OD with 25mm overall length

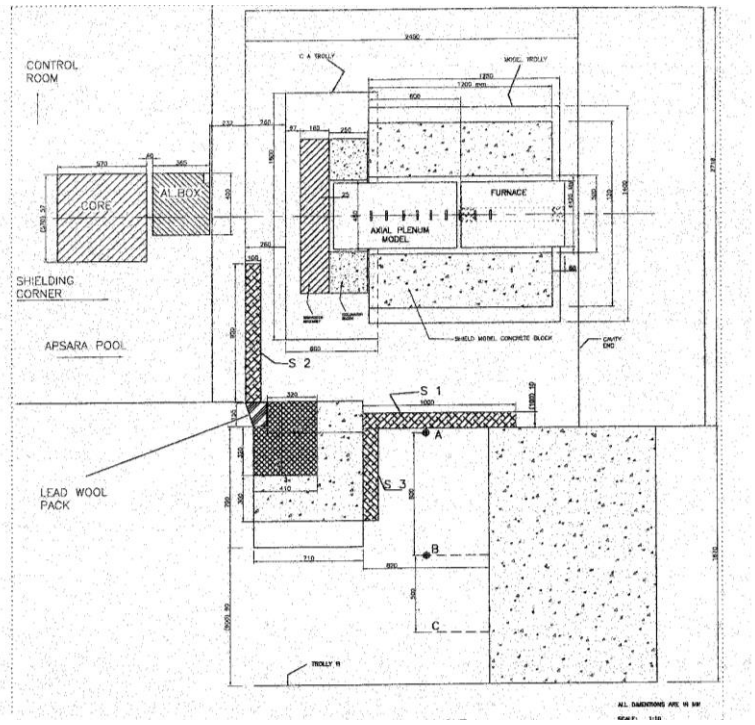

Fig. 2 The arrangement for Testing of HTFC at Apsara Shielding

In addition to this Apsara Reactor has been used for testing of High temperature Fission Counters to be used in PFBR (Fig. 2). The detectors, designed to operate in the pulse, Campbell and DC modes, is capable of operating at temperatures of up to 570°C and in gamma backgrounds up to 1MR/h. However, it is not feasible to test these detectors for their performance in their full range of operation at the required temperature. Hence, the prototype detectors were tested in the shielding corner of the reactor with the reactor operating in C` position. The set up consisted of a converter assembly, collimator block and axial plenum used to generate PFBR-like flux from the thermal flux obtained from the reactor. A suitable circular furnace capable of heating the detector up to 570°C was placed beyond the above set-up to irradiate the detector.

With this set-up it was possible to test the prototype detector for its performance and from the results obtained valuable insights were gained leading to improvement in the design.

6.0 Utilisation of AHWR-CF

India has large reserves of Thorium and its utilisation for power production is an important feature of the long-term Indian Nuclear Power Programme. As a part of this strategy, Critical Facility (CF) for an Advanced Heavy Water Reactor (AHWR) has been developed in BARC. Critical Facility (CF) is a low power research reactor with features like "enough flexibility to conduct a wide range of experiments, which helps in validating the computer codes for reactor physics of AHWR and in generating nuclear data about

material, such as Thorium – Uranium 233 based fuel, which have not been used extensively in the past". CF has been designed for a nominal power of 100 W for the average flux of 10^8 n/cm^2/s. Facility was commissioned and achieved first criticality in April 2008. The D9 and D 10 locations in the reactor provide excellent facility for testing of neutron detectors in fluxes up to 4 x10^7nv.
This reactor has been used extensively to test the following detector systems

Detector Type	Meant for	Use
Fission chambers	cLWR	For reactor control and safety in the range of 1 to 10^{10}nv
Compensated Neutron Ion Chambers	cLWR	For reactor control and safety in the range of $10^4$to 10^{10}nv
Pulse and DC instrumentation	cLWR	For reactor control and safety in the range of 1 to 10^{10}nv
He-3 detectors	P4	For the measurement neutron flux in range of 5x 10^{-4} nv to 50 nv
Pre-Start-up equipment	cLWR	For the measurement of in-core neutron flux 0.1 nv to 10^5 nv

a. Fission Chambers

Used in ex-core locations in the Source, intermediate and power ranges of the reactor, with typical neutron sensitivity of 1cps/nv (100fA/nv) and gamma tolerance up to 1MR/h. The dimensions are typically 50 mm OD X 600mm length

b. Compensated ion chambers

Used in ex-core locations in the intermediate and power ranges of the reactor, with typical neutron sensitivity of 10fA/nv and gamma sensitivity of 0.1pA/nv. The dimensions are typically 50 mm OD X 600mm length

c. He-3 Detectors

Used in the ex-core location of P4 with typical sensitivity of 200cps/nv

7.0 KAMINI Reactor utilization

KAMINI (Kalpakkam Mini reactor) is a Uranium-233 fueled, low power (30 kW) research reactor designed and built jointly by the Bhabha Atomic Research Centre (BARC) and Indira Gandhi Centre for Atomic Research (IGCAR), Kalpakkam. This reactor functions as a neutron source with a flux of 10^{12} neutrons/sqcm/second at core center and facilitates carrying out neutron radiography of radioactive and non-radioactive objects and neutron activation analysis.
The reactor fuel is an alloy of uranium-233 and aluminium in the form of flat plates and assembled in an aluminum, casing to form the fuel subassemblies. The reflector is beryllium oxide encased in zircaloy sheath. Demineralized light water is used as moderator, coolant as well as shield. Cooling of the reactor core is by natural convection. Start up and regulation of the reactor is done by adjusting the positions of two safety control plates made of cadmium, which is sandwiched in aluminum. These plates are provided with gravity drop mechanism for rapid shut down of the reactor. All reactor operations are carried out from a central control panel.

Further to closing down of old Apsara reactor, KAMINI reactor was used to test the HTFCs developed for PFBR.

A furnace of 3kW capacity and 1.5 m length was introduced into the pool of Kamini reactor for testing of HTFCs. The furnace was provided with sufficient cooling to take care that the pool temperature does not exceed the normal operating temperature.

With this set-up it was possible to test the HTFCs at different temperatures up to and including 570°C in fluxes of up to 10^7nv. The production lot detectors manufactured by ECIL were tested in this location before they were delivered to the site.

8.0 FBTR

Two locations – the detector pit and experimental canal – at the FBTR at Kalpakkam provided two different types of environment and flux types to test neutron detectors. The detector pit provides nearly thermalized flux, while the experimental canal a slightly harder spectrum. Also, it is possible to test detectors at temperatures up to 480°C in the experimental canal.

During the initial phase of development of HTFCs, the detector and electronics were tested in FBTR to establish various design parameters such as the sensitivity at higher temperatures, linearity of response pulse width, overlap between Pulse and MSV range etc.

References

1. Nuclear power reactor instrumentation systems handbook. Volume 1, Harrer, J.M. & Beckerley, J.G., Argonne National Laboratory, 1973.
2. "Neutron Detection" Allen W. D. George Newnes Ltd., London, 1960
3. "Neutron Ionisation Chambers" Grosshoeg, G., , North-Holland, Amsterdam, 1979
4. DuBrigde, R. A., *IEEE trans. Nucl. Sci*. NS-14(1), 241, 1967
5. Thomas, H. A., and McBride, A. C., *IEEE trans. Nucl. Sci*. NS-15(1), 15, 1968

Author Information

Dr. V. Balagi joined the Electronics Division of BARC, after graduating from the 37th Batch of BARC Training School in 1994. He earned his M. Sc From MG university, Kottayam, Kerala in 1992. Since joining, Dr. Balagi has been involved with the design, development and supply of neutron and gamma detectors for various projects of DAE. He obtained doctoral degree in 2006 from Mumbai University for the thesis entitled "ANALYTICAL AND EXPERIMENTAL STUDIES ON ION CHAMBERS". He was involved in various projects of DAE like PRP, P4, PFBR etc. He has developed and transferred the technology for High Temperature Fission Chambers (capable of operation up to 570°C) to ECIL. His current activities include development of Fission counters for various projects.

Utilization of Research Reactors for testing of Fusion Reactor Materials

Shashank Chaturvedi

Institute for Plasma Research, Gandhinagar, Gujarat-382428, India
(Author email: shashank@ipr.res.in*)*

1.0 Introduction:

In a fusion reactor, deuterium (D) and tritium (T) nuclei fuse together to generate neutrons of mean energy 14.1 MeV. These neutrons, carrying 80% of the fusion energy release, are required for the power generation, tritium breeding and other applications. At the same time, they poses serious challenges to the integrity of reactor structure & sub-systems, proper functioning of the sub-systems, maintenance operations etc. due to radiation damage, helium production, transmutation, volumetric heat generation etc. In order to put things in perspective, the source neutron yield of a 1 GW_t DT fusion power reactor would be 3.5×10^{20} n/s. This can induce radiation damage of ~3 dpa/FPY (Full Power Year) in steel and ~20 appm (atomic parts per million) of He production in steel at the First Wall surrounding the hot plasma. Therefore, it is necessary to qualify materials proposed to be used in a fusion reactor after irradiating them under appropriate conditions.

Fusion reactors have a range of components/sub-systems that are required for the confinement of the fusion plasma inside a magnetic "cage", heating of the plasma, removal of heat flowing out of the plasma and the support structure of various sub-systems. These include the superconducting/copper magnets, vacuum chamber, structural materials, plasma-facing components, breeding blankets, pumping systems, fuelling systems etc.

This paper reports on theoretical and experimental work done so far at IPR for the design and development of fusion reactor materials, including collaborative studies with other institutions. Possible areas of Research Reactor utilisation for fusion-relevant studies are also identified.

2.0 Irradiation studies for Superconducting/copper magnets:

Electromagnets producing high magnetic fields are a key element of fusion reactors for the confinement and shaping of "burning" plasmas. Apart from the current-carrying part of the magnet, which can be made of superconducting material or copper, they also contain insulation and support structure. Superconducting materials belong to two categories – low-temperature materials like NbTi and Nb_3Sn and high-temperature (HTS) materials like Bismuth strontium calcium copper oxide (BSCCO) & Rare earth barium copper oxide (REBCO). When these materials are subjected to 14 MeV neutron irradiation, it leads to changes in electrical and mechanical properties due to transmutation, e.g., critical current, critical temperature, electrical resistivity and microstructural properties. For example, beyond a certain neutron fluence threshold, Nb_3Sn ceases to be superconducting. For insulating materials like FRP Tapes, Epoxy Resin, Bisphenol, Cyanate Ester, Kapton Film and superinsulation, there are changes in Electrical Resistivity, Voltage Breakdown, Flexural Strength, Compressive Strength and Inter-laminar shear strength. In structural materials like SS316LN and SS304, there are changes in mechanical properties like creep strength, thermal properties, etc. Apart from these areas, there can be changes in properties of sensors and instrumentation cables used in these magnets.

The detailed structure of superconducting materials used for a typical superconducting magnet in fusion applications is shown in Fig. 1.

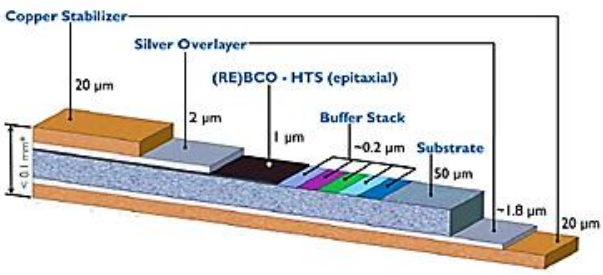

High Temperature Superconducting Tape

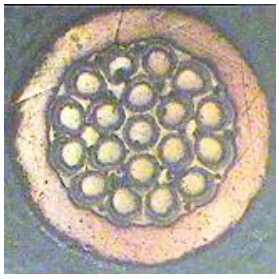

Nb_3Sn Strand

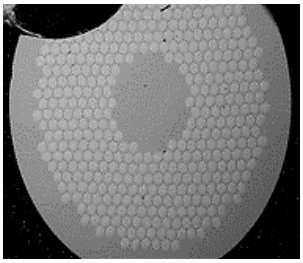

NbTi Strand

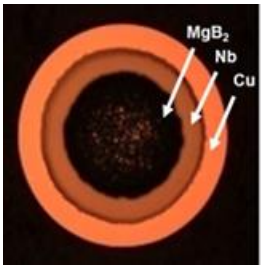

MgB_2 Strand

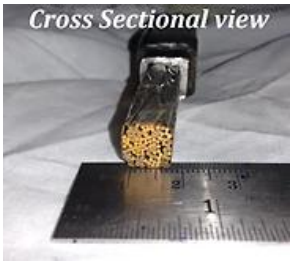

Cable In Conduit Conductor (CICC)

Figure 1: *Detailed structure of a superconducting magnet used in fusion applications*

a. D^+ ion beam irradiation studies:

An ion irradiation study aimed at studying the change in critical current and temperature of HTS due to ion beam irradiation has been conducted with Sumitomo Di-BSCCO HTS tape of width 4.42 mm and thickness 0.34 mm at IPR [1]. The irradiation was performed using a 100 keV deuterium (D+) ion beam. Results of the measured voltage-current (V-I) characteristics of irradiated sample and comparison with the unirradiated sample at 77 K is shown in Fig. 2.

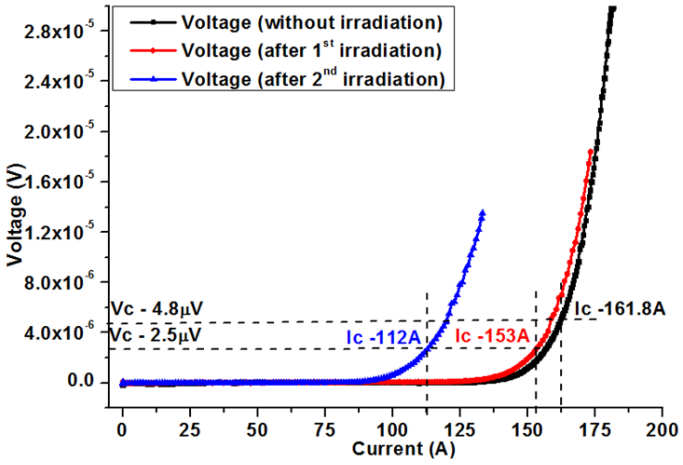

Figure 2: Measured V-I characteristics of unirradiated and irradiated sample of Di-BSCCO HTS tape at 77 K (Fluence levels for blue and red plots are 1.06×10^{16} ions/cm^2 and 9×10^{14} ions/cm^2).

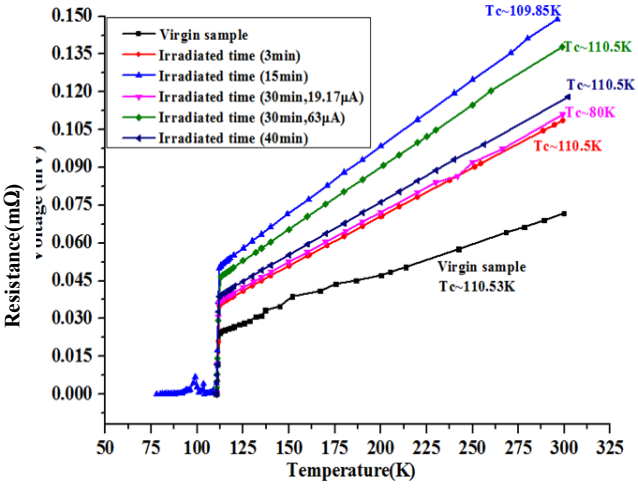

Figure 3: Measured R-T characteristics of unirradiated and irradiated samples of Di-BSCCO HTS. The deuterium fluence used for this study is 9×10^{14} ions/cm^2

It can be seen from Fig. 2 that the surface damage caused by the D^+ ions significantly reduce the critical current of the HTS sample from 161.8 A to 112 A (~30% reduction). Results of the measured R-Temperature characteristics of unirradiated and irradiated samples is shown in Fig. 3.

b. Fast neutron irradiation studies of magnet insulation material GFRP:

Glass Fibre Reinforced Plastics (GFRP) G-10 CR grade composite consisting of S-glass and Liquid modified Bisphenol Epoxy A with Liquid aromatic amine hardener was irradiated in the Fast Breeder Test Reactor (FBTR) at IGCAR, Kalpakkam [2]. The irradiation parameters are listed in Table 1.

Table 1: Neutron irradiation parameters for GFRP G-10 magnet insulating material in Fast Breeder Test Reactor (FBTR)

Parameter	**Unit**	**Value**
Reactor power	MW_{th}	32
Neutron flux at irradiation location (E-5 pit)	$n/cm^2/s$	2.2×10^{10}
Irradiation time	days	60
Neutron fluence	n/m^2	1.1×10^{21}

Fig. 4 shows GFRP insulation material at the irradiation location in FBTR. The composition of the GFRP material developed at IPR is given in Table-2.

Figure 4: GFRP magnet insulation material at irradiation site in FBTR.

Table 2: Composition of GFRP magnet insulating material irradiated in FBTR [2]

Glass Fiber	In-house Epoxy Resin System
S2 -glass fabric of 600 GSM , 64-68 % wt and Resin: 32-36%	Two component, Liquid modified Bisphenol Epoxy A with Liquid aromatic amine hardener
Density: 2.48 g/cc	Mixed viscosity: 2000 mPa.s
Softening temp ° C: 1056	Shear strength at 77 K: ≥ 19.2 MPa
Thermal coefficient (ppm °C): 3.8	Specific gravity: 1.15 -1.20
Dielectric strength (kV/mm) : 13.0	Heat deflection temp: 58 ºC
Composition: SiO_2 : 64-66% wt., AL_2O_3 : 24-25 % wt, CaO: 0-0.18, MgO: 4.5-10.2, Na_2O+K_2O: 0-0.2, Fe_2O_3 : 0-0.1	Epoxy value: 0.30-0.35 eq/100 g

The performance tests carried on the irradiated samples were tensile strength (as per ASTM: D638-1991 standard), shear strength (as per IS: 4248-1967 standard) and breakdown strength (as per ASTM: D 149 2009 standard). Results of mechanical tests conducted on unirradiated and irradiated samples is given in Fig. 5. It was found that there is no significant degradation in the tensile & shear strengths of neutron irradiated samples upto 1.1×10^{21} n/m^2 fluence – these properties changed by only 2% and 4% respectively. The electrical breakdown strength of the samples was also not degraded significantly, suggesting that these materials can be used in a reactor environment where fluence levels are below 1.1×10^{21} n/m^2.

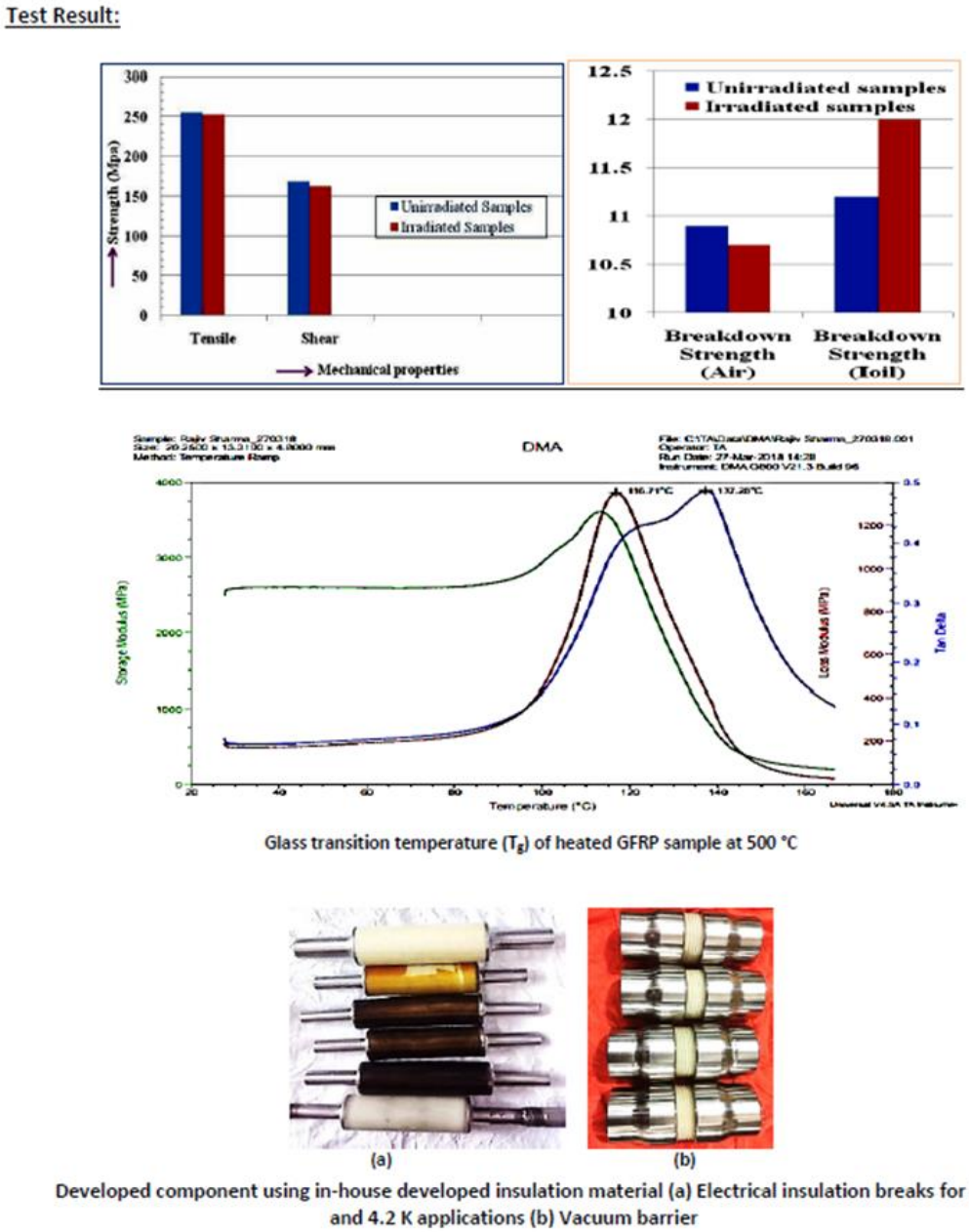

Figure 5: Results of the mechanical tests performed on the irradiated insulating samples and compared with unirradiated samples

c. Future plan of irradiation studies of Superconducting magnet materials:

Deuterium ion irradiation upto 200 keV energy at IPR is planned to check the effects of ion irradiation on the important properties of HTS and to study the microstructural properties using transmission electron microscopy (TEM). Further tests under different neutron spectra are planned at a newly-installed 14 MeV DT neutron generator facility at IPR. In order to study the effect of neutron spectrum, the study could greatly benefit from irradiation in Dhruva at BARC and FBTR at IGCAR.

3.0 Development of structural and functional materials for blanket:

Various materials have been developed for fusion blanket such as India specific Reduced Activation Ferritic Martensitic Steels (IN-RAFMS) structural material, functional materials (Li_2TiO_3, Be and Pb-16Li) at IPR in collaboration with BARC, IGCAR and other research & academic institutions in India.

The physical, mechanical and thermal properties for these materials have been generated as part of database generation [3].

a. IN-RAFM Steel:

Several variations of steels were investigated to develop RAFM steels with high-temperature mechanical properties and microstructural stability that is equivalent to the original heat-resistant steel with a high irradiation resistance. The most promising composition with these attributes contains a Cr concentration of 7 to 9 wt% with a maximum *W* concentration of 2 wt% [3]. IN-RAFM steel is based on the chemical composition of the conventional Grade-91 steel [9Cr–1Mo–0.06Nb–0.2V–0.05N], which is modified by substitution of molybdenum by tungsten and niobium by tantalum. For the development of IN-RAFM steel, a three-phase development programme was initiated in collaboration with IGCAR, Kalpakkam and Mishra Dhatu Nigam Limited (MIDHANI), Hyderabad.

i.) In the pilot scale development phase, three heats of steel weighing of 200 kg each were melted at Mishra Dhatu Nigam Limited (MIDHANI). Strict control was exercised on the radioactive tramp elements (Mo, Nb, B, Cu, Ni, Al, Co, Ti) and on the elements that promote embrittlement (S, P, As, Sb, Sn, Zr, O). Physical and mechanical properties were evaluated to achieve the internationally established RAFM steel;

ii.) four heats of the steel were melted with different chemical composition (tungsten and tantalum contents in the ranges 1–2 wt% and 0.06–0.14 wt%, respectively);

iii.) Finally, 1.4 wt% tungsten with 0.06 wt% tantalum was found to possess optimum combination of impact, tensile, low cycle fatigue and creep properties and was selected to be India-specific RAFM steel.

Commercial scale heats of Indian RAFM steel, each weighing about 1500 kg, have been produced and short-term mechanical properties have been evaluated. Different physical and thermos-mechanical characterizations have been performed on the unirradiated IN-RAFMS samples. Fig. 5 shows the Yield stress, ultimate tensile strength and Impact properties.

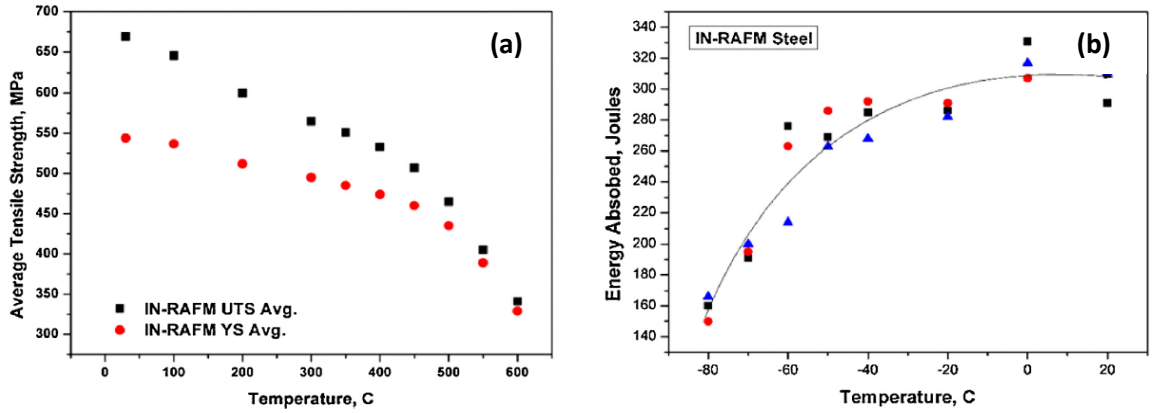

Figure 6: (a) Yield stress and ultimate tensile strength **(b)** Impact properties of IN-RAFMS

Creep test of IN-RAFM steel is being carried out at temperatures of 550 °C and 600 °C with a stress range of 240 -180 MPa up to10,000 h. Long-term creep tests of the steel are presently in progress. The variation of impact energy with temperature showed a typical ductile-to-brittle transition (DBTT) curve as shown in Fig. 6 (b). The DBTT estimated for IN-RAFM steel is less than -70°C [3,4].

The fusion blanket structural materials will be subjected to high heat loads and high flux 14 MeV fusion neutrons, and will experience internal pressure loads, thermal stresses, substantial electromagnetic forces in case of plasma disruptions, and high pressure loads in the case of a coolant ingress. Degradation of microstructure of structural materials under neutron irradiation as a result of displacement damage accumulation and production of transmutation products, i.e., helium and hydrogen, will strongly

influence materials' performance. Various RAFM steel developed by other countries have been neuron irradiated at different dpa and temperature ranges in research reactors. IN-RAFM steel also needs to be neutron irradiated followed by various Post Irradiation Examination (PIE) studies such tensile test, impact properties, swelling phenomena and other mechanical and thermal behaviour to be studied out at irradiation dose (dpa) and temperature.

b. Functional materials:

The lithium ceramics (Li_2TiO_3, Li_4SiO_4) and Beryllium (Be) are considered as tritium breeder and neutron multiplier material in a fusion reactor blanket. These materials will be operated under harsh conditions, in particular, they will be exposed to considerable levels of neutron irradiation. Severe irradiation environment would bring damage to the microstructure of the materials and affect the stable operation and tritium recovery from the blanket. Therefore, their optimum properties must be tested under relevant neutron irradiation conditions. Li_2TiO_3 & Li_4SiO_4 show excellent thermal performance, ease of tritium recovery, and good irradiation behaviour. The spherical form (pebble) of Li_2TiO_3 and Be are kept as a packed bed in the breeder module. Li_2TiO_3 powder and pebbles are prepared by solid state reaction and spheronization process respectively [5]. At every stage of preparation, various characterizations on the powder, pebbles and pebble bed have been carried out to meet the desired properties. Test facilities for the measurement of effective thermal conductivity (K_{eff}) of the pebble bed using steady-state Axial and transient hot-wire method have been designed and built indigenously at IPR.

Neutron irradiation may lead to the transformation of materials. Therefore, PIE should be done on these irradiated Li_2TiO_3 material to estimate the compositional changes which result in changes in properties, e.g., melting point, tritium diffusivity, and thermo-mechanical performance.

4.0 IPR 14 MeV DT neutron generator facility:

IPR has recently set up an accelerator-based D-T neutron facility with a design yield of $5x10^{12}$ n/s. Figure 7 shows a photograph of the facility. The source consists of an Electron Cyclotron Resonance Ion Source (ECRIS), Low Energy Beam Transport (LEBT) system, Electrostatic Acceleration, Medium Energy Beam Transport (MEBT) system, 300kV, 50 mA High Voltage Power Supply (HVPS), Beam diagnostic system (BDS), Switching Magnet (SM) and Rotating tritiated target. Deuterium ions produced from a 2.45 GHz ECR source are accelerated by a 300 kV high voltage power supply and impinge on a Titanium tritide (TiT) thin-film rotating target [6]. This produces 14 MeV neutrons which can be used to study their effect on fusion blanket materials, benchmark experiments for Fusion Evaluated Nuclear Data (FENDL), neutron spectroscopy measurements, double differential cross-section measurements, and effect on plasma-facing components of fusion machines. Various neutron diagnostic systems have been installed, such as alpha particle, foil activation, and gas-filled detectors [6,7]. The neutron yield has been measured and estimated using these diagnostics. The uncertainties and correction factors associated with all measurement techniques have been assessed and incorporated into the final results. Initial operations have shown a neutron yield of 7×10^{11} n/s. Deuterium ion irradiation experiments have also been performed for surface damage studies [1,8].

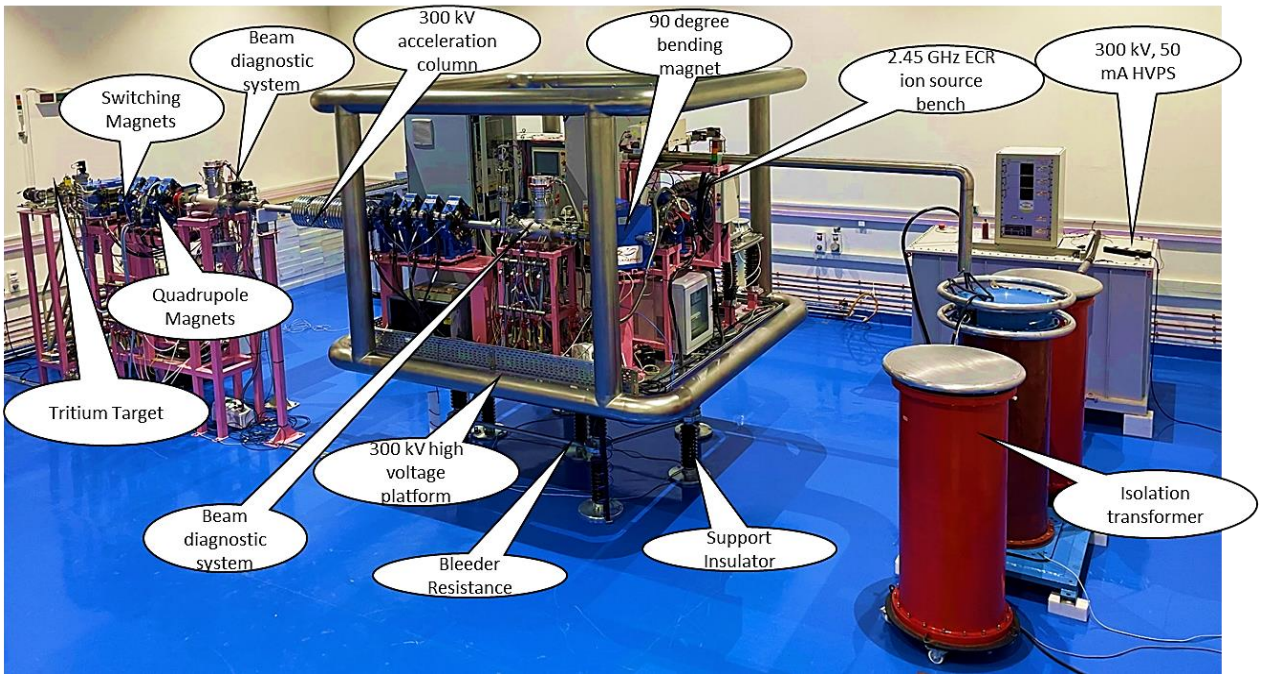

Figure 7: IPR 14 MeV DT neutron generator facility

5.0 Irradiation Studies in Tungsten Plasma-Facing Materials:

Although tungsten-based materials are the most promising candidates for plasma-facing components in fusion power reactors owing to their high melting point, low erosion yield and low affinity for hydrogen isotopes, radiation damage created by fusion neutrons and □-particles can adversely affect these properties. At present, there exists no fusion-relevant test facility -- the lack of predictable experimental data under 14 MeV neutron irradiation makes it necessary to resort to predictive modelling with a set of experimentally-benchmarked models. Surrogate particle irradiation using energetic ions and electrons, □-rays, and fission neutrons can be synergistically employed to create a set of experimental benchmarks. The rationale for this can be understood from a typical neutron and the primary-knock-on atom (PKA) spectrum at the tungsten divertor in ITER shown in Fig. 8 (a,b) where the low energy part causes transmutation reactions and the high energy tail results in displacement damage and helium production [9]. The primary-knock-on-atom (PKA) spectra produced by the neutrons is shown in Fig. 8 (b) with a maximum PKA energy of about 300 keV set by the kinematic limit of energy transfer.

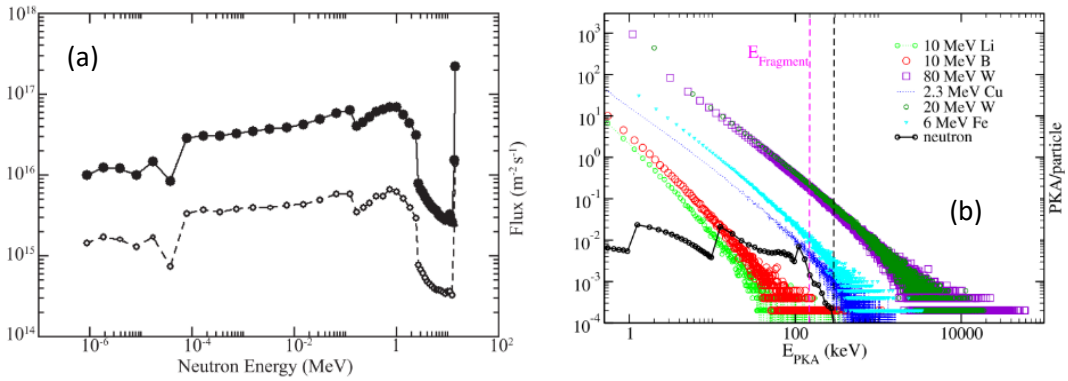

Figure 8: The neutron flux (a) and the PKA spectrum of neutrons and ions (b). The cascade-fragmentation threshold energy is shown by dashed vertical lines [9]

One of the open problems in comparing the neutron and surrogate particle damage is whether the total displacement event characterized by dpa will be a reasonable comparison or the nature of the energy

transfer and the subsequent defect created by the incident particles will make a difference in the material properties [10]. The latter can be tested experimentally by creating a variety of PKA spectra by using different ions which is also shown in Fig. 8 (b). In order to explore this, we have carried out extensive experiments and modelling using a low (H, D He), medium (B) and high mass ions (Au, W) with impinging energy ranging from 50 keV to 80 MeV on tungsten by using ion irradiation facilities across India and the defects were characterized using positron annihilation spectroscopy (PAS), TEM, SEM, XRD and EBSD techniques. The depth profile of the ions was characterized by secondary ion mass spectroscopy (SIMS) and elastic recoil detection analysis (ERDA) [9-12].

Table 3: Details of ion-irradiation experiments

Sample	Ion	Energy (MeV)	Flux (m^{-2} s^{-1})	Fluence (m^{-2})	R (μm)	dpa s^{-1}	dpa ($E_d = 90$ eV)
HeLF	He^+	3.0	1.12×10^{15}	7.5×10^{18}	4.4	2.24×10^{-7}	0.001
HeHF	He^+	3.0	1.12×10^{15}	2.25×10^{19}	4.4	2.24×10^{-7}	0.003
BLF	B^{3+}	10.0	8.67×10^{14}	1.3×10^{18}	4.3	6.66×10^{-7}	0.001
BHF	B^{3+}	10.0	8.67×10^{14}	1.0×10^{19}	4.3	6.66×10^{-7}	0.008
Au	Au^{7+}	80.0	9.63×10^{13}	1.3×10^{18}	4.6	2.56×10^{-5}	0.22
250 keV He	He^+	0.25	9.8×10^{16}	5.0×10^{19}	0.45	4.31×10^{-5}	0.022

The list of ions irradiated is given in Table 3 and the TEM images of the defects is shown in Fig. 9 (a) and the defect size distribution in Fig. 9 (b). While high energy Au ions produce dense clusters of small defects, high energy boron produces large defects which are fewer in number.

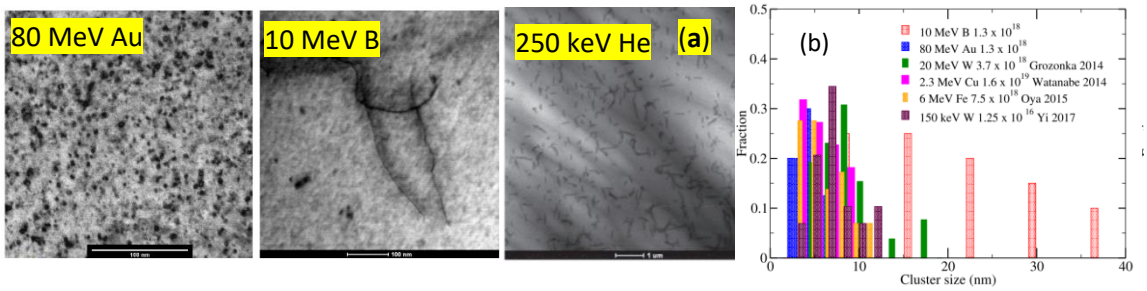

Figure 9: HRTEM images of the defects produced by 80 MeV Au, 10 MeV B and 250 keV He ions (a) and the defect-size distribution (b) [10-11].

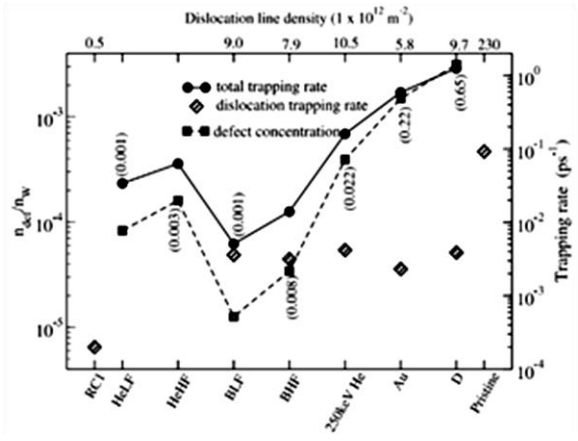

Figure 10: The defect density obtained from TEM (upper X-axis) and from PAS (left Y-axis). The dpa values are given in parenthesis for each sample. The total positron trapping rate is marked on right Y-axis [11].

For the same dpa, different ions produce different type of defects and the defect density estimated using TEM and PAS is shown in Fig. 10. This study shows that for the same dpa, different ions produce different defects. The modelling of the defect structures carried out using molecular dynamics simulations shows that above a certain threshold energy of the PKA (160 keV), cascade fragments and the energy is distributed among several small cascades leading to numerous small defect clusters which is the case with heavy ions as seen from the PKA spectrum of Fig. 8 (b).

For the same type of ions, the ion energy also plays a crucial role in the defects. While 250 keV He ion shows extensive dislocation line

formation, the 3 MeV helium forms small defect clusters with no dislocation lines observed which could be due to the difference in the way helium participates in the cascade and the differences are being explained in the basis of competitive capture of defects during and post-cascade phases [8,9].

6.0 Future plan:

At present the ion-irradiation experiments are being extended to iron and copper alloys that are relevant for structural as well as high heat-flux materials. While the displacement damage at high energy can be well modelled by ions, the major caveat lies in the limited ion penetration range (~ m) which makes material testing data unreliable since the sample bulk is relatively unaffected. -rays, on the other hand, can penetrate throughout the sample (~cm) and the utilization of energetic -rays in creating defects in tungsten is currently being explored. The low energy part of the neutron spectrum is capable of creating defects along with transmutations and the proposed activity is aimed at investigating the transmutation reactions and displacement damage in tungsten due to both thermal and high (E > 1 MeV) part of the fission neutron spectrum using research reactors.

7.0 Conclusions:

Ion beam and neutron irradiation studies for Di-BSCCO HTS tape & developed magnet insulation material at IPR have been initiated and databases have been generated. These studies will be further extended to fully qualify them for the fusion reactor environment. Commercial scale heats of Indian RAFM steel proposed to be used as structural material have been produced and short term mechanical properties have been evaluated. Different physical and thermos-mechanical characterizations have been performed on the un-irradiated IN-RAFMS samples. Blanket functional material Li_2TiO_3 has been developed in-house and characterised for its desired properties. Irradiation studies for these materials are planned in research reactor facilities.

A 14 MeV DT neutron generator facility has been developed at IPR for neutron activation studies, neutron diagnostics development, benchmark experiments for the validation of neutron cross-section libraries and low-fluence irradiation studies such as performance degradation of electronics.

High energy ion beam irradiation studies for tungsten plasma facing components have been performed and damage produced by them is correlated with the neutron damage using PKA spectrum. These studies are planned to be extended of neutron irradiation in research reactors.

References:

1. M. Rajput et al., "Deuterium ion irradiation impact on the current-carrying capacity of DI-BSCCO superconducting tape," Nuclear Engineering & Technology, https://doi.org/10.1016/j.net.2022.02.008.
2. Rajiv Sharma et al 2017 IOP Conf. Ser.: Mater. Sci. Eng. **171** 012149.
3. E. Lucon et al, "The European effort towards the development of a demo structural material: Irradiation behaviour of the European reference RAFM steel EUROFER", Fusion Engineering and Design, Volume 81, Issues 8–14, February 2006, Pages 917-923.
4. E. Rajendrakumar, K.N. Vyas, T. Jayakumar, "Overview of LLCB TBM design and R&D activities in India", Fusion Engineering and Design **109–111** (2016) 1522–1527.
5. R. Knitter, P. Chaudhuri, Y.J. Feng, T. Hoshino, I.-K. Yu, "Recent developments of solid breeder fabrication, J. Nucl. Mater. **442** (2013) S420–S424.
6. Sudhirsinh Vala et al., "Rotating tritium target for intense 14-MeV neutron source", Fusion Eng. Des. **123**, Nov 2017, Pages 77-81.
7. Sudhirsinh Vala, et al., "Development and performance of a 14-MeV neutron generator", Nuclear Inst. and Methods in Physics Research, A, **959** (2020) 163495.
8. P.N. Maya et al., Studies on the near-surface trapping of deuterium in implantation experiments. 2021 Nucl. Fusion **61** 036007.
9. P.N. Maya et al., (2019) Nucl. Fusion **59** 076034.
10. S. P. Deshpande et al., APID for Fusion, IAEA Vol. 18, 3-44, (2019) ISSN 1018-5577.
11. P.N. Maya et al., Nucl. Fusion **62** (2022) 016005.
12. P. Sharma et al., Microscopy and Microanalysis (2019), 1–7.

Author Information

Dr. Shashank Chaturvedi got his B.Tech. in Chemical Engineering from IIT Delhi, where he was awarded the Silver Medal for standing first in the Dept. He then got his Ph.D. in Chemical Engineering from Princeton University, USA. His PhD work involved the computational study of a novel Nuclear Fusion Reactor concept.

He was awarded the Homi Bhabha Science & Technology Award of DAE in 2005. He is a Fellow of the Indian National Academy of Engineering and Senior Professor in the Homi Bhabha National Institute (HBNI).

He has earlier served as Head, Computational Analysis Division in the Bhabha Atomic Research Centre (BARC), Visakhapatnam. He is presently serving as Director of the Institute for Plasma Research, Gandhinagar, Gujarat.

His research interests include numerical modelling of pulsed-power & plasma systems, including Magneto-hydrodynamics, radiation-hydrodynamics, high-speed impact & shock waves, pulsed electromagnetics, High Performance Computing (HPC), Theoretical and experimental determination of materials properties (opacity, equation-of-state) under extreme conditions and automated processing of signals, voice, image & video data.

Applications of Radioactive Particle Tracking Technique for Flow Visualization in Industrial Process System

D. Jaiswal[1], H. J. Pant[2], R. K. Upadhyay[1*]

[1]Department of Chemical Engineering and Technology, Indian Institute of Technology (BHU) Varanasi, Varanasi-221005, Uttar Pradesh, India
[2]Isotope and Radiation Application Division, Bhabha Atomic Research Centre, Trombay, Mumbai – 400085, India
(**Corresponding author email:* rku.che@itbhu.ac.in)

Abstract

Multiphase flow reactors are the heart of many industries. However, even after decades of their use for many industrial processes, the design and scale-up of such reactors are still based on some heuristics rule. This is mainly due to the poor understanding of their complex flow physics, which is mainly due to the lack of suitable measurement technique. The radioactive particle tracking (RPT) technique is a state-of-the-art non-invasive velocity measurement technique which can measure the flow field for variety of multiphase flow system with same fidelity at all the scale. The current contribution discusses the details of RPT techniques and its implementation for investigation of different multiphase flow systems at different scale.

1.0 Introduction

Multiphase flows are significant in industrial applications across a wide range of industries. Multiphase flow reactors are used in many industries such as petrochemicals, refineries, fine chemicals, mineral extractions, power generations, paper production, and food manufacturing [1]. For better design and scale-up of such reactors it is important to understand the velocity field and phase distribution inside these reactors. Further, it is critical to understand not only the mean quantities but also the local and fluctuating components of these variables. In current contribution, we will limit our discussion on velocity field measurement in multiphase flow reactors. In literature, invasive and non-invasive techniques are used for measurement velocity field in variety of multiphase flow reactors. Invasive approaches involve inserting a probe into the vessel or reactor of concern to evaluate the velocities of the phase of interest. Some of the broadly adopted invasive techniques for velocity measurements are pitot tube, hot wire anemometry and optical probe. Pitot tubes are a typical method for analysing localized velocity in the flow field of single-phase. This technique was used by pioneer fluid flow researchers like Osborne Reynolds to measure the flow dynamics in a single-phase flow vessel. commonly, a five-hole Pitot tube is used [2 3]. The main tube is flanked by four tubes in this arrangement. Each of the surrounding tubes' ends are narrowed at a 45° angle to the main tube. A manometer is linked from every hole. The central hole measures total pressure, whereas the other four are associated with measurement of static pressure. The Pitot tube works on the principle of estimating the difference of static and stagnation pressure at a specific point in the fluid. Another invasive technique is hot wire anemometry (HWA), which uses the change of resistance in an electrically resistant wire caused by the loss of heat by the moving fluid to measure the velocity of the fluid around the wire. Platinum-iridium, platinum, tungsten and nickel film are commonly used materials to make the wire. Convection transmits a specific quantity of heat as fluid travels throughout the probe, which can be quantified averse to the local velocity of liquid. Either, a feedback system containing constant resistance or a fixed heating current, is used to connect the probe, but generally constant resistance method is used because of response time improvement due to reduction in variation of the probe temperature magnitude. Davis et al. [4] Mudde and Saito [5] employed another invasive technique called optical fibre probes to quantify local fraction of gas, size of bubble, and

velocity of bubble, in two and three phase system. As a result, this measurement emphasis as multi-functional. The basis of optical fibre probes is based on the refractive index difference of the various materials that make up the fluid flows. Lights get emitted from one end of the probe, commonly using a pulsed laser. Some fraction of the light that is reflected backward at the other end, due to the aftereffects of the optical fibre's refractive indices. A photo-detector is used to determine the intensity of reflected light, which is dependent on the flowing fluid's refractive index. Though these invasive techniques are simpler and cheaper compared to the non-invasive techniques, they change the flow field at the point of measurement itself due to their invasive nature. Further, they cannot be used with same accuracy in dense multiphase systems like gas-solid fluidized bed or gas-liquid system with high gas fraction.

In non-invasive velocity measurement techniques, velocity fields are measured without disrupting the flow. However, these are indirect measurement methods, which means that the obtained information will be in mode of signals or images, that must be processed further to obtain velocities. laser Doppler anemometry (LDA), particle image velocimetry (PIV), positron emission particle tracking (PEPT), radioactive particle tracking (RPT), and magnetic resonance imaging (MRI) are some of the more commonly used non-invasive velocity measurement techniques.

In LDA, a moving object's velocity is determined by lighting it with laser light and detecting the Doppler shift in the light frequency, dispersed by the flowing fluid. LDA is a very well determined approach for measuring velocity in flow of single phase.[6] Several researchers have also used LDA to measure the flow field in multiphase flow systems. However, this is used in visible light range and hence its application is limited for the dilute system where discrete phase fraction is low. PIV is another laser-based imaging technique, though it is set up differently from LDA. A strong laser beam is focused through within a cylindrical lens, in traditional 2D PIV, which moulds the transmitting ray into a thin flat sheet of laser light containing higher intensity. This sheet is created at a specific moment in time. The thickness of sheet is usually in the range of 2 to 5 mm. Many researchers have used PIV technique to diagnosed the floe filed in multiphase flow reactors.[7] However similar to LDA, PIV also works in visible range and hence cannot be used for opaque system. To minimise the noise generated due to the light scatter it is generally recommended to use this technique for dilute system where discrete phase fraction is low. Hence, the applicability of these techniques for industrial scale system are limited.

PEPT is another technique which is used for mapping the flow field in multiphase flow reactors. It is based on radiation. In this technique a positron source is used as a tracer. When this tracer particle emits a positron, it instantly annihilated with the free electron, resulting in a pair of 511 keV gamma rays travelling in different directions following straight line pathways (180° apart). Two huge positron sensitive detectors (commonly referred to as positron cameras) detect these gamma rays. Only those photon-capture events that are recorded by both detectors within a 12 ns of resolving time are deliberated as defendable measurements. PEPT is used to measure the flow field in gas-solid and gas-liquid systems.[8—11] As it's based on gamma-radiation it can also be used for opaque and dense system. However, due to the low energy of gamma-rays produced due to annihilation, this technique can only be used for smaller system.

MRI was first used to examine multiphase flow in the 1980s and 1990s. To induce a magnetization, a huge and very strong magnet (5 Tesla or higher strength) is concentrically installed around the vessel. For sending and receiving signal, radio wave antenna is being used. The measurement of phase velocity is performed with this technique by photographing the spatial heterogeneity in magnitude of magnetization magnitude. At a specific time, a spin lump (a primordial quantity associated to elementary particles that comprise everything) is linked to a radio frequency (R.F.) excitation, and its

relaxation is photographed at later stages. As a result, the velocity is estimated using the spins' displacement over two excitations and the spin vector's relaxation rate.[12—14] This technique is quite efficient however, due to the requirement of large magnetic field this is used for system having maximum diameter of 5 cm only till date. This limits the application of this technique for laboratory scale system only. Therefore, it is vital to develop a technique which can be used for both dilute and dense multiphase flow system with equal fidelity at all the scale.

The 'Radioactive Particle Tracking' (RPT) technique is the one of the non-invasive velocity measurement tools that has shown a good prospect in recent years. [15—17] This contribution will look methodologies and RPT application in multiphase systems in detail.

2.0 Radioactive Particle Tracking (RPT) Technique

In RPT, a single radioactive particle (emits gamma ray) is utilised as the identifier of the 'phase' whose velocity profile is to be mapped [2,18—21] When tracking a liquid phase, the tracer particle is rendered ambiguously buoyant in relation to the liquid.[22 19] If a solid (granular particulates) is being tracked, the tracer particle's shape, size and density are adjusted to match the solids in the stream.[2 18 20 21] The tracer particle is left free in the system and moves with the phase of interest. An array of NaI (Tl) scintillation detectors, strategically positioned around the desired vessel, are used to detect the counts emitted by the tracer particle. This photon count time series recorded on each detector are then used to calculate the Lagrangian position time series map by using the suitable reconstruction algorithm. The Lagrangian trace of this particle is then used to deduce the instantaneous velocity time series. A data set of flow fields such as turbulence kinetic energies, mean velocity fields, shear stresses, coefficient of dispersion, and also other parameters that demonstrate the dominating flow patterns and flow conditions is measured based on this data.[23 2 24 16] Fig 1 shows the schematic and flow diagram of RPT data processing. Due to the use of gamma-ray, RPT can be used to investigate the flow field in opaque as well as dense and dilute multiphase flow systems. The activity and energy of the tracer particle can be tailor made by the using the nuclear reactor. This gives the flexibility to use the technique at laboratory, pilot and industrial scale system with equal fidelity. The RPT is implemented on variety of multiphase flow systems like gas-solid [18 16 25], gas-liquid systems [23 19], liquid-solid system [20 21] and gas-liquid-solid systems [19]. The different case studies of RPT implementation on such systems are shown below.

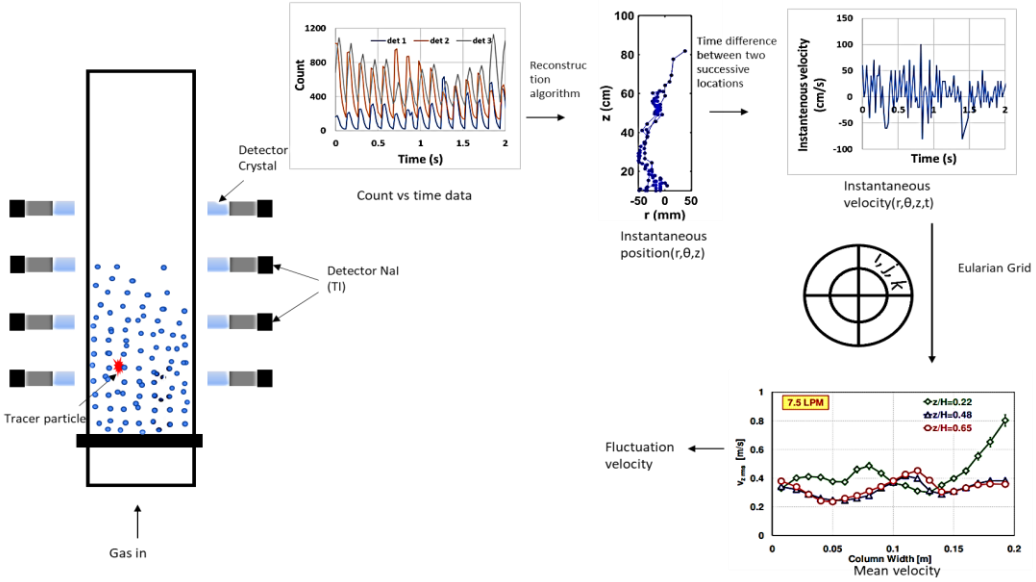

Fig. 1- Schematic of RPT setup and RPT data processing flow diagram

3.0 Implementation of RPT in laboratory scale gas-solid fluidized bed

Many applications in the chemical industry, petrochemical, and metallurgical industry, as well as energy generation and food processing, require gas-solid interactions. Gas-solid fluidized systems, in particular, are broadly used in these industries due to their distinct advantages, like the ability to maintain isothermal conditions across the bed, extremely good heat and mass transfer rates, and the ability to operate continuously. These features are beneficial in both circumstances where solid is reactant and when the solid is catalyst. [26] [27] [16] Most of these gas-solids beds are poly-dispersed in nature. However, the design and scale-up strategies for such beds are mainly available for monodispersed beds (particle of uniform size). In current work, the hydrodynamics behaviour of binary fluidized beds with the same density and different size is examined by using RPT technique in a laboratory scale setup. The experiments are performed for different bed compositions and gas inlet velocities. All of the experiments are carried out in a Perspex® fluidized bed column (cylindrical) with an ID of 11.5 cm. A perforated plate distributor of hole size 2mm and pitch 8 mm is used for gas distribution. Above the distributor, a filter cloth with a mesh size of 200 is employed to avoid particles from sliding back towards the distributor zone. The gas flow rate is controlled by a series of rotameters. The glass beads of 1 mm and 0.6 mm sizes and density 2600 kg/m^3 are used as a solid phase and air is used as gas phase. It should be noted that at a time the flow behaviour of only one particle is tracked. Hence, for all the conditions experiments are performed twice, once with 1 mm tracer particle and another for 0.6 mm tracer particle to decipher the flow physics of the complete bed. In both the cases Sc-46 doped in glass beads of desired size are used as a tracer particle. The mass of bed was kept constant at 3 kg for all the experiments. Fig 2a shows the photograph of the experimental setup.

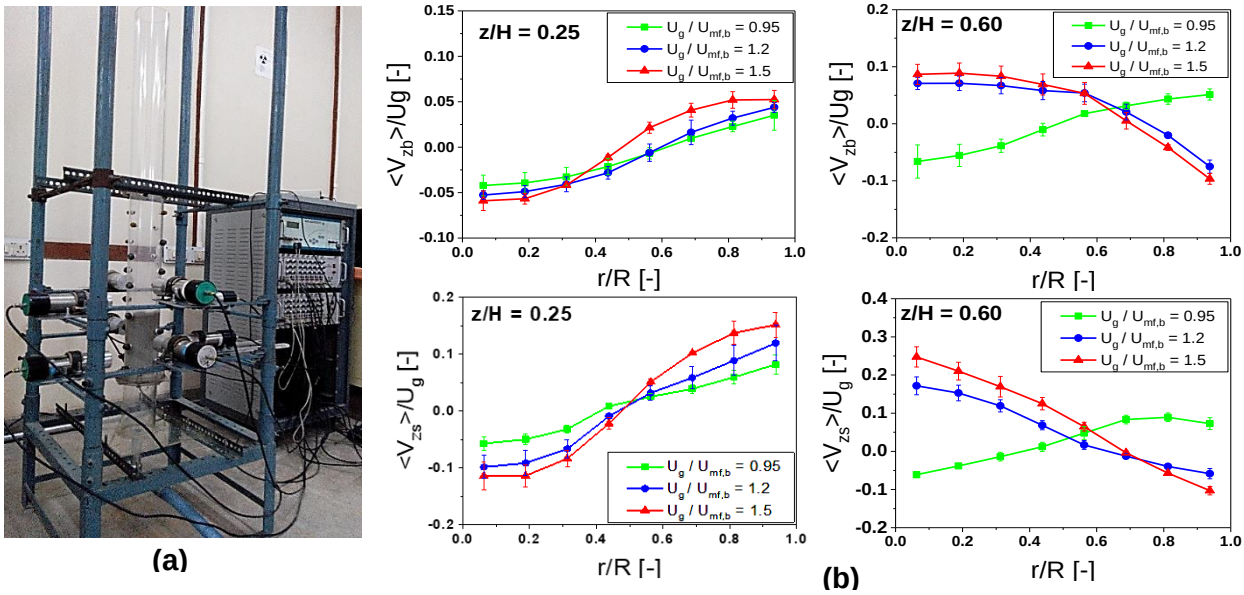

Fig. 2 (a) Photograph of the experimental setup **(b)** radial variation of the normalized mean axial velocity at different gas inlet velocities for 50:50 bed composition

The experiments are performed for different bed composition and gas velocities and the motion of both the particles was tracked by using RPT technique for each condition. The data are plotted at two different heights, z/H=0.25 which refers to bottom section and z/H=0.6 which represents top section. Fig. 2b shows the radial variation of normalized mean axial velocity of both the solids at two different axial planes for 50:50 binary bed composition. Results show that both the solids move downward at the centre and upward near the wall at the bottom section while moves upward at the centre and downward near the wall at the top section of the bed. The velocity of both the solid increases with the

air velocity. However, the increase is more in smaller solid compared to the bigger solid. It is interesting to observe that bigger solid fluidized at a velocity lower than its minimum fluidization velocity and have similar velocity magnitude as of the smaller particle. This was achieved mainly due to the particle-particle interaction which plays critical role at this condition. It should be noted that no other technique will able to give such detailed information other than RPT as its use's radiotracer.

4.0 Implementation of RPT in pilot-plant scale gas-solid circulating fluidized bed (CFB)

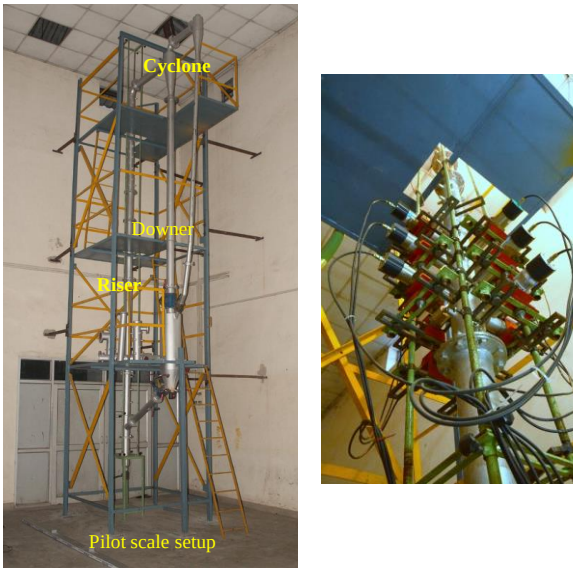

Fig. 3 Photograph of the pilot plant scale CFB setup with RPT facility

RPT is further implemented in a pilot plant scale circulating fluidized bed (CFB). Experiments are performed in a clod flow CFB of riser diameter 10 cm and height 6.8 m. Glass beads of mean diameter of 600 μm and density 2500 kg/m^3 is used as sloid phase, and air at ambient temperature through an air blower is used as gas phase. Sc-46 doped in the glass beads of same size is used as a tracer particle. The tracer particle is prepared in such a manner that the surface property of tracer particle and glass beads remain same. This scandium doped tracer particle is then sent to nuclear reactor for irradiation. The motion of this single radioactive particle is tracked by using 12 NaI (Tl) scintillation detectors, which are used to record the photon counts emitted by the tracer particle during its path. Suitable reconstruction algorithm is used to reconstruct the position of the particle by using photon-count series recorded on each detector. In this case the particle motion is only tracked at the middle section of the riser where the flow is already developed. As the wall of the reactor is made of mild steel, a tracer particle of high activity (800 μCi) is used. This is the major advantage of the RPT experiment, where based on the requirement the activity of the tracer particle can be tailor made by using available nuclear facility in Bhabha Atomic Research Center (BARC). The experiments are performed for different solid flux (70-126 kg/m^{2}s) at a constant gas velocity of 9.7 m/s. The data is acquired at 100 Hz frequency for all the cases. As the system size is large for each case data is continuously acquired for 7 days. Hence, a huge data set are generated which used for further processing.

Fig 4 shows the axial mean velocity of solids at the height of 3.8 m for all the fluxes at constant gas velocity of 9.7 m/s. Along the radial direction, mean axial velocity gradient is very low. With increase in the flux, velocity increases. When the solid flux is increased from 90 kg/m^{2}s to 110 kg/m^{2}s, mean axial velocity is

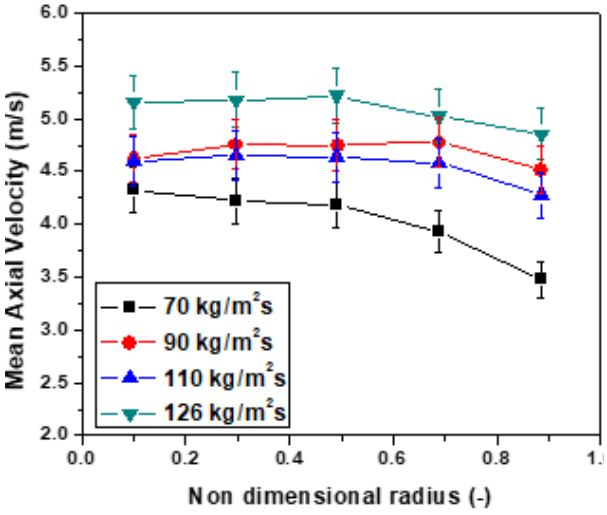

Fig. 4 Mean axial velocity of solids in CFB riser at the height of 3.8 m for different flux

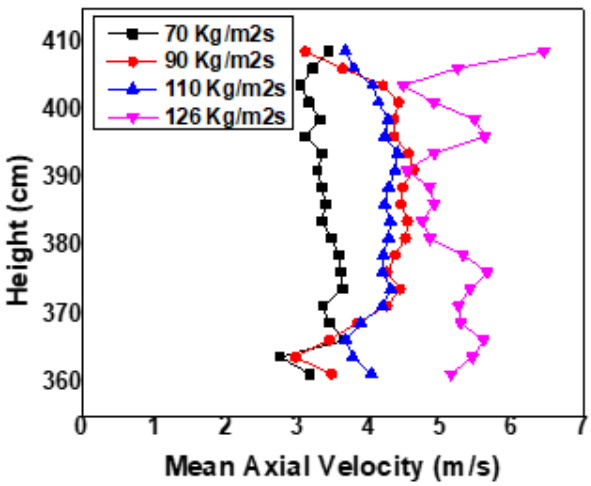

Fig. 5 Mean axial velocity of solid along the height of the column near the wall

decreased. This might be due to the flow structure change accompanying the regime. Further increasing the flux at the same superficial gas velocity increases mean axial velocity. Fig 5 shows the axial mean velocity along the height near the wall. It can be clearly seen that the mean axial velocity along the height for the flux of 70 and 90 kg/m^{2}s is not varying much. The reason behind the fluctuation of mean axial velocity along the height for 110 and 126 kg/m^{2}s has to be explored. In fast fluidization, core annulus flow has been reported by many authors. Solids accumulation near the wall also has been confirmed by the number of occurrence map in this work (not shown here). Again, such a detailed information is not possible from other technique at this scale.

5.0 Conclusion

The current contribution summarises the various aspects of radioactive particle tracking (RPT) technique. RPT is a very versatile technique for studying the hydrodynamic behaviour of gas -solid, gas-liquid and gas-liquid solid systems. Recently we have also implemented the RPT in a liquid-liquid system. The use of radioisotope gives the flexibility to use the technique for different multiphase flow system at different scales with almost similar accuracy. The technique provides a large data set and can be used to investigate the detailed velocity field. The technique not only provide mean velocities but it also provides the PDF of instantaneous and fluctuating velocity at each location inside the system of interest. This huge data set can be used to analyse the system in detail. The data generated can also be used to validate the CFD models. It can also be used to developed a better design and scale-up strategies.

References

1. M. P. Dudukovic, Science, 325, 698-701 (2009)
2. F. G. Larachi et al., Nucl. Instrum. Methods Phys. Res., Sect. A, 338 (2-3), 568-76 (1994).
3. A. M. C. Chen, D. Bzovey, Nucl. Eng. Des., 122, 95-104 (1990).
4. M. R. Davis, J. Phys. E: Sci. Instrum., 3, 15-20 (1970).
5. R. F. Mudde, T. Saito J. Fluid. Mech., 437, 203-228 (2001).
6. Durst et al., Principles and Practice of Laser Doppler Anemometry. Second Edition (1981).
7. R. J. Adrian, Ann. Rev. Fluid. Mech., 23, 261-304 (1991).
8. Hawkesworth et al., Nucl. Instru. Meth. 253, 145-157 (1986).
9. Parker et al., Chem. Eng. Sci., 52, 2011-2022 (1997).
10. Parker et al., Nucl. Instrum. Meth. A, 236, 592-607 (1993).
11. Parker et al., Nucl. Instrum. Meth. A, 348, 583-592 (1994).
12. P. T. Callaghan, Clarendon Press, Oxford (1991
13. L. F. Gladden, P. Alexander, Meas. Sci. Technol., 7, 423-435 (1996)

14. L. F. Gladden, Chem. Eng. Sci., 49, 3339-3408 (1994).
15. Chaouki et al., Ind. Eng. Chem. Res., 36 (11), 4476-4503 (1997).
16. R. K. Upadhyay, S. Roy, Can. J. Chem. Eng. 88, 601-610, 2010
17. Kalo et al., Chem. Eng. Sci., 207, 702-712, 2019
18. Roy et al., AIChE J., 51, No. 3, 802-835 (2005).
19. Upadhyay et al., Eng. Sci., 96, 152-164, 2013.
20. Jain et al., Particuology, 33, 112-122, 2017.
21. Kalo et al., Ind. Eng. Chem. Res., 59, 20943, 2020
22. Devanathan, et al., Chem. Eng. Sci., 45(8), 2285–2291 (1990).
23. N. Devanathan, D.Sc. Thesis, Washington University, USA, (1991).
24. S. Degaleesan. D.Sc. Thesis, Washington University, USA (1997).
25. Kalo et al., 2020. Ind. Eng. Chem. Res. 59, 20943–20952 (2020).
26. Devidson et al., "Fluidization" Academic Press (1985).
27. M. Kwauk. Fluidizaton – Idealized and Bubbleless, Ellis Horwood (1992).

Author Information

Dr. Rajesh Kumar Upadhyay has obtained his PhD degree from IIT Delhi in 2010. He has worked for 9 years in IIT Guwahati as an Assistant Professor and Associate professor positions. Thereafter he has joined the IIT (BHU), Varanasi in year 2019 as an Associate Professor and working their till now. He has published around 25 international journal papers and around 60 international conference papers. His major expertise is: multiphase flow reactors, measurement techniques, radiotracer-based techniques like radioactive particle tracking, and gamma-ray densitometry, novel reactor design and hydrogen energy.

Enhancing The Efficiency Of Chemical Processes: The Triad Of Radiotracing, Radioactive Particle Tracking (RPT) And Computational Fluid Dynamics (CFD)

Shantanu Roy[1], H. J. Pant[2]

[1] Department of Chemical Engineering, Indian Institute of Technology (IIT) – Delhi, New Delhi-110016, India
[2] Isotope and Radiation Applications Division, Bhabha Atomic Research Centre, Mumbai-400085, India
(Author email: [1]roys@chemical.iitd.ac.in, [2]hjpant@barc.gov.in)

Abstract
Residence Time Distribution (RTD) measurements were conducted by pulse radiotracer (Au-198) injection in a 'hot' industrial fluidized bed coal gasifier. The data obtained was treated and analyzed employing a network model based on a cascade of perfectly mixed tanks in series. Based on the non-ideality of flow, flow schemes are proposed whose RTD function was deduced in the Laplace domain. These RTD functions were numerically transformed into the time domain and were compared with that measured using radiotracing. It was noted that Scheme 3, which was based on the backflow of solids in the bed could satisfactorily predict the actual RTD function. Besides, the parameters of the model provided insights into the actual solids flow pattern in the gasifier. Furthermore, the model demonstrated its adaptability in analyzing RTD of similar studies reported earlier for both single as well as pulse injection of tracer.

Keywords: Residence Time Distribution (RTD), Fluidized Bed, Coal Gasification

1.0 Introduction

The design and scale-up of chemical reactors is a problem of continuing interest to chemical and process engineers. While many problems and challenges in the design and scale-up of multiphase reactors have been addressed, the emergence of novel (and typically difficult) feedstocks as well as the need to reduce the environmental footprint of process units continues to open and evolve new challenges in this field. Many of these challenges relate to the inherently complex and scale-dependent nature of these dispersed multiphase flows. Other transport effects in reactors, in turn, get determined by the nature of these flows.

Radiotracer techniques are widely used for measurement of hydrodynamic parameters, troubleshooting and process optimization in full-scale industrial reactors because of their many advantages such as high detection sensitivity, on-line detection and availability of a wide range of compatible radiotracers for various applications and utility in harsh industrial environments. Built on the legacy of classical reactor engineering and residence time distribution (RTD) theory, radiotracer imaging involves the injection of radioactive material in a suitable physico-chemical form similar to that of the process material. The passage of these radiotracers in their sojourn through the system of interest is monitored at strategically selected locations using radiation detectors. In spite of their wide use in the industry, radiotracer techniques have several limitations in their interpretation, not often widely discussed, and thus their use for scale-up and scale-down of multiphase flow reactors and validation Computational Fluid Dynamic (CFD) models is limited.

The other end of the spectrum of radiation-based imaging techniques is represented by single-particle radiotracing methods, such as Radioactive Particle Tracking (RPT), Positron Emission Particle Tracking (PEPT) and X-Ray Particle Velocimetry (XPTV). For instance, RPT, which has been widely discussed in the open literature, is based on the principle of following a single gamma-ray emitting tracer particle

through its many realizations in the process vessel of interest, and then back-projecting the photon counts time series to yield a Lagrangian velocity time series. From the latter information, many flow quantities of interest are evaluated, including ensemble averaged profiles of velocity, turbulence and flow regime information, and dispersion coefficients. In that sense such techniques come close to other "optical" velocity measurement methods like PIV and LDA. Such single particle radiotracer data thus yields rich databases for benchmarking CFD models, but the issues related to both experimenting with such techniques at large scales and well as having grid-converged CFD models at large scales essentially limits such validation research to small-scale laboratory systems.

This contribution dwells on the challenges in "bridging this gap" in radiotracer techniques between these scales.

As an illustrative application, the talk will focus on coal gasification as an application, where all these techniques have been applied. The talk will show how having a judicious application of these three apparently diverse expertise can help to aid chemical processing and reduce the environmental footprint of chemical reactors.

2.0 Gasifier based on Indian Coal

Gasification for syngas generation constitutes a critical step towards cleaner utilization of coal. Of late, among several applications of syngas, its usage as a raw material for the production of methanol has received thrust as it can not only be used as a clean fuel but also, is an important feed for the synthesis of a wide range of liquid and high-value chemicals [1]. While gasification of coal and its subsequent conversion to methanol has been a proven technology worldwide, the processing of low-grade coal with high ash content (> 35-40%) poses unique challenges. The presence of highly abrasive ash can be a major roadblock in a gasifier, as well as in the downstream gas cleanup and methanol reactor. Thus, a critical bottleneck to syngas production is the gasification of coal. Based on the gas (air/O_2 + steam) and solid (coal) contacting patterns, there exits several successful commercial technologies like – The Lurgi Fixed Bed Dry Bottom (FBDB) Gasification™ of Air Liquide, Shell Coal Gasification (SCG) Technology™, and mixed-flow Winkler (HTW) ™ of ThyssenKrupp Uhde GmbH [2]. As the primary mode of gasification is through fluidization, the technologies similar to HTW is doggedly sought wherein relatively superior mixing ensures uniformity in temperature and aids in quicker dispersion of solids. With the fuel content typically within 1-5 % of the entire weight of bed material, the intense churning of the bed ensures rapid heating of injected particles and subsequent efficient consumption. Further, clinker formation is avoided as the operating temperature rarely overshoots 900 ^{O}C, and the ash extracted in dry form; a feature aptly suited for high ash low-grade coal. In case a high carbon conversion is warranted, a portion of entrained solids can be fed back into the bed through a recycle loop. These traits thus offer tremendous flexibility over a fixed or entrained bed gasification in terms of grade of fuel and the air-to-fuel ratio [2].

Notwithstanding the superior bed hydrodynamics and fuel flexibility, coal gasification in fluidized beds has inherent challenges as well. Fluidized Beds are known to give rise to maldistributions in the form of rising gas pockets devoid of solids. In the case of the gasifier, this passage lowers the gas residence time leading to lesser and slower diffusion of oxygen/steam from the bubbles to the suspended coal particles. Deficiency in oxygen supply can lead to incomplete coal conversion and lesser heat generation, which in turn might pose difficulty in maintaining bed temperature. In extreme situations, this may even lead to a lowering of bed temperature [3]. From the point of view of the operation, this decrease in bed temperature might be deceptive and can innocuously dictate an increase in coal/ air/oxygen feed rate to enhance combustion

Figure 1 Clinkers formed in Fluidized Bed Gasifier

reactions or discharge rate of ash from the bottom. However, such an erroneous decision can cause a sudden rise in bed temperature, *albeit* after a time lag, which can have a catastrophic cascading effect. Excess coal might increase the bed temperature to the extent that it is closer to the ash fusion temperatures causing slag formation and clinkering. Subsequently, the clinkers as large as few millimeters cause further agglomeration and lead to particle growth which can potentially set in de-fluidization (**Fig. 1**). Despite sufficient feed, a significant fraction of unburned coal leaves the reactor. Thus, a maldistribution in flow of solids (Coal) and gases (oxygen/air + steam) can have a detrimental effect on the continuous operation of fluidized bed gasifiers.

With this backdrop, the present study thus focusses on studying the solids flow in an industrial fluidized bed gasifier. To this effect, pulse tracer injection of radioisotope labeled coal particles was employed to determine the Residence Time Distribution (RTD) and estimate solid maldistribution. The RTD measurements and subsequent analysis employing a network model provide a degree of axial mixing, which can be useful for troubleshooting and retrofitting of existing reactors.

3.0 Radiotracing

Residence Time Distribution (RTD) is a versatile tool to quantify flow maldistribution in a continuous system based on the amount of time that material spends in the domain of interest [4]. Besides, it quantifies the macromixing characteristics of fluid elements, expressed typically in terms of moments of the RTD distribution function, Dispersion (Bondestein/Peclet) number, and the number of equivalents of perfectly mixed-flow systems. One of the key features of RTD measurements is to ensure that barring a distinct property that distinguishes from bulk solid, the tracer designed should be hydro-dynamically similar to the phase of interest. In order to conform to this condition, a multitude of techniques for RTD estimation in laboratory-scale fluidized beds has been reported. Some of the popular intrusive (also referred to as disruptive) methods like -- impulse injection of solids impregnated with a saturated solution of table salt [5], direct measurement of salt concentration[6,7]. These techniques involve withdrawing samples from various definite locations from the bed which was then washed and filtered. The salt concentration of the filtrate is estimated based on pre-calibrated conductivity measurements. These methods are innately slow due to elaborate sample withdrawing mechanisms and thus cannot account for stochastic solid flow. A popular non-invasive measurement technique involves tracking Phosphorescent Tracer [8–15]. The 'tracer injection' involves excitation of phosphor-coated particles by a sudden flash of high-intensity light source, essentially rendering the process immune to cause any disturbance to the actual flow. The detection of solid dispersion was effected through the measurement of the intensity of emitted light by the 'light tagged' tracers downstream by an elaborate arrangement of optical fiber and photo-multiplier tube. However, in spite of its several advantages, being an optical technique, only the particles close to the wall could be excited. Although a modification was later introduced in the form of planar injection, the fact that once excited, phosphorescence lasts only for few minutes is a significant hindrance in its applicability to an industrial bed where a longer tracer activity is often required [13]. Nevertheless, another class of measurements attempted to exploit the magnetic permeability of ferromagnetic tracers to measure RTD [16–19]. A small batch of crushed ferromagnetic material (steel, Mn-Zn) with identical particle size

distribution to that of bed material was injected by an electro-pneumatic valve synchronized with the injection controller. Similarly, sensing coils placed downstream generates a voltage signal corresponding to variation in concentration. In spite of sophisticated instrumentation, the measurements are susceptible to parasitic impedance and electrostatic charging, the influence of which is highly likely in case of measurements in 'hot' fluidized beds. Sublimation of CO_2 pellets was also used as solid tracers to measure RTD but with limited success due to complications in data interpretation [20].

Notwithstanding the challenges faced in RTD measurements of solids in a fluidized bed, significant headway was achieved by employing radioisotopes. Being a high energy γ emitter, they are aptly suited for *in-situ* measurements in dense industrial beds of large diameters (~ 1m). This also allows data acquisition, both at injection and outlet relatively simpler. Thus, several studies in the past have focused on RTD measurements through radioisotopes. These studies can be broadly classified into two categories -- the former being RTD measurements using single radioisotope [21–28] and the latter approach involve stimulus-response of radioisotope tagged bed solids [29–33]. The single-particle measurement utilizes the concept of well-known trajectory length distribution (TLD) to estimate the RTD moments [22–24,34]. This concept is based on the assumption that multiple tracer navigation in a circulating system simulates the movement of fluid elements and that the path (and hence the residence time) for each of these instances to be mutually exclusive events. Thus, the distribution of an ensemble of the residence time of such events can represent the RTD of the system [35]. Although readily adapted for laboratory-scale circulating systems, the accuracy of RTD estimation with a single radioisotope depends on the collection of sufficient statistics and is thus time-consuming, particularly for a pilot-scale reactor. Such limitation is largely overcome in the latter approach in which a small batch of radioisotope labeled solids is injected in the bed [29–33]. An approach like this is analogous to pulse injection of the tracer. This alteration eliminates the requirement of matching tracer properties with that of bed material. Thus, it can be readily applied to any industrial beds without any modifications for RTD studies. Numerous studies in the past showed that within the limited scope of measurements, the CFB boiler behaves as a train of well-mixed tanks [33]. Similar measurements in pilot-scale coal gasifiers performed for both 'hot' and ambient runs analyzed the mixing pattern at the bottom outlet [29,30]. A tank-in-series model was fitted agreed satisfactorily with the actual discharge rate of solids from the bottom. Further refinement of the model established that solids exiting from bottom behave similar to tank-in-series with backflow and a recycle fraction under 'hot' conditions [32]. Whereas, under 'cold' operation, a fraction of solids was found to additionally follow a bypass stream. A detailed compilation of the RTD measurements of solids in a fluidized bed is discussed in [13,19,36].

From the preceding discussion, it is recognized that in order to execute RTD measurements in industrial fluidized beds, radiotracers are by far the best alternative. The primary motive of this study is thus twofold. Firstly, an analysis of RTD measurements of an industrial fluidized bed gasifier is presented. Subsequently, a network model is developed which examines various schemes of solid flow in the bed. The model is then not only employed to estimate the RTD of solids.

4.0 Experimental

4.1 Fluidized Bed Gasifier

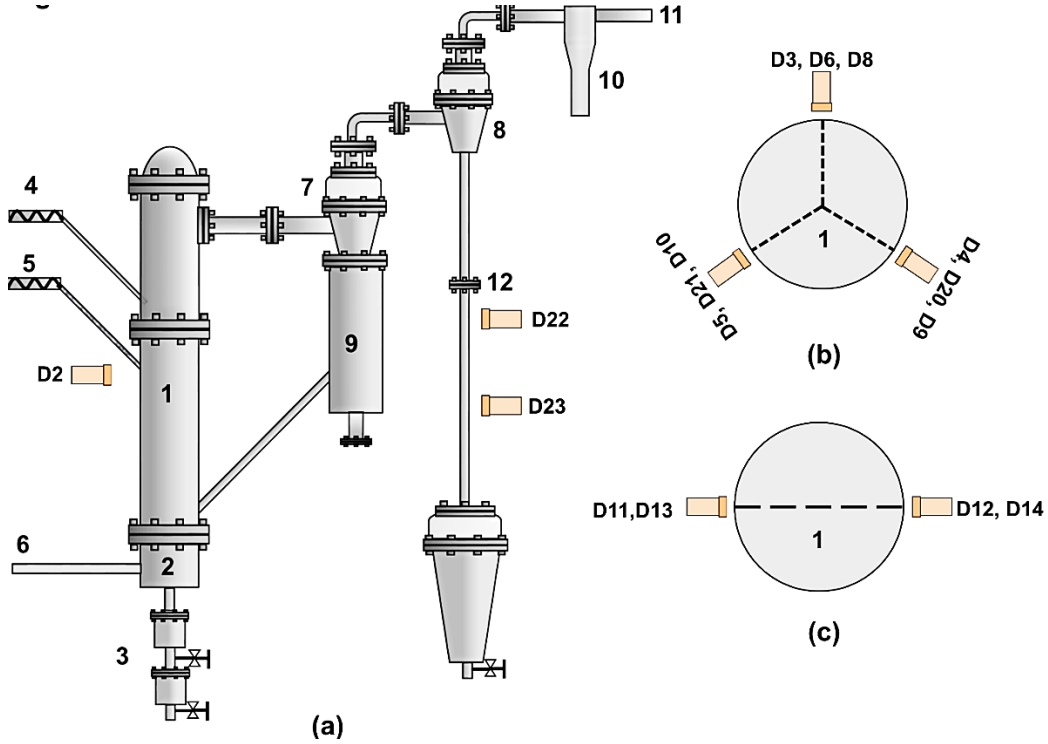

Figure 2 (a) Schematic representation of fluidized bed gasifier (1. Fluidized Bed, 2. Plenum, 3. Ash Discharge, 4. Bed Material, 5. Coal Inlet, 6. Air and Steam/Oxygen Inlet, 7. Cyclone 1, 8. Cyclone 2, 9. Downer, 10. Syngas Cooler, 11. Syngas Outlet to Ventruri Scrubber, 12. Standpipe)
(b) Location of bed detectors
(c) Location of freeboard detectors

RTD measurements were conducted in a pressurized Fluidized bed gasifier (**Fig. 2a**). The system consists of various subsystems such as gasifier, coal/bed material feeding system, air compressor, steam supply system, and ash extraction system. Several utilities (not shown in the figure) like steam boiler, lock hopper, air compressor in upstream as well as venturi scrubber, droplet separator, filter press, and settling chamber in the downstream complements the gasifier systems. The gasifier has an internal diameter of 200 mm and was designed for gasifying sub-bituminous coal. Pre-mixed hot air/oxygen and steam were injected in the plenum where it was further distributed in the bed through a conical distributor. The freeboard section is slightly tapered with internal diameter reducing to 140 mm. For precise control, both the gasifier and freeboard sections were provided with multiple tappings for temperature and pressure measurements. Initially, the gasifier was filled with a known quantity of crushed refractory as bed material (0.5-2 mm) and coal particles (0.5- 2 mm) through respective feed injection systems. Subsequently, the mixture of fluidizing air/steam was fed to the gasifier. During the gasification, the bed temperature was typically maintained at ~820-850 ^{o}C. Fine ash/ unburned coal particles in the gases produced were separated in a system of cyclones at the exit. Further, gas cleaning was effected in venture scrubber and droplet separator. The syngas thus generated was cleaned and burned in a combustor.

4.2 Residence Time Distribution Measurements

As indicated above, the radiotracer technique was adopted to measure the RTD of the coal particles being fed into the gasifier. However, critical to such studies is the selection of a suitable radiotracer. In particular, the physicochemical characteristics should match closely like that of the process material. As the present study involves tracing of solid coal particles, it was required that the radiotracer thus chosen resembles it. Yet another important criterion for selection of radiotracer, is its half-life, which should be long enough compared to the duration of actual experiments. This is to ensure that the radioactive decay has minimal effect on the actual experiments. As radioisotopes are high energy gamma emitters that can penetrate thick walls, they are suitable for online tracing in industrial process vessels. Based on the above consideration, for the present study, Au-198 was selected for the RTD studies. Prior studies on adsorption characteristics of Au- 198 on coal particles have indicated its suitability for such purposes [37]. Moreover, as Au 198 has a half-life of 2.7 days, its usage in an open industrial environment was also prudent from safety considerations. In the present study, for tracer preparation approximately, 3 ml of radioactive $AuCl_4$ was adsorbed in a sample of 100 gms of coal particles. In terms of the activity, in each experiment about 3mCi of Au-198 labeled over coal particles was used.

A total of 15 experimental runs was performed to determine the RTD of solids. Such exhaustive span of the experimental matrix spanned over two modes (Oxy and air-blown) with operating pressures at 2 and 4 bar. However, to maintain brevity, runs 3, 8, and 12 will be discussed here. A set of 22 NaI detectors mounted strategically around the gasifier was employed to gather tracer signal. The radiotracer prepared was instantaneously injected into the coal feed line using a specially fabricated injection arrangement and registered in detector D2. Subsequently, its movement in the gasifier was monitored using the ring detectors in the bed and at the freeboard (**Figs. 2b** and **c**). To avoid the detection of any spurious counts, all the detectors were suitably collimated and mounted along the bed. The tracer signal versus time data was acquired in an online data acquisition system and for further data analysis, the counts obtained by D22 and D23 placed the standpipe were used.

5.0 Network Modeling

Any complex flow systems can be analyzed as a network of ideal subsystems whose RTD function $E(t)$ has an explicit mathematical definition [38,39]. Typically, such models consist of a physical structure associated with the architecture of the model. In the case of reactors, these architectures may consist of elementary multiple Continuous Stirred Tank Reactors (CSTRs), Plug Flow Reactors (PFRs), internal as well as external recycle streams arranged in any order of precedence. Additionally, models developed can account for non-ideality like – short-circuiting, bypass, and dead space as well [39–41]. Now, assemblage of these models through a set of parameters completes the description of any closed network. In case of present study, for an assumed flow scheme, the overall de-convoluted $\overline{E}(s)$ representing the combination of the subsystems is then derived with regression of suitable parameters. Likewise, in the present study, the solids flow in the fluidized bed gasifier is also analyzed. Three such phenomenological flow schemes have been proposed as described below.

5.1 Scheme 1 – Recycle

In this model, the gasifier is assumed to have four conceptual zones (subsystems) from the bottom – bottom bed, top bed, freeboard, and a recycle stream (**Fig. 3**). The fraction of solids $(1-\alpha)C_0Q$ entering the reactor unites with a recycle stream that emerges after traversing through the recycle and bottom bed with

a residence time of $\beta_3\tau$ and $\beta_1\tau$ min respectively. The merged fraction C_BQ then enters the top bed and leaves with a rate of C_TQ. Subsequently, it is assumed that only a fraction $(1-\alpha)C_TQ$ of this stream actually proceeds to the freeboard. Finally, the outlet stream from the freeboard with material flow rate $(1-\alpha)C_{out}Q$ leaves, which in the present case is interpreted as the output signal (photon counts) for D22/D23 and will thus be employed in all subsequent analyses.

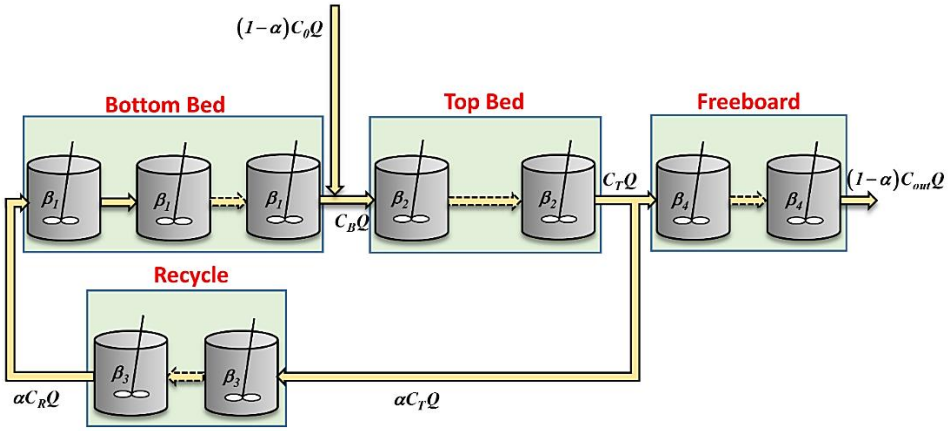

Figure 3 Schematic of flow Scheme 1

Now, assuming the RTD function to be represented by a cascade of perfectly mixed systems with net volume V_B, the material balance at the outlet of the bottom bed can be expressed as.

$$\frac{dV_BC_B}{dt} = -\alpha C_BQ \tag{1}$$

Taking the Laplace transform of the above equation and subjecting to the initial condition $C_B(0) = C_{B,in}$ of an impulse response, the eventual function transfer function is represented by **Eq. 3** below.

$$\tau s\overline{C}_{B,1}(s) - \overline{C}_{B,in}(s) = -\alpha\overline{C}_{B,out}(s) \tag{2}$$

$$\overline{E}_{B,1}(s) = \frac{\overline{C}_{B,1}(s)}{\overline{C}_{B,in}(s)} = \frac{1}{\beta_1\tau_{mod\,el}s + \alpha} = \frac{\alpha}{1 + \frac{\beta}{\alpha}\tau_{mod\,el}s} \tag{3}$$

When extended for a battery of N_B tanks in series, it reduces to **Eq. 4**.

$$\overline{E}_B(s) = \frac{1}{\left(\frac{\beta_1\tau_{mod\,el}}{N_B}s + \alpha\right)^{N_B}} \tag{4}$$

Although an analytical inversion in the form of **Eq. 5** exists for **Eq. 4**, when used in combination with other flow schemes, the eventual transfer function may require a numerical treatment.

$$E(t)=\frac{1}{\left(\frac{\beta}{N\alpha}\right)\tau_{mod\,el}}\left[\frac{t}{\left(\frac{\beta}{N\alpha}\right)\tau_{mod\,el}}\right]^{N-1}\frac{N^N}{(N-1)!}\frac{exp\left[-\,tN\Big/\left(\frac{\beta}{N\alpha}\right)\tau_{mod\,el}\right]}{\left(\frac{\beta}{N\alpha}\right)\tau_{mod\,el}} \tag{5}$$

Similar transfer functions may be derived for top bed, recycle and freeboard. The corresponding transfer functions for individual subsystems are tabulated in **Table 1**. Now, an assumption that a solid element undergoes M trips in the recycle would tantamount to $M+1$ trips in forward (top bed) loop. Thus, the net transfer function of the subsystem $\overline{E}_{TBR}(s)$ with the recycle$\left(\overline{E}_R(s)\right)$, bottom bed$\left(\overline{E}_B(s)\right)$ and the top bed $\left(\overline{E}_T(s)\right)$can be represented as

$$\overline{E}_{TBR_1}(s)=\frac{1}{1+\alpha}\overline{E}_T(s)\sum_{M=0}^{\infty}\left(\frac{1}{1+\alpha}\right)^M\left[\overline{E}_T(s)\overline{E}_B(s)\overline{E}_R(s)\right]^M \tag{6}$$

When $M\to\infty$, $\overline{E}_{TBR}(s)$ can be further simplified by computing the infinite sum of the geometric progression (**Eqs. 7, 8**).

$$\overline{E}_{TBR_1}(s)=\frac{1}{1+\alpha}\overline{E}_T(s)\frac{1}{1-\left(\frac{1}{1+\alpha}\right)\left[\overline{E}_T(s)\overline{E}_B(s)\overline{E}_R(s)\right]} \tag{7}$$

$$\overline{E}_{TBR_1}(s)=\frac{\overline{E}_T(s)}{1+\alpha\left[1-\overline{E}_T(s)\overline{E}_B(s)\overline{E}_R(s)\right]} \tag{8}$$

Thus, the net transfer function $\overline{E}_{TBRF}(s)$ representing the system would be

$$\overline{E}_{TBRF_1}(s)=\overline{E}_{TBR_1}(s)\overline{E}_F(s) \tag{9}$$

Substituting $\overline{E}_R(s)$, $\overline{E}_B(s)$, $\overline{E}_T(s)$ and $\overline{E}_F(s)$, the overall transfer function denoting Scheme 1 is (**Eq. 10**)

$$\overline{E}_{TBRF_1}(s)=\frac{\left(\frac{1}{\left[1+\left(\frac{\beta_2}{N_T}\right)\tau_{mod\,el}s\right]^{N_T}}\right)\left(\frac{(1-\alpha)^{N_F}}{\left[1+\left(\frac{\beta_4}{N_F}\right)\frac{1}{(1-\alpha)}\tau_{mod\,el}s\right]^{N_F}}\right)}{1+\alpha\left[1-\left(\frac{1}{\left[1+\left(\frac{\beta_2}{N_T}\right)\tau_{mod\,el}s\right]^{N_T}}\right)\left(\frac{\alpha^{N_B}}{\left[1+\left(\frac{\beta_1}{N_B\alpha}\right)\tau_{mod\,el}s\right]^{N_B}}\right)\left(\frac{\alpha^{N_R}}{\left[1+\left(\frac{\beta_3}{N_R\alpha}\right)\tau_{mod\,el}s\right]^{N_R}}\right)\right]} \tag{10}$$

Here, $\beta_1,\beta_2,\beta_3,\beta_4$ represent the fractional volumes, whereas, N_B, N_T, N_R, N_T refer to the number of equivalent tanks in the cascade of bottom bed, top bed, recycle and freeboard respectively. As the estimation of poles of $\overline{E}_{TBRF_1}(s)$ is difficult, its analytical inversion is non-trivial. Hence, in order to

estimate the parameters of the system represented by $\overline{E}_{TBRF_1}(s)$, **Eq. 10** is numerically inverted by Zakian inversion method to corresponding $E_{FBRC_1}(t)$ and regressed [42]**.**

Table 1 Transfer Functions of Subsystems

Subsystem	**Fraction of flow (α)[-]**	**Volume fraction of the subsystem (β)[-]**	**Number of equivalent tanks in subsystem (N)[-]**	**Transfer Function**
Bottom Bed	α	β_1	N_B	$\overline{E}_B(s)=\dfrac{\alpha^{N_B}}{\left[1+\left(\dfrac{\beta_1}{N_B\alpha}\right)\tau_{model}s\right]^{N_B}}$
Top Bed	**1**	β_2	N_T	$\overline{E}_T(s)=\dfrac{1}{\left[1+\left(\dfrac{\beta_2}{N_T\alpha}\right)\tau_{model}s\right]^{N_T}}$
Recycle	α	β_3	N_R	$\overline{E}_R(s)=\dfrac{\alpha^{N_R}}{\left[1+\left(\dfrac{\beta_3}{N_R\alpha}\right)\tau_{model}s\right]^{N_R}}$
Freeboard	$1-\alpha$	β_4	N_F	$\overline{E}_F(s)=\dfrac{(1-\alpha)^{N_F}}{\left[1+\left(\dfrac{\beta_4}{N_F(1-\alpha)}\right)\tau_{model}s\right]^{N_F}}$

6.0 Results and Discussion

In this section, the detailed analysis of the flow schemes as a part of the network synthesis model is discussed. An integral step for a successful tracer test is in ensuring perfect injection. **Figure 4a** illustrates that the entire tracer injection was within very short which negates any possibility of tracer backmixing the inlet itself. Typically, raw signals from radiotracers are noisy. For, subsequent processing thus, the signals were filtered employing low – pass Butterworth filter (**Fig. 4b**). Now, the filtered signals were treated for background and injection point correction (**Fig. 4c**). Consequently, the tracer count so obtained was normalized to estimate $E(t)$. Based on the measured $E(t)$, a detailed analysis of the flow was accomplished by employing the flow schemes based on network modeling of the solids flow.

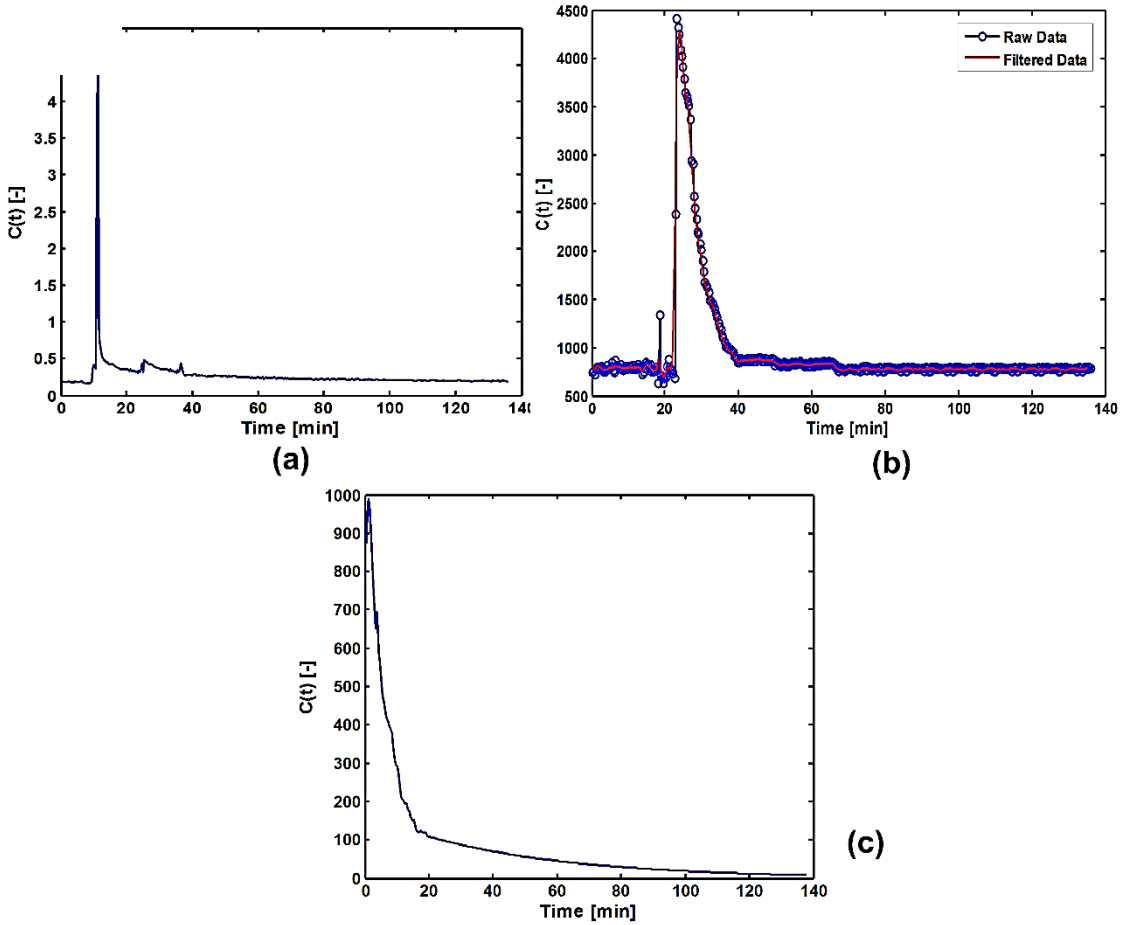

Figure 4. (a) Count vs time at the injection detector D2, **(b)** Raw and filtered count of Run 8 at D22, **(c)** Injection and background corrected count of Run 8 at D22

6.1 Flow behavior of solids in fluidized bed coal gasifier

As discussed earlier, the tracer coal particles injected were detected by D2. Once, in the bed, they undertake a complex flow path, a fraction of which ultimately exits from the top. As the passage of coal from the top was continuous, the tracer signal obtained by detectors D22 and D23 located closely in the standpipe was used for analysis. Closer examination of the experimental measurements of solids RTD indicated strong axial mixing. A single parameter model like Axial Dispersion Model (ADM) may not provide a suitable description of such solids flow. Besides, with such dominant contribution of mixing non-idealities like strong internal recirculation, the formation of dead zones and bypass also exist. Hence, for an adequate explanation, additional parameters may be needed. As the present study primarily deals with an industrial gasification system, the flow complications are expected to be manifold.

It was notable that in spite of the flow complexities, the mean residence time of solids flow computed by the model ($\mu_{1,model}$) fairly agreed with that measured ($\mu_{1,exp}$). Whereas the μ_1 of RTD function denotes the mean residence time distribution, the nature of mixing is characterized by σ^2. Now, as the network model of Scheme 3 represented the convolution of RTD functions of several phenomenological sub-systems, it would have been improper to represent the overall distribution based on a single parameter σ^2

. Instead, the dimensionless parameters - α , $\beta_1 - \beta_4$, γ , δ , N_B , N_F , N_R and N_S in Scheme 3 takes into account the contribution of each of the non-idealities and thus indicate the possible nature of mixing governing the flow. The parameters $\beta_1 - \beta_4$, along with α and γ showed that the entire bed behaved as a highly heterogeneous unit. Moreover, it was also noted that irrespective of the run conditions, there was considerable back-mixing of solids in the bottom bed. Although the network analysis of RTD yielded a phenomenological description of the industrial coal gasifier, the influence of operating pressure and mode of operation (oxy/air) on solids mixing pattern is difficult to be determined conclusively. However, in the following section, the applicability of the Scheme 3 model to predict RTD in fluidized beds as reported earlier, is being presented, which demonstrated its scalability as well.

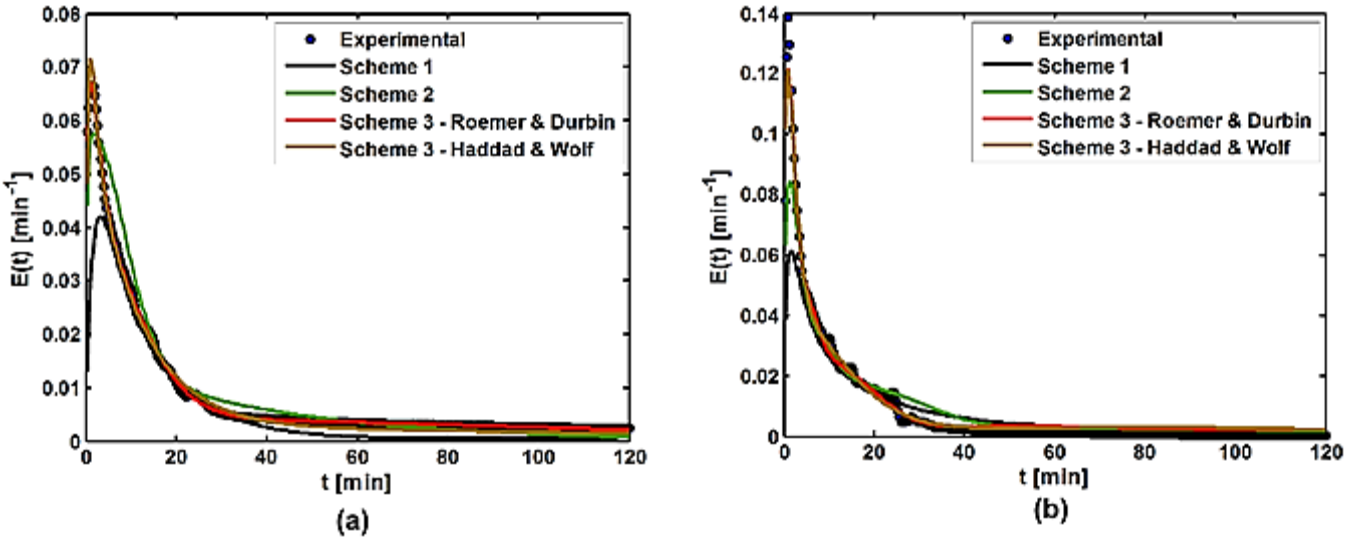

Figure 5. $E(t)$ vs t of Run 3 at **(a)** D22 and **(b)** D23

7.0 Conclusions

The flow pattern of solids in fluidized beds is very complex. In spite of the fact that they have been a topical area of research, understanding the underlying flow pattern governing hydrodynamics remains unresolved. Primarily, flow maldistributions arise due to RTD of the phases.

Thus, in this study, RTD measurements were performed in a Winkler type industrial coal gasifier employing radiotracer. Experimental data for three runs operated under oxygen/air-blown mode and two pressures 2, 4 bars were used for investigation. A detailed analysis of the flow non-ideality was carried out based on the network of a cascade of perfectly mixed tanks in series. Although the effect of pressure and the operating mode was not distinctly identified, the extent of non-ideality could be quantified. Besides, these models were also tested for RTD data reported earlier and were found to satisfactorily agree with the experimental observations [7,24]. Such analysis exhibited that the proposed scheme was sufficiently robust, scalable and can be adapted for both single as well as pulse injection of tracer.

Notwithstanding the present study, analysis based on RTD yields only macromixing characteristics of the flow field. Additional hydrodynamic modeling through CFD with appropriate closures is required to decipher a comprehensive flow model for a fluidized bed coal gasifier.

References

[1] P. Mondal, G.S. Dang, M.O. Garg, Syngas production through gasification and cleanup for downstream applications — Recent developments, Fuel Processing Technology. 92 (2011) 1395–1410. doi:10.1016/J.FUPROC.2011.03.021.

[2] P. Basu, Combustion and gasification in fluidized beds, CRC press, 2006.

[3] A. Arjunwadkar, P. Basu, B. Acharya, A review of some operation and maintenance issues of CFBC boilers, Applied Thermal Engineering. (2016). doi:10.1016/j.applthermaleng.2016.04.008.

[4] E.B. Nauman, Residence time theory, Industrial and Engineering Chemistry Research. 47 (2008) 3752–3766. doi:10.1021/ie071635a.

[5] H.P. Cui, M. Strabel, D. Rusnell, H.T. Bi, K. Mansaray, J.R. Grace, C.J. Lim, C.A. McKnight, D. Bulbuc, Gas and solids mixing in a dynamically scaled fluid coker stripper, Chemical Engineering Science. 61 (2006) 388–396. doi:10.1016/J.CES.2005.06.014.

[6] M.J. Rhodes, S. Zhou, T. Hirama, H. Cheng, Effects of operating conditions on longitudinal solids mixing in a circulating fluidized bed riser, AIChE Journal. 37 (1991) 1450–1458. doi:10.1002/aic.690371003.

[7] R. Andreux, G. Petit, M. Hemati, O. Simonin, Hydrodynamic and solid residence time distribution in a circulating fluidized bed: Experimental and 3D computational study, Chemical Engineering and Processing: Process Intensification. 47 (2008) 463–473. doi:10.1016/J.CEP.2007.01.023.

[8] B. Du, L.S. Fan, F. Wei, W. Warsito, Gas and solids mixing in a turbulent fluidized bed, AIChE Journal. (2002). doi:10.1002/aic.690480907.

[9] F. Wei, Z. Wang, Y. Jin, Z. Yu, W. Chen, Dispersion of lateral and axial solids in a cocurrent downflow circulating fluidized bed, Powder Technology. 81 (1994) 25–30. doi:10.1016/0032-5910(94)02854-0.

[10] W. Wei, Fei, Jin Yong, Yu, Zhiqing, Chen, Lateral and Axial Mixing of the dispersed particles in CFB, Journal of Chemical Engineering of Japan. (1994) 506–510.

[11] F. Wei, J.-X. Zhu, Effect of flow direction on axial solid dispersion in gas—solids cocurrent upflow and downflow systems, The Chemical Engineering Journal and the Biochemical Engineering Journal. 64 (1996) 345–352. doi:10.1016/S0923-0467(96)85016-0.

[12] F. Wei, Y. Cheng, Y. Jin, Z. Yu, Axial and lateral dispersion of fine particles in a binary-solid riser, Canadian Journal of Chemical Engineering. 76 (1998) 19–26. doi:10.1002/cjce.5450760104.

[13] A.T. Harris, J.F. Davidson, R.. Thorpe, A novel method for measuring the residence time distribution in short time scale particulate systems, Chemical Engineering Journal. 89 (2002) 127–142. doi:10.1016/S1385-8947(02)00004-9.

[14] A.T. Harris, J.F. Davidson, R.B. Thorpe, Particle residence time distributions in circulating fluidised beds, Chemical Engineering Science. 58 (2003) 2181–2202. doi:10.1016/S0009-2509(03)00082-4.

[15] A.. Harris, J.. Davidson, R.. Thorpe, The influence of the riser exit on the particle residence time distribution in a circulating fluidised bed riser, Chemical Engineering Science. 58 (2003) 3669–3680. doi:10.1016/S0009-2509(03)00215-X.

[16] A. Avidan, J. Yerushalmi, Solids mixing in an expanded top fluid bed, AIChE Journal. 31 (1985) 835–841. doi:10.1002/aic.690310520.

[17] D.C. Guío-Pérez, T. Pröll, H. Hofbauer, Solids residence time distribution in the secondary reactor of a dual circulating fluidized bed system, Chemical Engineering Science. 104 (2013) 269–284. doi:10.1016/J.CES.2013.08.047.

[18] D.C. Guío-Pérez, T. Pröll, J. Wassermann, H. Hofbauer, Design of an inductance measurement system for determination of particle residence time in a dual circulating fluidized bed cold flow model, Industrial and Engineering Chemistry Research. 52 (2013) 10732–10740. doi:10.1021/ie400211h.

[19] D.C. Guío-Pérez, T. Pröll, H. Hofbauer, Measurement of ferromagnetic particle concentration for characterization of fluidized bed fluid-dynamics, Powder Technology. 239 (2013) 147–154. doi:10.1016/J.POWTEC.2013.01.040.

[20] D. Bellgardt, J. Werther, A novel method for the investigation of particle mixing in gas-solid systems, Powder Technology. 48 (1986) 173–180. doi:10.1016/0032-5910(86)80076-6.

[21] P.A. Ambler, B.J. Milne, F. Berruti, D.S. Scott, Residence time distribution of solids in a circulating fluidized bed: Experimental and modelling studies, Chemical Engineering Science. 45 (1990) 2179–2186. doi:10.1016/0009-2509(90)80093-T.

[22] K. Kiared, F. Larachi, C. Guy, J. Chaouki, Trajectory length and residence-time distributions of the solids in three-phase fluidized beds, Chemical Engineering Science. 52 (1997) 3931–3939. doi:10.1016/S0009-2509(97)00236-4.

[23] S. Roy, A. Kemoun, M.H. Al-Dahhan, M.P. Dudukovic, Experimental investigation of the hydrodynamics in a liquid-solid riser, AIChE Journal. 51 (2005) 802–835. doi:10.1002/aic.10447.

[24] S. Bhusarapu, M.. Al-dahhan, M.P. Dudukovic, Quantification of solids flow in a gas – solid riser : single radioactive particle tracking, Chemical Engineering Science. 59 (2004) 5381–5386. doi:10.1016/j.ces.2004.07.052.

[25] C. W. Chan, J.P.K. Seville, D.J. Parker, J. Baeyens, Particle velocities and their residence time distribution in the riser of a CFB, Powder Technology. (2010). doi:10.1016/j.powtec.2010.05.008.

[26] S. Mahmoudi, J. Baeyens, J. Seville, The solids flow in the CFB-riser quantified by single radioactive particle tracking, Powder Technology. (2011). doi:10.1016/j.powtec.2011.04.011.

[27] S. Mahmoudi, C.W. Chan, A. Brems, J. Seville, J. Baeyens, Solids flow diagram of a CFB riser using Geldart B-type powders, Particuology. 10 (2012) 51–61. doi:10.1016/J.PARTIC.2011.09.002.

[28] C.E. Weinell, K. Dam-Johansen, J.E. Johnsson, Single-particle behaviour in circulating fluidized beds, Powder Technology. 92 (1997) 241–252. doi:10.1016/S0032-5910(97)03245-2.

[29] H.J. Pant, V.K. Sharma, M. Vidya Kamudu, S.G. Prakash, S. Krishanamoorthy, G. Anandam, P. Seshubabu Rao, N.V.S. Ramani, G. Singh, R.R. Sonde, Investigation of flow behaviour of coal particles in a pilot-scale fluidized bed gasifier (FBG) using radiotracer technique, Applied Radiation and Isotopes. 67 (2009) 1609–1615. doi:10.1016/J.APRADISO.2009.04.003.

[30] H.J. Pant, V.K. Sharma, S. Goswami, J.S. Samantray, I.N. Mohan, T. Naidu, Residence time distribution study in a pilot-scale gas–solid fluidized bed reactor using radiotracer technique, Journal of Radioanalytical and Nuclear Chemistry. 302 (2014) 1283–1288. doi:10.1007/s10967-014-3528-9.

[31] S. Goswami, J. Biswal, J. Samantray, D.F. Gupta, H.J. Pant, Measurement of mixing time and holdup of solids in gas–solid fluidized bed using radiotracer technique, Journal of Radioanalytical and Nuclear Chemistry. 302 (2014) 845–850. doi:10.1007/s10967-014-3256-1.

[32] S. Goswami, H.J. Pant, V.K. Sharma, L. Varshney, Radiotracer investigation in a pilot-scale fluidized bed coal gasifier (FBCG), Applied Radiation and Isotopes. 149 (2019) 22–30. doi:10.1016/J.APRADISO.2019.04.013.

[33] W. Lin, C.E. Weinell, P.F.B. Hansen, K. Dam-Johansen, Hydrodynamics of a commercial scale CFB boiler-study with radioactive tracer particles, Chemical Engineering Science. 54 (1999) 5495–

5506. doi:10.1016/S0009-2509(99)00296-1.

[34] J. Villermaux, Trajectory Length Distribution (TLD), a novel concept to characterize mixing in flow systems, Chemical Engineering Science. 51 (1996) 1939–1946. doi:10.1016/0009-2509(96)00051-6.

[35] L. Sharma, K.D.P. Nigam, S. Roy, Axial dispersion in single and multiphase flows in coiled geometries: Radioactive particle tracking experiments, Chemical Engineering Science. 157 (2017) 116–126. doi:10.1016/J.CES.2016.05.012.

[36] L. Hua, J. Wang, Residence time distribution of particles in circulating fluidized bed risers, Chemical Engineering Science. 186 (2018) 168–190. doi:10.1016/J.CES.2018.04.027.

[37] S. Goswami, H.J. Pant, R.N. Ambade, B. Paul, L. Varshney, A. Dash, Study of adsorption characteristics of Au (III) onto coal particles and their application as radiotracer in a coal gasifier, Applied Radiation and Isotopes. 122 (2017) 127–135.

[38] E.B. Nauman, B.A. Buffham, Mixing in continuous flow systems, John Wiley & Sons Inc, 1983.

[39] L.T. Fan, C.Y. Wen, Models for flow systems and chemical reactors, Marcel Dekker, New York, 1975.

[40] D. Wolf, W. Resnick, Residence time distribution in real systems, Industrial and Engineering Chemistry Fundamentals. 2 (1963) 287–293. doi:10.1021/i160008a008.

[41] A. Haddad, D. Wolf, W. Resnick, Residence time distribution in multi-stage systems with recycle, The Canadian Journal of Chemical Engineering. 42 (1964) 216–218. doi:10.1002/cjce.5450420507.

[42] R.G. Rice, D.D. Do, Applied mathematics and modeling for chemical engineers, John Wiley & Sons, 2012.

[43] B.A. Buffham, Impulse response of infinite and semi-infinite sequences of identical stirred tanks with backflow, Industrial and Engineering Chemistry Fundamentals. 8 (1969) 428–430. doi:10.1021/i160031a011.

[44] M.H. Roemer, L.D. Durbin, Transient response and moments analysis of backflow cell model for flow systems with longitudinal mixing, Industrial and Engineering Chemistry Fundamentals. 6 (1967) 120–129. doi:10.1021/i160021a021.

[45] A.H. Haddad, D. Wolf, Residence Time Distribution Function for Multi-Stage Systems with Backmixing, The Canadian Journal of Chemical Engineering. 45 (1967) 100–104.

Author Information

Shantanu Roy is Professor of Chemical Engineering Indian Institute of Technology - Delhi, New Delhi, India. He holds a B. Tech. from IIT Delhi (1994), and an M.S. (1996) and D. Sc. (2000) from Washington University in St. Louis, USA, all in Chemical Engineering. Prior to joining IIT Delhi as full-time faculty in 2004, Dr. Roy was employed in Corning Incorporated in New York.

At present, Prof. Roy also holds the additional charge of Dean – Academics at IIT Delhi. He is also currently Institute Chair Professor at IIT Delhi.

Prof. Roy's research interests include computational flow modeling of multiphase reactors, non-invasive imaging of multiphase flows, and process intensification through monolithic and structured reactor systems and microreactors. In particular, he has been involved in the development and use of novel techniques like radioactive particle tracking (RPT) and different modes of process tomography. At present, he is also leading a major project pushed by Government of India on development of technology for methanol production from high-ash Indian coal. His other interests include mini and micro-scale reactors.

Prof. Roy is a recipient of the DuPont Young Faculty Award in 2004. He serves as an expert for International Atomic Energy Agency, Vienna for radiation-based experimental techniques and has lectured in several countries as IAEA expert. He also a member of the Scientific Advisory Committee of the Ministry of Petroleum and Natural Gas, Government of India, the Science and Engineering Research Board, and has been a member of several high-level committees of Government of India.

Prof. Roy has been on the Editorial Board of Advanced Powder Technology (Elsevier) and the Asia-Pacific Journal of Chemical Engineering. Prof. Roy serves as a reviewer of several top journals such as AIChE Journal, Chemical Engineering Journal, Chemical Engineering Science, etc. He has also served as member of advisory committees of several international conferences such as ISCRE (International Symposium of Chemical Reaction Engineering) and GLS (International Symposium of Gas-Liquid-Solid Reactor Engineering), and is the Co-Chair of the ISCRE 26 Conference in New Delhi.

Nuclear structure studies with thermal neutron induced reactions

Bency John

Nuclear Physics Division, Bhabha Atomic Research Centre, Mumbai-400085, India
(*Author Email:* bjohn@barc.gov.in / bencyv.john@gmail.com)

1.0 Introduction

The renaissance in low energy nuclear physics during the past couple of decades is credited largely due to the technological revolutions in terms of radioactive ion beam accelerators and high-resolution high-efficiency radiation detector systems. Along with the experimental developments, a qualitative change in theoretical modeling due to the progress in computer technologies and numerical algorithms is taking place, particularly in the areas of theoretical nuclear structure. Exploration in a selected section of thermal neutron induced reactions using a high resolution γ-ray detector setup can be stimulating in this background as we found in experiments carried out using the DURGA setup (Dhruva Utilization for Research using Gamma Array) at DHRUVA reactor. The primary aims of DURGA setup are to conduct nuclear structure investigations in neutron rich fission fragments produced in thermal neutron induced fission of fissile isotopes, and thermal neutron capture reactions in medium to heavier mass nuclei. First experiment with this setup was conducted in the year 2021 and further utilization is underway. Results from this experiment are presented in some detail after a brief description of the setup.

2.0 DURGA Facility

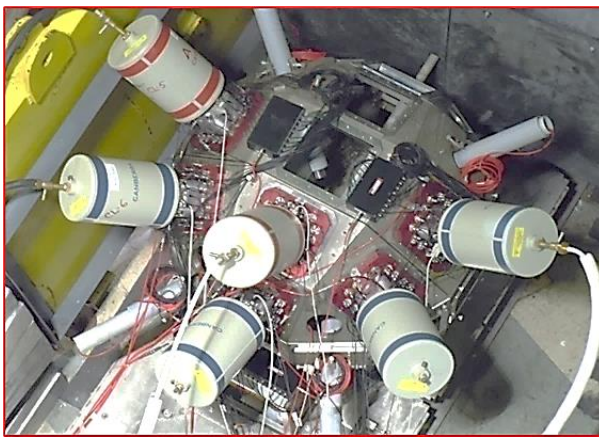

Figure 1. Top-view of the near-4π stainless steel frame that holds the HPGe clover detectors and the $LaBr_3$(Ce) fast scintillators. Thermal neutron beam hit the target placed at the geometrical center of the assembly, after drifting through the Al tube (~ 1 inch dia.), seen coming out from the grey coloured inner shield structure.

Figure 2. Inside-view of the near-4π frame with the target holder (white) at center and protruding $LaBr_3$(Ce) (cylindrical) and BGO ACS (square faced) detectors. HPGe clover detectors are housed inside the ACS shells.

The purpose of DURGA setup is high-resolution prompt gamma coincidence spectroscopic investigations of excited nuclei produced in neutron capture reaction (CGS: Capture-Gamma Spectroscopy) and fission reaction following thermal neutron capture (PFGS: Prompt Fission-Gamma Spectroscopy). A combination of High Purity Germanium (HPGe) clover configuration semiconductor detectors and fast timing Lanthanum Bromide ($LaBr_3$(Ce)) scintillation detectors is mounted at different

angles on a spherical mechanical structure, made of stainless steel, covering a near 4π solid angle (Figures 1 and 2). The 'near-4π' frame is designed in such a way that the front faces of clover-detectors are at a distance of 25 cm from the geometrical center of the mounting structure, with the accompanying anti-Compton shields (ACS) subtending an angle less than but close to 30 deg. A maximum of 32 clover detectors can be mounted in this manner with a maximum total solid angle coverage of approximately 25%. At the center of the near-4π frame, the target material of interest is placed as a foil or pellet of dia 10-15 mm. The experimental work space is a shielded enclosure of size 3.38 x 2.81 m built to utilize the beam tube R-3001 of DHRUVA research reactor (Figure 3). DHRUVA research reactor operates at maximum power of 100 MWth, and at the exit of the beam tube, the estimated maximum neutron flux is about 10^8 n/cm^2/s, which is primarily thermal. At the target position, which is further down-stream by 2.0 m, the neutron flux is found to be approximately 10^7 n/cm^2/s from flux measurements.

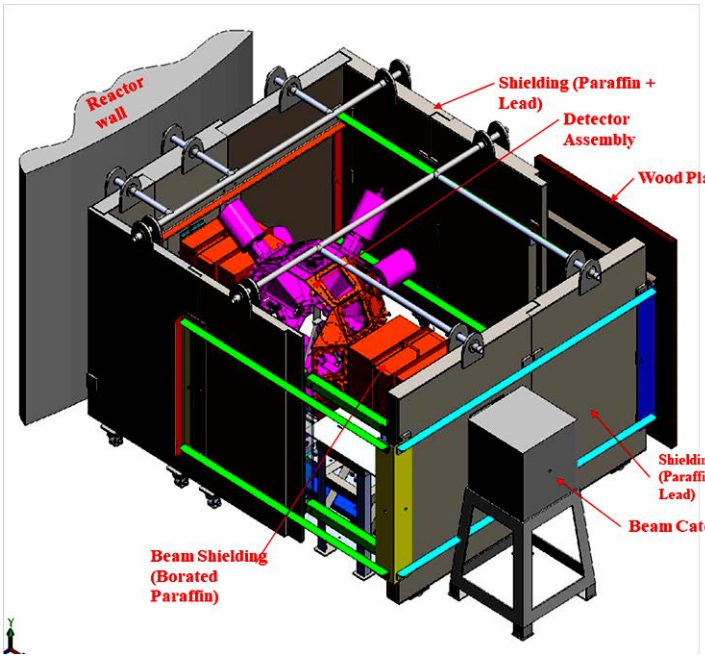

Figure 3. Schematic drawing of DURGA setup showing the reactor wall and relative positions of the outer shield structure (grey) and the 'near 4π' frame (pink) that hold the detectors in different angular positions.

If all the detector positions of the near-4π frame are occupied with the HPGe clover-detectors, a highly detailed prompt gamma coincidence spectroscopy can be performed over a wide range of nuclei, allowing detection of γ transitions as weak as approximately 10^{-4} of the total reaction cross section. However, at present, the number of HPGe clover detectors in DURGA are limited to six, and in near future it will be enhanced to eight detectors. Even with these many detectors, data on spins and parities of the excited states can be deduced with techniques such as γ-ray angular correlation. To obtain data on the excited states' lifetimes, and hence on nuclear moments, it is required that the HPGe clover detectors are coupled to suitable ancillary devices. The $LaBr_3$(Ce) fast scintillator detectors serve this purpose, and the DURGA setup is equipped with 11 such detectors.

Another significant step taken for the DURGA facility is to develop a dedicated multi-frequency digitizer-based digital data acquisition system and integrate it with the gamma detector array. The required software has been developed in collaboration with CAEN, Italy. The main advantages of such a system over the conventional analog one is well known. Presently, the acquisition system is designed for an array of 8 Compton-suppressed HPGe clover-detectors and 16 $LaBr_3$ fast scintillators which is upgradable to higher numbers. The analog signals from the HPGe clover-detector preamplifiers are sampled by four 8-channels 100 MSPS 14-bit V1724 CAEN digitizers, whereas one 16-channels 500 MSPS 14-bit V1730 CAEN digitizer takes care of the signals from the $LaBr_3$(Ce) fast scintillators. To make the system a self-sustained one, the signals from the BGO anti-Compton shields are also digitized by an 8-channels 250 MSPS 12-bit V1720 CAEN digitizer. Further details on DSP data acquisition system are given in a contributory presentation in this conference [1].

3.0 Detailed description of the setup

The radial beam tube R-3001of DHRUVA research reactor has been used for the DURGA setup. A beam collimator of total length 1.26 m, comprising of annular cadmium absorbers and annular lead absorbers with a bismuth plug suitably positioned at the center line with stainless steel and wood supports, is inserted in to the hole on the reactor wall to fill the beam tube, so that only a pencil beam of thermal neutrons comes out. As shown in the schematic drawing (Figure 3), just outside the reactor wall, a rectangular shielded outer enclosure, made up of MS and Pb sheets with paraffin filling in between, has been erected with suitable reinforcements. Overall size (LxBxH) of this outer shielding structure is 3.38 x 2.81 x 2.11 m and thickness of its wall varied at places in between 8 to 20 cm. In the gap between the end of the beam collimator and the outer enclosure, a second beam collimator comprising of boron carbide and lead has been placed in alignment. Thermal neutron streaming and gamma radiations were still too high to make the detector operation possible. A third, relatively thick set of lead, boronated rubber and cadmium shielding has been installed at the position before the detector holder frame. This inner shield reduced the above background considerably. It was not necessary to use borated paraffin blocks shown in saffron color in the schematic drawing (Figure 3), and hence they were removed. Thermal neutron beam of average diameter 16 mm at the geometric center of the near-4π structure has been achieved, and it has been verified by a neutron imaging camera.

4.0 Detectors used in DURGA

The task of the DURGA setup is not merely detecting gamma radiations but it should be able to assign them to a nucleus and even to the corresponding de-excitation process of the nucleus. When additional detectors for particle identification are *not* used, this task can become rather challenging. This is particularly true for fission experiments (PFGS) where several hundreds of different nuclei are produced in the reaction. The PFGS and CGS techniques are based on the knowledge of some initial information about the nucleus of interest, of at least one transition which is already assigned to the nucleus. The task outlined above demand high energy resolution and a maximum possible efficiency for the gamma detectors. Use of as many possible HPGe clover configuration detectors therefore is indispensable for detailed PFGS and CGS campaigns.

The HPGe clover configuration detectors used in DURGA were manufactured by Canberra, France, and are exactly similar to the one used in INGA set-up at the three accelerators centres in India. The initial size of the n-type high purity Ge crystals used are 50mm in diameter and 70 mm in length. Four such crystals are machined on the sides at an angle to taper down the first 36 mm in such a way that they pack into a close geometry (Ge-Ge distance only approximately 0.7mm) to form a 'clover' configuration. The sketch in Figure 4 (a) shows the faces of four crystals configured like a clove. This way of cutting maintains most of the original volume, up to ~ 90%. (The advantage being a significantly larger photo-peak efficiency and energy/timing resolutions for the clover configuration detectors, as discussed below.) The crystals, after fabricating each one a separate p-n diode, are enclosed in a vacuum aluminum housing which act as a common Ge cryostat (Figure 4 (b)). The front face of the aluminum housing has a thickness of 1.5 mm. The crystals and the first stage of preamplifier electronics are maintained at a temperature of approximately 95 K by a common cold finger from a liquid nitrogen Dewar. The liquid nitrogen Dewar has a static holding time in excess of 20h, when in vertical down-looking position with no high-voltage applied. Surrounding the Ge cryostat is a BGO anti-Compton shield (ACS) with its heavy metal collimator, acting as a veto detector. The ACS is of optimized design to match the Ge cryostat dimensions.

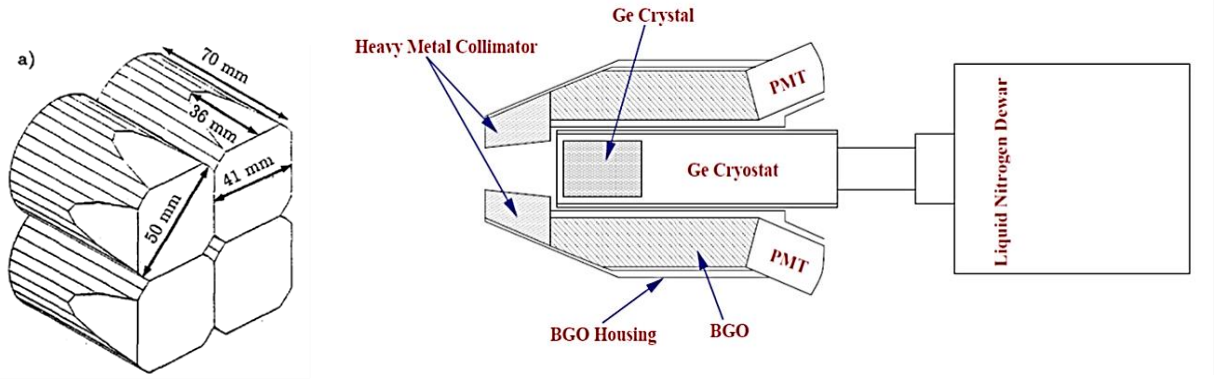

b)

Figure 4. a) Size and shape of the Ge crystals for a four-crystal clover detector; **b)** Schematic layout of a HPGe detector along with the BGO anti-Compton shield.

The detection of full energy of a gamma ray in a Ge clover-detector can be in two ways; (i) full energy in one segment, and (ii) in more than one segment. The first type is called a single event and the second a multiple event. In the second type, the full energy is obtained during the analysis by adding back energies in all the segments that are fired. An add-back factor F_{ab} can be defined given by the ratio of photopeak efficiency in the add-back mode to the singles event mode. The F_{ab} value of the clover detectors used in DURGA is around 1.4 at 1.33 MeV gamma energy. Typical normalized spectra obtained with a ^{152}Eu source in singles and add-back mode are shown in Figure 5. A plot of add-back factor vs. γ-ray energy employing ^{152}Eu radioactive source is also given in the lower panel of Figure 5. The advantage of Compton suppression employing BGO anti-Compton shield, which veto-out the Compton scattered events, is demonstrated in Figure 6.

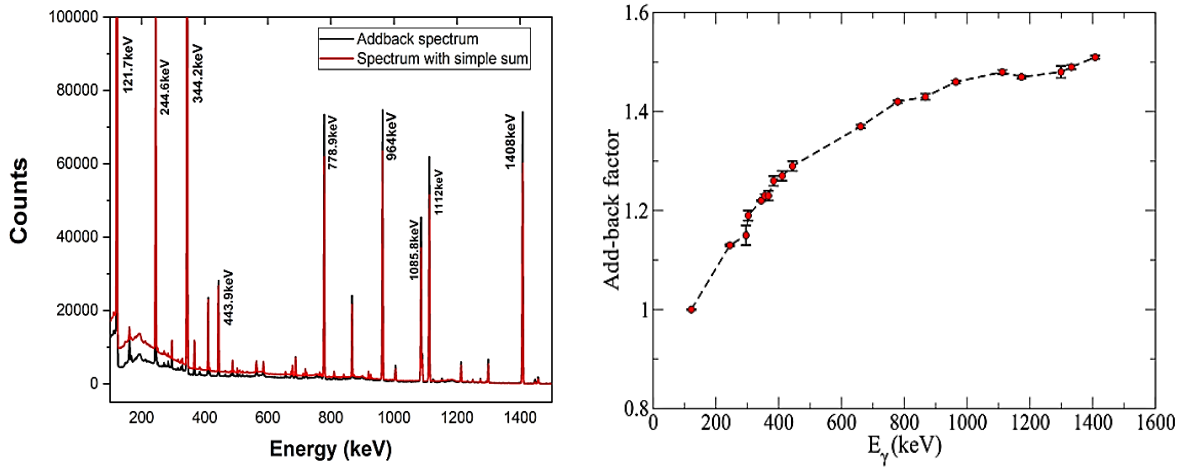

(a) (b)

Figure 5. (a) Typical add-back spectrum(black) and singles spectrum (simple sum of 4 clover segments (red color)); **(b)** Add-back factor as deduced from the clover data using ^{152}Eu radioactive source.

Energy resolutions in single event mode and add-back mode have been compared for these detectors, and the comparison has turned out to be excellent for these types of detectors. The timing resolutions obtainable from Ge detectors are moderate. But in case of clover configuration, because the signals are

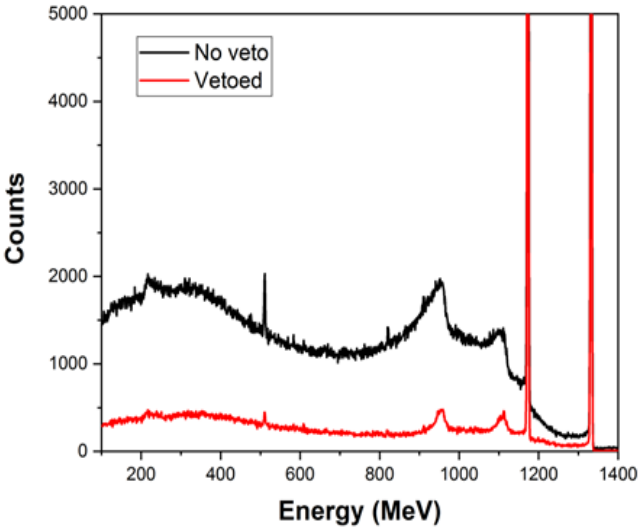

Figure 6. Effect of Compton suppression on the spectrum from the decay of a ^{60}Co source.

generated in 1/4th of the volume, the timing resolution is improved compared to a single detector of same overall size but without volume division.

5.0 $LaBr_3$(Ce) scintillation detectors

$LaBr_3$(Ce) scintillation detectors have been used in DURGA setup for life time measurements owing to its fast-timing resolution combined with good energy resolution. These detectors have an active volume of 43.5 cm^3. Lifetime measurements of nuclear excited states in sub to a few nanoseconds range can be carried out by the delayed coincidence technique. We have measured timing resolution of ~350 ps when $LaBr_3$ detectors are integrated with the digital data acquisition system. This feature makes the setup capable of searching for new isomer states among accessible nuclear excited states.

6.0 First experiment with DURGA: ^{163}Dy (n_{th}, γ) ^{164}Dy* (CGS)

Neutron capture state of even-even ^{164}Dy nucleus has energy above the ground state at 7584 keV. In the de-excitation of this state through E1, M1, E2,… photon cascades, the other states of lower energy are accessed. Electric dipole radiation E1 is highly favored in early part of the cascade as it has $(\varepsilon_\gamma)^3$ energy dependence. As a result, the primary transitions are usually of high energy E1 transitions. In subsequent 'secondary' transitions of generally lower photon energy, the nucleus reaches lower excitation energies and the transitions are strongly influenced by a variety of nuclear structural aspects and collective behaviors. The vibrations of β and γ types, multi-phonon excitations, rotation-vibration couplings, band-mixing and octupole-hexadecapole deformations are manifested depending upon the specific nucleus. Experimentally observed transition patterns for such phenomena may appear differently in some nuclei and in such a case the patterns provide a tool to study the underlying nuclear processes.

Two-phonon gamma-vibration in ^{164}Dy nucleus has been predicted theoretically to occur with $K^\pi=0^+$ and $K^\pi=4^+$ bandheads more than twice the energy of the single phonon $K^\pi=2^+$ γ-band. This brings certain difficulty in experimental observation of the same; such as $K^\pi=0^+$ and $K^\pi=4^+$ bandheads are close to the pairing gap, and hence under influence of an enhanced density of levels. The experimental vibration strength function may turn to be a fragmented one. Due to these difficulties, an elusive nature was accorded to the two phonon gamma vibration states in nuclei of similar structure, and it has been a debated theme among experimental and theoretical structure physicists over the past few decades. From among the candidate nuclei, for ^{166}Er, there exist some details of confirmation on two-phonon gamma-vibration. In the ^{164}Dy nucleus, one $K^\pi=4^+$ two-phonon state has been reported earlier.

In the first experiment with the DURGA array, we observed the lowest intrinsic $K^\pi=4^+$ state in ^{164}Dy at 1978.6 keV. This state along with three other newly observed states at 2206.7, 2261.5 and 2463.7 keV have clarified the related de-excitation properties. Inference from their decay properties is that they possibly form the elusive $K^\pi=4^+$ two-phonon gamma-vibrational band. In addition, a state at 2379.2 keV is observed with anharmonicity ratio 3.12 and it is a strong candidate for the $K^\pi=0^+$ two-gamma-phonon state. Partial level scheme of ^{164}Dy nucleus as obtained from the present data and relevant to above inferences are given in the accompanying contributory presentation [1]. Further experimental

and theoretical work is necessary to ascertain the extent of two-phonon collective components in the wave functions of the proposed states. It also remains an open question whether this particular excitation mode exits in other rare-earth nuclei.

7.0 Relevance of spin-isomer research for applications in science and technology

Importance of the research as discussed above is evident for the case of physics of low lying special collective states. Such detailed investigations in selected areas of the nuclear chart can guide to information on the 'door-way states' for specific activation of isomers of interest. Finding a method for production of isomers of suitable half lives in high specific activities suitable for radiation medicine applications is very important. As mentioned, the door-way states can only be located by detailed structure physics studies. Once their location and properties are known, direct activation of the door-way state using sufficiently high intensity photo-excitation can lead to isomer's production in sufficient specific activity. The latter because strongly populated door-way states via photo-excitation decay through intermediate states to the isomer of interest. Activation via thermal neutrons without selectivity generally do not lead to a favorable situation. This note does not imply that we found a favor in ^{164}Dy but only want to point out the importance of conducting research in this field.

8.0 Enhancement of DURGA as a national facility

Like in most laboratories in the world that pursue experiments in nuclear structure using HPGe detectors, the DURGA facility also provides a platform for installation of HPGe and complementary detectors. As mentioned earlier, DURGA has space for 32 clover detectors. To procure and maintain such a large number of HPGe clover detectors is not feasible for a single research laboratory, even in abroad. Pooling detectors, electronics, other related components, and human resources from other research institutes is a possible way out to smoothly operate and maintain a facility of the envisaged magnitude. Similar collaborative approach has successfully been demonstrated all over the world and also in India by the INGA (Indian National Gamma Array) collaboration. In INGA collaboration, all major stakeholders have in-house dedicated team of researchers, comprising of scientists, software engineers, technicians, research associates, students and other support staff. The related operational responsibilities, such as detector maintenance, electronics and data acquisition system, data sorting and analysis software development, mechanical maintenance, physics aspects etc are then generally shared among the core group of scientists, technicians and engineers in all such facilities. Therefore, a dedicated in-house gamma spectroscopy group consisting of the human resource components as mentioned above is the need of the hour, which will be crucial to realize the full potential of DURGA as a national facility.

9.0 Concluding remarks

Primary aims of the DURGA facility located in DHRUVA reactor are to conduct nuclear structure investigations in neutron rich fission fragments produced in thermal neutron induced fission of fissile isotopes (PFGS: Prompt Fission-Gamma Spectroscopy), and thermal neutron capture reactions in medium to heavier mass nuclei (CGS: Capture-Gamma Spectroscopy). This facility is unique in the country for nuclear structure investigations using thermal neutron beams. Details on the setup emphasizing on the high-resolution detectors and the 4π-frame used are given. A combination of High Purity Germanium (HPGe) clover configuration semiconductor detectors and fast timing Lanthanum Bromide ($LaBr_3$(Ce)) scintillation detectors is mounted in special configurations on a near spherical structure. First experiment with this setup on CGS has been conducted recently and interesting results on the structure of ^{164}Dy nucleus have been obtained.

Acknowledgements: Author gratefully acknowledge the able support of colleagues from DHRUVA, Gas and Movement Section, EmAID, and NPD in accomplishing the measurements. Special thanks to Dr. S. Mukhopadhyay for help in preparing the manuscript.

Reference(s):

1. S. Mukhopadhyay, B. V. John, Contributory papers in the DAE-BRNS Theme Meeting RRU-2022, May 6-7, 2022, Bhabha Atomic Research Centre, Mumbai.

Author Information

Dr. Bency Vilavinal John joined BARC in 1986 after graduating 29th Batch of BARC Training School in Physics discipline. Currently he is Scientific Officer/H and Head, Fission Physics Section of Nuclear Physics Division, BARC. He did his Ph. D. in experimental nuclear physics from Mumbai University and did post doctoral study at Cyclotron Institute, Texas A&M University, USA, in the same field. He is experienced in low energy nuclear physics experiments using Pelletron Linac Accelerator Facility. He is also experienced in using thermal neutron beam from Dhruva Reactor for nuclear physics experiments, in addition to theoretical model developments in the related fields. His main contributions are in basic research in nuclear fission, nuclear structure and level density, and in isoscalar giant resonances.

Ionizing Energy for Food Security, Safety and Promotion of International Trade of Agri-produce

Dr. S. Gautam

Food Technology Division, Bhabha Atomic Research Centre, Trombay, Mumbai-400085, India
(*Author email*: sgautam@barc.gov.in)

1.0 Principles of Radiation Processing of Food

Food irradiation is a physical process in which food and agricultural commodities, in pre-packed form or in bulk, are exposed to a controlled amount of radiation energy to achieve desirable effects such as inhibition of sprouting in underground vegetable like onion and potato; delay in ripening of certain fruits; killing of insect pests, parasites, pathogenic and spoilage microorganisms in various food including cereals, pulses, spices, herbals, flesh foods, minimally processed foods as well as Ready to Eat (RTE)/ Ready to Cook (RTC) Foods.

2.0 Radiation and Sources Approved for Processing of Food & Pharma products

Internationally statutory bodies including IAEA have approved following four radiation sources for treating foods & Pharma products

1. Gamma radiation (1.17/ 1.33 MeV) emitted by cobalt-60 radioisotope
2. Gamma radiation (0.66 MeV) emitted by cesium-137 radioisotope
3. X-rays from machine sources of energies not exceeding 5 MeV, and
4. Electrons from machine sources of energies not exceeding 10 MeV.

Food in packages is placed in containers that are moved by a conveyor into a shielded room, where it is briefly exposed to radiation emanating from a source. Radiation by its direct effect on macromolecules and indirect effect through radiolysis of water inactivates essential biomolecules of insects, parasites, and microorganisms, and destroys them. At very low doses, it also causes inhibition of sprouting and delay in ripening and senescence in fruits and vegetables. This technology is also used to sterilize surgical devices, medical and healthcare products.

3.0 Food Irradiation Facility

A radiation source (cobalt-60 or electron accelerator), biological shield (irradiation cell) and a conveyor system are the main features of a radiation processing facility. Walls and ceiling of an irradiation cell are 1.5 - 2.0 m thick of high-density cement concrete (2.5 g/cc). This ensures that no radiation escapes outside the cell and poses no health hazard to operators.

The radionuclide source, which continuously emits radiation, is normally stored under water when not in use (wet storage type irradiator). Water as shielding medium is generally preferred as it is cheap and easily available. On the other hand, machine sources like electron accelerators can be switched `on-off' at will and do not require any shielding in `off'' position. Using gamma sources big size containers can be irradiated due to high penetration power of gamma radiation, while with electrons thickness of product may become a limiting factor. However, this problem could be overcome by conversion of electrons to X-rays. The choice of an irradiator largely depends upon the nature of food, dose to be given, and throughput required.

4.0 Applications in food preservation

On the basis of radiation dose, food applications are classified into low dose (< 1 kGy), medium dose (1-10 kGy) and high dose (> 10 kGy) applications. Radiation dose is the measure of radiation energy absorbed per unit mass of material under consideration. The unit of absorbed dose is Gray (Gy). 1 Gray is the energy absorption of 1 Joule per kilogram.

5.0 Low Dose Applications

5.1 Sprout inhibition in bulbs and tubers:

Irradiation in the range of 0.06 to 0.15 kGy inhibits sprouting in tubers (e.g., potato), bulbs (e.g., onion), rhizomes (e.g., ginger) and corms (e.g., taro). In tropical climate chemical sprout inhibitor like maleic hydrazide (MH) and isopropyl-N (3-chlorophenyl) carbamate (CIPC) are not as effective as under subtropical or temperate climates. Conventionally, in commercial cold storage, potato is stored at 2-4 °C, and removed for sale as and when needed. Though sprouting is inhibited at this temperature, the commodity starts sprouting profusely as soon as it is taken out from the cold store and as it moves down the supply chain. This can be avoided by using radiation. Moreover, after irradiation (Dmin 75 Gy) potato can be stored at higher temperature of 14 ºC for around 7-8 months depending upon the quality of the product. This not only conserves energy, but also prevents sweetening of potato, commonly occurring at low temperatures. It gives advantage to the manufacturers of chips as the low sugar potato give desired lighter color to fries and chips.

Onion (Rabi crop) after irradiation (Dmin 60 Gy) can be stored at 0.5 to 1ºC and 65-68% Relative humidity in a proper ventilated structure for around 7-8 months depending upon the quality of the product.

5.2 Delayed ripening of fruits and vegetables:

India is a major producer of tropical fruits and vegetables. The Alphonso and Kesar varieties of mango are popular all over the world and have great export potential. Irradiation of these fruits at hard mature pre-climacteric stage at 0.25 to 0.75 kGy delays the ripening process by about 7 days, thus improving shelf-life. These doses are also effective in destroying quarantine pests.

At present, mangoes after radiation treatment as per USDA guidelines are exported to USA by air route. Because of high air transportation cost and limitation of volume, share of Indian mango in the USA remains relatively small and result in low export earnings. Use of sea route for transportation would result in substantial cost reduction and enable export of larger volumes enabling deeper penetration in the USA market. A technology has been developed for delayed ripening of Indian 'Kesar' mangoes which will enable its sea-route shipment to USA'. The SOP has been approved by the United States Department of Agriculture (USDA).

Irradiated fresh fruits and vegetables can be stored for longer duration, sometimes up to 30 d

at 10-14 ºC and in modified atmospheres. As observed in case of tomato harvested at green mature stage ripening can be delayed up to 2 months upon radiation processing (Dmin 650 Gy) when stored at 10-13 ºC.

Radiation treated mango
(Shelf life 35 days in cold storage)

Radiation treated tomato
(Shelf life 60 days in cold storage)

5.3 Radiation processing as a quarantine treatment:

Fresh, as well as stored agricultural commodities are often infested with insect pests and microbial pathogens. It is a major constraint in international trade in agricultural commodities. As fumigants like ethylene dibromide (EDB) and methyl bromide (MB) are being phased out, role of irradiation as a quarantine treatment is attracting greater attention. This may help boost exports of fresh fruits, vegetables, plantation products and cut flowers.

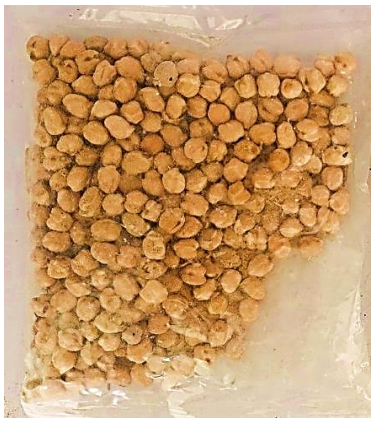

Non-irradiated

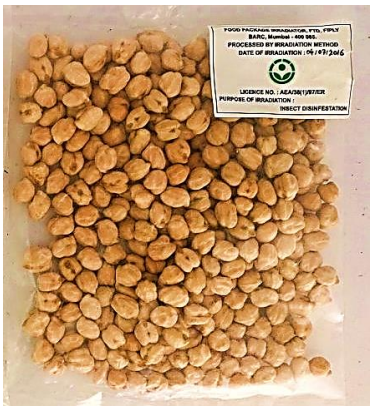

Irradiated

6.0 Medium Dose Applications

6.1 Shelf-life extension of sea-foods, meat and meat products:

India is one of the major producers and exporter of sea-foods. With a coastline of over 4500 km, fish production has steadily increased over the years. Fresh catch of fish is prone to rapid spoilage due to improper storage conditions, and contamination with pathogens under usual handling and processing practices. This poses serious health risk to consumers. Under ice, fish like Bombay duck, pomfret, Indian Salmon, Mackerel, and shrimp can be stored for about 7-10 days. Studies have demonstrated that irradiation at 1-3 kGy followed by storage at melting ice temperatures increases its shelf- life nearly threefold. In India, meat and meat products are marketed either fresh or in frozen form. Meat and meat products including poultry have a shelf-life of about a week at 0-3ºC, which could be extended up to four weeks by applying a dose of 2-5 kGy, which inactivates spoilage bacteria. Radiation treatment has been employed to enhance the shelf-life of intermediate moisture fish and meat products.

7.0 High Dose Applications

7.1 Hygienization of spices:

India is a major spice producing and exporting country. However, due to inadequate handling and processing conditions, spices get contaminated with insect eggs and microbial pathogens. When incorporated into semi-processed or processed foods, particularly, after cooking, the microbes, both spoilers and pathogens, in spices can outgrow causing spoilage and posing risk to consumers. An average absorbed dose of 10 kGy brings about near sterility while retaining the natural characteristics of spices. Irradiation at higher doses can also be used for total sterilization of diets for immune compromised patients, adventure sports, military and astronauts as well as ensuring safety of Ready to Eat (RTE) foods for calamity affected people.

Availability of nutritious, safe and ambient storable meal during calamities is an earnest need. Unpredictable disasters like flood and earthquakes may lead to failure of different logistics and worsen the food supply. A nutritious and safe RTE product 'Stuffed Baked Food (SBF)' locally called as 'Litti' was developed which upon radiation treatment can be stored for 8 months at ambient temperature. The product was supplied by DAE as a good will gesture for flood and land slide affected people of Himachal Pradesh in the year 2018, and also to various National Disaster Response Force (NDRF) units of the country.

8.0 Benefits of Radiation Processing

Globally a significant amount of agricultural produce is lost through postharvest spoilage due to insect infestation, microbial attack and other biological and physical damages. Prevention of postharvest losses can plug the widening gap between food production and requirement. The chemical fumigants like ethylene dibromide (EDB), methyl bromide (MB) and ethylene oxide (ETO) used for the control of insect pests, quarantine treatment of agricultural and horticultural produce and for microbial decontamination of food commodities are being phased out on account of their harmful effects on human health and environment. On the other hand, treatment with radiation energy is a very effective green and eco-friendly technology for elimination of pathogens and can be applied to pre-packaged commodities even under frozen conditions.

9.0 Advantages of Radiation Processing

Radiation processing is and effective alternative to chemical fumigants that endanger human health and environment. Being a cold process, it does not alter the fresh-like character of a food commodity. At the recommended doses it maintains sensory qualities, texture, nutritive value and appearance of food. It does not produce any toxic residues in food. Unlike chemical fumigants irradiation can be carried out in pre-packaged foods and hence no risk of post-irradiation contamination. Being highly penetrating and effective, large volumes of foodstuffs can be treated very efficiently. Radiation processing is an eco-friendly treatment and does not pollute environment. A single treatment of irradiation could suffice to achieve many desirable effects.

11.0 Wholesomeness of Irradiated Foods

Wholesomeness of food indicates attributes such as nutritional adequacy, organoleptic quality (flavor and aroma), and safety aspects. In context of irradiated food, wholesomeness has been thoroughly studied for parameters such as Induced radioactivity; Microbiological safety; Safety of chemical changes; and Nutritional adequacy in laboratories around the world for more than past five decades. At the energies of gamma rays from cobalt-60 (1.33 and 1.17 MeV), Cesium-137 (0.66 MeV) and those recommended for X-rays (≤5 MeV) and accelerated electrons (≤10 MeV), no induction of radioactivity is possible in atoms constituting food. Besides, in an irradiation facility the food while subjected to radiation treatment never comes into direct contact with the source of radiation. The microbiological analyses of radiation- processed foods have indicated that foods preserved by radiation do not pose any special problems in relation to microflora. The major concern about the safety of irradiated food was the formation of free radicals and radiolytic product(s). When food is exposed to high intensity radiation, free radicals and radiolytic products are formed due to interaction of radiation with matter, however, when thoroughly scrutinized at various levels and data generated were compiled and critically evaluated, no unique radiolytic products were found to be formed in radiation treated foods and most of the free radicals formed disappear depending on the nature of the commodity, either immediately after irradiation, or during its post- irradiation storage and processing. In fact, the chemical differences between radiation processed foods and non-irradiated foods are so small, that the detection of the radiation treated food remains a challenging issue. The investigations have proved that the free radicals or radiolytic products formed as a result of irradiation treatment do not compromise the safety of food. Radiation processing of food has not found to have any effect on the nutritive value of food as it does not affect important macronutrients, such as carbohydrates, proteins and fats, thus leaving the food fresh.

None of the short- or long-term animal feeding studies as well as the trials on human volunteers have shown any adverse effect. Recent study conducted in BARC, India has too affirmed the genotoxic safety of radiation treated foods when used for prolonged generations in various model systems. American astronauts and Russian cosmonauts have been consuming

irradiated rations on board during space missions. USA is importing radiation treated mango form India since 2007 and many other fruits from different parts of the world since many years. In China huge volume of radiation treated food is being consumed. Vietnam is exporting substantial quantity of radiation treated foods including flesh foods. Thus, on the basis of available information and scrutiny of scientific data, it has become amply clear that food irradiation technology provides maximum assurance of safety to consumers. Therefore, more than 60 countries all over the globe including India have approved radiation processing of food.

12.0 Regulatory approval

Determination of required radiation dose is one of the major parameters for optimal processing which is addressed through R&D activities at Food Technology Division, BARC, Mumbai. This is based upon the nature of commodity as well as the purpose. First of all, in 1994 Government of India amended Prevention of Food Adulteration Act (1954) Rules and approved irradiation of onion, potato and spices for domestic market. Recently 'Generic approval of radiation processing of food under Radiation processing of food and Allied Products Rules, 2012' has been gazette notified by the Government of India in 2016 (F.No.1-120(2)/Standards/Irradiation/FSSAI-2015).

13.0 The commissioning of an irradiation facility

It is carried out at different stages (Scrutinization of proposal, approval, site clearance, plant erection, source installation, safety assessments and guidance, supervision, commissioning, maintenance) which are affected and monitored by several organizations (Bhabha Atomic Research Centre, BARC; Board of Radiation & Isotope Technology, BRIT and Atomic Energy Regulatory Board, AERB) operating directly under the regulation of Department of Atomic Energy, India. Construction of the facility is a one-time investment and other expenditures include regular maintenance, running costs and occasional source replacement.

14.0 Food irradiation facilities

In India, the first pilot radiation processing facility, the Food Package Irradiator in Food Irradiation Processing Laboratory (FIPLY), was commissioned in 1967. Later four food irradiation facilities were commissioned in the Government sector in states of Maharashtra and Gujarat namely, Krishi Utpadan Sanrakshan Kendra (KRUSHAK) at Nashik; Irradiation Facility Centre (IFC), Maharashtra State Agriculture and Marketing Board (MSAMB), Vashi; Radiation Processing Plant (RPP), Vashi; Gujarat Agro Industries Corporation Limited, Ahmedabad. In the last two decades additional 21 plants have been established under private entrepreneurship. Presently, construction for many new plants have started and many more have been proposed.

15.0 Conclusion

Although India is the second largest producer of agricultural and horticultural commodities, it ranks 102 in the global hunger index (GHI). Post-harvest losses are one of the prime reasons behind this paradox. Besides contribution of agriculture sector in national GDP has shown a gradual

decline since independence. Technological and processing interventions could be considered as possible remedial measures. A significant amount of agricultural produce is lost during postharvest storage primarily due to insect infestations, microbial contaminations, and other biological and physical damages. Prevention of postharvest losses can help in ensuring food security to the greater extent. The chemical fumigants used for the control of insect pests, quarantine treatment of agricultural and horticultural produce and for microbial decontamination of food commodities are being phased due to their harmful effects on human health and environment. Therefore, there is an utmost need of an alternate environment-friendly green technology to address these issues. Radiation technology provides a very effective solution to the post-harvest losses of food while ensuring their safety too. Foods subjected to radiation treatment are gaining acceptance in society at a rapid pace, due to increased public understanding of the process and the underlying science. Worldwide consumers are purchasing radiation treated foods as per their availability because of their satisfaction with the quality and safety of the product. Irradiation technology has enabled the import of fruits and vegetables across the countries including into the USA that were once prohibited due to the fear of importing pests along with the produce. As the current numbers of food irradiation plants are minuscule in India with respect to the quantum of produce which is limiting the visibility of radiation treated food in domestic market(s), India is in dire need of many more food irradiation plants coupled with cold chain, storage and appropriate transportation facilities. With the expansion of educated population and rise in literacy, Indian buyers too are gradually being more concerned of quality and safety of foods where radiation processing has a great future and hope to cater the need.

Acknowledgement

The contributions from the past and present scientific & technical staffs of Food Technology Division, BARC, Mumbai in taking the national food irradiation program on a successful path is gratefully acknowledged.

Food -class based Generic approval of Radiation Processing

Class	Food	Purpose	Dose limit (kilo Gray) Minimum	Maximum
Class 1	Bulbs, stem and root tubers, and rhizomes	Inhibit sprouting	0.02	0.2
Class 2	Fresh fruits and vegetables (other than Class 1)	Delay ripening	0.2	1.0
		Insect disinfestation	0.2	1.0
		Shelf-life extension	1.0	2.5
		Quarantine application	0.1	1.0
Class 3	Cereals and their milled products, pulses and their milled products, nuts, oil seeds, dried fruits and their products	Insect disinfestation	0.25	1.0
		Reduction of microbial load	1.5	5.0
Class 4	Fish, aquaculture, seafood and their products (fresh or frozen) and crustaceans	Elimination of pathogenic microorganisms	1.0	7.0
		Shelf-life extension	1.0	3.0
		Control of human parasites	0.3	2.0
Class 5	Meat and meat products including poultry (fresh and frozen) and eggs	Elimination of pathogenic microorganisms	1.0	7.0
		Shelf-life extension	1.0	3.0
		Control of human parasites	0.3	2.0
Class 6	Dry vegetables, seasonings, spices, condiments, dry herbs and their products, tea, coffee, cocoa and plant products	Microbial decontamination	6.0	14.0
		Insect disinfestation	0.3	1.0
Class 7	Dried foods of animal origin and their products	Insect disinfestation	0.3	1.0
		Control of moulds	1.0	3.0
		Elimination of pathogenic microorganisms	2.0	7.0
Class 8	Ethnic foods, military rations, space foods, ready-to-eat, ready-to-cook/ minimally processed foods	Quarantine application	0.25	1
		Reduction of microorganisms	2	10
		Sterilization	5	25

Dose Limits for Radiation Processing of Allied Products

			Dose limit (kGy) Minimum	Maximum
1.	Animal food and feed	Insect disinfestations Microbial decontamination	0.25 5.0	1.0 10.0
2.	Ayurvedic herbs and their products, and medicines	Insect disinfestations Microbial decontamination Sterilization	0.25 5.0 10	1.0 10.0 25
3.	Packaging materials for food/allied products	Microbial decontamination Sterilization	5.0 10.0	10.0 25
4.	Food additives	Insect disinfestations Microbial decontamination Sterilization	0.25 5.0 10	1.0 10.0 25
5.	Health foods, dietary supplements and nutraceuticals	Insect disinfestations Microbial decontamination Sterilization	0.25 5.0 10	1.0 10.0 25
6.	Body care and cleansing products	Microbial decontamination Sterilization	5.0 10	10.0 25
7.	Cut flowers	Quarantine application Shelf-life extension	0.25 0.25	1.0 1.0

Map of food irradiation plants operational in India

Currently 25 food irradiation plants (Government sector: 4; Private sector: 21) are operational in the country.

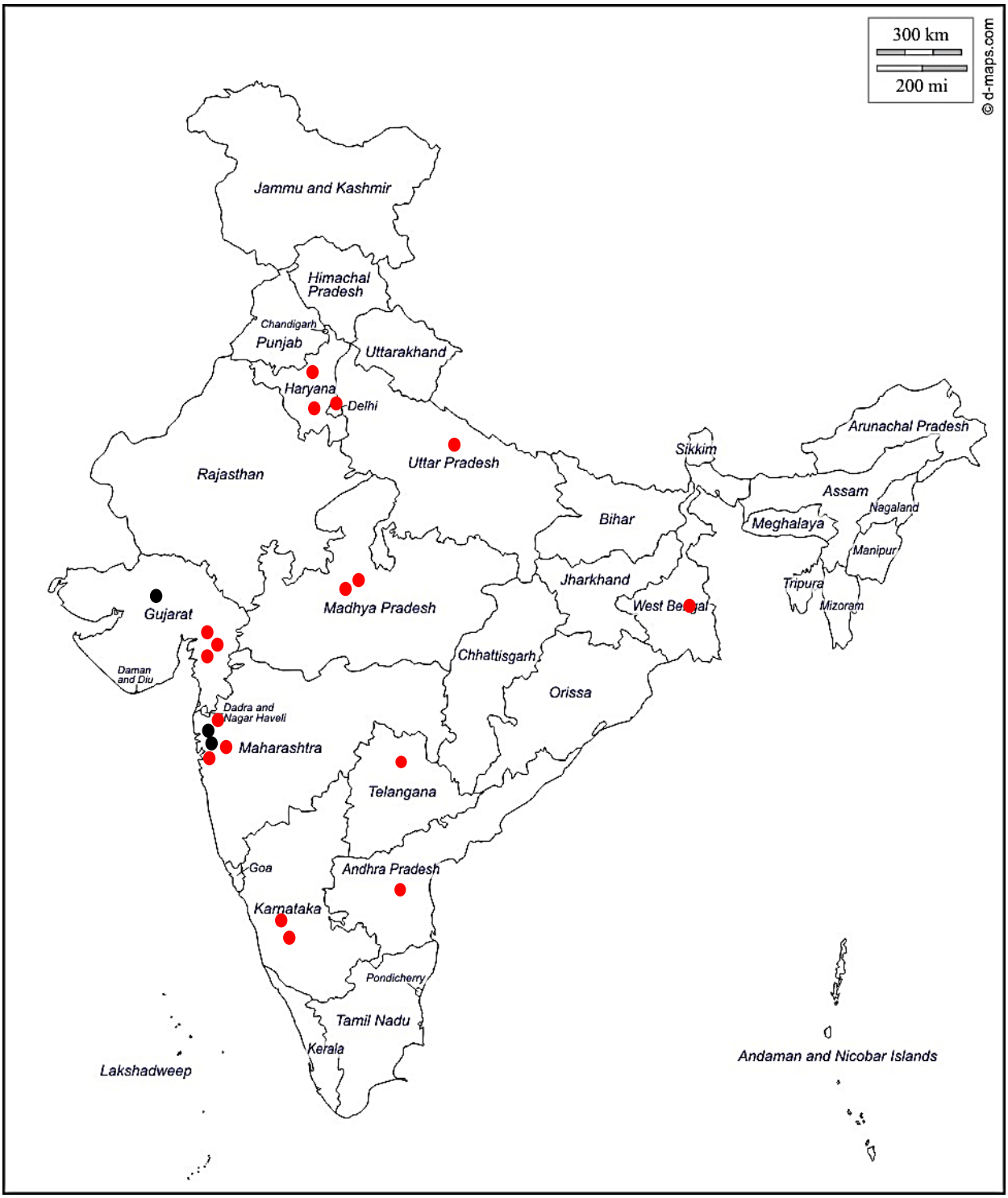

Author Information

Shri S. Gautam joined BARC in 1994 through prestigious BARC-Training School Program, and later joined Food Technology Division. After that he completed his doctorate degree in science from University of Mumbai, and two years post-doctoral studies (2005-07) at University of Medicine and Dentistry, New Jersey, USA. Dr. Gautam has worked extensively on the preservation of foods, primarily fruits and vegetables, development of special purpose ready-to-eat meal for calamity affected people, disaster response forces, and other targets using radiation technology. Besides, Dr. Gautam has worked on the understanding the potential nutraceutical applications of fruits, vegetables and allied products. He has also carried out fundamental studies to reveal the mechanism of cell death in stressed bacterial cells. Dr. Gautam has 116 publications in peer reviewed journals and books, alongside many abstracts in conferences. He is currently serving as Head, Food Food Technology Division, BARC, Mumbai and also Professor at Homi Bhabha National Institute (HBNI), DAE, Trombay, Mumbai. Dr. Gautam has been awarded DAE-Homi Bhabha Science & Technology Award (2016) for outstanding contributions in the area of Food Technology. Besides he also got DAE Group Achievement Awards twice (2009 & 2011). Dr. Gautam is a fellow of Maharashtra Academic Sciences and Scientific panel member in the Food Safety and Standards Authority of India (FSSAI).

Chemical Characterization of Materials by NAA and PGNAA utilizing Research Reactors at BARC

Raghunath Acharya

Radiochemistry Division, BARC, Trombay, Mumbai-400085, India
(*Author email:* racharya@barc.gov.in / racharyabarc@gmail.com)

Chemical characterization of materials is the most important step under chemical quality control (CQC) exercise and it involves quantification of major, minor and trace elements present in the sample. Presently, atomic and mass spectroscopic techniques are widely used for this purpose. Radioanalytical techniques in general and Nuclear Analytical Techniques (NATs) in particular like Neutron Activation Analysis (NAA) and Ion Beam Analysis (IBA) have added advantages in analyzing direct solid samples without chemical dissolution for obtaining simultaneous multi-elemental determination from major to trace elements. NAA is a powerful isotope specific nuclear analytical technique for simultaneous determination of elemental concentrations of major, minor and trace elements in diverse matrices. The technique has many advantageous properties including inherent accuracy and precision and it is capable of yielding high analytical sensitivity and low detection limits (ppm to ppb) due to availability of high thermal neutron flux from research reactors. Due to higher penetration power of neutrons and gamma rays, NAA experiences negligible matrix effects in the samples of different origins. Depending on the sample matrix and element of interest NAA technique is used non-destructively, known as instrumental neutron activation analysis (INAA), or through chemical dissolution methods. This technique in combination with on-line NAA (PGNAA) is capable of analyzing about $2/3^{rd}$ of the elements (~ 70 elements) in the periodic table. The NAA and PGNAA have been applied almost all fields of Science and Technology. It has been applied for multielement analysis in the fields like environment, biology, geology, archaeology, material sciences, nuclear technology and forensic sciences as well as industrial samples like coal, cement and gemstones. Under our R&D programs of the department as well as collaborative work utilizing research reactors, NAA has been extesively applied for multielemental determination in samples like sediments, ores, manganese nodules, cereals, medicinal / edible leaves, wheat, milk, packaged foods, renal calculi, ancient pottery/bricks, precious stones, gunshot residues, viscera samples, automobile windshield glasses, alloys such as stainless steel, zircaloys, coal, coal ash, catalysts and dross. This is possible because of availability of high flux (about 10^{14} n/cm^2/s) research reactors like 100MW$_{th}$ Dhruva and 2MW$_{th}$ upgarded Apsara (Apsara-U) at BARC, Trombay. On the other hand, PGNAA is a truly non-destructive technique capable of determining elements like H, B and other neutron poisons (like Cd, Gd, Sm, Eu , Dy and Hf) as well as almost all elements at minor or trace concentration levels. A dedicated PGNAA facility will find vast applications to finished reactor materials, archaeology/museum smaples, forensic specimens/evidences as well as glass, ceramics and alloys that are difficult to destroy and samples can be returned after analysis is over as there will be not much gross activity since it is an online measurement method with low neutron flux from thermal neutron beam lines (10^5 to 10^8 n/cm^2/s).

Acknowledgements: Author is thankful to all contributors and collaborators as well as Reactor Group, BARC in general and Director, RG, Head, ROD and Head, RRSD and Head, RPNES (RRSD) in particular. Author thanks Dr. S.B, Manohar, Dr. AVR Reddy, Dr. A. Goswami Dr PK Pujari, Dr S. Kannan and Dr. P.K. Mohaptra of RC&IG, BARC for their support and encouragement in NAA & PGNAA work.

Author Information

Dr. Raghunath Acharya after completing his M.Sc (Chemistry) with first-class first position from Ravenshaw College (Aautonomous) (now University) under Utkal University joined 37th Batch of BARC Training School. After successfully completing one-year training course in 37th Batch (1993-94), he joined Radiochemistry Division, BARC and since then he is engaged in R&D work on Nuclear Analytical Chemistry utilizing research reactors and particle accelerators. He is instrumental in developing k_0-based (Single Comparator) conventional and internal monostandard neutron activation analysis (NAA) and prompt gamma NAA (PGNAA) as well as in situ current normalized Particle Induced Gamma-ray Emission (PIGE) methods for the first time in India and these techniques are helpful for non-destructive chemical characterization of various materials having relevance to DAE and Society. Since 1994, he has extensively utilized research reactors (Apsara, CIRUS, Dhruva, AHWR Critical Facility, KAMINI and Apsara-U) for various R&D programs and collaborated with many Indian Universities/Institutes under BRNS, UGC-DAE CSR and CSIR projects He obtained his PhD degree in 2000 from University of Mumbai and pursued his Postdoctoral studies in Dalhousie University, Canada during 2000-2002. He is a recipient of IANCAS Dr. Tarun Datta Memorial Award 2003, Young Scientist Award 2008 (YSA 2008) of the International Committee of Activation Analysis (ICAA) and "Scientific and Technical Excellence Award" of the DAE for the year 2009. He has obtained more than 160 peer reviewed international journal publications, more than 300 conference presentations. He is an elcted member of k_0-International Scientific Committee since 2009 and Secretary of ICAA since 2019. Currently, he is Heading Nuclear Analytical and Actinide Spectroscopy Section of Radiochemistry Division, BARC, Mumbai.

RRU-2022

Dr. Tej Singh, a postgraduate in Physics from Agra University, Uttar Pradesh, joined Research Reactor Services Division in the year 1990 after completion of one year orientation course in Nuclear Engineering from 33rd batch (Physics Discipline), BARC Training School. He did his PhD in physics from Mumbai University. His areas of expertise are reactor physics, safety & shielding design optimization, core management studies & operational reactor physics of present and upcoming research reactors. At present, he is heading the reactor physics and nuclear engineering section of Research Reactor Services Division. He is responsible for providing reactor physics support for safe and smooth operation of the research reactors at BARC. He has developed computer codes NEMSQR and HEXNEM, based on nodal expansion method, for reactor core design calculations & core management studies, respectively. He also developed safety analysis codes IQSHEX & DINHEX Space time kinetics based on nodal expansion methods and RITAC & SACRIT based on point kinetics model coupled with thermal hydraulics for research & power reactors for analysis of reactivity-initiated accidents.

Shri Kunal Chakraborty, Outstanding Scientist, is the Head, Reactor Operations Division, BARC. He is from 32nd batch of BARC Training School. His field of expertise is operations, utilization and safety Management of Research Reactors. He is responsible for effective utilization of the reactor like regular irradiation and supply of radioisotopes, irradiation of new fuels and other experimental assemblies, testing of detectors, utilization of beam tube by commissioning of neutron radiography facility etc. He is one of the key person for co-ordination with other services and sections as required for timely action to correct/rectify the deficiencies in the system and equipment.

Shri C. G. Karhadkar, Outstanding Scientist, is the Director, Reactor Group, BARC. He is from 31st batch of BARC Training School. His field of expertise is research reactor operations, safety review of nuclear reactors, reactor utilization, radioisotope production, NTD silicon production, fission molly production and mechanical design. He has designed various rigs for utilization of the reactor for various experiments. He was instrumental in planning for long shut down of Dhruva for repair of leaky heat exchanger and executed the same ahead of schedule. He was one of the key person to oversee the first criticality of the Apsara-U reactor.

Dr. Raghunath Acharya, Head, Nuclear Analytical and Actinide Spectroscopy Section, Radiochemistry Division, BARC, is an expert in the field of Nuclear Analytical Chemistry. He completed his M.Sc (Chemistry) with first-class first position from Ravenshaw College (Autonomous) (now University) under Utkal University and joined 37th Batch of BARC Training School. After successfully completing one-year training course in 37th Batch (1993-94), he joined Radiochemistry Division, BARC. Since 1995, he is engaged in R&D work on chemical characterization of various materials utilizing research reactors and particle accelerators at BARC. He is instrumental in developing k_0-based NAA and PGNAA as well as in situ current normalized IBA/PIGE methods for the first time in India. He obtained his PhD degree in 2000 from University of Mumbai and pursued his Postdoctoral studies in Dalhousie University, Canada during 2000-2002. He is a recipient of IANCAS Dr. Tarun Datta Memorial Award 2003, Young Scientist Award 2008 (YSA 2008) of the International Committee of Activation Analysis (ICAA) and "Scientific and Technical Excellence Award" of the DAE for the year 2009. He is an elected member of k_0-International Scientific Committee and General Secretary of ICAA.

Dr. P.K. Pujari, Distinguished Scientist, is the former Director, Radiochemistry and Isotope Group at Bhabha Atomic Research Centre. He has developed a state of the art positron laboratory including positron accelerator at BARC, and has overseen R&D in the area of nuclear chemistry, radioanalytical sciences, specialized radiation measurements, actinide chemistry and quality control of nuclear materials as well as radiation and radioisotope applications in the area of healthcare and industry. He is a recipient of Homi Bhabha Medal (1985), IANCAS Dr. Tarun Datta Memorial Award (1997), Japan Society for the promotion of Sciences (JSPS) Fellowship (1998-2000), DAE-SRC Outstanding Research Investigator Award (2008) and Homi Bhabha Science and Technology Award (2008). Dr. Pujari is a member of the International Committee of Positron Annihilation (ICPA) and was elected as Chair of the International Committee of Positron and Positronium Chemistry during 2014-17. Presently, he is President of IANCAS and SPAN, c/o RCD, BARC.

Azadi Ka Amrit Mahotsav

प्रकाशक:
Published by:
अध्यक्ष, वैज्ञानिक सूचना संसाधन प्रभाग
Head, Scientific Information Resource Division
भाभा परमाणु अनुसंधान केंद्र, ट्रॉम्बे, मुंबई – 400085, भारत
Bhabha Atomic Research Centre, Trombay, Mumbai 400085, India

TECHNOLOGIES FOR NEW INDIA@75